Production of plant-derived punicic acid in engineered yeast platforms

by

Juli Wang

A thesis submitted in partial fulfillment of the requirements for the degree of

Doctor of Philosophy

in

Plant Science

Department of Agricultural, Food and Nutritional Science
University of Alberta

Abstract

Punicic acid (PuA) is a high-value edible conjugated fatty acid with strong bioactivities and has important potential applications in nutraceutical, pharmaceutical, and oleochemical industries. Since the production of PuA is severely limited by the fact that its primary natural source, pomegranate seed oil, is not readily available on a large scale, there is considerable interest in understanding the biosynthesis and accumulation of this plant-based unusual fatty acid in transgenic microorganisms to support the design of biotechnological approaches for PuA production via metabolic engineering and fermentation.

In the first study, the effectiveness of genetic engineering and precursor supply in PuA production in the model yeast strain *Saccharomyces cerevisiae* was tested. The results revealed that the combination of precursor feeding and co-expression of selected genes in acyl channeling processes created a 'Push-Pull' approach to increase PuA content. Coupled with the deletion of a yeast lipid metabolism regulator, the feeding of 0.05% linoleic acid, and the introduction of *PgFADX* and other genes from pomegranate, PuA content was increased to 3.4% of total fatty acids.

Due to the complexity of plant-derived unusual fatty acid biosynthetic pathways, individually testing each gene for pathway functionality and obtaining the best gene combination are time-consuming. A rapid workflow is necessary to facilitate the study of plant unusual fatty acid metabolism and the synthesis of plant-derived lipids in microorganisms. Therefore, in the second study, genes potentially contributing to PuA synthesis were directly shuffled within the yeast genome by targeting the yeast Ty retrotransposon, resulting in a recombinant yeast library with varying PuA content. The screening of 1752 strains led to the identification of a recombinant *S. cerevisiae* capable of accumulating 26.7% of total fatty acids as PuA without

requiring linoleic acid precursor feeding. In shake flask cultivation, the PuA titer reached 424.6 mg/L. Subsequent analysis showed the combination of several upstream and downstream genes conducive to PuA accumulation. Moreover, PuA constituted over 22% of total fatty acids in the triacylglycerol (TAG) fraction of yeast single-cell oil, demonstrating a significant increase compared to PuA levels in the TAG fraction of transgenic plants. Following the increase of PuA production in yeast, substantial changes in the yeast lipidome, including TAG and major polar lipid species, were observed.

Many non-conventional oleaginous yeasts have emerged as prominent candidates in biotechnological studies for their ability to produce single-cell oil and utilize cost-effective, renewable feedstocks. In the third study, the capability of oleaginous yeast *Rhodosporidium toruloides* to produce PuA was investigated. The initial expression of pomegranate *PgFADX* allowed *R. toruloides* to accumulate 3.7% of its total fatty acids as PuA. Subsequent genomic integration of genes encoding codon-optimized delta-12 acyl lipid desaturase (PgFAD2) or diacylglycerol acyltransferase 2 (PgDGAT2) significantly increased PuA levels. The engineered *R. toruloides* strain with *PgFADX* and *PgFAD2* coexpression accumulated 12% of its lipids as PuA from glucose, which translated into a PuA titer of 451.6 mg/L in shake flask cultivation. The content of PuA achieved 6.4% when wood hydrolysate was used as the substrate, showcasing *R. toruloides'* potential in the bioconversion of lignocellulosic feedstock into high-value PuA.

In summary, the work included in this PhD thesis has led to two PuA-producing microbial platforms, including an engineered model yeast *S. cerevisiae* strain with a high PuA content, and a non-conventional oleaginous yeast *R. toruloides* strain that is capable of converting renewable agricultural and forestry waste substrate into high-value PuA. A novel Ty

retrotransposon-targeted random gene shuffling workflow for efficiently engineering baker's yeast for producing PuA was also developed. The findings of this thesis provide knowledge and valuable insights into the enrichment mechanism of PuA in yeast and will benefit the development of innovative microbial platforms for producing other plant-derived high-value fatty acids.

Preface

This thesis is based on the research presented in the following papers. My detailed contribution to each paper is summarized below. In general, I was responsible for most of the work including project design, experiment design, conducting experiments, data collection, data analysis, and manuscript preparation. My supervisor, Dr. Guanqun Chen, provided all the required resources for the experiments completed in this thesis, as well as initial project design, valuable discussions, and editing of the manuscripts. Dr. Stacy D. Singer and Dr. David C. Bressler were also involved in the discussion and editing of the manuscripts and thesis.

Chapter two is based on a submitted manuscript to *Biotechnology Advances*, which is currently under revision: Wang, J., Singer, S.D., Chen, G., Biotechnological advances in the production of unusual fatty acids in transgenic plants and recombinant microorganisms

I conceptualized the review and drafted the manuscript. Dr. Guanqun Chen provided all the required resources and supervision. All authors contributed to the manuscript revision.

Chapter three is based on a published paper: Wang, J., Xu, Y., Holic, R., Yu, X., Singer, S.D., Chen, G., 2021. Improving the Production of Punicic Acid in Baker's Yeast by Engineering Genes in Acyl Channeling Processes and Adjusting Precursor Supply. J. Agric. Food Chem. 69, 9616–9624. https://doi.org/10.1021/acs.jafc.1c03256

I conceptualized the "push and pull" approach used in this project, performed all experiments, analyzed the data, and drafted the manuscript. Dr. Guanqun Chen provided supervision, discussion, and all the required resources. Dr. Roman Holic provided certain codon-optimized pomegranate genes, plasmids, and yeast mutants used in this study. All coauthors contributed to the revision of the manuscript.

Chapter four is based on a manuscript in preparation: Wang, J., Chen, G., Optimization of pomegranate-derived punicic acid accumulation in *Saccharomyces cerevisiae* by Ty retrotransposon-targeted random gene shuffling.

I conceptualized the idea of using Ty retrotransposon-targeted random gene shuffling to screen candidate genes that facilitate PuA production, designed the project, performed the experiments, analyzed the data, and drafted the manuscript. Dr. Guanqun Chen provided supervision, all the required resources, valuable discussions, and editing of the manuscripts. The lipidomic analyses described in this work were performed by the Kansas lipidomic research center analytical laboratory.

Chapter five is based on a submitted manuscript, which is currently under review: Wang, J., Haddis, D.Z., Xiao, Q., Bressler, D.C., Chen, G., Engineering *Rhodosporidium toruloides* for the production of pomegranate-derived punicic acid.

I conceptualized the idea of using *R. toruloides* to produce PuA, designed the research, performed the experiments, analyzed the data, and drafted the manuscript. Dr. Guanqun Chen provided supervision and all the required resources. Dagem Zekaryas Haddis from Dr. Bressler's lab prepared and provided wood hydrolysate. Qiong Xiao from Dr. Chen's lab conducted the RT-PCR analysis. All coauthors contributed to the revision of the manuscript.

Other publications and my contributions during my PhD study are listed in the appendix.

Acknowledgments

Looking back on my PhD journey, I am incredibly grateful to all the people who have provided constant support and encouragement. Without the motivation and help of these individuals, this doctoral thesis would not be possible. First and foremost, I would like to express my sincere thanks to Dr. Guanqun Chen, my supervisor. Over four and a half years ago, Dr. Chen introduced me to the field of plant science by accepting me as a PhD student in his lab. Under Dr. Chen's guidance, I immersed myself in the complexities of plant lipid metabolism and focused on interdisciplinary research involving applied microbiology and plant lipid biotechnology. From the very first day of my PhD study, Dr. Chen has been a constant source of inspiration and motivation. His deep passion for the field and his dedication to research motivated me to continually push for higher achievements in my work. Moreover, Dr. Chen was always encouraging of my research efforts and strongly supported the ideas I proposed. His support not only made the work in this thesis possible but also gave me the confidence to conduct independent research and consider a future career in academia.

My sincere gratitude goes out to my supervising committee members, Dr. Stacy D. Singer and Dr. David C. Bressler, for their kind support and insightful comments in forming the manuscripts included in this thesis. Their scholarly insights have expanded my thinking and enhanced the quality of this work. I also want to thank Dr. David Stuart and Dr. Jonathan Curtis for serving as the examiners and Dr. Doug Korver for serving as the Chair of my candidacy exam. I am also truly thankful to Dr. Yang Qu for agreeing to be the external examiner and Dr. Habibur Rahman for serving as the Chair of my thesis defense. I deeply appreciate the time and effort they invested in reviewing my study.

To my dear colleagues and collaborators, I extend my sincerest thanks. In particular, I want to express my heartfelt gratitude to Professor Yang Xu from the University of Guelph, Canada. Dr. Xu, who previously conducted postdoctoral research in our lab, has been an invaluable source of support throughout this journey. Her dedication coupled with her

remarkable talent as a researcher, has been truly an inspiration to me. I also thank Dr. Roman Holic from the Slovak Academy of Sciences, Slovakia, for providing valuable discussions concerning yeast expression systems, the synthesized pomegranate genes, and various yeast strains at the beginning of this research. I extend my thanks to Dr. Bin Shan, our lab technician, for her diligent efforts in ensuring the smooth operation of our lab and the success of our research projects.

I also want to express my heartfelt gratitude to the wonderful individuals and cherished friends I have had the pleasure of meeting in the Chen group: Qiong Xiao, Kethmi Jayawardhane, Udaya Subedi, Yingyi Liu, and Dr. Qiyuan Shan. In times of challenge, their support has been a source of strength. Our time together was filled with unforgettable moments and their help has been truly appreciated.

I am deeply thankful to the University of Alberta and the Department of Agricultural, Food, and Nutritional Science for providing the resources, facilities, and academic environment necessary for the completion of this research. I am privileged to have been a part of this vibrant academic community. I extend my sincere gratitude to the funding sources that have supported my PhD study, including Alberta Innovates, Results Driven Agriculture Research, Natural Sciences and Engineering Research Council of Canada, Canada Poultry Research Council, Cargill/Diamond V, Canada Foundation for Innovation-John R. Evans Leaders Fund and Research Capacity Program of Alberta, as well as the providers of the various graduate scholarships I have received during my PhD studies at the University of Alberta.

My thanks extend to my family for their everlasting love, encouragement, and understanding throughout my PhD study. Their belief in me has been a continual source of strength, encouraging me to strive for excellence, and I am deeply thankful for their sacrifices and unwavering support.

Thank you all for being a part of this journey.

Table of Contents

List of Tables

List of Figures

List of Abbreviations

ACC/ACCase	acetyl-CoA carboxylase
BHT	butylated hydroxytoluene
ACP	acyl carrier protein
ATP	adenosine triphosphate
cDNA	complementary DNA
CoA	coenzyme A
CPT	choline phosphotransferase
DAG	diacylglycerol
DGAT	acyl-CoA: diacylglycerol acyltransferase
DGK1	diacylglycerol kinase 1
ELO	fatty acid elongase
EPT	ethanolamine phosphotransferase
ER	endoplasmic reticulum
FAD2	delta(12) fatty acid desaturase
FAD3	delta(15) fatty acid desaturase
FADX	bifunctional fatty acid conjugase/delta(12) fatty acid desaturase
FAE	fatty acid elongase
FAS	fatty acid synthase
FAT	acyl-ACP thioesterase
G3P	sn-glycerol-3-phosphate
GC	gas chromatography
GPAT	glycerol-3-phosphate acyltransferase

GRAS	generally recognized as safe
LA	linoleic acid
LACS	long-chain acyl-CoA synthetase
LPAT	lysophosphatidic acid acyltransferase
LPC	lysophosphatidylcholine
LPCAT	lysophosphatidylcholine acyltransferase
LPE	lysophosphatidylethanolamine
MAG	monoacylglycerol
MFA	monounsaturated fatty acid
OLE1	acyl-CoA desaturase
PA	phosphatidic acid
PAP	phosphatidate phosphatase
PC	phosphatidylcholine
PDAT	phospholipid: diacylglycerol acyltransferase
PDCT	phosphatidylcholine: diacylglycerol cholinephosphotransferase
PE	phosphatidylethanolamine
PG	phosphatidylglycerol
PI	phosphatidylinositol
PL	polar lipid
PLA2	phospholipase A2
PLC	phospholipase C
PS	phosphatidylserine
PuA	punicic acid

PUFA	polyunsaturated fatty acid
SAD	stearoyl-ACP desaturase
SFA	saturated fatty acid
sn	stereospecific numbering
SNF	sucrose non-fermenting
TAG	triacylglycerol
UFA	unusual fatty acid

Chapter 1 – Introduction

Punicic acid (PuA; 18: 3 $\Delta^{9cis, 11trans, 13cis}$), is an unusual plant-derived conjugated polyunsaturated fatty acid (Grossmann et al., 2010) (Figure 1). Studies have shown that PuA possesses a broad spectrum of health benefits, including anti-diabetic, anti-obesity, and anti-carcinogenic properties (Aruna et al., 2015; Holic et al., 2018; Vroegrijk et al., 2011). In addition, due to the presence of conjugated double bonds, conjugated fatty acids have strong chemical reactivity and polymerization ability, making them useful as cross-linking agents (Adekunle, 2015; He et al., 2014; Lee et al., 2021). Therefore, the market potential of PuA extends beyond health benefits to industrial uses, such as the manufacture of resins, paints, polymers, and drying oils. Given these emerging applications of PuA in the nutraceutical, cosmetic, and chemical industries, its potential market is expected to experience significant growth in the coming years (Paul and Radhakrishnan, 2020). As a result, the market price of pomegranate seed oil, depending on its purity, has been reported to be relatively high (Holic et al., 2018; Urbanikova et al., 2023), ranging from 10 to 70 CAD per kg (www.alibaba.com, accessed on 1 June 2024).

The primary natural source of PuA is pomegranate (*Punica granatum*), which contains up to 80% PuA in its seed oil (Kaufman and Wiesman, 2007; Khoddami et al., 2014; Takagi and Itabashi, 1981). A few other plant species, such as *Trichosanthes kirilowii*, also produce this fatty acid, although at lower levels compared to pomegranate (Hennessy et al., 2016; Shabbir et al., 2017). Compared to oilseed crops, the oil content of pomegranate seeds is relatively low. For instance, canola (mainly *Brassica napus*) seeds contain 45% or more oil on a dry weight basis (Rahman et al., 2013), whereas pomegranate seeds only contain less than 20% oil (Fadavi et al., 2006; Lansky and Newman, 2007; Özgül-Yücel, 2005). Moreover, the yield of pomegranate

seeds is low and subject to a range of influences, including the fruit's genotype and climatic conditions (Fadavi et al., 2006; Khoddami et al., 2014; Özgül-Yücel, 2005). Therefore, this low and unstable oil yield may affect the feasibility and cost-effectiveness of PuA production from pomegranate seeds. Although initial efforts are underway to produce PuA in transgenic plants, the productivity has been relatively low so far (Mietkiewska et al., 2014; Xu et al., 2020b). Compared to plant sources, the production of PuA through microbial fermentation presents a promising alternative. Using metabolically engineered microorganisms, microbial fermentation would offer a more controlled and scalable production of PuA without large arable land requirements. Furthermore, utilizing agricultural and industrial waste materials as feedstock could significantly reduce the production costs of PuA when using engineered microorganisms.

In pomegranate, the synthesis of PuA is catalyzed by the bifunctional fatty acid desaturase and conjugase PgFADX (Iwabuchi et al., 2003) (Figure 1). In addition, previous studies have demonstrated that the enrichment of unusual fatty acids (UFAs) in plant oils is facilitated by a series of enzymatic reactions occurring in the developing seeds (Cahoon and Li-Beisson, 2020; Napier, 2007). These processes form an acyl-editing and triacylglycerol (TAG) assembly network, crucial for transferring UFAs from phospholipids to the storage lipid TAG and maintaining a normal fatty acid composition of plant cell membrane structure (Cahoon and Li-Beisson, 2020). Investigating this multi-enzyme network in plant hosts and transferring it to transgenic crops for PuA production presents challenges due to the intricate nature of plant genomes, regulation, and their long growth cycles. Conversely, many conventional and non-conventional microbial platforms provide a feasible alternative option due to their fast growth rates, advanced molecular tools, and short timeframe of commercialization.

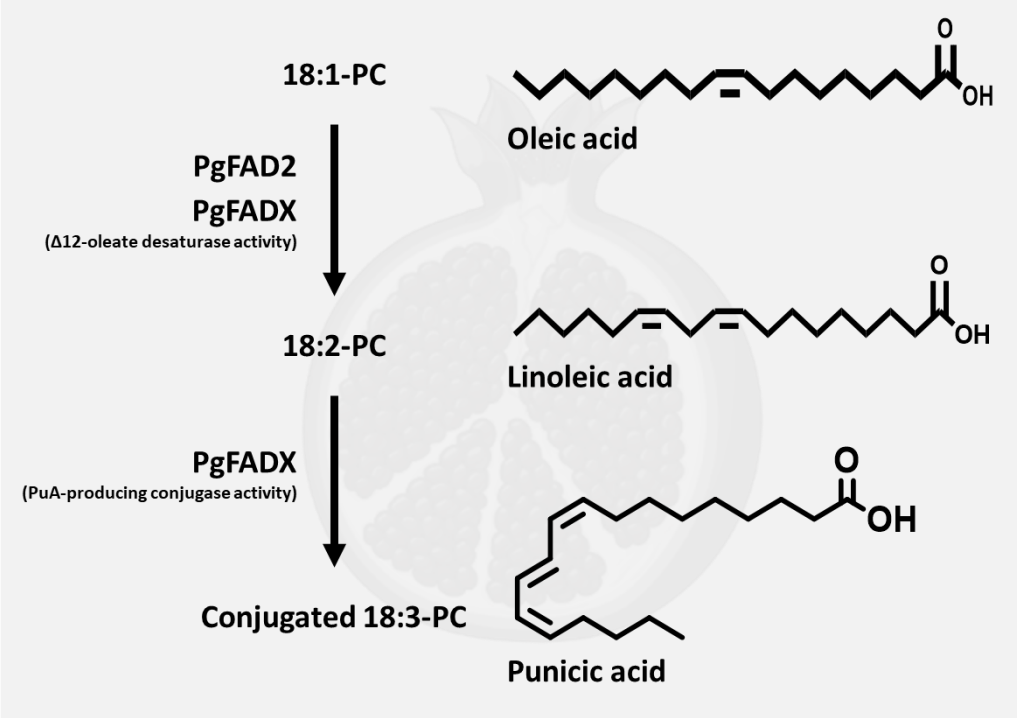

Figure 1. Illustration depicting the pomegranate PuA biosynthetic pathway. Abbreviations: PgFAD2, Δ12 fatty acid desaturase; PgFADX, fatty acid conjugase; PC, phosphatidylcholine.

Therefore, the overall objective of this study is to develop genetically engineered microbial platforms for cost-effective PuA production and to study the metabolic network involved in PuA biosynthesis in microbial hosts. The following specific objectives were targeted: Reconstitution of efficient PuA biosynthesis in the model yeast *Saccharomyces cerevisiae*; development of a metabolic engineering strategy for PuA production optimization and identify a working combination of candidate genes in favor of yeast PuA accumulation; and transformation of non-conventional oleaginous yeast into a PuA-producing platform using traditional substrate or agricultural waste as the feedstock. The current research was based on the following hypotheses:

1. Given that *S. cerevisiae* BY4741 has a functional fatty acid and TAG synthesizing pathway, this model yeast strain can be modified to synthesize PuA by transforming pomegranate *PgFADX*-containing plasmids.
2. Since linoleic acid (LA) is the direct precursor of PuA, improving the availability of this fatty acid precursor will increase the accumulation of PuA in heterologous hosts. This can be achieved by selecting a delta-12 fatty acid desaturase (FAD2) with higher catalytic performance from various sources. Since *S. cerevisiae* can readily assimilate exogenous free fatty acid, direct feeding of LA to the culture medium will also lead to a more efficient precursor supply for PuA production in yeast cells.
3. Since PuA production is subject to the control of yeast native lipid metabolism, the metabolic engineering of lipid metabolism-associated master regulators or lipid degradation pathways can direct carbon flux to PuA synthesis while protecting the PuA product from degradation, thus increasing PuA production in yeast cells.
4. The lack of specialized enzymes limits product channeling from phosphatidylcholine (PC) to TAG in PuA-producing *S. cerevisiae*. Incorporating pomegranate enzymes into yeast cells can improve PuA flux to TAG, and thereby increase PuA production.
5. The pathways involved in PuA biosynthesis and accumulation are interconnected and the conventional plasmid-based gene-stacking approach is inefficient and insufficient for creating a strain with increased PuA production. Shuffling pomegranate-derived genes and precursor-providing genes directly on the yeast genome, together with high-throughput analysis, will accelerate development and produce a yeast strain with higher PuA levels.
6. Due to the natural shift in fatty acid profile and potential post-translational regulation of heterologous desaturase-like enzymes in yeast cells, changing the growth temperature will

affect PuA production. Using the response surface methodology to optimize culture parameters in yeast fermentation processes will substantially increase PuA production.

7. By leveraging the natural ability of oleaginous yeast *R. toruloides* to accumulate high levels of lipids under nitrogen-limited conditions, coupled with the introduction of pomegranate genes, PuA production in this non-conventional yeast could be significantly enhanced.
8. Since *R. toruloides* can utilize a wide array of substrates, including pre-treated agricultural and forestry wood waste, engineered *R. toruloides* could convert such substrates to PuA, resulting in a more cost-effective and sustainable production process.

Accordingly, this thesis started from a literature review concerning the recent progress in producing UFAs in transgenic plants and microorganisms, with conjugated and hydroxy fatty acids as representatives (Chapter 2). The initial engineering of the model yeast *S. cerevisiae* using a plasmid-based expression of genes encoding PgFADX and PgFAD2 resulted in the accumulation of 0.3% of total fatty acids as PuA. Through a "push and pull" metabolic engineering strategy, the PuA content was increased to 3.4% with LA feeding (Chapter 3). A novel high-throughput workflow was then developed, leading to a recombinant *S. cerevisiae* strain with substantially improved PuA-accumulating ability. Using the response surface methodology, subsequent culture condition optimization led to 26.7% of yeast's total fatty acids as PuA without requiring LA precursor feeding. In shake flask cultivation, the PuA titer reached 425 mg/L (Chapter 4). Additionally, the non-conventional yeast *R. toruloides* was engineered to produce PuA. The strain with *PgFADX* and *PgFAD2* coexpression accumulated 12% of its lipids as PuA from glucose, which translated into a PuA titer of 452 mg/L in shake flask cultivation due to the oleaginicity of the yeast. The strain could also grow well with wood hydrolysate and produce 310 mg/L of PuA in flask cultivation (Chapter 5). These advances not only demonstrate

the potential for enriching plant-derived UFAs in microbial hosts via fermentation but also provide knowledge and valuable insights into the production of other high-value fatty acids.

Chapter 2 – Literature Review

2.1. Introduction

UFAs are a special class of lipid molecules with significantly different chemical structures than common fatty acids. Generally speaking, unlike the five common fatty acids in vegetable oils (palmitic acid, stearic acid, oleic acid, linoleic acid, and α-linolenic acid) (Li-Beisson et al., 2013), UFAs consist of several medium-chain fatty acids (e.g. C10:0, capric acid; C12:0, lauric acid), long chain fatty acids (e.g. C22:6, docosahexaenoic acid; C24:1, nervonic acid), or fatty acids with unique carbon chains structures such as double bond positions and orientations, acetylenic or triple bonds, modifications to carbon side-chains (such as conjugation, hydroxylation, epoxidation and cyclopropanation), or a combination of these structural characteristics (Cahoon and Li-Beisson, 2020). Among the hundreds of plant fatty acids (Cahoon and Li-Beisson, 2020; Ohlrogge et al., 2018), a number of UFAs, such as hydroxy fatty acids (HFAs), conjugated fatty acids (CFAs) and omega-3 polyunsaturated fatty acid (omega-3 PUFAs), have distinct physiochemical characteristics, and therefore, high value and important applications in nutraceutical, pharmaceutical, food, feed and oleochemical industries (Aruna et al., 2015; Holic et al., 2018).

CFAs are fatty acids that have two or more conjugated double bonds. One of the most well-studied CFAs is conjugated linoleic acid (CLA), which has two conjugated double bonds and is typically produced by animal commensal bacteria in the form of c9, t11-CLA, and t10, c12-CLA (Coakley et al., 2003; Verhulst et al., 1987). The metabolisms of CLA isomers have been well studied due to their significant health implications in humans (Basak and Duttaroy, 2020; den Hartigh, 2019), in which c9, t11-CLA is often studied for its alleviation in cardiovascular disease and cancer, while t10, c12-CLA has been primarily considered for its role

in body weight control or adiposity loss (Basak and Duttaroy, 2020; den Hartigh, 2019). While only a trace amount of CLA is found in the plant oil product (Carpenter and Slover, 1973), many plant seed oils naturally contain a wide array of CFAs with a higher degree of unsaturation (Cahoon et al., 1999; Dib et al., 2023; Hennessy et al., 2016; Kaufman and Wiesman, 2007; Zhan et al., 2016). For example, tung oil, extracted from the seeds of the tung tree (*Vernicia fordii*) has a high content of eleostearic acid (C18:3 c9, t11, t13, EsA) with quick-drying properties, and is therefore an ideal choice for wood finishes and varnishes, offering a durable and waterproof coating (Shockey et al., 2016b). Punicic acid (C18:3 c9, t11, c13, PuA) is the major fatty acid in pomegranate (*Punica granatum*) seeds and occupies 60%-80% of seed fatty acid composition (Kaufman and Wiesman, 2007; Khoddami et al., 2014; Paul and Radhakrishnan, 2020; Takagi and Itabashi, 1981). Pomegranate seed oil is well-recognized for its health benefits and could be used as a functional ingredient in food and nutraceuticals (Holic et al., 2018; Paul and Radhakrishnan, 2020). For instance, a previous study found that administering PuA reduced intestinal inflammation via the activation of PPARγ and δ, which control the metabolic network involved in lipid metabolism and inflammation (Bassaganya-Riera et al., 2011). When mice were fed a high-fat diet for 12 weeks, 1% of the pomegranate seed oil supplement ameliorated the diet-induced obesity and insulin resistance and lowered weight gain (Vroegrijk et al., 2011).

HFA, another class of well-studied UFA, contains one or more hydroxyl groups attached to its carbon chain. Based on the number and position of the hydroxyl groups, HFA could be categorized into mono-HFAs, di-HFAs, and poly-HFAs (Cao and Zhang, 2013). The most abundant and widely used mono-HFA in the oleochemical industry is from plant sources, such as ricinoleic acid (RA) and lesquerolic acid, which are naturally present in castor beans (*Ricinus*

communis) and Lesquerella (*Physaria fendleri*), respectively. Castor oil contains up to 90% of the total lipid as RA (da Silva Ramos et al., 1984; Román-Figueroa et al., 2020; McKeon et al., 2016), and lesquerolic acid levels in Lesquerella seed oil exceed 60% (Hayes and Kleiman, 1996; Isbell et al., 2008; McKeon et al., 2016). As the major natural source of HFA, castor oil is widely used in the chemical industry, food industry, and pharmaceutical industry, including the making of paints, coatings, plastics, cosmetics, and lubricants (Caupin, 1997; Metzger and Bornscheuer, 2006). Nevertheless, the corresponding supply of castor oil is limited due to the toxin ricin and allergenic 2S albumins in castor seeds, undesirable agronomic features, and difficulties in mechanical harvesting and castor oil refining (Lee et al., 2015; McKeon et al., 2016). The efforts of developing ricin-detoxified castor elite cultivars via conventional and molecular breeding approaches have so far achieved limited success (De Sousa et al., 2022; McKeon et al., 2016).

Beyond CFA and HFA, the spectrum of UFA includes a wide range of other structurally unique fatty acids with important biological and industrial relevance. For example, owing to the shorter carbon chain lengths, medium-chain fatty acids have unique physicochemical characteristics that make them useful for the production of biofuel (Chen et al., 2012; Kannengiesser et al., 2016). Cyclic fatty acids, characterized by their intramolecular carbocyclic ring configurations, are naturally found in certain bacteria (Brian and Gardner, 1968), and plant species such as *Sterculia foetida*, which contains up to 78% of sterculic acid (C19:1 cyclic fatty acid) in its seed oil (Badami and Patil, 1980; Herrera-Meza et al., 2014; Pasha and Ahmad, 1992). Hydrogenation of cyclic fatty acids leads to the branched-chain fatty acids through ring opening (Bianchini et al., 1983), which could be useful in the oleochemical industry. Acetylenic fatty acids, featured by their triple bonds, are the major seed fatty acid species of specific plants,

such as *Crepis alpina* (about 70% of the seed oil) (Lee et al., 1998; Samuelsson and Johansson, 2001). Epoxy fatty acids, produced through the epoxidation reaction that introduces an epoxide ring into the fatty acid chain (Singh et al., 2001), have various biological effects (Spector and Kim, 2015), and industrial applications such as plasticizers production (Greenspan and Gall, 1956). Nervonic acid, a vital long-chain monounsaturated fatty acid, is crucial for the development and maintenance of nerve cell membranes and brain health (Li et al., 2019). Likewise, many long-chain polyunsaturated fatty acids, including stearidonic acid (C18:4, SDA), eicosapentaenoic acid (C20:5, EPA), and docosahexaenoic acid (C22:6, DHA), are also important lipid nutrients in health management (Guil-Guerrero, 2007; Russell and Bürgin-Maunder, 2012; Siriwardhana et al., 2012). Various nutrition products rich in these fatty acids have already been developed and are available on the market (Kleiner et al., 2015; Xie et al., 2015). In addition, the characterization of UFAs with complex structures, such as long-chain di-HFAs nebraskanic acid (C24:1 di-HFA) and wuhanic acid (C24:2 di-HFA) in the seed oil of *Orychophragmus violaceus*, further underscore the potential of UFA's industrial application given that these long-chain di-HFAs provide superior lubrication properties at high temperatures (X. Li et al., 2018).

Collectively, UFAs found in plants and microorganisms are of significant biological and industrial importance due to their unique structures and potential applications. Since many of the original sources of UFAs are not ideal for large-scale production, it is attractive to produce them in crops and industrial microorganisms via synthetic biology. Transgenic oilseed crops are commonly regarded as excellent for large-scale UFA production in agriculture, and engineered industrial microorganisms present an attractive alternative as they can produce UFAs in a controlled bioreactor in short production cycles with greatly reduced arable land requirements.

In this review, we explore recent biotechnological breakthroughs in understanding the biosynthesis routes of UFAs, using CFA and HFA as examples but also including additional UFAs. The review begins with a discussion of UFA biosynthesis and transgenic production in plants, as well as the characterization of the important enzymes involved. Next, advances in microbial production of UFA are introduced, including the use of natural producers and engineered microorganisms for UFA production via bioconversion and neosynthesis. We then review advances in integrating plant and microbial biotechnology for UFA production, followed by an extensive discussion concerning the challenges and associated possible solutions in the neosynthesis of UFA in heterologous hosts, with the aim of facilitating the development of advanced biotechnology for increasing the heterologous production of UFAs.

2.2. Unusual fatty acid biosynthesis in plants

2.2.1. *de novo* fatty acid biosynthesis in plants and engineering of associated enzymes for improving UFA production

Storage lipid production in plants begins with *de novo* fatty acid biosynthesis in plastids (Figure 2.1A), where in the first step acetyl-CoA carboxylase (ACCase) converts acetyl-CoA into malonyl-CoA. Plastid ACCase is a complex of four discrete enzymatic proteins: biotin carboxyl carrier protein (BCCP), biotin carboxylase (BC), α-carboxyltransferase (α-CT), and β-carboxyltransferase (β-CT), and its activity is regulated through various biochemical mechanisms (Salie and Thelen, 2016). For example, a recent study revealed that plant ACCase undergoes light-dependent activation in response to changing physiological conditions in plastids and attenuation by the envelope docking owing to interactions between carboxyltransferase interactors and the α-carboxyltransferase subunit of ACCase (Ye et al., 2020). Constitutive expression of ACCase in oleaginous algae *Phaeodactylum tricornutum* in the chloroplast

increased oil body formation and the relative neutral lipid content by 1.77-fold (D.-W. Li et al., 2018).

Malonyl-CoA: acyl carrier protein malonyltransferase converts malonyl-CoA to malonyl-ACP, which serves as the basic building block for further fatty acid synthesis catalyzed by type II fatty acid synthase in a pseudo-cyclic system (Li-Beisson et al., 2013). In the first condensation reaction, Ketoacyl-ACP synthases III (KAS III) uses acetyl-CoA with malonyl-ACP to form a C4 acyl chain. A previous study showed KAS III from *Cuphea wrightii* is inhibited by medium-chain end products of native fatty acid biosynthesis, and the KAS III mutant that was freed from this inhibition in *in vitro* experiments led to an increase in short to medium-chain acyl-ACPs (Abbadi et al., 2000). Subsequently, KAS I catalyzes the elongation of acyl-ACPs from C4 to C16, whereas KAS II specifically targets the elongation of C16 acyl-ACPs to C18. As a result, KAS activity offers a potential control point for regulating the ratio of shorter/longer chain fatty acids to fit the precursor requirement of different UFAs. For instance, the overexpression of *Jatropha curcas KAS II* in *Arabidopsis thaliana* led to an increase in C18 fatty acids at the expense of C16 fatty acids (Wei et al., 2012). Combined with other modifications, this may contribute to the synthesis of UFAs using C18 fatty acid as the precursor. On the other hand, the KAS from *Cuphea* species, which naturally accumulates over 90% of C10 and C12 fatty acids in its seed oil (Phippen et al., 2006), is strongly correlated with the synthesis of medium-chain fatty acids (Slabaugh et al., 1998). The introduction of CwKAS A1 further shifted fatty acid synthesis toward shorter chains in *Arabidopsis* seeds expressing *Cuphea* FatB thioesterases (Leonard et al., 1998), which demonstrated potential for medium-chain fatty acid production.

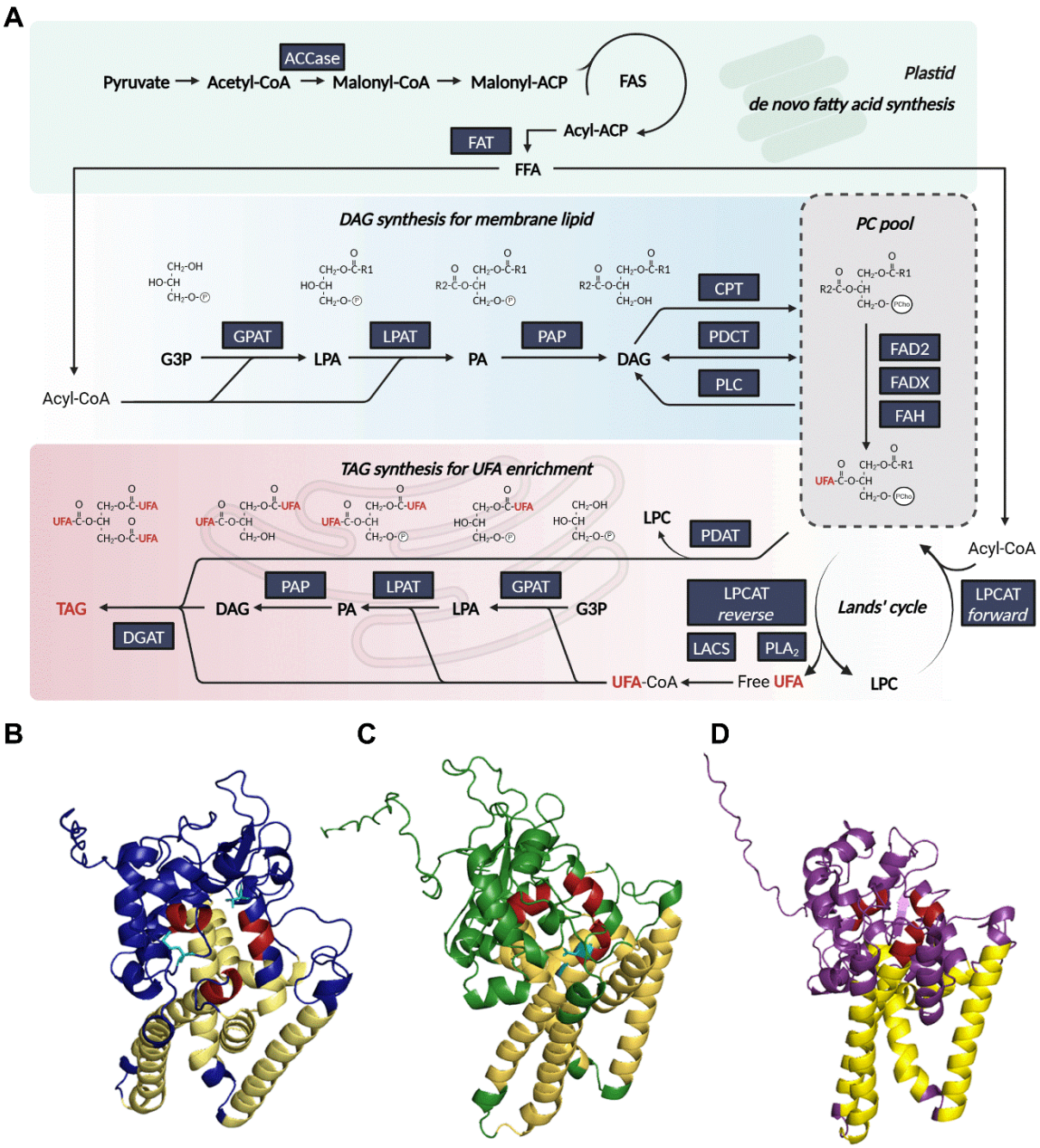

Figure 2.1. Plant unusual fatty acid biosynthetic pathway.

(A) Illustration of the metabolic pathways involved in the synthesis of UFA-enriched TAG. Abbreviations: DAG, diacylglycerol; DGAT, acyl-CoA: diacylglycerol acyltransferase; G3P, glycerol-3-phosphate; GPAT, glycerol-3-phosphate acyltransferase; LACS, long-chain acyl-CoA

synthetase; LPA, lysophosphatidic acid; LPAT, lysophosphatidic acid acyltransferase; LPC, lysophosphatidylcholine; LPCAT, lysophosphatidylcholine acyltransferase; PA, phosphatidic acid; PAP, phosphatidate phosphatase; PC, phosphatidylcholine; PDAT, phospholipid: diacylglycerol acyltransferase; PDCT, phosphatidylcholine: diacylglycerol cholinephosphotransferase; PLA2, phospholipase A2; ACCase, acetyl-CoA carboxylase; FAS, fatty acid synthase; FAT, fatty acid thioesterase; CPT, cholinephosphotransferase; TAG, triacylglycerol; PLC, phospholipase C; FADX, bifunctional fatty acid conjugase/desaturase; FAD2, Δ12 fatty acid desaturase; FAH, fatty acid hydroxylase. Made with biorender.com. (B-D) Predicted 3D structures of *Arabidopsis* monofunctional Δ12 fatty acid desaturase (AtFAD2), *M. charantia* conjugase (McFADX), and *R. communis* hydroxylase (RcFAH), respectively. The 3D models were predicted by the AlphaFold Protein Structure Database (Jumper et al., 2021; Varadi et al., 2022). The membrane-spanning and transmembrane domains were analyzed using the TMHMM server (CBS; Denmark) and labeled in yellow. The conserved metal-binding histidine motifs were labeled in red. The M324 and T148 in AtFAD2 and the G111 and D115 in McFADX were marked in cyan, which are important amino acid sites determining the fatty acid product ratio.

The biosynthesis of monounsaturated fatty acids also occurs in plastids, where Δ9 stearoyl-ACP desaturase introduces a double bond into 18:0-ACP to form 18:1-ACP. Plants may have partially redundant Δ9 stearoyl-ACP desaturases, and they have important functions in seed development and storage lipid production during the maturation phase (Kazaz et al., 2020). In addition, SAD may also play a critical role in UFA production. For instance, a recent study showed that the mRNA levels of tung tree *VfSAD1* and *VfSAD2* were largely upregulated in the seed during the oil accumulation period (Chen et al., 2023), which presumably contributed to the supply of C18:1 as the precursor for EsA synthesis. Subsequently, fatty acyl-ACP thioesterase (FAT) releases the fatty acid moiety from acyl-ACP, thereby terminating fatty acid production. In many plant species, FATs are selective for fatty acid chain length and saturation degree, which has a significant impact on the fatty acid composition of storage lipids in plants. In general, FAT can be classified into FATA and FATB subfamilies, which exhibit distinct substrate preferences. FATA specifically targets monounsaturated (oleoyl) acyl-ACP (Aznar-Moreno et al., 2016), whereas FATB family proteins have specificity for saturated, short or medium-chain fatty acids (Salas and Ohlrogge, 2002). FATs from the natural producers of UFAs may have substrate specificity to the UFA-containing acyl-ACP and thus have high biotechnological value. For instance, the expression of FAT from medium-chain fatty acid-producing *Umbellularia californica* (UcFatB1) in *A. thaliana* and *Brassica napus* led to the accumulation of high levels of lauric acid (Yuan et al., 1995).

Moreover, the substrate specificity of FATs can be modified by engineering the catalytic domain, enabling it to selectively target acyl chains ranging from 6 to 14 carbons (Kalinger and Rowland, 2023). Interestingly, a recent study has shown that FATs may be selective for their ACP partners (Beld et al., 2014). Therefore, the introduction of FAT for metabolic engineering

purposes may work better with the coexpression of ACP from the same species. Since the combined function of KAS and FAT enzymes plays a critical role in determining the chain lengths and initial saturation levels of fatty acids produced in plastids, they are often targeted in studies aimed at modifying plant lipid profiles. Taken together, *de novo* fatty acid biosynthesis supplies the essential fatty acid precursors for UFA production and produces certain UFAs such as medium-chain fatty acids. Therefore, investigating the function, regulation, and protein-protein interaction of the key plastidial enzymes, such as ACCase, FASII, and FAT, would be highly valuable for UFA production in plant lipid biotechnology.

2.2.2. Characterization and structure analysis of fatty acid desaturase 2-like enzymes

Acyl-editing on phosphatidylcholine (PC) plays an important role in the production of certain UFA species with special double bonds or carbon side-chain modifications in plants. Following the *de novo* synthesis within the plastid, fatty acids are moved to the endoplasmic reticulum (ER) and converted to these UFAs on PC (Chapman and Ohlrogge, 2012; Chen et al., 2015; Harwood et al., 2017). A variety of enzymes contribute to UFA production on PC, with fatty acid desaturase 2 (FAD2)-like proteins playing an essential role. FAD2 is responsible for the introduction of a second double bond at the Δ12 position of oleic acid, converting it into linoleic acid (LA), which, together with oleic acid, are the key fatty acid precursors for the synthesis of many UFAs (Chapman and Ohlrogge, 2012; Dyer et al., 2002). In pomegranate, further desaturation and conjugation of LA lead to PuA, which is catalyzed by *P. granatum* bifunctional fatty acid desaturase and conjugase PgFADX, a FAD2-family enzyme, on the *sn-2* position of PC (Hornung et al., 2002; Iwabuchi et al., 2003). In castor, the oleoyl chain on the *sn-2* position of PC is hydroxylated by *R. communis* oleate hydroxylase (RcFAH), another FAD2-like enzyme, to generate RA (Broun and Somerville, 1997; van de Loo et al., 1995). Similarly,

the biosynthesis of some plant epoxy fatty acids, acetylenic fatty acids, as well as some other CFAs and HFAs are also catalyzed by FAD2-like enzymes (Lee et al., 1998; Carlsson et al., 2004; Broun et al., 1998a; Qiu et al., 2001; Dyer et al., 2002). Since these enzymes belong to a structurally similar protein family (Broun et al., 1998b), the characterization and structural analysis of FAD2 and FAD2-like enzymes can provide a good reference for understanding the basis of PC-derived UFA formation.

In general, FAD2-like enzymes are ER-localized proteins with multiple transmembrane domains (Figure 2.1B). An aromatic amino acid-containing sequence that acts as an ER retrieval motif was found in the C-terminus of *Arabidopsis* FAD2 (McCartney et al., 2004). FAD2 contains three conserved histidine-rich motifs, which coordinate the di-iron center to catalyze the acyl-editing on PC (Figure 2.1B). The same structure configuration can also be found in FADX (Figure 2.1C) or FAH (Figure 2.1D). As a result, the desaturase, conjugase, or hydroxylase activities of FAD2, FADX, or FAH are not strictly separated, and altering the amino acids sites around the histidine motifs could lead to changes in product profile (Broun et al., 1998a; Iwabuchi et al., 2003). For instance, PuA-producing pomegranate PgFADX is a bifunctional enzyme catalyzing both desaturation and conjugation reactions (Garaiova et al., 2017; Iwabuchi et al., 2003). Moreover, the alteration of a few amino acids in the monofunctional desaturase *Arabidopsis* FAD2 sequence can effectively convert it into a mutant enzyme with hydroxylase activity (Broun et al., 1998b). By comparing the amino acid sequences of plant oleate desaturases with the hydroxylases from *Lesquerella fendleri* and *R. communis*, seven residues were found to be strictly conserved. By replacing these seven residues in *Arabidopsis* FAD2 with their counterparts in the hydroxylase from *Lesquerella fendleri* (also known as *Physaria fendleri*) (A63V, A104G, T148N, Y217F, A295V, S322A, and M324I), *Arabidopsis* FAD2 was

transformed into a bifunctional desaturase/hydroxylase which is capable of producing LA and low amount of RA (0.5%) when being expressed in yeast (Broun et al., 1998b). By replacing four of these sites with counterparts from RcFAH (A104G, T148I, S322A, and M324V), the resulting AtFAD2 mutant exhibited a high hydroxylation/desaturation product ratio when being expressed in *Saccharomyces cerevisiae*, where T148 and M324 likely had major roles in determining the product ratio (Broadwater et al., 2002).

In the study of *Momordica charantia* conjugase (McFADX), the second transmembrane helix and the first histidine box were determined as important regions affecting conjugase product partitioning. While the wild-type McFADX mainly produces EsA, by domain swapping of these regions with the counterparts from *Arabidopsis* FAD2, the chimera enzyme (Chimera 7, AtFAD2 aa 1–116; McFADX aa 126 –399) could produce similar levels of PuA and EsA simultaneously when expressed in transgenic *Arabidopsis* seeds (Rawat et al., 2012). Additionally, residues 111 and 115 in McFADX were identified as important sites for imparting PuA-producing conjugase activity, and the substitution of the two amino acids (G111V/D115E) could substantially increase the PuA accumulation compared to the wild-type enzyme.

It appears that many plant enzymes for the synthesis of PC-derived UFAs have varied progress along their respective evolutionary path. For example, LfFAH retained both hydroxylase and desaturase activities in contrast to the hydroxylase activity only of RcFAH (Broun et al., 1998a), while FADXs from pomegranate and tung tree seems to be a relatively newly evolved conjugase retaining a considerable amount of fatty acid desaturase activity (Dyer et al., 2002; Iwabuchi et al., 2003). The significant change in product partitioning caused by the relatively small change in protein structure makes these enzymes excellent candidates for

studying the mechanism of UFA synthesis, as well as for the potential rational design of enzymes with better catalytic ability.

2.2.3. Glycerophospholipid remodeling for heterologous production of UFAs in plants

The Lands' cycle is an important metabolic route for modifying phospholipid acyl chains in plant lipid metabolism, which involves the deacylation of fatty acid chains from PC by phospholipase A_2 (PLA_2) and reacylation of the resulting lysophosphatidylcholine (LPC) with acyl-CoAs by lysophosphatidylcholine acyltransferase (LPCAT) (Chen et al., 2015). In this process, the lipid composition of the cellular membrane is adjusted, and UFA can be released from PC for further enrichment in neutral lipids (Wang et al., 2012). Plant PLA_2s are small proteins that carry out calcium-dependent hydrolysis, specifically targeting the *sn*-2 position of phospholipids (Ryu et al., 2005). They participate in metabolic pathways related to plant development and responses to environmental stress (Gupta and Dash, 2017). Previous studies have shown that *Arabidopsis* $PLA_2\alpha$ exhibited substrate selectivity on both acyl-chain species and phospholipid headgroup (Ryu et al., 2005). In terms of UFA synthesis, castor *RcPLA₂α* has high expression in endosperm and the recombinant protein prefers ricinoleic-PC over regular PC as the substrate *in vitro* (Bayon et al., 2015), suggesting its potential role in modifying seed lipid compositions for improved HFA production. However, the coexpression of $RcPLA_2\alpha$ with RcFAH in transgenic *Arabidopsis* did not improve, but greatly reduced the seed HFA content in both PC and the neutral lipids (Bayon et al., 2015).

In addition to PLA_2, the PLA family also includes other complex groups of enzymes with unique structures, catalytic preferences, and physiological functions, such as PLA_1 and the patatin-like PLA (Ali et al., 2022; Chen et al., 2011). In contrast to small PLA_2s, which target the *sn*-2 position, PLA_1 enzymes hydrolyze phospholipids at the *sn*-1 position (Noiriel et al., 2004).

While lecithin: cholesterol acyltransferase like PLA_1 (LCAT-PLA_1) belongs to the PLA_1 group (Chen et al., 2011), a recent study demonstrated that the LCAT-PLA from *Physaria* or *R. communis* could cleave acyl chains at both the *sn*-1 and *sn*-2 positions of PC and display substrate selectivity towards *sn*-2-ricinoleoyl-PC over *sn*-2-oleoyl-PC (Xu et al., 2021). Although overexpressing the coding regions of these LCAT-PLAs in the *Arabidopsis RcFAH12/fae1Δ* line did not lead to significant alterations in HFA levels, the distribution of HFAs at the *sn*-1/3 positions of TAG was enhanced (Xu et al., 2021). Plant patatin-like PLAs (pPLAI, pPLAIIs, and pPLAIIIs) are structurally related to patatins, the major storage proteins in potato tubers, and demonstrate combined activity on both *sn*-1 and *sn*-2 positions (Chen et al., 2011; Scherer et al., 2010). Similar to castor small $PLA_2\alpha$ (Bayon et al., 2015), a previous study found that the overexpression of castor pPLAIIIβ in *Arabidopsis* also led to a significant reduction in seed HFA content, suggesting castor pPLAIIIβ may catalyze the removal of HFAs from PC in developing seeds (Lin et al., 2019).

Following the activity of phospholipase, long-chain acyl-CoA synthetase (LACS) activates free fatty acids to acyl-CoAs, which not only contributes to the fundamental processes of lipid metabolism but also plays an important role in the plant's biotic and abiotic stress tolerance conferred by lipid modifications (Li et al., 2022; Wei et al., 2022; Zhao et al., 2021). Many oilseed plants contain multiple LACS homologs with different expression patterns. For example, *Arabidopsis* LACS8 is predominantly expressed in seeds, whereas LACS1, LACS4, and LACS9 are predominantly transcribed in stem, leaf, and floral tissues, respectively (Zhao et al., 2010), highlighting their pivotal functions in regulating plant growth. Plant LACS enzymes also exhibit varying substrate specificity. LuLACS8A from flax (*Linum usitatissimum*) showed significantly higher specificity for α-linolenic acid (C18:3 c9, c12,c15), the major fatty acid in

flax seed lipid (Xu et al., 2018b), whereas castor RcLACS2 prefers to activate ricinoleate (He et al., 2007). Since RcLACS2 has much higher expression in germinating seeds rather than developing seeds, it may play a more substantial role in activating ricinoleate for lipid degradation to provide the seedling with energy (He et al., 2007). Nevertheless, the additional expression of castor *RcLACS1*, *RcLACS4*, or *RcLACS8* in *Arabidopsis* transformed with $RcPLA_2\alpha$ and RcFAH did not further improve RA accumulation (Bayon et al., 2015), suggesting the exact role of LACS in UFA enrichment still needs further investigation.

LPCAT is another key enzyme that is important for glycerophospholipid remodeling, where it catalyzes both forward and reverse reactions with different specificities (Lager et al., 2013). The influence of LPCAT activity on the UFA biosynthetic pathway was studied in both *in vitro* and *in vivo* assays (Lager et al., 2013; Lunn et al., 2020). The forward reaction of LPCAT involves the acylation of LPC with newly synthesized acyl-CoA to produce PC. The *in vitro* assay revealed that in the forward reaction, RcLPCAT prefers LPC over lysophosphatidylethanolamine and lysophosphatidic acid as the acyl receptor and acylates C16:0-LPC, C18:0-LPC and C18:1-LPC at similar rates. In terms of the acyl donor, RcLPCAT exhibits a preference for using monounsaturated fatty acyl-CoA over saturated and ricinoleoyl-CoA as the acyl donor (Arroyo-Caro et al., 2013a; Lager et al., 2013), which implies the potential role of RcLPCAT in recruiting specific acyl-CoA (e.g. 18:1-CoA) into PC for UFA synthesis. In contrast, sunflower (*Helianthus annuus*) LPCATs have a preference for acyl-CoAs with a higher degree of unsaturation (18:3>18:2>18:1) in the forward reaction (Mapelli-Brahm et al., 2020).

The reverse reaction of LPCAT involves the direct release of acyl groups from PC into the acyl-CoA pool. In *Camelina sativa*, the calculated potential transfer of fatty acids from PC to

the acyl-CoA pool via the reverse reactions of CsLPCATs varied from approximately 100% to around half of the total fatty acids incorporated into TAG at various stages of seed development (Klińska et al., 2019). In the reverse reaction, *Arabidopsis* LPCAT2 was able to catalyze the rapid release of the ricinoleoyl groups 6-fold faster than C18:1 groups esterified to the *sn*-2 position of PC. However, in the forward reaction, AtLPCAT2 has limited utilization of the ricinoleoyl substrate (Lager et al., 2013), thus suggesting its potential role in regulating the acyl-CoA composition in plant hosts with HFA biosynthesis. It is possible that the reverse reaction of LPCAT might require the function of other enzymes to efficiently channel the released ricinoleic-CoA to storage lipids. For example, yeast assays revealed the biochemical coupling of the flax LPCAT1-catalyzed reverse reaction with the DGAT1-catalyzed reaction for incorporating PUFAs into TAG (Pan et al., 2015). Moreover, the additional expression of castor *RcLPCAT* in an HFA-producing *Arabidopsis* line reduced HFA and total seed oil yield, whereas the gene stacking of *RcLPCAT* on top of castor phospholipid: diacylglycerol acyltransferase (*RcPDAT*) expression increased HFA and oil content (Lunn et al., 2020).

Several other enzymes also participate in acyl-editing on glycerophospholipids. For instance, phospholipase C (PLC) hydrolyzes phospholipids into diacylglycerol (DAG), which can act as a lipid messenger involved in various membrane remodeling, stress response, and developmental processes in plants (Ali et al., 2022; Fan et al., 2023). In addition to important cellular and physiological functions, the DAG produced by PLC can also potentially serve as a precursor for TAG biosynthesis. Consistently, the overexpression of nonspecific PLC (NPC6) in both *Arabidopsis* and *Camelina* led to an increase in seed oil content and seed weight, and the knockout of NPC6 resulted in a notable reduction in seed oil content and seed size (Cai et al., 2020). Apart from the accumulation of TAG, evidence also indicated the possible involvement of

PLC in the synthesis of UFAs. The expression of a PLC-like protein from castor bean (RcPLCL1) in an HFA-producing *Camelina* line heterologously expressing *RcFAH12* further increased HFA accumulation (C18:1-OH and C18:2-OH) in seeds, at the expense of common C18:2 and C18:3 fatty acids (Aryal and Lu, 2018). Additionally, RcPLCL1 expression resulted in reduced HFA accumulation in the PC fraction of the mature seed, indicating that RcPLCL1 enhanced the channeling of HFAs from PC to TAG (Aryal and Lu, 2018).

Phosphatidylcholine: diacylglycerol choline phosphotransferase (PDCT) is responsible for the interconversion between PC and DAG by catalyzing the transfer of the phosphocholine headgroup (Figure 2.1A) and plays an important role in glycerophospholipid remodeling. The *Arabidopsis pdct* mutant significantly reduced PUFA accumulation in seed TAG by 40%, while its PC retained higher PUFA levels (Lu et al., 2009). Furthermore, the heterologous expression of flax *LuPDCT1* and *LuPDCT2* in *Arabidopsis* increased PUFA by 16.4%-19.7% at the expense of oleic acid in seeds (Wickramarathna et al., 2015), and the seed-specific overexpression of native *CsPDCT* in *Camelina* led to increased seed yield, seed oil content, and oil yields per plant with altered PUFA content (Abdullah et al., 2024). These results suggest that PDCT may be involved in both the reverse transfer of PUFA product into the DAG pool for TAG biosynthesis and the transfer of fatty acid precursor into PC for further editing. Moreover, PDCT also contributes to the accumulation of UFAs. For example, the coexpression of *Escherichia coli cyclopropane synthase* (*EcCPS*) with lychee (*Litchi chinensis*) *PDCT* (*LcPDCT*) in *Camelina* increased the content of cyclopropane fatty acid (CPA) in seed oil by more than 50% and doubled the conversion of CPA-PC to CPA-DAG (Yu et al., 2019). Similarly, it was shown that PDCT efficiently promoted the mobilization of HFAs from PC into DAG and increased HFA levels in TAG of the HFA-producing transgenic *Arabidopsis* seeds (Hu et al., 2012).

With *RcFAH* expression, the *PDCT*-deficient *Arabidopsis* mutant accumulated only about half the amount of HFA compared with the wild-type *Arabidopsis* background, whereas the seed-specific coexpression of castor *RcPDCT* with *RcFAH* in *Arabidopsis* doubled HFA accumulation from 9.9% to 19.9% and partially restored the negative effect of *RcFAH* expression on seed oil content (Hu et al., 2012). Castor seed contains a high level of TAG with all three positions esterified to RA, but the microsome fraction of developing castor endosperm has a very low amount of ricinoleoyl groups (Bafor et al., 1991; Lin and Arcinas, 2007). A recent study revealed that castor PDCT is possibly one of the key enzymes responsible for this distribution pattern (Demski et al., 2022). The results showed RcPDCT could utilize DAGs with ricinoleoyl groups, as well as DAGs with common acyl groups, but has a 10-fold selectivity for DAG with a single ricinoleoyl group (1-OH-DAG) over DAG with two ricinoleoyl groups (2-OH-DAG). After converting to PC, the ricinoleoyl group from 1-OH-DAG could be recycled for the synthesis of TAG with a higher degree of HFAs, while the PC-derived nonricinoleate DAG is used as the substrate for synthesizing membrane lipids with common fatty acid composition (Figure 2.1A) (Demski et al., 2022).

2.2.4. Specialized TAG assembly for unusual fatty acid enrichment in plants

In oilseed crops, TAG serves as a primary form of carbon and energy storage, and it is often the final destination of UFA. The acyl-CoA-dependent TAG biosynthesis pathway, also known as the Kennedy pathway, is comprised of *sn*-glycerol-3-phosphate acyltransferase (GPAT), lysophosphatidic acid acyltransferase (LPAT or LPAAT), phosphatidic acid phosphatase (PAP), and diacylglycerol acyltransferase (DGAT), and is responsible for sequentially integrating fatty acyl-CoA into the *sn*-1, *sn*-2, and *sn*-3 positions of glycerol-3-phosphate (G3P) to form TAG (Figure 2.1A) (Kennedy, 1961; Chen et al., 2022). In plants,

many GPAT homologs exist, and GPAT9 is particularly interesting due to its specific ER localization and important function in TAG biosynthesis (Payá-Milans et al., 2016; Shockey et al., 2016a; Singer et al., 2016). Transgenic tobacco plants heterologously expressing *Perilla frutescens PfGPAT9* significantly increased total oil and unsaturation degree in both the seeds and leaves, and PfGPAT9 displayed a strong preference for 18:1 and 18:3 fatty acid substrates (Zhou et al., 2023). When *JcGPAT2* from *J. curcas* was overexpressed heterologously, transgenic *Arabidopsis* accumulated between 42 and 60% more oil (Misra et al., 2017). In contrast, the heterologous expression of *Arabidopsis GPAT9* in *B. naups* did not seem to have a role in increasing seed oil content (Liao et al., 2022).

Numerous studies have demonstrated that LPAT2 has important functions in TAG biosynthesis and UFA production in seeds. Analysis of transgenic *Lesquerella* seed TAG suggested that heterologously expressed *RcLPAT2* was able to increase the acylation of 18:1-OH to the *sn*-2 position of lysophosphatidate up to 17% and thus increase the level of tri-HFA-TAG species (Chen et al., 2016). When ricinoleoyl-lysophosphatidate was the acyl acceptor, RcLPAT2 preferred ricinoleoyl-CoA over other acyl donors (Arroyo-Caro et al., 2013b). In addition, LPAT2 has been shown to promote the heterologous synthesis of other UFAs, including conjugated PUFAs, very long-chain fatty acids (VLCFAs), and CPA (Shockey et al., 2019; Yin et al., 2022; Yu et al., 2018). In *Arabidopsis*, the expression of tung tree *VfLPAT2* on top of *VfFADX* and *VfDGAT2* increased EsA up to 13% (Shockey et al., 2019), and the overexpression of *Camelina CsLPAT2* led to 2.8 times higher VLCFA-containing phosphatidic acid and substantially higher VLCFA content in TAG (Yin et al., 2022). Regarding CPA synthesis, further expression of *Sterculia foetida SfLPAT* resulted in higher amounts of CPA in CPA-producing transgenic *Arabidopsis* seeds (Yu et al., 2014). Consistently, in CPA-producing

Camelina lines, coexpressing *SfLPAT* resulted in a 90% increase in CPA levels, and an increase in CPA in DAG and TAG from 14 to 26% and 6% to 12%, respectively (Yu et al., 2018). An altered spatial distribution of mono- and di-CPA-PC was also observed by mass spectrometry imaging of PC molecular species in seed sections (Yu et al., 2018).

Within the Kennedy pathway, DGAT is often considered a key enzyme responsible for the hyperaccumulation of UFAs since it catalyzes the final step in TAG biosynthesis (for a detailed review, see (Chen et al., 2022)). ER-bound DGAT1 and DGAT2 are the two most extensively studied types of DGAT enzymes and have been commonly investigated in the study of UFA production. DGAT1 belongs to the membrane-bound O-acyltransferase (MBOAT) family and has a larger protein size with more transmembrane domains, whereas DGAT2 belongs to a different family of acyltransferase and has a more compact structure with fewer transmembrane domains. DGAT1 is considered to be the major contributor to the bulk of TAG biosynthesis in common oil-producing plants and displays a relatively broad substrate specificity (Chhikara et al., 2018; Li et al., 2010b). Compared to DGAT1, some DGAT2s were shown to have a different substrate preference, utilize different substrate pools, and be strongly induced in developing seeds at the beginning of oil accumulation in UFA producers (Li et al., 2010a; Regmi et al., 2020; Shockey et al., 2006; Zhou et al., 2013). For instance, in contrast to *AtDGAT1*, *AtDGAT2* overexpression specifically led to an increase in the PUFA content of TAG (Zhou et al., 2013). Although RcDGAT1 displays higher activity towards diricinolein substrate than *Arabidopsis* AtDGAT1 (McKeon and He, 2015), it appears that RcDGAT2 plays a more prominent role in contributing to a high ratio of RA content in TAG (Kroon et al., 2006). Biochemical analyses demonstrated that when diricinolein was used as the acyl acceptor instead of diolein or dilinolein, RcDGAT2 produced nearly ten times more TAG, and the expression of

RcDGAT2 in HFA-producing *Arabidopsis* boosted HFAs from 17% to nearly 30% (Burgal et al., 2008). Furthermore, tung tree VfDGAT1 and VfDGAT2 were found to be differentially localized in the ER of transformed tobacco cells. The expression of VfDGAT2 in yeast cells in the presence of tung oil and a nonspecific lipase led to a significant increase in trieleostearin content, which is the major UFA in tung oil (Shockey et al., 2006). Similar findings have been reported regarding the accumulation of epoxy fatty acid (vernolic acid), with DGAT2 having a greater influence than DGAT1 (Li et al., 2010a).

In addition to DGAT, the UFA acyl-chain can also be transferred directly from the *sn*-2 position of PC to the *sn*-3 position of DAG, producing TAG and LPC, catalyzed by PDAT in acyl-CoA-independent TAG synthesis (Dahlqvist et al., 2000). It has been observed that various plant PDATs display different substrate preferences (Dahlqvist et al., 2000; Pan et al., 2013; Banaś et al., 2013; Ståhl et al., 2004). Expressing *RcPDAT1* in HFA-producing *Arabidopsis* significantly increased the accumulation of total HFA to over 25% in seed oil (Kim et al., 2011; van Erp et al., 2011). Further gene stacking of *RcPDAT1A* with *RcDGAT2* in HFA-producing *Arabidopsis* lowered the HFA levels in PC and recovered a substantial part of the reduction in seed oil, which was caused by *RcFAH* expression (van Erp et al., 2011). It is worth noting that a dependence between the actions of different TAG assembly enzymes was observed occasionally. The single expression of these enzymes might only lead to limited enhancement in the UFA level. For instance, the lone expression of either *RcGPAT9* or *RcLPAT2* did not lead to a dramatic improvement in HFA content in the T_2 bulk seed compared to the control (Kim et al., 2020; Lunn et al., 2019). In contrast, when three castor acyltransferases (RcGPAT9, RcLPAT2, and RcPDAT1A) were simultaneously introduced into HFA-producing *Arabidopsis*, HFA accumulation was greatly increased to 34% of the total seed oil, where 44% of the HFA was in

3-HFA-TAG (Lunn et al., 2019). Meanwhile, homozygous *RcGPAT9*, *RcLPAT2,* and *RcDGAT2* coexpression lines also achieved a total TAG HFA content of 37%, which is almost double the content observed in the CL37 background line (*fae1Δ* with *RcFAH12* overexpression) (Shockey et al., 2019). Similarly, in another study, the coexpression of *RcDGAT2*, *RcPDAT*, *RcPDCT*, and *RcLPCAT*, on top of *RcFAH* expression and *fae1Δ Arabidopsis*, led to over 31% of HFA product with significantly increased seed size, weight, and total oil per seed (Park et al., 2022).

2.3. Biosynthesis of unusual fatty acids in microorganisms

2.3.1. Oleaginous microbial platforms as an alternative approach for lipid production

Vegetable oils and microbial single-cell oils represent two distinct sources of lipids. Due to variables including feedstock availability, production technology, and environmental impact, each has particular benefits and challenges. For traditional oil extraction from oilseed crops, plants must be harvested, cleaned, shelled, and processed, which may be energy intensive. On the other hand, establishing a microbial fermentation facility may require a higher initial investment compared to traditional agricultural operations, however, lipid-rich microbial biomass may be treated more effectively thus lowering manufacturing costs. In terms of microorganisms, many oleaginous yeasts, molds, algae, and bacteria are capable of accumulating lipids to more than 20% of their biomass. For example, *Rhodococcus opacus* PD630 and *Rhodococcus jostii* RHA1 are bacterial strains that showed significant TAG synthesizing ability (Amara et al., 2016; Chatterjee et al., 2020; Hernández et al., 2008). Using simple carbon sources such as gluconate or benzoate, they can store over 50% of the cell dry weight as lipids under nutritionally limited conditions (Alvarez et al., 2021; Cappelletti et al., 2020; Kim et al., 2019). Compared to these oleaginous bacteria, yeasts have been more extensively studied for enhancing single-cell oil and plant-derived lipid production as they provide several advantages. The US

Food and Drug Administration (FDA) has declared no objection to certain yeast strains, such as genetically modified *S. cerevisiae* and *Yarrowia lipolytica*, to be "Generally Recognized as Safe" (GRAS) microorganisms for food and feed industries (United States Food and Drug Administration, 2021, 2015, 2011, 2005). Furthermore, since both yeasts and plants are eukaryotes, they have similar cellular structures with membrane-bound organelles (Farhi et al., 2011; Shi et al., 2021). These membrane structures may be important for the localization of plant-derived UFA-producing enzymes that have multiple transmembrane structures (Broadwater et al., 2002; Rawat et al., 2012). Conversely, bacteria are prokaryotic organisms without membrane-bound organelles, which may add extra challenges in producing plant-based UFAs via genetic engineering. In addition, oleaginous *Rhodococcus* strains have not yet been included in the GRAS list.

Many yeast species have superior capabilities in terms of accumulating high lipid contents (J. Wang et al., 2022). For instance, *Rhodosporidium toruloides* is a non-conventional yeast capable of the concomitant production of TAG and carotenoids. By adjusting the ratio of carbon to nitrogen in the growth medium, the production of lipids in wild-type *R. toruloides* can be significantly boosted to more than 72% of cell dry weight (González-García et al., 2017; Saini et al., 2021). Furthermore, *R. toruloides* is a promising choice for converting lignocellulosic biomass into valuable bioproducts for sustainable bioproduction processes because of its ability to use a wide range of substrates, including glucose and xylose (Adamczyk et al., 2023). This yeast species also showed robust growth in the presence of various inhibitors, which are typically found in pretreated agricultural wastes (Boviatsi et al., 2020; Fernandes et al., 2023; Jiao et al., 2021; Qi et al., 2020). Similarly, *Lipomyces starkeyi* and *Trichosporon fermentans* were able to accumulate 40% to 60% of single-cell oil, using not only lignocellulose-derived sugars but also

other waste materials as substrates (Huang et al., 2009; Liu et al., 2020; Zhu et al., 2008). *Y. lipolytica*, another well-characterized oleaginous yeast, has been developed as a platform for producing microbial single-cell oil. It can grow on a variety of carbon sources, such as lipids, glucose, fructose, or glycerol, and store 36% of its biomass as lipids (Zhang et al., 2014). A *Y. lipolytica* strain with up to 77% lipid content has been engineered with the overexpression of DGAT (*DGA1*) from *R. toruloides*, a DGAT (*DGA2*) from *Claviceps purpurea*, and deletion of the native *TGL3* lipase regulator (Friedlander et al., 2016).

Nutritional stress, particularly nitrogen deprivation, has been shown to trigger significant lipid accumulation in microorganisms as it redirects carbon flux towards lipid storage (Figure 2.2). This process is partially regulated by key enzymes such as ATP: citrate lyase (ACL) in oleaginous microorganisms, which respond to nitrogen-limited conditions and convert excess citrate to acetyl-CoA for fatty acid synthesis (Ratledge, 2004; Zhang et al., 2014). Recently, metabolic engineering has shown great potential in enhancing the accumulation of lipids in yeast. For instance, although the model yeast *S. cerevisiae* is not commonly recognized as a good lipid producer, by deleting the gene encoding ADP-activated serine/threonine kinase (SNF1) and overexpressing DGAT in an engineered industrial *S. cerevisiae* strain D5A with a relatively high initial lipid content, lipid accumulation was boosted to nearly 50% of its biomass (Knoshaug et al., 2018). Furthermore, by mating haploid *S. cerevisiae* strains with better lipid accumulation and the further introduction of a deregulated ACCase mutant, the deletion of one regulatory subunit of casein kinase 2 (CKB1), the overexpression of the DGAT, and the disruption of competing pathways and TAG hydrolysis, a *S. cerevisiae* strain capable of accumulating TAG content of 65% of dry biomass was obtained (Arhar et al., 2021). With these advances in lipid

accumulating abilities, yeast thus has the potential to become a preferable microbial cell factory for the synthesis of a wide range of plant bioproducts, including plant UFAs.

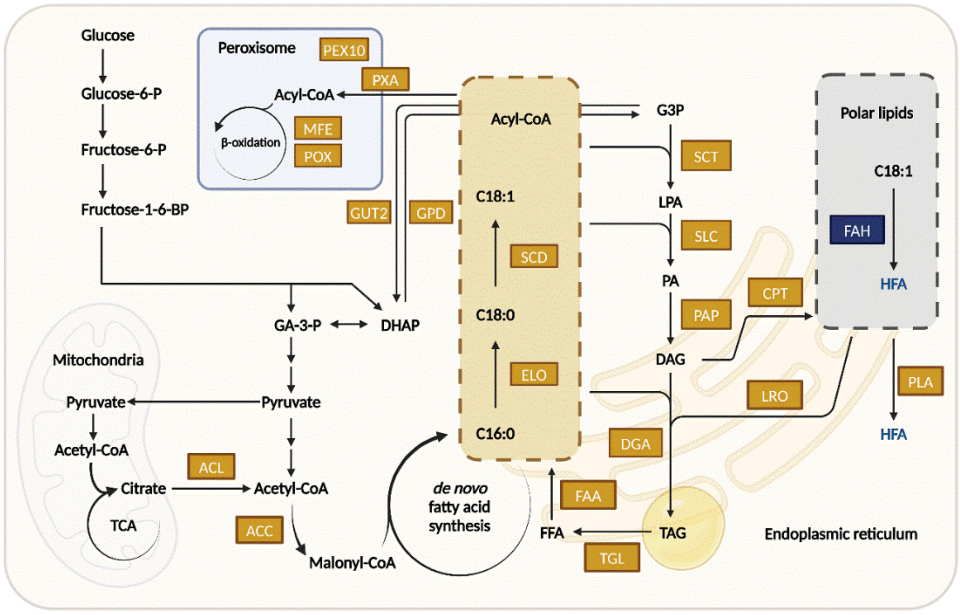

Figure 2.2. Schematic diagram showing typical lipid metabolism in oleaginous yeast.

The fatty acid hydroxylase (FAH) was included as an example of UFA synthesis in a yeast platform. Made with biorender.com. Abbreviations: SCT, glycerol-3-phosphate acyltransferase; FAA, acyl-CoA synthetase; SLC, lysophosphatidic acid acyltransferase; PAP, phosphatidate phosphatase; LRO, phospholipid: diacylglycerol acyltransferase; PLA, phospholipase A; ACC, acetyl-CoA carboxylase; ELO, fatty acid elongase; CPT, choline phosphotransferase; GA-3-P, glyceraldehyde 3-phosphate; DHAP, dihydroxyacetone phosphate; G3P, glycerol-3-phosphate; LPA, lysophosphatidic acid; PA, phosphatidic acid; DAG, diacylglycerol; TAG, triacylglycerol; HFA, hydroxy fatty acid; DGA, diacylglycerol acyltransferase; TGL, triacylglycerol lipase; FFA, free fatty acid; ACL, ATP-citrate lyase; GPD, glyceraldehyde-3-phosphate dehydrogenase;

GUT2, glycerol-3-phosphate dehydrogenase; POX, peroxisomal acyl-CoA oxidase; MFE, peroxisomal β-oxidation multifunctional enzyme; PXA, peroxisomal fatty acid import protein; PEX10, peroxisomal biogenesis factor.

2.3.2. Natural unusual fatty acid accumulation in microorganisms

Certain microorganisms possess the natural ability to synthesize UFAs with functional groups such as conjugated double bonds and hydroxyl groups. Some well-studied bacterial UFA-producing enzymes recognize free fatty acids as substrate, in contrast to the above-mentioned plant-derived fatty acid conjugase and hydroxylase, which specifically edit fatty acyl chains on PC molecules (Kishino et al., 2011; B. Zhang et al., 2012). For instance, much effort has been made in the last few decades to direct the conversion of free LA into CLA using bacteria, such as *Butyrivibrio* (Hussain et al., 2016; Kim et al., 2000), *Propionibacterium* (Wang et al., 2007), *Lactobacillus* (X.-X. Liu et al., 2021) and *Bifidobacterium* (Mei et al., 2022). Results suggested that the bioconversion rate from LA to CLA can reach over 90% using the above-mentioned bacteria, demonstrating their potential as highly efficient whole-cell catalysts (Gao et al., 2020; Mei et al., 2022).

Different CLA isomer profiles were generated during microbial bioconversion, mainly as a result of the specificity of the LA isomerase/isomerization system found in different microorganisms. The proportion in which the two most biologically significant CLA isomers (c9, t11-CLA and t10, c12-CLA) are produced varies greatly based on the microbial source. Being a stable, soluble, and cytoplasmic protein, t10, c12-CLA-specific *Propionibacterium acnes*' linoleate isomerase (PAI)'s crystal structure in apo- and product-bound forms have been elucidated (Liavonchanka et al., 2006). In contrast, analyses of potential linoleate isomerase (LI) enzymes from certain *Lactobacillus* and *Bifidobacterium* suggested these LIs are membrane-bound proteins (Macouzet et al., 2010). Moreover, in *Lactobacillus plantarum*, the CLA was identified as the product of a multi-enzymatic complex comprising hydratase (CLA-HY) in the membrane fraction, as well as dehydrogenase (CLA-DH) and isomerase (CLA-DC) in the

soluble fraction (Kishino et al., 2011). CLA was only produced by recombinant *E. coli* when all three transformants expressing CLA-HY, CLA-DH, and CLA-DC were present as catalysts.

The production of HFAs by microorganisms mainly occurs through the hydroxylation reaction, which is catalyzed by hydratase (Seo et al., 2013), P450 monooxygenase (Jung et al., 2011), or desaturase-like hydroxylase, etc. (Meesapyodsuk and Qiu, 2008). Hydratase, such as the CLA-HY found in *L. plantarum*, catalyzes the selective addition of a water molecule to the double bond position in unsaturated fatty acids, which generates mono-HFA with high efficiency. In contrast to microbial hydratases that catalyze hydration independently of reducing cofactors, enzymes such as cytochrome P450 monooxygenases require NAD(P)H as the cofactor for their oxygenation activity (Van Bogaert et al., 2011). The structural variation of cytochrome P450s enables them to have a broad range of catalytic abilities, which can be divided into α-hydroxylase and ω-hydroxylase activities according to the preference in catalytic sites (Jiang et al., 2021). α-hydroxylases catalyze the hydroxylation of fatty acids near the carboxyl group of the fatty acid chain, whereas ω-hydroxylases, such as members of the well-studied CYP102 family, are responsible for hydroxylation near the methyl end of the fatty acid chain (Jung et al., 2011). CYP102A1 (also known as $P450_{BM3}$) is a fatty acid hydroxylase from *Bacillus megaterium* with a self-sufficient electron transport system (C. Whitehouse et al., 2012). This enzyme has been extensively investigated for years due to its high catalytic rates, and many mutagenesis, as well as directed evolution efforts, have been made aimed at broadening its substrate range and improving its catalytic activity (Carmichael and Wong, 2001; Vincent et al., 2021).

In addition to hydratase and P450, desaturase-like oleate hydroxylases were also found in certain microorganisms that have the natural ability to synthesize HFAs. *C. purpurea*, which is a

fungal pathogen known for causing ergot disease in cereal grains, has the ability to synthesize RA in its sclerotia (Billault et al., 2004). *C. purpurea* hydroxylase (CpFAH) was found to be responsible for RA accumulation and the heterologous expression of *CpFAH* in *S. cerevisiae* also provided Δ12 desaturase activity on C16 and C18 monounsaturated fatty acids, suggesting that CpFAH is a bifunctional Δ12-hydroxylase/desaturase (Meesapyodsuk and Qiu, 2008).

Similar to plant hydroxylase, CpFAH contains multiple transmembrane domains and three histidine-box motifs (Robin et al., 2019). By constructing chimeras of CpFAH with monofunctional desaturase CpFAD2, it was shown that only the cytosolic domains have an impact on hydroxylation/desaturation activity distribution (Robin et al., 2019). Replacing the CpFAH cytosolic domain near the second histidine-box eliminated all hydroxylase activity and converted CpFAH into a monofunctional desaturase. Further mutagenesis identified I198 as the most important site for hydroxylation activity and various mutations at this position led to different hydroxylation/desaturation product ratios. Interestingly, further alignments of desaturases/hydroxylases across plants and microorganisms showed a threonine (T) is always found at this position in desaturases, whereas hydroxylases tend to have isoleucine (I) (RcFAH and CpFAH) or asparagine (N) (PfFAH) instead (Robin et al., 2019).

2.3.3. Engineered microorganisms for UFA production via bioconversion

Since the direct extraction of UFAs from plant natural producers may not be cost-effective, many plant species have been genetically modified for the improved production of UFAs (Table 2.1) (Holic et al., 2018; Xu et al., 2020b). However, several challenges remain with plant-based systems. Scaling up UFA production by plant cultivation requires a large amount of arable land, which may compete with food production and affect food security. In addition, climate conditions, pests, and diseases may influence crop yields, and in-depth studies and field

trials are necessary to address concerns regarding transgenic plants' fitness costs, as well as interactions with surrounding ecosystems (Fu and Song, 2018; Hackett and Bonsall, 2016; Kumar et al., 2020; Lu et al., 2016). For instance, when transgenic plants are grown in an open environment, gene flow between transgenic crops and their non-modified relatives requires careful assessment to avoid potential unintended ecological consequences (Hancock, 2003; Kumar et al., 2020; Ohadi et al., 2017; Snow, 2002).

Therefore, developing microbial platforms for lipid and UFA production may serve as an alternative approach. Due to fast growth rates and capabilities for high-density fermentation, microorganisms can be efficiently cultured on non-arable land and have higher productivities per unit area when used to produce lipid-related bioproducts (Adams et al., 2013; Chisti, 2008; J. Wang et al., 2022). Compared to transgenic plants, engineered microorganisms can be cultured in closed, controlled, and regulated environments such as bioreactors, which are less susceptible to environmental influences and have limited interactions with surrounding ecosystems if proper downstream processing measures are taken. In addition, many microorganisms can grow on a wide range of substrates, including wastewater or by-products from agricultural and food industries (Lan et al., 2015; Savakis and Hellingwerf, 2015), demonstrating their versatility in cost-effective and sustainable production.

Table 2.1. Representative studies of UFA production in transgenic plants.

UFA	Plant host	Engineering strategies	UFA level	Reference
PuA	*A. thaliana*	*T. kirilowii TkFADX*	10.2%	(Iwabuchi et al., 2003)
	A. thaliana	*PgFADX, PgFAD2, fad3Δ, fae1Δ*	21.2%	(Mietkiewska et al., 2014)
	B. napus	*PgFADX, PgFAD2*	11.1%	(Xu et al., 2020b)
t10, c12-CLA	*N. tabacum*	*PAI*	0.3% of esterified FA 15% of free FA	(Hornung et al., 2005)
CPA	*A. thaliana*	*EcCPS, S. foetida SfLPAT, fad2Δ, fae1Δ*	35%	(Yu et al., 2014)
	C. sativa	*EcCPS, S. foetida SfLPAT, fad2Δ, fae1Δ*	20%	(Yu et al., 2018)
	C. sativa	*EcCPS, L. chinensis LcPDCT, fad2Δ, fae1Δ*	8%	(Yu et al., 2019)
RA-containing	*A. thaliana*	*RcFAH, fae1Δ*	17%	(Lu et al., 2006)
	A. thaliana	*RcFAH, RcDGAT2, fae1Δ*	30%	(Burgal et al., 2008)
	A. thaliana	*CpFAH, fad2Δ, fae1Δ*	25%	(Meesapyodsuk and Qiu, 2008)
	A. thaliana	*CpFAH*	19.7%	(Meesapyodsuk and Qiu, 2008)
	A. thaliana	*RcFAH, RcPDAT1A, fae1Δ*	27%	(van Erp et al., 2011)
	A. thaliana	*RcFAH, RcPDCT, fae1Δ*	23.3%	(Hu et al., 2012)
	A. thaliana	*RcFAH, RcDGAT2, RcPDCT, fae1Δ*	28.5%	(Hu et al., 2012)
	A. thaliana	*RcFAH, AtWRI1, fae1Δ*	20.9%	(Adhikari et al., 2016)
	A. thaliana	*RcFAH, RcGPAT9, RcLPAT2, RcPDAT1A, fae1Δ*	34%	(Lunn et al., 2019)

	A. thaliana	*RcFAH, RcLPCAT, RcPDAT, fae1Δ*	29%	(Lunn et al., 2020)
	A. thaliana	*RcFAH, RcDGAT2, RcPDAT, RcPDCT, RcLPCAT, fae1Δ*	31%	(Park et al., 2022)
	C. sativa	*RcFAH, RcPLCL1*	24%	(Aryal and Lu, 2018)
	B. carinata	*C. graeca 3-ketoacyl-CoA synthase (KCS)*	44%	(Taylor et al., 2009)
Nervonic acid	*B. carinata*	*L. annua 3-ketoacyl-CoA synthase (KCS)*	30%	(Guo et al., 2009)
	C. sativa	*L. annua 3-ketoacyl-CoA synthase (KCS)*	6-12%	(Huai et al., 2015)

Fatty acid product profiles, cultivation conditions, and genetic manipulations summarized in this table do not include all specific details, but only those that are unique and of concern to this review. In the descriptions of desaturase and elongase, the Δ character denotes specificity for a fatty acid substrate, whereas other Δ characters denote gene disruptions.

In the microbial production of UFAs, bioconversion plays an important role by utilizing microorganisms or their enzymes to directly transform readily available fatty acid precursors into modified value-added lipids (Table 2.2). Reactions with high stereo- and regioselectivity can be achieved by selecting specific natural or engineered microbes as whole-cell catalysts. For example, in the production of CLA, some *Bifidobacterium breve* strains have been shown to convert LA precursor into nearly 100% of c9, t11-CLA (Coakley et al., 2003; Gao et al., 2020), whereas *P. acnes* produced solely t10, c12-CLA from LA (Liu et al., 2024; Verhulst et al., 1987). In contrast to complex metabolic engineering approaches, bioconversion often involves simpler and shorter metabolic pathways. Therefore, higher efficiency in converting substrates into target products can result from this simplicity (Wang et al., 2021; Zhang et al., 2013). For instance, by expressing the oleate hydratase from *Stenotrophomonas maltophilia* in *E. coli* ER2566, whole cell catalyst converted 50 g/L oleic acid into 49 g/L 10-hydroxystearic acid, reaching a conversion yield of 98% (w/w) (Joo et al., 2012). When external lipids serve as the substrate for microbial catalysts, reduced fatty acid degradation and enhanced fatty acid assimilation abilities are beneficial for improving the overall efficiency of bioconversion. Accordingly, by removing *E. coli* β-oxidation-associated enzymes FadE and FadD, as well as enhancing the import of fatty acid precursors through the overexpression of the native fatty acid transporter FadL, the concentrations of medium-chain ω-HFAs products were significantly improved in recombinant *E. coli* strains harboring the AlkBGT hydroxylation system from *Pseudomonas putida* (He et al., 2019).

In addition to bacteria, oleaginous yeasts have also emerged as good candidates for UFA bioconversion. By culturing in a medium supplemented with soybean oil, an engineered *Y. lipolytica* strain harboring *P. acnes* PAI and *Mortierella alpina* Δ12-desaturase accumulated t10,

c12-CLA up to 44% of total fatty acids, and 4 g/L CLA production was achieved in the bioreactor (Zhang et al., 2013). Using safflower seed oil as the substrate, along with the additional deletion of *PEX10* (encoding a protein involved in peroxisomal biogenesis and β-oxidation), a decreased t10, c12-CLA degradation rate and increased t10, c12-CLA production to 7.4 g/L was achieved in *Y. lipolytica* with multiple copies of the PAI gene (B. Zhang et al., 2022). Engineered microorganisms have also been used for the bioconversion of common fatty acids into several UFAs commonly found in plants. For example, by replacing native oleate hydroxylase CYP52M1 with an RA-producing hydroxylase in *Starmerella bombicola*, an RA production titer reaching 2.96 g/L was achieved using oleic acid as feedstock (Chatterjee et al., 2022). *S. bombicola* is a yeast species known for secreting glycolipid biosurfactant (sophorolipids), and RA in an engineered strain was bound with sophorolipid first intracellularly and then secreted into the medium, followed by hydrolysis to recover RA, thus avoiding the build-up of RA in the cell membrane and alleviating intracellular toxicity (Chatterjee et al., 2022). Being a GRAS yeast strain, *S. cerevisiae* has been modified to produce 1.6% (w/w) pomegranate-derived PuA by supplying a *PgFADX*-expressing recombinant strain with LA (Hornung et al., 2002). Since *S. cerevisiae* has a relatively simple fatty acid profile consisting of only saturated and monounsaturated fatty acids (Sec et al., 2015), supplying the exogenous LA in a bioconversion manner is conducive to PuA accumulation. In line with this, after a push and pull approach by combining the deletion of a yeast lipid metabolism regulator with the heterologous expression of *PgFADX* and pomegranate acyl-editing genes, along with the feeding of 0.05% LA, *S. cerevisiae* was engineered to produce 3.4% of total fatty acids as PuA (Wang et al., 2021).

Table 2.2. Representative studies and metabolic engineering strategies for UFA production in recombinant microorganisms.

UFA	Platform	Engineering strategies	UFA level	Reference
PuA	*S. cerevisiae*	*PgFADX*	1.6%	(Hornung et al., 2002)
	S. cerevisiae	*PgFADX, PgPDAT, PgLPCAT, snf2Δ*	3.37% (7.2 mg/L)	(Wang et al., 2021)
	S. pombe	*PgFADX, PgFAD2*	25.1% (38.71 mg/L)	(Garaiova et al., 2017)
	Y. lipolytica	*PgFADX, DGA2, GPD1, eyk1Δ, pox1-6Δ, tgl4Δ*	0.5% (36.6 mg/L)	(Urbanikova et al., 2023)
	Y. lipolytica	*PgFADX, YlFAD2, YlCPT, PgLPCAT, YlLRO1, GPD1, P. graminis Δ9 desaturase, MaELO2, YlELO1, pex10Δ, gut2Δ, lro1Δ, fad2Δ, scdΔ, lip1Δ, scp2Δ*	4.77% (100.56 mg/L) in flask 6.19% (3072.72 mg/L) in bioreactor	(Wang et al., 2024)
Calendic acid	*S. pombe*	*CoFADX-2, PgFAD2*	8.7% (4.4 mg/L)	(Garaiova et al., 2023)
EsA	*S. cerevisiae*	*VfFADX*	2.1%	(Dyer et al., 2002)
t10, c12-CLA	*Y. lipolytica*	*PAI*	5.9%	(B. Zhang et al., 2012)
	Y. lipolytica	*PAI, M. alpina* Δ12 desaturase	9.8% (44.9 mg/L)	(Zhang et al., 2013)
	Y. lipolytica	*PAI, M. alpina* Δ12 desaturase	44% of cells, 30% of culture medium (4 g/L) in bioreactor	(Zhang et al., 2013)
	Y. lipolytica	*PAI,* Δ12 desaturase, cells of the yeast were permeabilized by freeze/thawing, β-oxidation weakened by sodium acetate	15.6 g/L	(Zhang et al., 2016)
	Y. lipolytica	*PAI, YlFAD2, pox1-6Δ, fad2Δ, dga1Δ, dga2Δ, lro1Δ*	6.5% (52 mg/L)	(Imatoukene et al., 2017)

	Y. lipolytica	*PAI, YlFAD2, pox1-6Δ, fad2Δ, dga1Δ, dga2Δ, lro1Δ*	6% of cells, 3.4% of culture medium (302 mg/L) in bioreactor	(Imatoukene et al., 2017)
	Y. lipolytica	*PAI, pex10Δ,* Δ12 desaturase	7.4 g/L (2.8 g/L in cells and 4.6 g/L in media)	(B. Zhang et al., 2022)
	M. alpina	*PAI,* 5 μM long-chain acyl CoA synthetase inhibitor was added	1.2% (29 mg/L)	(Hao et al., 2015)
	S. cerevisiae	*PAI*	4.3% of all esterified fatty acids 5.7% of all free fatty acids	(Hornung et al., 2005)
	Y. lipolytica	*EcCPS, DGA1, pex10Δ, mfe1Δ*	32% (3 g/L) in bioreactor	(Markham and Alper, 2018)
CPA	*Y. lipolytica*	*EcCPS, tgl4Δ, pox1-6Δ*	45.8% (2.3 g/L) in bioreactor	(Czerwiec et al., 2019)
	Y. lipolytica	*EcCPS, GPD1, DGA2, LRO1, pox1-6Δ, tgl4Δ*	19.6% (7.49 g/L) in bioreactor	(Imatoukene et al., 2020)
10-hydroxy stearic acid	*E. coli*	Oleate hydratase from *Stenotrophomonas maltophilia*	49 g/L	(Joo et al., 2012)
Medium -chain ω-HFAs	*E. coli*	*AlkBGT, FadL, fadEΔ, fadDΔ*	309 mg/L ω-hydroxydecanoic acid	(He et al., 2019)
RA	*P. pastoris*	*CpFAH, CpDGAT1, fad2Δ*	55.7% (171.44 mg/L)	(Meesapyodsuk et al., 2015)
	S. pombe	*CpFAH*	52.6% (137.4 mg/L)	(Holic et al., 2012)

EPA	*Y. lipolytica*	*CpFAH12, LRO1, pox1-6Δ, fad2Δ, dga1Δ, dga2Δ, lro1Δ*	43%	(Beopoulos et al., 2014)
	Y. lipolytica	*CpFAH,* fatty acid elongase *(MaC16E),* PC biosynthesis *(CDS1, PSD1, CHO2, and OPI3), pah1Δ, app1Δ, dga1Δ, mef1Δ, pex10Δ, fad2Δ,* with Triton X-100 treatment	74% (2 g/L of free RA)	(Park and Hahn, 2024)
	Y. lipolytica	*M. alpina* elongase*, YlCPT1, F. Moniliforme* Δ12 desaturase*, P. aphanidermatum* Δ17 desaturase*, E gracilis* Δ5 desat*urase,* Δ8 desaturase, Δ9 elongase*, Peridinium sp.* Δ5 desaturase, *Eutreptiella sp.* Δ9 elongase*, pex10Δ, YALi0C18711gΔ, leu2Δ, lip1Δ, scp2Δ*	56.6%	(Xue et al., 2013)
	Y. lipolytica	*ScDGAT2C, ScGPAT2, ScG6PD, ScPDC, ScACC, ScACS,* Δ12-Δ9-Δ8-Δ5-Δ17 desaturase	266.44 mg/L	(Jia et al., 2024)
Nervonic acid	*S. cerevisiae*	*ChFAE1, MoKCS, elo2Δ*	57 mg/L	(Y. Zhang et al., 2022a)
Nervonic acid Erucic acid	*R. toruloides*	*C. abyssinica* and *C. graeca KCS* in CECT 13085	38.4% (8 g/L nervonic acid, 5.8 g/L erucic acid) in bioreactor	(Fillet et al., 2017)

Fatty acid product profiles, cultivation conditions, and genetic manipulations summarized in this table do not include all specific details, but only those that are unique and of concern to this review. In the descriptions of desaturase and elongase, the Δ character denotes specificity for fatty acid substrate, whereas other Δ characters denote gene disruptions.

2.3.4. Neosynthesis of unusual fatty acids in engineered microorganisms

In contrast to bioconversion, the neosynthesis of UFAs often involves a more intensive modification of microbial metabolic pathways, so that non-native UFAs can be synthesized from simple substrates such as glucose (Table 2.2). Since neosynthesis has potential advantages in terms of reducing dependence on specific feedstocks and lowering production costs, many metabolic engineering efforts have been made to explore the efficiency of *de novo* synthesis of UFAs in microbial platforms, including VLCFAs, PUFAs, CFAs, and HFAs, etc. (Holic et al., 2012; Wang et al., 2021; Xue et al., 2013; Y. Zhang et al., 2022a). Nervonic acid, for example, is a C24 monounsaturated VLCFA that is important for the development and maintenance of nerve cell myelin. Efforts to boost nervonic acid production have focused on carefully manipulating elongase activity in engineered microorganisms. By heterologously expressing a gene encoding elongase and knocking out endogenous elongase (ELO2) in *S. cerevisiae*, up to 57 mg/L of nervonic acid was obtained in a shake flask culture (Y. Zhang et al., 2022a).

In terms of the microbial production of RA, model yeasts *Schizosaccharomyces pombe* and *Pichia pastoris* have been engineered to produce RA by introducing *CpFAH* from *C. purpurea* (Holic et al., 2012; Meesapyodsuk et al., 2015). 75% of the total fatty acid in fission yeast *S. pombe* is naturally present as oleic acid, which may offer an abundant supply of fatty acid precursors for the synthesis of RA. Results showed that the growth of *S. pombe* cells with *CpFAH* expression was impaired at 30 °C but was recovered under 37 °C. By shifting the temperature, engineered *S. pombe* produced 52.6% of total fatty acids as RA, equivalent to 137.4 μg/mL of culture (Holic et al., 2012). Although the natural oleic acid content in wild-type *P. pastoris* was only around 51%, by removing native Δ12 desaturase activity, this common fatty acid precursor content was increased to 77.85% (Meesapyodsuk et al., 2015). Subsequently,

when coupled with *CpFAH* and *CpDGAT1* coexpression, the engineered strain without Δ12 desaturase activity produced 56% of total fatty acids as RA. RA was found mostly in free fatty acid form and total RA production reached 171 μg/mL of culture (Meesapyodsuk et al., 2015).

In terms of CFA production, fission yeast was also engineered to produce PuA (Garaiova et al., 2017) and calendic acid (Garaiova et al., 2023) by expressing conjugase and desaturase cloned from *P. granatum* and *Calendula officinalis*, respectively. Without LA precursor supplementation, PuA and calendic acid production reached approximately 39 mg/L and 4.4 mg/L respectively. Collectively, although model microorganisms such as *S. cerevisiae*, *S. pombe,* and *P. pastoris* can be readily modified due to their advanced genetic tools, it seems that the production of UFAs in these yeasts was limited by their relatively low lipid-accumulating ability. Consequently, after modifying acyl channeling processes and adjusting precursor supply, an *S. cerevisiae* strain expressing pomegranate-derived *PgFADX* and *Y. lipolytica YlFAD2* could only produce 1.23% of total fatty acids as PuA (Wang et al., 2021). Recently, we developed a genetically modified *S. cerevisiae* strain that can accumulate more than 26% of its total fatty acid content as PuA, achieving a PuA concentration of over 400 mg/L without requiring the addition of LA precursor (unpublished data), although extensive metabolic engineering efforts were necessary to achieve this outcome.

On the other hand, many oleaginous yeasts may serve as a better platform for UFA production due to their higher overall efficiency in lipid synthesis. For nervonic acid production, the engineered oleaginous *R. toruloides* expressing the gene encoding elongase from plants synthesized up to 8 g/L of nervonic acid in bioreactor cultivation (Fillet et al., 2017). DuPont (USA) has also successfully produced eicosapentaenoic acid (EPA), a healthy 20-carbon PUFA with five double bonds, at high levels in the oleaginous yeast *Y. lipolytica* through the knockout

of *PEX10* and integration of 30 copies of nine different elongase and desaturase genes (Xue et al., 2013). The engineered strain produced EPA at 56.6% of total fatty acids and accumulated lipids at up to 30% of the dry cell weight. Additionally, a recent study showed that by incorporating *ScDGAT2C*, *ScGPAT2*, *ScACC*, glucose 6-phosphate dehydrogenase (*ScG6PD*), pyruvate dehydrogenase (*ScPDC*), and acetyl-CoA synthetase (*ScACS*) from the PUFA natural producer *Schizochytrium* sp., the flux of EPA into TAG storage could be increased in EPA-producing *Y. lipolytica* and led to 266.44 mg/L EPA titer (Jia et al., 2024).

Given that castor plants contain the highly toxic protein ricin, and *C. purpurea* produces harmful ergot alkaloids that have historically led to ergotism outbreaks (Kim and Oh, 2013), the oleaginous "GRAS" yeast *Y. lipolytica* appears to be a safer alternative for the production of RA. A recent study demonstrated that in engineered *Y. lipolytica*, the heterologous expression of *CpFAH*, fatty acid elongase (*MaC16E*), and enzymes responsible for PC biosynthesis (*CDS1*, *PSD1*, *CHO2*, and *OPI3*) via the CDP-DAG pathway, as well as the deletion of phosphatidic acid phosphatase genes (*PAH1* and *APP1*), diacylglycerol acyltransferase (*DGA1*), genes related to fatty acid degradation (*MEF1* and *PEX10*) and oleic acid desaturation (*FAD2*), C18 fatty acid flux was boosted towards the PC pool and led to significantly higher levels of RA product (Park and Hahn, 2024). Similar to *P. pastoris*, RA was also mainly found in the form of free fatty acid. By further inducing RA secretion via Triton X-100 treatment, the engineered strain produced over 2 g/L of free RA, constituting 74% of total fatty acids (Park and Hahn, 2024).

The synthesis of conjugated UFAs in *Y. lipolytica* was relatively challenging, as in the metabolically engineered obese *Y. lipolytica* with *PgFADX* overexpression, the level of PuA only reached 0.5% of total fatty acids (Urbanikova et al., 2023). Using the high oleic acid *Y. lipolytica* strain 2Pg2E (K. Wang et al., 2022), further improving endogenous LA precursor supply,

overexpressing multiple copies of *PgFADX*, modulating acyl-editing and PC biosynthesis pathways by overexpressing *YlCPT* and *PgLPCAT*, downregulating fatty acid turnover, enhancing G3P as well as TAG synthesis, the comprehensively modified *Y. lipolytica* strain accumulated 4.77% of total fatty acids as PuA in shake flask fermentation, and the PuA titer reached 100.56 mg/L (Wang et al., 2024). In addition, we have recently engineered the oleaginous yeast *R. toruloides* to produce PuA. With simple *PgFADX* and *PgFAD2* coexpression, the recombinant strain accumulated 12% of its lipids as PuA from glucose under nitrogen-limited conditions, which translated into a PuA titer of 451 mg/L in shake flask cultivation (data unpublished). Due to the capability of assimilating lignocellulosic hydrolysate feedstock, engineered *R. toruloides* also achieved 6.4% PuA accumulation when wood hydrolysate was used as the substrate, showcasing the benefits of using oleaginous yeast as a platform for UFA production.

2.4. Advances in integrating microbial and plant biotechnology for potential improvement in unusual fatty acid production

As outlined in sections 2.2.3 and 2.2.4, plant UFA enrichment often relies on the concerted effort of multiple enzymes. Considering the intricate nature of the pathways involved and the time-consuming steps of plant transgenic work, model microorganisms offer an alternative and highly efficient platform for the identification and characterization of plant enzymes due to their rapid growth rates, cost-effectiveness, and ease of genetic manipulation. *S. cerevisiae*, in particular, has been extensively utilized for studying cellular and molecular functions in eukaryotes due to the presence of membrane-bound organelles. In the study of plant lipid biosynthesis, yeast expression systems have been frequently used for the isolation of plant membrane fatty acid desaturases and conjugases, such as FAD2 and FADX (Dyer et al., 2002;

Iwabuchi et al., 2003; Petranovic and Nielsen, 2008; Vrinten et al., 2005). In addition, a variety of microorganism mutants have been constructed and are readily available for the identification and functional characterization of plant enzymes involved in lipid metabolism, including DGAT1, DGAT2, PDAT, LACS, LPCAT, GPAT, and LPAT (Arroyo-Caro et al., 2013a, 2013b; Demski et al., 2019; Payá-Milans et al., 2016; Xu et al., 2019, 2018a), thus highlighting the significance of microbiological tools in the study of plant lipids.

Via the bioconversion method detailed in section 2.3.3, microorganisms are capable of transforming low-value plant lipids into unique and value-added UFAs. Since many well-studied model microorganisms are not oleaginous, this interdisciplinary approach combining the large volume of knowledge regarding plant oil production with efficient microbial whole-cell catalysts has proven itself as a promising strategy for UFA production. Indeed, many plant lipids, such as *Acer truncatum bunge* seed oil (Chen et al., 2017) and LA from oats (Vahvaselkä et al., 2004), have been tested for microbial bioconversion into CLA. Using bioconversion, the lipid substrate spectrum for UFA production is not limited by the microorganism's natural lipid composition. In addition to converting common fatty acids, some UFAs derived from plants may also undergo further bioconversion, which introduces additional functional groups and raises the reactivity and potential value of the fatty acid. For instance, a recombinant oleate hydratase from *Lysinibacillus fusiformis* was able to convert RA to a novel compound 10,12-dihydroxystearic acid. Indeed, a 90 % (w/w) conversion rate could be achieved under optimized conditions, and the emulsifying activity of 10,12-dihydroxystearic acid was shown to be higher than that of oleic acid or RA (Seo et al., 2013).

Given the diversity of the microbial world, certain enzymes derived from microorganisms have proven to be effective in boosting the production of UFAs, sometimes outperforming

enzymes that originate from plants. For instance, in engineered *Y. lipolytica*, the expression of castor *RcFAH* only led to 7% of total fatty acids as RA, whereas the expression of *CpFAH* from the fungus *C. purpurea* resulted in 29% RA accumulation (Beopoulos et al., 2014). As demonstrated by HFA production in transgenic *Arabidopsis*, the heterologous expression of *CpFAH* also led to a higher level of HFA accumulation than was previously observed in *Arabidopsis* carrying plant-derived fatty acid hydroxylases (Meesapyodsuk and Qiu, 2008). CpDGAT2 was also isolated from *C. purpurea* which exhibited a preference for RA as a substrate (Mavraganis et al., 2010). Similarly, in the heterologous synthesis of CPA, it was found that the expression of a gene encoding *E. coli* cyclopropane fatty acid synthase (EcCPS) led to higher UFA accumulation in *Arabidopsis* than the expression of CPS from cotton or *Sterculia foetid*a (Yu et al., 2019, 2014). On the other hand, introducing plant-derived enzymes into microorganisms, such as the overexpression of *B. napus* long-chain acyl-CoA synthetase 4 (BnLACS4) or BnDGAT1 (Greer et al., 2015; Tan et al., 2014), has also been found to enhance the lipid content of yeast. Collectively, these findings highlight the crosstalk between microbial biotechnology and plant biotechnology for advancing UFA production.

2.5. Challenges of producing UFAs in heterologous hosts and potential strategies for improving UFA production

It has been observed that UFAs frequently dominate the seed fatty acid composition of many natural producers, such as castor bean or pomegranate, with levels as high as 80% to 90% (da Silva Ramos et al., 1984; Kaufman and Wiesman, 2007; Khoddami et al., 2014; McKeon et al., 2016; Paul and Radhakrishnan, 2020; Takagi and Itabashi, 1981). Although many comprehensive metabolic engineering efforts have been made, the levels of UFAs achieved in transgenic plants or microorganisms are still significantly lower than in natural producers (Wang

et al., 2021; Xu et al., 2020b). In the context of heterologous production, several challenges arise in the *de novo* synthesis of UFAs. These challenges include but are not limited to, the insufficient *in vivo* availability of precursor substrates, inefficient channeling of UFAs into storage lipids via native lipid metabolism, stress and fitness costs induced by UFA accumulation, and unexpected variations in the stability and regulation of expressed UFA-producing pathways.

2.5.1. Challenges arise from the availability of upstream precursors in heterologous hosts

In heterologous hosts, the activity of upstream metabolic pathways responsible for providing fatty acid precursors can be quite limited, and the presence of downstream competing pathways may affect the final UFA output. For instance, in *Arabidopsis*, the ER-localized fatty acid elongase (FAE1) is responsible for the elongation of C18:1 fatty acid into C20:1 and C22:1 (Kunst et al., 1992). The mutation of *fae1Δ* led to a dramatic reduction in VLCFA level and increased C18:1 content, which is the precursor for HFA synthesis (Kunst et al., 1992). Consequently, the *RcFHA12*-transformed *Arabidopsis fae1Δ* mutant line accumulated a significantly higher content of C18:1 (38% of total fatty acids) and total HFA (17% of total fatty acids) (Hu et al., 2012; Lu et al., 2006). In contrast, heterologously expressed *RcFHA12* in the wild-type *Arabidopsis* (Col-0) line only led to around 19.6% C18:1 and 9.9% HFA (Hu et al., 2012). Moreover, by inhibiting the activities of both *Arabidopsis* native Δ15 desaturase (FAD3) and FAE1, the content of LA could be increased to over 50% (Smith et al., 2003). Since LA is the direct precursor for PuA synthesis, the overexpression of *PgFADX* in the *Arabidopsis fad3Δ/fae1Δ* double mutant led to 2.6-fold higher amounts of PuA (Mietkiewska et al., 2014), in contrast to the content achieved with the wild-type *Arabidopsis* background (Iwabuchi et al., 2003). Further gene stacking of *PgFAD2* and *PgFADX* in the *fad3/fae1* mutant line boosted the content of PuA to 21.2% of total fatty acids (Mietkiewska et al., 2014).

In microorganisms, the most obvious example of precursor challenge in the production of UFAs is in the well-studied model yeast *S. cerevisiae*. Although *S. cerevisiae* is a well-known GRAS microorganism that has many merits, its natural fatty acid profile is over-simplified and not ideal for the production of certain UFAs. For instance, wild-type *S. cerevisiae* contains a high level of C16 fatty acids (>60%) (Sec et al., 2015), whereas many plant UFA biosynthetic pathways require C18 fatty acids as a direct precursor. Consequently, when testing plant fatty acid conjugase activity in *S. cerevisiae,* exogenously supplied LA has often been required to make the final product detectable (Hornung et al., 2002; Iwabuchi et al., 2003), even though many plant FADXs are capable of catalyzing both the conversion of oleic acid to LA and further conversion to CFA (Garaiova et al., 2017; Hornung et al., 2002). In line with this, in *S. cerevisiae* coexpressing *VfFAD2* and *VfFADX*, the amount of synthesized EsA (0.3%) was much lower than in cells containing *VfFADX* alone cultivated with exogenously supplied LA (2.1%) (Dyer et al., 2002).

In contrast, despite its structural similarity with desaturase-like FADX, the expression of plant *FAD2* alone in *S. cerevisiae* readily led to a high content of common LA product (Hornung et al., 2002; Iwabuchi et al., 2003; Wang et al., 2021), suggesting that substrate availability is a limiting factor with a stronger influence on UFA synthesis, at least in *S. cerevisiae*. Although plant FAD2 and FAD3 are known to form heterodimers, in which oleate is converted to linolenate without releasing the linoleate intermediate (Lou et al., 2014), limited information is available on the *in vivo* metabolic channeling between hosts' native common fatty acid biosynthetic pathways and heterologous UFA synthesis. Nonetheless, in terms of the *de novo* production of C18 UFAs, microbial platforms containing a higher amount of oleic acid could be used to improve the issue with precursor supply. Indeed, by using a high-oleic *Y. lipolytica*

variant or *S. pombe* (>75% oleic acid) as the starting strains, the production of PuA was significantly improved (Garaiova et al., 2017; Urbanikova et al., 2023; Wang et al., 2024).

2.5.2. Inefficient channeling of UFAs into storage lipids through native lipid metabolism in heterologous hosts

In heterologous hosts, the inefficiency in channeling UFAs into storage lipids is another bottleneck often associated with neosynthesis. After synthesis on PC, the majority of plant UFAs are released and integrated into TAG in natural producers via several distinct metabolic pathways. For example, in castor, oleic acid at the *sn*-2 position of PC is hydroxylated by RcFAH to generate an RA moiety, and most of the RA is further deposited in castor seed oil, occupying 90% of TAG at all three positions (da Silva Ramos et al., 1984; Román-Figueroa et al., 2020; McKeon et al., 2016). However, RA-producing *Arabidopsis* only accumulated 17% HFAs in seed oil at maturity and retained up to 10% to 12% of the PC fraction as HFAs, whereas in castor, HFAs only temporarily accumulated up to 5% in PC during the mid-stage of seed development (Lu et al., 2006; van Erp et al., 2011). In additional studies, as well as in our previous engineering efforts, similar observations have been made in the heterologous production of CFAs in *Arabidopsis*, *B. napus,* and *S. cerevisiae* (Cahoon et al., 2006; Mietkiewska et al., 2014, 2014; Wang et al., 2021; Xu et al., 2020b). The PuA produced by transgenic *A. thaliana* accounted for 12.5% of total fatty acids in PC, which was significantly higher than its relative content in TAG (6.6%) (Mietkiewska et al., 2014), and in transgenic *B. napus* lines, close proportions of PuA (5–10.6%) were found in TAG and PL fractions (Xu et al., 2020b). The heterologous synthesis of PuA in engineered *S. cerevisiae* led to 4.8% of total fatty acids as PuA in the PL fraction, which is 1.28-fold higher than in TAG (Wang et al., 2021). In contrast, CFAs comprise over 60% of TAG but are extremely rare in the PL of *P. granatum* or

M. charantia seeds, which are natural producers of CFAs (Banaś et al., 2023; Mietkiewska et al., 2014).

Collectively, a key difference between the accumulation of UFAs in natural producers and heterologous hosts lies in their distribution patterns (Lin et al., 2003). One possible explanation for the retention of UFAs in PL in heterologous hosts could be the lack of specific acyl-editing and TAG assembly networks, which may further lead to feedback inhibition and a reduction in the production of UFAs (Bates and Browse, 2011; Cahoon and Li-Beisson, 2020; Demski et al., 2022; van Erp et al., 2011). For this reason, many previous studies have focused on promoting product channeling efficiency by introducing natural producers' acyl-editing and TAG assembly enzymes into recombinant hosts (Table 2.1), which often led to a higher level of UFAs in TAG and reduced level of UFAs in polar lipids (detailed in section 2.2.3 and 2.2.4).

2.5.3. Stress and fitness costs induced by UFA synthesis

The connection between host fitness and lipid composition has been well-established. For instance, the overexpression of the *FAD3* or *FAD8* desaturase genes in tobacco plants and tobacco cell cultures led to increased tolerance to drought/osmotic stress and varied heat sensitivity (Zhang et al., 2005). Moreover, loss of FAD2 activity has been found to increase sensitivity to salt stress in *Arabidopsis*, which is caused by a reduction in vacuolar/plasma Na^+/H^+ antiporter activity (J. Zhang et al., 2012). Presumably, the heterologous expression of UFA biosynthetic pathways may also have a major effect on host fitness. Being non-native metabolites, the significant buildup of UFAs within the membrane fraction may induce stress or cellular toxicity through various mechanisms, and UFA accumulation within storage lipids could be challenging for the heterologous host to mobilize, which might eventually affect normal growth (Arroyo-Caro et al., 2013b). In terms of transgenic plants, *Arabidopsis* seeds

accumulating more than 11% CPA showed significantly reduced germination and establishment, and seeds accumulating more than 15% CPA displayed little to no germination (Yu et al., 2018, 2019, 2014). The introduction of the CFA biosynthetic pathway into wild-type *Arabidopsis* yielded seeds with low germination rates and wrinkled morphology, although these phenotypes were absent when the *Arabidopsis fad3Δ/fae1Δ* mutant was used (Cahoon et al., 2006). In addition to fitness costs, expressing UFA biosynthetic pathways in transgenic plants also led to a significant reduction of oil accumulation in seeds (Bates and Browse, 2011; Burgal et al., 2008; Dauk et al., 2007; Yu et al., 2018), which affects the final yield of UFAs. In *Arabidopsis* seeds expressing castor *RcFAH, in vivo* metabolic labeling revealed that the rate of *de novo* fatty acid synthesis within transgenic seeds dropped to approximately half that of control seeds and led to up to a 50% reduction in total seed oil content (Bates et al., 2014).

To overcome fitness costs and oil decreases due to the synthesis of UFAs, the further transfer of natural producers' acyl-editing and TAG assembly genes into heterologous hosts seems to be a viable option. As covered in section 2.2, castor PDCT and DGAT2 may work together to supply nonricinoleate lipids for membrane biosynthesis and raise the levels of tri-ricinoleoyl glycerol in castor seeds (Demski et al., 2022, 2019). Correspondingly, *RcPDCT* expression in *Arabidopsis* increased HFA accumulation and partially restored the negative effect of *RcFAH* expression on seed oil content (Hu et al., 2012), and the expression of castor *RcDGAT* or *RcPDAT* also alleviated the reduced rate of fatty acid biosynthesis and decline in seed oil accumulation (Bates et al., 2014). In addition, in *RcFAH*-transformed *Camelina* seeds, impaired germination was shown to be partially restored by introducing castor PLC (Aryal and Lu, 2018). The overexpression of plant oil biosynthesis master regulator Wrinkled1 (WRI1) in HFA-producing *Arabidopsis* also rescued deficiencies in average seed weight and seed yield caused by

the expression of *RcFAH*, although it resulted in further a reduction and delay in seed germination (Adhikari et al., 2016).

In terms of microbial platforms, the expression of the *RcFAH* was shown to cause the cessation of growth in *S. cerevisiae* (Broadwater et al., 2002). Similarly, RA synthesis was also harmful to *S. pombe* and led to poor growth at the normal growth temperature of 30 °C (Yazawa et al., 2013). Subsequent screening of an *S. pombe* cDNA library identified plg7, which encodes an endogenous PLA2, as a functional suppressor of RA levels in phospholipids as well as the growth defect induced by RA synthesis (Yazawa et al., 2013). While limited information is available about the cellular fitness of engineered yeast-producing CFAs, previous studies have demonstrated that *S. cerevisiae* strains transformed with the Δ12 desaturase gene from the tropical rubber tree (*Hevea brasiliensis*) were susceptible to oxidative stress induced by the addition of paraquat, tertbutyl hydroperoxide, or hydrogen peroxide (Cipak et al., 2006), possibly due to the harmful reactive oxygen species that arise from PUFA's lipid peroxidation. However, over an extended time of adaptation, the yeast strain developed increased resistance to oxidative stress, which was attributed to a rise in endogenous catalase activity (Cipak et al., 2008).

2.5.4. Stability and potential regulation of UFA biosynthetic pathways in heterologous hosts

Potential transcriptional and post-translational regulatory mechanisms may also play crucial roles in modulating lipid biosynthesis in heterologous hosts, influencing both the efficiency and stability of the biosynthetic pathways involved. Considerable evidence suggests that environmental factors are strong inducers of altered PUFA levels in plants and microorganisms. In terms of yeast platforms, *FAD2* transcription in *Y. lipolytica* was upregulated at low temperatures (12 °C) or in the presence of n-alkanes or oleic acid (Tezaki et al., 2017), which may affect the production of unusual PUFAs in this oleaginous yeast. In plant fatty acid

desaturation systems, however, PUFA content also increases with decreasing temperature, but changes in the corresponding fatty acid desaturase mRNA abundances are often minor (Lou et al., 2014). By expressing *B. napus* fatty acid desaturases in *S. cerevisiae*, a temperature-dependent increase in linolenic acid content was observed at cooler growth temperatures, while untransformed yeast cells responded to cooler temperatures by shortening fatty acid chains (Dyer et al., 2001). This increase was not due to transcriptional levels of fatty acid desaturase genes, but rather a temperature-induced, post-translational regulation of plant desaturase enzyme (Dyer et al., 2001; O'Quin et al., 2010; Tang et al., 2005). Further investigation identified the N-terminal sequences of plant fatty acid desaturases can confer rapid proteasome-dependent protein degradation in both plant and yeast cells, which are responsible for regulating membrane composition during temperature shifts (Khuu et al., 2011; O'Quin et al., 2010; Tang et al., 2005).

In terms of UFA synthesis, it has also been found that high levels of *LfFAH* mRNA accumulation in transgenic *Arabidopsis* did not fully translate into high levels of protein accumulation (Broun et al., 1998a). Given the structural similarities between various UFA-producing enzymes and FAD2, further characterization of their post-translational regulation in heterologous hosts may aid in the design and engineering of a more stable enzyme, thereby improving the final product output. Indeed, protein engineering has proven to be a very effective method of boosting lipid metabolism. Previously, we observed that the overexpression of *B. napus BnDGAT1* increased TAG biosynthesis in *S. cerevisiae*, and further investigation showed that adding an N-terminal tag could mask the deleterious influence of BnDGATs' native N-terminal sequence, resulting in increased protein accumulation and enzyme activity (Greer et al., 2015). Furthermore, a previous study demonstrated that the fusion of acyl-CoA binding protein to the N-terminus of *Chromochloris zofingiensis* CzDGAT1 improved protein accumulation and

increased the enzyme's affinity for acyl-CoAs, which raised the levels of oil accumulation in tobacco leaves and yeast cells (Xu et al., 2020a). Therefore, it would be interesting to investigate the properties of N-terminal sequences in desaturase-like UFA-producing enzymes and TAG assembly enzymes originating from UFA-producing plants. Protein engineering targeting this region may lead to improvements in UFA production, especially in heterologous hosts.

In addition to resolving these possible challenges, other aspects might also be considered when attempting to enhance the UFA accumulation in heterologous hosts. For instance, the overexpression of cytochrome b5, which is the electron donor needed by various fatty acid desaturation processes, enhanced the synthesis of PUFA at 30 °C in *S. cerevisiae* (Yazawa et al., 2010). Also, isozyme competition has been considered a limiting factor in the engineering of UFAs in heterologous plants, and higher UFA accumulation was achieved by suppressing *Arabidopsis* native *AtDGAT1* while expressing *DGAT* from UFA natural produces (van Erp et al., 2015). Collectively, the versatility and complexity of lipid metabolism in both plants and microorganisms led to several bottlenecks in the neosynthesis of UFAs in heterologous hosts. To overcome these obstacles, comprehensive engineering strategies are necessary to realize the efficient synthesis of UFAs.

2.6. Conclusions and perspectives

UFAs hold considerable biological and industrial significance due to their unique properties and wide range of applications. These special lipids are produced by many unique plant and microorganism species through specialized lipid metabolic pathways. The study of various UFA-producing enzymes in plants and microorganisms has paved the way for innovative approaches to produce UFAs in heterologous hosts. Plant systems, particularly those with high oil contents, are good platforms for UFA production. By targeting various glycerophospholipid

remodeling and specialized TAG assembly networks, the accumulation of UFAs could be enhanced. To minimize arable land requirements and achieve a faster production cycle, microorganisms have also been modified to accumulate UFAs. Considering the intricate nature of lipid metabolic pathways and the long cultivation cycles required for plants, exploring the synthesis of plant-derived UFAs in well-characterized microorganisms offers a more efficient alternative.

In addition to model microorganisms with advanced molecular tools, many oleaginous microorganisms known for their robust lipid accumulation capabilities have also emerged as promising platforms for UFA production. Through bioconversion or neosynthesis, different UFAs have been successfully produced by bacteria or yeast. However, despite significant metabolic engineering efforts, transgenic plants or microorganisms still produce UFAs at much lower levels than natural producers. Several bottlenecks have been identified in the heterologous production of UFAs, including limited precursor availability, inefficient integration into storage lipids, fitness costs induced by UFA accumulation, and unclear stability and regulation of the engineered pathways. Addressing these challenges may further improve the performance of engineered hosts. Leveraging both plant and microbial systems, the heterologous production of UFAs has the potential to significantly increase their industrial availability, making large-scale production more sustainable and cost-effective.

Chapter 3 – Improving the Production of Punicic Acid in Baker's Yeast by Engineering Genes in Acyl Channeling Processes and Adjusting Precursor Supply

3.1. Introduction

Punicic acid (PuA; 18: 3 $\Delta^{\mathbf{9}cis,\,\mathbf{11}trans,\,\mathbf{13}cis}$), an edible linolenic acid with three conjugated double bonds, has great potential in nutraceutical and pharmaceutical applications due to its strong antioxidant, antidiabetic, anticancer, anti-obesity, and anti-inflammatory bioactivities. (Holic et al., 2018). PuA can also be used in the production of high-quality alkyd resins, paints, varnishes, polymers, and drying oils due to its susceptibility to auto-oxidation and subsequent polymerization, fast drying rates, and water resistance. The major natural source of PuA is pomegranate (*Punica granatum*), which contains up to 80% PuA in its seed oil (Takagi and Itabashi, 1981), although a few other plant species also produce this fatty acid, albeit at lower levels. Unfortunately, none of these plants are suitable for the large-scale production of PuA due to low oil yields and restricted cultivation conditions (Holic et al., 2018). Although initial efforts are underway to produce PuA in transgenic plants, the productivity of this unusual fatty acid has been relatively low thus far (Hornung et al., 2002; Iwabuchi et al., 2003; Mietkiewska et al., 2014; Xu et al., 2020b). As a result of these factors, there is a growing interest in producing PuA using other approaches such as fermentation to fulfill rising demands for this high-value fatty acid (Holic et al., 2018).

PuA is a high-value edible conjugated fatty acid with applications in food, feed, and nutraceuticals, and therefore it is attractive to produce PuA in Generally Recognized as Safe (GRAS) microorganisms. As a GRAS microorganism with a substantial amount of genetic information, baker's yeast (*Saccharomyces cerevisiae*) has been used as a platform to produce various high-value compounds via metabolic engineering, and the edible purified final products,

as well as the edible yeast biomass containing the final products, can be easily commercialized for down-stream applications (Jaakola et al., 2006; Napier, 2007). Moreover, *S. cerevisiae* is a model yeast species with a simple fatty acid profile (approximately 40% palmitoleic acid, 30% oleic acid, 20% palmitic acid, and 5% stearic acid). Such characteristics theoretically provide an ideal foundation for the exploration of metabolic engineering strategies to heterologously produce PuA and other plant-based UFAs. However, in the few reports describing the synthesis of PuA in baker's yeast, the heterologous expression of the *P. granatum fatty acid conjugase* (*PgFADX*), which catalyzes the synthesis of PuA, only resulted in up to 2% PuA (as a percentage of total fatty acids) (Hornung et al., 2002; Iwabuchi et al., 2003). These findings indicate that extensive genetic engineering research will be necessary to generate *S. cerevisiae* strains that can accumulate large quantities of PuA.

In *P. granatum*, the synthesis of PuA from oleic acid (18:1) is generally considered to be catalyzed by Δ12-acyl-lipid-desaturase (PgFAD2) and PgFADX, where the former catalyzes the desaturation of oleic acid to linoleic acid (LA; 18:2 $\Delta^{\mathbf{9}cis,\ \mathbf{12}\mathrm{cis}}$) at the *sn*-2 position of phosphatidylcholine (PC) and the latter converts LA to PuA (Figure 3.1A) (Hornung et al., 2002; Iwabuchi et al., 2003; Mietkiewska et al., 2014). PuA is then channeled from PC to the storage lipid triacylglycerol (TAG) (Holic et al., 2018). The efficient synthesis and channeling of PuA and other UFAs in plants that can accumulate large amounts of these fatty acids often requires the contribution of enzymes with special substrate specificities and selectivities. Some such enzymes have been reported in acyl-editing, lipid biosynthetic and lipid regulatory steps, including phospholipase A_2 (PLA_2), lysophospholipid acyltransferase (LPCAT), phosphatidylcholine: diacylglycerol cholinephosphotransferase (PDCT), phospholipid: diacylglycerol acyltransferase (PDAT) and acyl-CoA: diacylglycerol acyltransferase (DGAT)

(Bates et al., 2014; Dahlqvist et al., 2000; He et al., 2004a, 2004b; Holic et al., 2018; Kroon et al., 2006; McKeon and He, 2015; Wickramarathna et al., 2015). These acyl-editing enzymes may be crucial for enhancing PuA assembly into TAG and thus provide valuable candidates for engineering PuA production. In addition to manipulating TAG assembly ('Pull'), other metabolic engineering strategies for increasing PuA production in microorganisms include increasing fatty acid biosynthesis ('Push') and preventing TAG turnover ('Protect') (Leplat et al., 2018; Maeo et al., 2009). To date, PuA has been heterologously synthesized in *S. cerevisiae*, *Schizosaccharomyces pombe*, *A. thaliana,* and *Brassica napus* (Garaiova et al., 2017; Iwabuchi et al., 2003; Mietkiewska et al., 2014; Xu et al., 2020b). However, these studies only evaluated the result of *PgFADX* and *PgFAD2* expression, and other important factors that may affect PuA production, such as genes in acyl editing, storage lipid accumulation and lipid degradation, transcription factors, and the functions of precursor supply and their various combinations, have not been well studied in yeast or plants as of yet.

This study aims to explore the effectiveness of combining different metabolic engineering strategies ('Push', 'Pull' and 'Protect') on the biosynthesis and accumulation of PuA in *S. cerevisiae*. As demonstrated in numerous previous studies, this model yeast is an ideal platform to study the mechanism of lipid accumulation in eukaryotes due to a plethora of genomic information and various available genetic modification tools. The results of this study will be of value for the heterologous production of this high-value fatty acid via fermentation and will also expand our understanding of the biosynthesis of plant-based UFAs

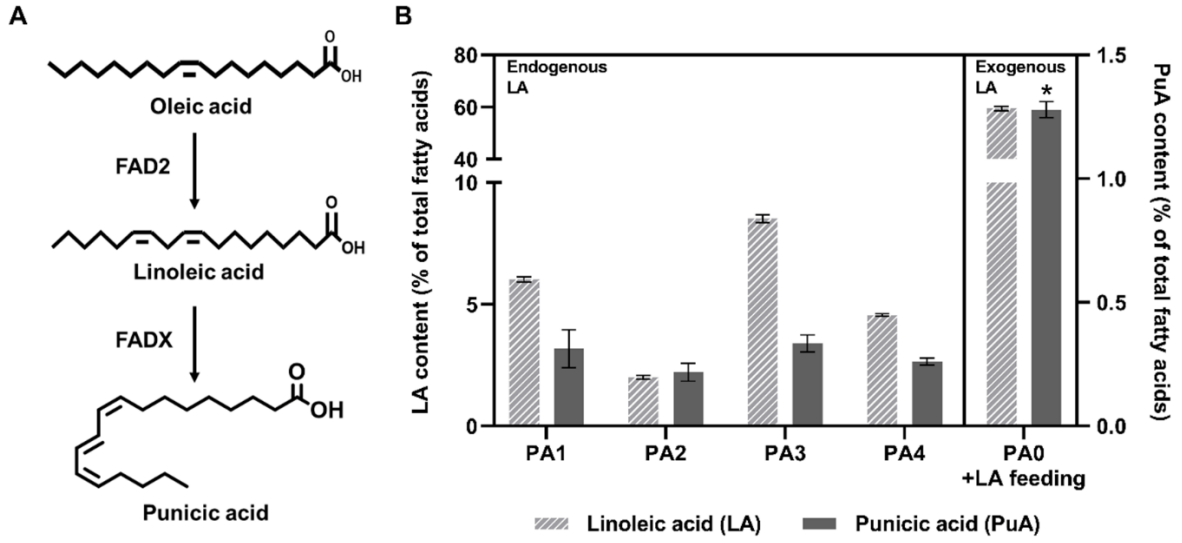

Figure 3.1. Reconstitution of the pomegranate-derived PuA synthetic pathway in *S. cerevisiae.*

(A) Illustration of PuA biosynthesis. Abbreviations: FAD2, Δ12 fatty acid desaturase; FADX, fatty acid conjugase; PuA, punicic acid. (B) Contents of LA and PuA in recombinant yeast strains with different sources of precursor. Strain names are listed in Table 3.1. Data represents the mean values of biological replicates ± SD (*n*=3). ∗, $P < 0.05$ (Student's t-test).

3.2. Materials and methods

3.2.1. Strain and culture conditions

All strains used in this study are listed in Table 3.1. In brief, *S. cerevisiae* BY4741 (*MATa, his3Δ1, leu2Δ0, lys2Δ0, ura3Δ0*) was used as the background strain, and *Escherichia coli* DH5α was used for plasmid construction and amplification. *Yarrowia lipolytica* E122 and *Lipomyces starkeyi* NRRL Y11557 were cultured for RNA isolation and cDNA synthesis. *E. coli* cultures were grown in Luria-Bertani (LB) medium containing 50 mg/L ampicillin at 37 °C with constant shaking at 225 rpm. For PuA production, individual colonies of transformed yeast cells

were first grown in yeast nitrogen base (YNB) (Sigma Y-0626) medium supplemented with the appropriate amino acid drop-out mix and 2% raffinose for 24 h at 30 ºC with shaking at 225 rpm. Cells were then inoculated into an induction medium consisting of 10 mL YNB, 1.2 g/L ammonium sulfate, 1% raffinose, and 2% galactose in 50 mL tubes at an initial OD_{600} of 0.2. Inoculum for PuA accumulation experiments was grown for 48 h at 20 °C in an incubated shaker with constant shaking at 225 rpm. For LA feeding experiments, LA was first dissolved in ethanol and then mixed with an induction medium containing 0.1 % (v/v) tyloxapol to assist with its distribution.

3.2.2. Genes, plasmids, and yeast transformation

Genes encoding various desaturases, including pomegranate-derived *PgFADX*, *PgFAD2*, and *Acheta domesticus AdFAD2*, were synthesized by Twist Bioscience (San Francisco, USA) and codon-optimized for yeast expression. In order to obtain the template for cloning *FAD2*s from *Y. lipolytica* and *L. starkeyi*, total RNA was isolated from yeast cells at the mid-log phase using the RNeasy kit (Qiagen, Toronto, Canada), and cDNA was synthesized using the SuperScript IV first-strand cDNA synthesis kit (Invitrogen, Burlington, Canada). Putative gene sequences encoding pomegranate acyl-editing and TAG assembly enzymes were predicted through searches of deep sequencing data (unpublished data) of *P. granatum* seeds or by performing Blast searches using the publicly available draft genome of *P. granatum* (Luo et al., 2020), and then synthesized by Twist Bioscience. The resulting coding sequences were then inserted into the multiple cloning sites of pESC-Ura or pESC-Leu using conventional restriction-based cloning methods or the ClonExpress One Step Cloning Kit (Vazyme Biotech). Control strains used in this study consist of empty vectors pESC-Ura or pESC-Ura and pESC-Leu,

respectively. Yeast transformations were performed using the lithium acetate and PEG3350 method as described previously (Gietz and Schiestl, 2007a).

3.2.3. Lipid extraction and separation of lipid classes

Total lipids were extracted from yeast samples as described in our previous study (Mietkiewska et al., 2014). Briefly, yeast biomass was collected by centrifugation, washed, lyophilized, and suspended in 800 µL of cold lipid extraction mix consisting of chloroform, isopropanol (2:1, v/v) and antioxidant butylated hydroxytoluene at a final concentration of 0.01 %. Cells were then disrupted (3 × 1 min) using a bead beater (Biospec, Bartlesville, OK) with glass beads (diameter 0.5 mm) and 2 min cooling between each cycle. The organic phase from each sample was separated by centrifugation and collected. The extraction procedure for each sample was performed twice. The combined organic phase containing lipids was dried under a stream of nitrogen and resuspended in 200 µL cold chloroform. For the separation of lipid classes, single yeast colonies were inoculated into a 25 mL induction medium in 250 mL flasks for 48 h. Total lipids were extracted from lyophilized biomass and then separated on thin layer chromatography (TLC) plates (0.25 mm Silica gel, DCFertigplatten, Macherey-Nagel, Germany) with a solvent system containing hexane/ diethyl ether/ acetic acid (80: 20: 1) (Mietkiewska et al., 2014). Lipid fractions on the TLC plate were visualized through primulin staining, and bands corresponding to TAG and PC were scraped off, methylated, and analyzed by gas chromatography.

3.2.4. Fatty acid analysis

Lipid transmethylation was carried out using the base-catalyzed method with 1 mL of 5 % sodium methoxide dissolved in methanol with C17:0-TAG as the internal standard (Mietkiewska et al., 2014; Xu et al., 2020b). After incubation at 30 °C for 30 min, 1.5 mL of

0.9% (w/v) sodium chloride solution was added to stop the reaction, and fatty acid methyl esters (FAME) were extracted with 1 mL of chromatographic grade hexane. The hexane phase was collected, dried and FAMEs were then resuspended in 100 µL hexane and analyzed on an Agilent 6890N Gas Chromatograph (GC) equipped with a 5975 inert XL Mass Selective Detector (MS, Agilent Technologies) and flame ionization detector (FID) using the method described in our previous study (Xu et al., 2020b). Briefly, FAMEs were separated on a capillary column DB23 (30 m×0.25 mm×0.25 µm, Agilent Technologies, Wilmington, DE, USA) using the following program: 5:1 split ratio, 1 µL injection. 4 min at 165 °C, then increased to 180 °C (10 °C/ min) and held for 5 min, and increased to 230 °C and held for 5 min. Individual FAME peaks were identified by MS and further confirmed with the comparison with the authentic standards of FAMEs with various chain lengths and unsaturation degrees. Quantification of lipids was performed using the C17:0 triacylglycerol as the internal standard with the peaks measured with GC-FID.

3.2.5. Statistical analysis

Unless otherwise noted, all data represent the mean values of biological replicates ± SD (n=3). Statistical analyses were conducted with Student's *t*-test using the GraphPad Prism (v8) software.

Table 3.1. Strains used in this study

Strain name	Relevant genotype/property	Source
Escherichia coli DH5a	*endA1, recA1, gyrA96, thi-1, hsdR17, relA1, supE44 ΔlacU169, Φ80d lacZΔM15*	Invitrogen
Saccharomyces cerevisiae		
BY4741	*MATa, his3Δ1, leu2Δ0, lys2Δ0, ura3Δ0*	(Baker Brachmann et al., 1998)
ira2Δ	BY4741-*ira2::KanMX*	Euroscarf
snf2Δ	BY4741-*snf2::KanMX*	Euroscarf
snf1Δ	BY4741-*snf1::KanMX*	Euroscarf
tgl3Δ	BY4741-*tgl3::KanMX*	Euroscarf
pxa1Δ	BY4741-*pxa1::KanMX*	Euroscarf
pxa2Δ	BY4741-*pxa2::KanMX*	Euroscarf
PA0	BY4741/pESC-Ura-*PgFADX*	This report
PA1	BY4741/pESC-Ura-*PgFADX-PgFAD2*	This report
PA2	BY4741/pESC-Ura-*PgFADX-AdFAD2*	This report
PA3	BY4741/pESC-Ura-*PgFADX-YlFAD2*	This report
PA4	BY4741/pESC-Ura-*PgFADX-LsFAD2*	This report
PA5	BY4741-*ira2Δ*/pESC-Ura-*PgFADX-YlFAD2*	This report
PA6	BY4741-*snf2Δ*/pESC-Ura-*PgFADX-YlFAD2*	This report
PA7	BY4741-*snf1Δ*/pESC-Ura-*PgFADX-YlFAD2*	This report
PA8	BY4741-*ira2Δ*/pESC-Ura-*PgFADX*	This report
PA9	BY4741-*snf2Δ*/pESC-Ura-*PgFADX*	This report
PA10	BY4741-*snf1Δ*/pESC-Ura-*PgFADX*	This report
PA11	BY4741-*tgl3Δ*/pESC-Ura-*PgFADX-YlFAD2*	This report
PA12	BY4741-*pxa1Δ*/pESC-Ura-*PgFADX-YlFAD2*	This report
PA13	BY4741-*pxa2Δ*/pESC-Ura-*PgFADX-YlFAD2*	This report
PA14	BY4741-*tgl3Δ*/pESC-Ura-*PgFADX*	This report
PA15	BY4741-*pxa1Δ*/pESC-Ura-*PgFADX*	This report
PA16	BY4741-*pxa2Δ*/pESC-Ura-*PgFADX*	This report
PA17	PA6 with pESC-Leu-*PgPLA$_2$-PgLPCAT*	This report
PA18	PA6 with pESC-Leu-*PgDGAT2-PgLPCAT*	This report
PA19	PA6 with pESC-Leu-*PgDGAT2-PgPLA$_2$*	This report

PA20	PA6 with pESC-Leu-*PgDGAT2-PgPDCT*	This report
PA21	PA6 with pESC-Leu-*PgPDAT-PgPDCT*	This report
PA22	PA6 with pESC-Leu-*PgPDAT-PgLPCAT*	This report
PA23	PA9 with pESC-Leu-*PgPLA$_2$-PgLPCAT*	This report
PA24	PA9 with pESC-Leu-*PgDGAT2-PgLPCAT*	This report
PA25	PA9 with pESC-Leu-*PgDGAT2-PgPLA$_2$*	This report
PA26	PA9 with pESC-Leu-*PgDGAT2-PgPDCT*	This report
PA27	PA9 with pESC-Leu-*PgPDAT-PgPDCT*	This report
PA28	PA9 with pESC-Leu-*PgPDAT-PgLPCAT*	This report

3.3. Results and Discussions

3.3.1. Establishment of punicic acid synthesis in *Saccharomyces cerevisiae* via the heterologous expression of various *FATTY ACID DESATURASE 2* genes and exogenous linoleic acid supplementation

In order to produce baker's yeast containing PuA, we first expressed *PgFAD2* and *PgFADX* in *S. cerevisiae* BY4741 using single plasmid pESC-Ura under the control of the inducible promoters *GAL1* and *GAL10*, respectively, resulting in yeast strain PA1 (Table 3.1). As shown in Figure 3.1B, PA1 accumulated up to 6% and 0.3% of total fatty acids as LA and PuA, respectively, whereas the control strain harboring the corresponding empty plasmid did not synthesize LA and PuA. To further enhance PuA production in baker's yeast, we then assessed the performance of other *FAD2* genes in this context. To achieve this, we replaced *PgFAD2* in the pESC-Ura- *PgFADX-PgFAD2* construct with *FAD2*s originating from the insect *A. domesticus* as well as the oleaginous yeasts *Y. lipolytica* and *L. starkeyi*, and generated yeast strains PA2, PA3 and PA4, respectively (Table 3.1). The PA3 strain hosting *YlFAD2* was found to accumulate 8.5% of total fatty acids as LA, which was significantly higher than the other *FAD2*s; however, this construct did not lead to a higher PuA content (Figure 3.1B). As an

alternative approach, we also evaluated the effect of supplying a yeast strain bearing *PgFADX* with exogenous LA since this fatty acid serves as the precursor for PuA synthesis. In this case, we found that supplying BY4741 transformed with the pESC-Ura-*PgFADX* vector (strain designated as PA0) with 0.05% exogenous LA increased cellular LA to 60% and resulted in 1.3% of total fatty acids as PuA, which is more than 3-fold higher than the PA1-PA4 strains (Figure 3.1B). Since the PA0 strain with LA supplementation enhanced LA and PuA levels, and PA3 was found to accumulate a relatively high proportion of LA, the two corresponding constructs (pESC-Ura-*PgFADX* and pESC-Ura-*PgFADX*-*YlFAD2*) were selected for further analysis.

The expression of *FAD2* is considered to be important in this context since LA is a precursor for PuA synthesis and *S. cerevisiae* does not have the inherent ability to synthesize this polyunsaturated fatty acid. However, the co-expression of *PgFAD2* and *PgFADX* led to the production of low amounts of PuA, but relatively high levels of LA in yeast cells (Figure 3.1), which were below the levels observed in fission yeast *S. pombe* when *PgFAD2* and *PgFADX* were coexpressed (Garaiova et al., 2017). Although this study used yeast codon-optimized coding gene sequences, strong inducible promoters, and a high copy number plasmid for the expression of *PgFAD2* and *PgFADX*, the PgFADX could still be subjected to strong post-translational regulation. For example, when *Arabidopsis thaliana FAD2* and *FAD3* were expressed in yeast, AtFAD3 was more efficiently degraded by the yeast proteasome than AtFAD2 (Lou et al., 2014). Moreover, yeast post-translational regulation of *Brassica napus* and *Vernicia fordii* FAD3 has been found to be temperature-sensitive, where the half-life of FAD3 was much longer under low temperatures (O'Quin et al., 2010).

The comparison of three alternative FAD2s with PgFAD2 indicated that the heterologous expression of *YlFAD2* led to the production of the highest levels of LA (Figure 3.1B), which suggests that the FAD2 from this oleaginous yeast strain performed better than PgFAD2 in *S. cerevisiae*. Among the four FAD2s tested, AdFAD2 is known to be able to convert oleoyl-CoA to linoleoyl-CoA in the acyl-CoA pool (Borgeson and Blomquist, 1993; Cripps et al., 1990; Zhou et al., 2008). Since acyl chains esterified to various head groups are subject to dynamic acyl-editing (Bates et al., 2012), we hypothesized that LA produced in the acyl-CoA pool might be quickly moved to PC and used for PuA synthesis by PgFADX. However, AdFAD2 resulted in the lowest LA content (Figure 3.1B), indicating that newly synthesized linoleoyl-CoA might not be efficiently converted to 18:2-PC for PuA synthesis. It should be also noted here that the level of LA in *S. cerevisiae* was far below what was achieved previously in fission yeast over-expressing *PgFAD2* (Garaiova et al., 2017). This suggests that the production of LA is inefficient in budding yeast *S. cerevisiae*, which might be caused by the significant difference in the palmitoleic acid and oleic acid levels of these two yeasts or enhanced post-translational degradation of PgFAD2 protein in *S. cerevisiae* cells.

Although the co-expression of *FAD2* with *PgFADX* did lead to the production of LA and PuA in *S. cerevisiae*, LA supplementation led to a much higher accumulation of these two fatty acids (Figure 3.1B), indicating that precursor feeding is an effective approach to increase PuA production, which is consistent with previous reports focused on yeast *S. cerevisiae* (Hornung et al., 2002; Iwabuchi et al., 2003). Similar findings were obtained by Dyer et al. (2002) whereby the heterologous co-expression of tung tree *VfFAD2* and *VfFADX* in yeast led to significantly lower levels of α-eleostearic acid (the major UFA in tung tree seed oil) than when *VfFADX* was

expressed alone with supplementation with exogenous fatty acid precursor (0.3% vs. 2.1%, respectively) (Dyer et al., 2002).

3.3.2. Effects of *Saccharomyces cerevisiae* lipid metabolism regulators ('push') and triacylglycerol mobilization ('protect') genes on punicic acid synthesis

Fatty acid biosynthesis and accumulation in *S. cerevisiae* could be modulated by regulators such as *snf1*, which encodes an ADP-activated serine/threonine kinase, *snf2*, which encodes a general transcription factor involved in the regulation of lipid accumulation, and *ira2*, which encodes a GTPase-activating protein involved in glucose-induced signaling (He et al., 2018; Kamisaka et al., 2006, 2007a, 2013; Knoshaug et al., 2018; Seip et al., 2013). In this study, we tested the functions of *snf1, snf2,* and *ira2* in PuA synthesis. Yeast strains bearing deletions of *ira2*, *snf2,* and *snf1*, respectively*,* were transformed with the plasmid pESC-Ura-*PgFADX*-*YlFAD2*, resulting in strain PA5, PA6 and PA7, respectively (Table 3.1). The *snf2* or *snf1* mutation led to higher PuA content in strains PA6 and PA7 (Figure 3.2). In order to evaluate the effects of these transcription factors under LA feeding, we also constructed yeast strains PA8, PA9, and PA10 by transforming *ira2*, *snf2,* and *snf1* mutants with plasmid pESC-Ura-*PgFADX*. With supplementation of 0.05% LA, PA8 and PA9 also accumulated higher amounts of PuA than the control strain PA0 (Figure 3.2). PA9 possessing *PgFADX, snf2* deletion, and 0.05% LA feeding accumulated the highest PuA content (2.7%).

Since TAG is the final deposition site for various fatty acids including PuA, the deletion of genes related to TAG mobilization may partially block turnover of the PuA product and increase PuA content in yeast cells (Athenstaedt and Daum, 2003; Klug and Daum, 2014). In light of this, yeast mutants of TAG lipase (encoded by *tgl3*) and peroxisomal long-chain fatty acid importers (encoded by *pxa1* and *pxa2*), were transformed with pESC-Ura-*PgFADX*-*YlFAD2*

or pESC-Ura-*PgFADX*, respectively, resulting in six engineered strains (PA11-PA16, Table 3.1). Somewhat surprisingly, none of the gene deletions benefited overall PuA accumulation, regardless of LA feeding or not. Taken together, our results demonstrate that among the six tested genes encoding transcription factors and TAG mobilization, the *snf2* deletion leads to the greatest improvement of PuA accumulation in *S. cerevisiae*. As such, the remaining experiments were carried out using the *snf2Δ* strain (PA6 and PA9; Table 3.1).

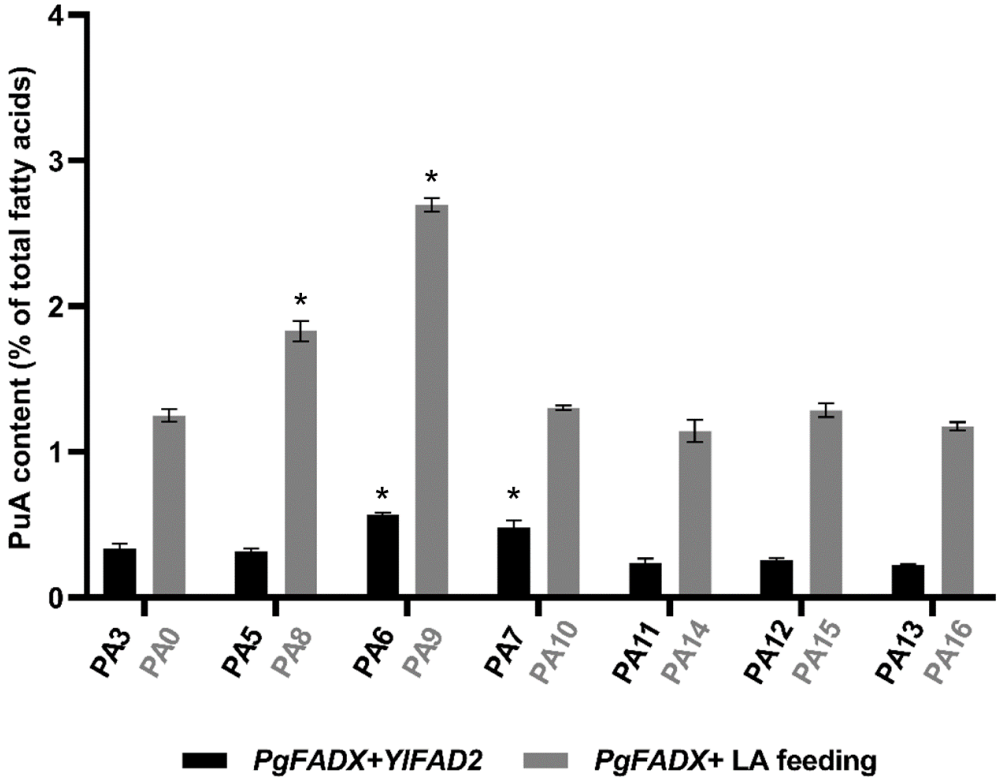

Figure 3.2. The disruption of the genes encoding lipid metabolism regulators led to improvements in punicic acid (PuA) content.

Strain names are listed in Table 3.1. Data represent means ± SD of three biological replicates. ∗, $P < 0.05$ (Student's t-test).

The heterologous biosynthesis of PuA in yeast may be regulated to a substantial degree by the native lipid metabolism of the host strain. Therefore, we further evaluated whether the 'Push' of fatty acid biosynthesis could enhance PuA production. The process of storage lipid accumulation involves complex interactions between carbon and energy relocation. Regulators such as Snf1p and Snf2p have been proven to be effective in increasing neutral lipid content in yeast in previous studies (Kamisaka et al., 2007a; Knoshaug et al., 2018). For instance, *SNF1* knockout in *Y. lipolytica* and *S. cerevisiae* significantly increased lipid accumulation (Knoshaug et al., 2018; Seip et al., 2013). *SNF1* encodes an ADP-activated serine/threonine kinase and plays an important role in yeast lipid synthesis (He et al., 2018; Knoshaug et al., 2018; Seip et al., 2013). In yeast cells, it controls carbon homeostasis and stress responses by regulating lipid synthesis and nitrogen metabolism (Chumnanpuen et al., 2012). Snf1p negatively controls the first committed step of fatty acid synthesis by directly phosphorylating and consequent inactivation of acetyl-CoA carboxylase (Mitchelhill et al., 1994; Usaite et al., 2009; Woods et al., 1994).

Moreover, *SNF2* is a transcription factor forming part of the SWI/SNF (switching/sucrose nonfermenting chromatin-remodeling) complex and a recent study showed that *snf2* knockout resulted in a significant increase of lipid content in *S. cerevisiae* (Kamisaka et al., 2007a). It is assumed that Snf2p might regulate the accumulation of phospholipids and storage lipids, and the incorporation of exogenous fatty acids into the *snf2*Δ mutant was found to be improved, suggesting potential regulation of fatty acid transporters by Snf2p (Kamisaka et al., 2006). All of the above characteristics are likely to be the cause of the increased PuA content in either FAD2-harboring strains or strains with exogenous LA feeding. To date, many metabolism regulators in model microorganisms have been annotated, however, only a few of them have been linked to

native lipid metabolism, let alone the heterologous synthesis of UFAs. Therefore, as demonstrated in this study, the use of metabolic engineering to study their function is of great significance to the rational design of recombinant yeast enriched in UFAs.

Our results indicate that among the three tested genes, the deletion of *snf2* increased the LA and PuA content in recombinant yeast expressing *PgFADX* (Table 3.2). Our results, along with reports that the *snf2* mutant can effectively incorporate exogenous fatty acids and increase lipid content in *S. cerevisiae* (Kamisaka et al., 2007a, 2010a), demonstrate that the 'Push' of fatty acid production by manipulation of endogenous transcription factors could be an effective approach to improve PuA production in yeast.

Table 3.2. Linoleic acid (LA) and punicic acid (PuA) content of recombinant yeast cells.

Strain	LA feeding	LA content	PuA content (% total fatty acids)
PA0	0.05%	59.6 ± 1.0	1.3 ± 0.04
PA9		73.4 ± 0.3	2.7 ± 0.1
PA27		66.4 ± 5.3	3.3 ± 0.2
PA28		64.2 ± 1.6	3.4 ± 0.02
PA3	-	8.5 ± 0.2	0.3 ± 0.03
PA6		8.1 ± 0.2	0.6 ± 0.02
PA21		15.4 ± 1.5	1.2 ± 0.2
PA22		17.3 ± 1.6	1.2 ± 0.1

3.3.3. Effects of pomegranate acyl-editing and triacylglycerol assembly genes ('pull') on punicic acid synthesis in *Saccharomyces cerevisiae*

Acyl-editing and TAG assembly processes play a pivotal role in the enrichment of UFAs in higher plants (Figure 3.3A) (He et al., 2004a, 2004b; Kroon et al., 2006; McKeon and He, 2015). The lack of such a specialized metabolic network in yeast could cause the retention of PuA in PC, which may trigger potential feedback inhibition and reduce the accumulation of PuA in storage lipids. To test the functions of related genes in PuA synthesis in yeast, five putative acyl-channeling genes from pomegranate, including *PLA$_2$*, *LPCAT*, *DGAT2*, *PDCT,* and *PDAT*, were synthesized and cloned into pESC-Leu in pairs. The resulting plasmids pESC-Leu-*PLA$_2$-LPCAT*, pESC-Leu-*DGAT2-LPCAT*, pESC-Leu-*DGAT2-PLA$_2$*, pESC-Leu-*DGAT2-PDCT*, pESC-Leu-*PDAT-PDCT*, and pESC-Leu-*PDAT-LPCAT* were then transformed into strains PA6 (BY4741-*snf2Δ*/pESC-Ura-*PgFADX-YlFAD2*) and PA9 (BY4741-*snf2Δ*/pESC-Ura-*PgFADX*), respectively, generating strains PA17-PA28 (Table 3.1).

In strains harboring *YlFAD2* and *PgFADX*, coexpression of acyl-editing and TAG assembly genes generally led to a 67% - 128% increase in PuA content (Figure 3.3B, Table 3.2). Among the genes assessed, strain PA22 bearing *PgPDAT* and *PgLPCAT* produced 17.3% and 1.23% of total fatty acid as LA and PuA, respectively. In contrast, improvements were less obvious when LA was acquired exogenously without the presence of *YlFAD2* (strains PA23-28). When compared to PA9, only PA27 and PA28 led to increases in PuA content (by 20%) with 0.05% LA supplementation (Figure 3.3B), accumulating the highest PuA levels of 3.3% and 3.4% of total fatty acids, respectively. While PuA contents in these two strains are similar, both exhibit levels that are 10 times higher than the starting strain PA1 heterologously expressing *PgFAD2* and *PgFADX* (0.3% of total fatty acids) (Figure 3.1 & 3.3).

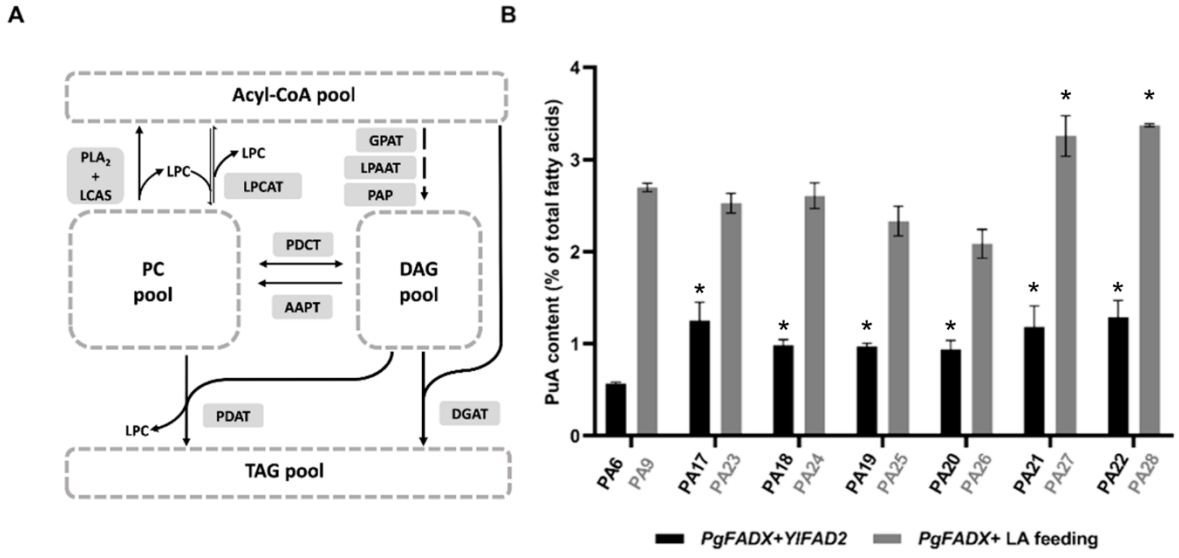

Figure 3.3. Introduction of pomegranate-derived acyl-channeling genes.

(A) Illustration of acyl-channeling process among different substrate pools. Abbreviations: AAPT, choline/ethanolamine phosphotransferase; DGAT, acyl-CoA: diacylglycerol acyltransferase; GPAT, glycerol-3-phosphate acyltransferase; LACS, long-chain acyl-CoA synthetase; LPAAT, lysophosphatidic acid acyltransferase; LPC: lysophosphatidylcholine; LPCAT: lysophosphatidylcholine acyltransferase; PAP, phosphatidic acid phosphatase; PC, phosphatidylcholine; PDAT, phospholipid: diacylglycerol acyltransferase; PDCT, phosphatidylcholine: diacylglycerol cholinephosphotransferase PLA_2, phospholipase A_2; (B) Introducing pomegranate-derived acyl-channeling genes moderately increased PuA content. Strain names are listed in Table 3.1. Data represents the mean values of biological replicates ± SD (n=3). ∗, $P < 0.05$ (Student's t-test).

Given the importance of PuA channeling from PC to TAG, we further examined the distribution of PuA in lipid fractions in our engineered yeast cells. In PA9, PuA accounted for 6.3% and 1.4% of total fatty acids in PL and TAG fractions, respectively (Figure 3.4A). In strain PA27, the relative PuA content in TAG was increased by 50%, compared with PA9 ($P< 0.05$; Figure 3.4A). When comparing the two strains accumulating the highest amounts of PuA in cells, the co-expression of *PgPDAT* and *PgPDCT* (PA27) led to a higher proportion of PuA in TAG than the co-expression of *PgPDAT* and *PgLPCAT* (PA28) (Figure 3.4A). Similar results were also observed in lipid samples extracted from strains heterologously expressing *YlFAD2* without LA feeding (PA6 and PA21). Although PuA contents in both TAG and PL fractions were less than 0.5% of total fatty acids in these strains, the co-expression of *PDAT* and *PDCT* (PA21) still increased PuA proportions by 65% and 87% in TAG and PL fractions, respectively (Figure 3.4B).

PuA is synthesized on the membrane lipid PC but is deposited in the storage lipid TAG in pomegranate seeds (Mietkiewska et al., 2014), and a similar scenario is seen with the accumulation of many other UFAs in higher plants (Cahoon and Li-Beisson, 2020; Napier, 2007). The channeling of UFAs from PC to TAG (the "Pull" of PuA assembly into TAG) has been considered a major bottleneck in the heterologous synthesis of UFAs, and the expression of related genes from native producers of the UFA in transgenic plants has been shown to be an effective approach to increase production (Cahoon and Li-Beisson, 2020; Napier, 2007). In this study, we assessed whether the co-expression of pomegranate genes involved in acyl-editing and TAG assembly could increase PuA content in engineered yeast. The expression of all different combinations of the selected genes, along with *YlFAD2* and *PgFADX*, effectively increased PuA content in our system (Figure 3.3B), suggesting that this approach also works well for PuA

production in yeast. The beneficial effect of acyl-channeling genes on strains supplemented with exogenous LA was less obvious. Only the combination of *PDAT+LPCAT* and *PDAT+PDCT* increased PuA content (Figure 3.3B) by approximately 2- to 4-fold times higher compared to previous reports (Hornung et al., 2002; Iwabuchi et al., 2003). In future studies, it would be interesting to further characterize the channeling of UFAs from PC to TAG. In addition, a detailed analysis of PuA distribution in lipid classes with lipidomic would expand our understanding of PuA channeling among lipid classes and shed light on novel strategies to channel PuA to TAG by engineering the related genes.

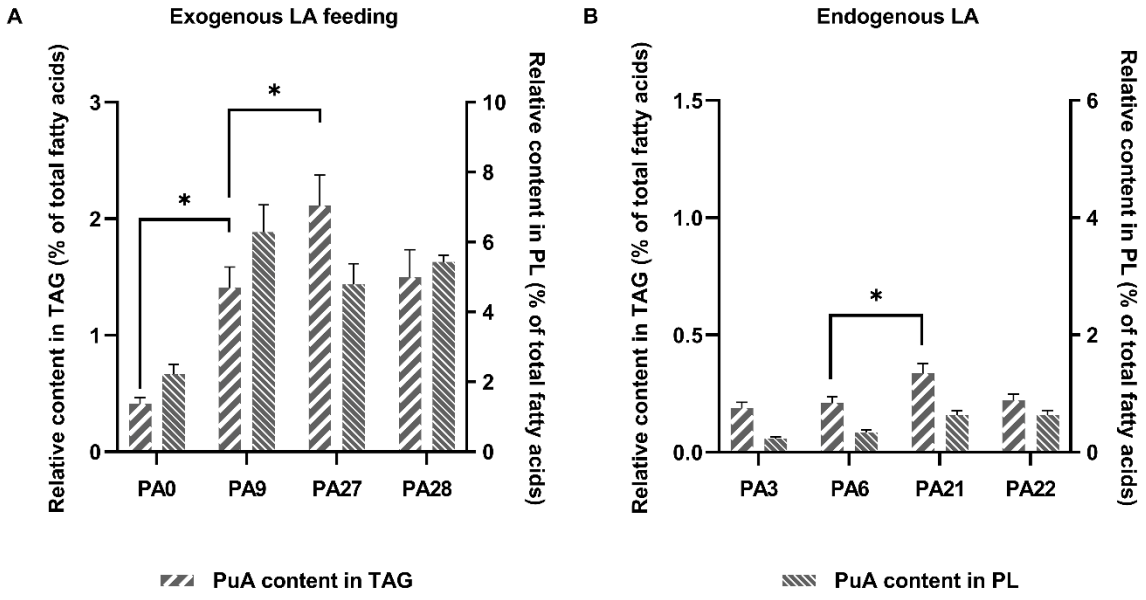

Figure 3.4. Relative punicic acid (PuA) content in TAG and polar lipids extracted from recombinant yeast cells with linoleate (LA) supplementation or co-expression with *YlFAD2*. Strain names are listed in Table 3.1. The data shown represent the mean values of biological replicates ± SD (n=3). ∗, $P < 0.05$ (Student's t-test).

Further analysis of PuA content in TAG and PL lipid classes indicated that although the co-expression of both *PgPDAT*+ *PgPDCT* and *PgPDAT*+ *PgLPCAT*, respectively, can increase PuA content with or without LA supplementation (Figure 3.3), the former performed better than the latter in terms of channeling PuA from PC to TAG (Figure 3.4). In addition, we noticed that upon LA supplementation, the content of LA in engineered *S. cerevisiae* reached approximately 60% in PL fraction which is much higher compared to LA level in cells over-expressing *FAD2*. Although a comparable high level of endogenous LA in *S. pombe* cells can be achieved by over-expressing *PgFAD2*, only a moderate increase in PuA (25%) was observed (Garaiova et al., 2017). Taken together, our results indicate that different genes and gene combinations may provide distinct contributions to PuA accumulation in different yeast species. Moreover, many enzymes catalyzing plant lipid biosynthesis actively interact with and influence each other. Therefore, complex plant metabolomes and interactomes may likely work in concert with UFA enrichment in TAG (Bates et al., 2014; Cahoon et al., 2006; Cahoon and Li-Beisson, 2020). Given the multifaceted nature of the acyl-channeling apparatus, single gene expression or a simple combination of genes cannot fully transfer PuA biosynthesis from pomegranate to yeast. Further studies such as the shuffling of plant-derived acyl-channeling genes and interactomes from the native PuA producer to yeast may provide more comprehensive solutions for producing PuA, as well as other UFAs, in *S. cerevisiae*.

PuA has great potential in nutraceutical, pharmaceutical, and oleochemical applications due to its three conjugated double bonds and the associated strong antioxidant, antidiabetic, anticancer, anti-obesity, and anti-inflammatory bioactivities. However, its production is severely limited due to the fact that the major natural source of PuA is pomegranate seed oil, which is not readily available on a large scale (Holic et al., 2018). Similar to other UFAs and high-value

bioproducts, it is thus attractive to provide a stable and economical supply of PuA in engineered microorganisms. To achieve this objective, it will be of critical importance to expand our knowledge of PuA accumulation in yeast and to use this information in the design of effective metabolic engineering strategies. Therefore, we evaluated the combination of various metabolic engineering strategies for engineering PuA production in *S. cerevisiae* and found that a 'Push-Pull' approach with the combination of *snf2* deletion, along with the heterologous expression of *PgFADX*, *PgPDAT,* and *PgPDAT/LPCAT*, and supplementation with 0.05% LA in the culture medium resulted in approximately 3.4% of total fatty acids as PuA. This was a 10-fold increase compared to the background yeast strain heterologously expressing *PgFAD2* and *PgFADX*, and approximately two to four-fold enhancement compared to previous reports focused on *S. cerevisiae* (Iwabuchi et al., 2003). Although the content of LA in strains with precursor feeding (PA23-PA28) largely remains the same, in strains coexpressing *YlFAD2* (PA17-PA22), engineering genes in acyl channeling processes seems to improve the content of both LA and PuA (Table 3.2, Supplementary Table S3.1). After incubation, yeast cultures with exogenous LA accumulated higher lipid content and slightly less biomass compared to yeast coexpressing *YlFAD2*, possibly due to the inhibition from the high concentration of fatty acid feeding (Supplementary Table S3.1). Taken together, the dry cell weight of strain PA28, which accumulates the highest PuA content, is 1.7 mg/mL culture and the total lipid content is around 12.6%, which corresponds to 7.2 μg/mL PuA of liquid culture.

Nevertheless, the percentage of PuA in total fatty acids was relatively low and was also lower than LA (Figure 3.1), suggesting the conversion rate of LA to PuA by PgFADX is modest in *S. cerevisiae*. Since the expression of PgFADX in *Arabidopsis* and fission yeast results in over 20% of total fatty acids as PuA, the catalytic ability of PgFADX itself should be acceptable, and

the low percentage of PuA might be due to other issues with the baker's yeast platform. These potential issues could be rather complex, including but not limited to post-transcriptional regulatory apparatus targeting FAD2-like enzymes in baker's yeast, rapid PuA turnover, cellular localization of PgFADX, its spatial distance to LA storage sites, and the inefficient incorporation of PuA into TAG. In this study, we investigated PuA synthesis in baker's yeast mutants to address this issue and found that the disruption of genes encoding master regulators that modulate multiple metabolic pathways can significantly improve the content of PuA.

3.4. Conclusions

In summary, we engineered *S. cerevisiae* to produce PuA as a means of expanding our knowledge in the context of generating this high-value unusual fatty acid in baker's yeast. Among the genes tested, a 'Push-Pull' approach by combining the disruption of *snf2* with the heterologous expression of *PgFADX*, *PgPDAT,* and *PgLPCAT,* along with the feeding of 0.05% LA, resulted in *S. cerevisiae* cells yielding 3.4% of total fatty acids as PuA. To further improve PuA production in baker's yeast, subsequent studies are required, including the evaluation of PgFADX enzymatic activity and enzyme engineering, its subcellular localization and stability, coupled with comprehensive metabolic engineering of PgFADX and other genes in lipid biosynthesis and accumulation, and carbon fluxing. Moreover, the strain used in the current proof-of-concept study is a common laboratory baker's yeast strain with four auxotrophic markers in its genome to facilitate genetic manipulation. By transferring the knowledge reported in this study to other yeast species, especially oleaginous yeast species such as *Y. lipolytica*, the generation of industrial-level PuA-producing yeast strains may be possible following optimization.

3.5. Supplementary material

Supplementary Table S3.1. Fatty acid precursor contents, dry cell weight, and total fatty acid content of recombinant yeast cells.

The values represent the average of three independent experiments ± standard deviation.

Abbreviations: FA, fatty acids; OA, oleic acid; LA, linoleic acid; PuA, punicic acid; DCW, dry cell weight.

Strain	FA (% of total fatty acid)			DCW (mg/mL)	Total FA (% of DCW)
	OA	LA	PuA		
			Endogenous LA		
PA6	36.0 ± 1.0	8.1 ± 0.2	0.6 ± 0.02	2.5 ± 0.4	7.9 ± 0.6
PA17	34.5 ± 1.8	17.5 ± 1.8	1.3 ± 0.2	1.7 ± 0.1	7.9 ± 0.6
PA18	33.3 ± 0.1	14.0 ± 0.4	1.0 ± 0.1	2.4 ± 0.1	10.1 ± 1.0
PA19	33.0 ± 0.3	14.1 ± 0.4	1.0 ± 0.03	2.4 ± 0.2	8.3 ± 0.6
PA20	32.6 ± 0.2	14.4 ± 0.3	0.9 ± 0.1	2.4 ± 0.1	9.1 ± 0.7
PA21	32.5 ± 0.3	15.4 ± 1.5	1.2 ± 0.2	2.1 ± 0.1	8.0 ± 1.5
PA22	33.0 ± 0.7	17.3 ± 1.6	1.3 ± 0.2	1.9 ± 0.2	6.8 ± 1.4
			LA feeding		
PA9	4.6 ± 0.1	73.4 ± 0.3	2.7 ± 0.1	2.2 ± 0.1	14.3 ± 1.0
PA23	10.4 ± 0.8	63.6 ± 1.8	2.5 ± 0.1	1.6 ± 0.1	11.2 ± 0.8
PA24	11.4 ± 0.5	62.1 ± 1.0	2.6 ± 0.1	1.8 ± 0.2	13.0 ± 1.0
PA25	11.3 ± 1.3	63.8 ± 2.6	2.3 ± 0.2	2.0 ± 0.1	12.0 ± 1.2
PA26	15.6 ± 2.0	56.7 ± 2.5	2.1 ± 0.2	2.1 ± 0.1	13.5 ± 1.7
PA27	10.4 ± 0.9	66.4 ± 5.3	3.3 ± 0.2	2.0 ± 0.2	11.7 ± 0.5
PA28	9.9 ± 1.0	64.2 ± 1.6	3.4 ± 0.02	1.7 ± 0.2	12.6 ± 0.9

Chapter 4 – Optimization of Pomegranate-Derived Punicic Acid Accumulation in *Saccharomyces cerevisiae* by Ty Retrotransposon-Targeted Random Gene Shuffling

4.1. Introduction

In addition to the key enzymes that directly catalyze the synthesis of PuA, pathways upstream and downstream of PuA synthesis in transgenic hosts may not effectively synergize with each other to achieve optimal production. Since *S. cerevisiae* has a relatively simple lipid profile and contains no LA (Sec et al., 2015), an efficient supply of the LA precursor is crucial for converting this model yeast into a PuA-producing platform (Wang et al., 2021). Moreover, the enrichment of UFAs in plant oils involves a series of enzymatic reactions that occur in developing seeds (Cahoon and Li-Beisson, 2020; Napier, 2007; Chen et al., 2022; Wickramarathna et al., 2015; Demski et al., 2022). These reactions form the acyl-editing and TAG assembly network, which dominates the flow of UFAs from phospholipids into TAG for their stable storage in lipid droplets.

Given that the presence of this network efficiently enhances UFA accumulation in plant seeds, it is not surprising that UFA levels in the seed TAG of natural producers are significantly higher than in engineered transgenic hosts (da Silva Ramos et al., 1984; Kaufman and Wiesman, 2007; Khoddami et al., 2014; McKeon et al., 2016; Mietkiewska et al., 2014; Paul and Radhakrishnan, 2020; Román-Figueroa et al., 2020; Takagi and Itabashi, 1981; Xu et al., 2020b). In line with this, while PuA is the major fatty acid species in pomegranate seed TAG, engineered *Brassica napus* and *Arabidopsis thaliana* only accumulate 6.6% and 10.6% of PuA in seed TAG fractions, respectively (Mietkiewska et al., 2014; Xu et al., 2020b). Given the complexity of the pathways involved in plant-derived UFA synthesis, it is time-consuming to test each gene separately to achieve pathway functionality, and even more challenging to efficiently obtain the

best gene combination for their transgenic production. Thus, a more effective process is required to facilitate the study of plant UFA metabolism and the heterologous synthesis of plant-derived lipids in microorganisms.

The objective of this study, therefore, was to develop a rapid and efficient workflow for producing PuA in the model yeast *S. cerevisiae*, which would shed light on the production of other high-value plant-derived UFAs. By targeting the locations of yeast Ty retrotransposons, the current study directly shuffled genes that potentially contribute to PuA synthesis in the yeast genome and generated a recombinant yeast library with various contents of PuA. After screening 1752 strains, a recombinant *S. cerevisiae* strain capable of accumulating 26.7% of total fatty acids as PuA was obtained without the need for LA precursor feeding, which, to the best of our knowledge, is the highest PuA content achieved in engineered microorganisms to date. In shake flask cultivation, the PuA titer reached 424.6 mg/L. Subsequent analysis identified the presence of a *PgFADX*-containing expression cassette, as well as genes encoding pomegranate phosphatidylcholine: diacylglycerol cholinephosphotransferase (PgPDCT), lysophospholipid acyltransferase (PgLPCAT), acyl-CoA: diacylglycerol acyltransferase 2 (PgDGAT2), PgFAD2 and fatty acid elongase from *Rattus norvegicus* (RnELO2), indicating the workflow efficiently identified a yeast strain with a preferred gene combination. Furthermore, lipidomic and positional analyses revealed substantial changes in the yeast lipidome resulting from PuA synthesis, where PuA comprised over 22% of total fatty acids in the TAG fraction of yeast single-cell oil, which is much higher than that in transgenic *A. thaliana* and *B. napus* (Mietkiewska et al., 2014; Xu et al., 2020b).

4.2. Materials and methods

4.2.1. Strains, genes, and plasmids

All strains used in this study are listed in Table S4.7. In brief, *Escherichia coli* DH5α was used for routine plasmid construction and preparation. *S. cerevisiae* BY4741- *snf2Δ* obtained from the Euroscarf collection was used as the starting strain in this study. *S. cerevisiae* H1246 quadruple mutant lacking lipid biosynthetic ability was used to test the performance of pomegranate genes. Yeast transformations were performed using the traditional lithium acetate and PEG3350 method as described previously (Gietz and Schiestl, 2007b). To obtain the template for cloning TAG assembly and acyl-editing genes from *P. granatum*, total RNA was isolated from *P. granatum* tissues using the Spectrum Plant Total RNA Kit (Sigma-Aldrich, Oakville, Canada) and cDNA was synthesized using the SuperScript IV first-strand cDNA synthesis kit (Invitrogen, Carlsbad, USA). Putative sequences coding for pomegranate acyl-editing and TAG assembly enzymes were obtained by performing an NCBI Basic Local Alignment Search Tool (BLAST) search against the online draft genome of *P. granatum* (Luo et al., 2020). The target Ty retrotransposon region was analyzed based on the S288C reference genome from the *Saccharomyces* Genome Database (SGD) (http://www.yeastgenome.org/). Similarity and identity searches for target sequences in Ty retrotransposons were conducted using BLAST. Plasmids providing donor DNA were derived from pUC19. Four components, including upstream homology sequence, gene expression cassette, selection marker with truncated promoter region (*leu2*, *his3*, and *ura3* for round 1, 2, and 3 integrations, respectively), and downstream homology sequence were inserted. To release donor DNAs from the pUC19 backbone, either PCR or double digestion of SmaI sites flanking the donor DNA was conducted. For different genes, 500 fmol of each donor DNA were pooled together. To facilitate integration,

CRISPR/Cas9 expression vectors (based on plasmid pCRCT, obtained from Addgene, plasmid #60621) targeting different locations on Ty retrotransposons were constructed and co-transformed into yeast cells with donor DNA (Bao et al., 2015). Three 20bp sequences that are adjacent to the PAM sites that occur frequently in the respective target regions were selected as the spacer sequences for delivering crRNA (Table S4.8). These sequences were ordered as single-stranded, complementary oligos and annealed to obtain double-stranded DNAs. By adding homology arms, these sequences were inserted between two Eco31I restriction sites on the pCRCT plasmid.

4.2.2. Culture conditions and optimization

For plasmid construction and preparation, *E. coli* was cultured at 37 °C in the Luria-Bertani (LB) medium with shaking at 225 rpm. To sustain the plasmids in *E. coli*, 100 mg/L ampicillin was applied. For testing PuA accumulation in shake flask cultivation, individual colonies of transformed yeast cells were first grown in 5 mL yeast nitrogen base (YNB) supplemented with an appropriate amino acid drop-out mix and 2% glucose for 24 h at 30 °C with shaking. Seed cultures were then inoculated into 1 L shake flasks containing 60 mL synthetic complete medium (6.7 g/L YNB, 2 g/L synthetic complete supplement mixture of amino acids, and 6% glucose). The inoculum for PuA production experiments was grown for 72h at 20 °C or 30 °C, using an incubated shaker with a shaking speed of 250 rpm. For culture condition optimization, the Box–Behnken design was employed for response surface methodology. The factors considered for optimization included carbon level (X1), initial pH (X2), and initial OD_{600}. They were examined at three levels (6%, 10.5%, and 15% for glucose; 5.3, 6.5, and 7.6 for initial pH; 0.2, 0.6, and 1 for initial OD_{600}). The two responses considered for analysis were PuA content (% of total fatty acids) and PuA titer (mg/L). Based on the results,

second-order polynomial equations were fitted to predict the optimal points within experimental constraints (Table S4.6).

4.2.3. **Preparation of plant oil hydrolysate and fatty acid feeding**

Preparation of free fatty acids from pomegranate seed oil was conducted using chemical hydrolysis (Salimon et al., 2011). In brief, 50 g of pomegranate seed oil was mixed with 12 g potassium hydroxide, 117 mL pure ethanol, and 35 mL H_2O in a shake flask flushed with nitrogen. 1.65 mL of butylated hydroxytoluene (BHT) solution (50 mg/mL) was added to the mixture to protect PuA. The reactor was then sealed and maintained at 50 °C with constant shaking. After 1 hour of incubation, removal of the unsaponifiable matter was performed three times by mixing 100 mL of distilled water and 100 mL of hexane. Free fatty acids were extracted with 100 mL hexane and dried over anhydrous sodium sulfate. The solvent was then removed under vacuum to obtain pomegranate oil hydrolysate. When fatty acid feeding was required, 0.03% v/v ethanol dissolved LA or pomegranate oil hydrolysate was supplemented to the culture medium along with 0.2% non-ionic surfactant NP-40 (TERGITOL™ solution) for even distribution of fatty acid in the aqueous medium.

4.2.4. Nile red staining of neutral lipids in yeast

Nile red fluorescence detection was conducted as described previously (Pan et al., 2013). Briefly, 100 µl aliquots of the yeast cell suspension were transferred to a 96-well dark flat-bottom plate. Background fluorescence was measured using a Synergy H4 Hydrid multimode microplate reader (Biotek Instrument, Inc.) with emission and excitation filters set to 485 and 538 nm, respectively. A newly prepared methanolic Nile red solution (0.1 mg/mL) was added,

and the second fluorescence intensity was measured. The Nile Red values were calculated based on the change in fluorescence over OD_{600} ($\Delta F/OD_{600}$).

4.2.5. Lipid extraction and separation of lipid class using TLC

Prior to lipid extraction, yeast biomass was harvested from liquid culture via centrifugation. The supernatant was then removed and 800 µL of a cold lipid extraction mixture comprising chloroform and isopropanol (2:1, v/v) was added, along with glass beads (0.5mm) and BHT at a final concentration of 0.01%. Subsequently, cellular disruption was achieved through three cycles of bead beating (1-minute duration each) using a Biospec bead beater (Biospec, Bartlesville, OK), with 2-minute cooling on ice between each cycle. The extraction procedure was repeated twice for each sample. The collective organic phase, containing both polar lipids and TAG, was dried under nitrogen and resuspended in 200 µl chloroform.

For lipid class analysis, the lipid extracted from each sample was separated using TLC with silica gel-coated plates (0.25 mm Silica gel, DCFertigplatten, Macherey-Nagel, Germany). The TLC plates were developed using a solvent mixture comprising hexane/diethyl ether/acetic acid (in a 70:30:1 ratio) (Xu et al., 2020b). Lipid fractions on the TLC plate were visualized via 0.05% primulin staining under UV light. Bands corresponding to target lipid fractions were scraped, extracted, derivatized, and subsequently analyzed.

4.2.6. Positional analysis of TAG and polar lipids

The fatty acid distribution between *sn-2* and *sn-1/3* TAG was analyzed using previously described enzymatic reactions (Luddy et al., 1964; Xu et al., 2020b). Briefly, after TLC separation, TAG was recovered from the silica gel, and dried under nitrogen. Subsequently, 1 mL Tris-HCl buffer (1 mM, pH 8.0), 100 µL 2.2% $CaCl_2$, and 250 µL 0.1% deoxycholate was added.

Each mixture was vortexed for 2 minutes and sonicated for 60 seconds to emulsify the lipid. The mixture was pre-warmed in a water bath at 40 °C for 30 s, and then 20 mg pancreatic lipase (pancreatic lipase type II, Sigma) was added to initiate hydrolysis. The mixture was further incubated for 3 min at 40 °C, and the reaction was terminated by adding 500 μL of 6 M HCl. The resulting lipids, containing unreacted TAG, DAG, monoacylglycerol (MAG), and free fatty acids, were extracted twice with 3 mL of diethyl ether and then separated using TLC. The *sn-2* MAG was subsequently analyzed.

The positional analysis of polar lipids was performed by cleaving the fatty acids at the *sn-1* position of polar lipids using phospholipase A1 (Vikbjerg et al., 2006; Xu et al., 2020b). In brief, phospholipase A1 was first mixed with water in a 1:4 (v/v) ratio. Polar lipids were recovered from the silica gel and dissolved in 2 mL of diethyl ether, and 1 mL of phospholipase A1 (Sigma) solution was added to initiate hydrolysis. The mixture was then vortexed at maximum speed for 5 min and the reaction was terminated by evaporation of diethyl ether under nitrogen. The hydrolyzed lipids were extracted and separated by TLC, and cleaved fatty acids were subsequently analyzed.

4.2.7. Lipid transmethylation, analysis and lipidomic profiling

To prepare fatty acid methyl esters (FAMEs), transmethylation was carried out via a base-catalyzed method using 1 mL of 5% sodium methoxide dissolved in methanol (Mietkiewska et al., 2014). After incubation at 30 °C for 1 hour, the reaction was stopped by adding 1.5 mL of 0.9% (w/v) sodium chloride solution. Fatty acid methyl esters were then extracted with 1 mL of hexane. Subsequently, the FAMEs were analyzed on an Agilent 6890N Gas Chromatograph equipped with a 5975 inert XL Mass Selective Detector and Flame Ionization Detector (Agilent Technologies) using a method described in our previous study (Wang et al., 2021). Briefly,

FAMEs were separated on a capillary column DB23 (30 222 m×0.25 mm×0.25 μm, Agilent Technologies, Wilmington, DE, USA) using the following program: 2:1 split ratio, 1 μL injection. 4 min at 165 °C, then increased to 180 °C (10 °C/ min) and held for 5 min, and increased to 230 °C and held for 5 min. The lipidomic analyses described in this work were performed at the Kansas Lipidomic Research Center analytical laboratory. The lipidome of four chosen yeast strains was investigated. In the analyses, four cultures of each yeast strain were used as replicates. All biological replicates were cultured under the same conditions, and samples were collected after 96h.

4.3. Results and Discussion

4.3.1. Functional validation of pomegranate TAG-assembly genes in yeast and construction of PgFADX variants

Acyl-editing and TAG assembly pathways are important biochemical processes involved in the modification of fatty acids in plants, particularly in those that produce UFAs (Figure 4.1A). Within these pathways, specialized enzymes collaborate to modify and exchange specific acyl groups, redistributing them across various lipid pools and enriching the target fatty acid within the TAG fraction (Cahoon and Li-Beisson, 2020). Since most pomegranate enzymes involved in TAG biosynthesis have not been verified functionally, we first identified and isolated genes encoding acyl-editing and TAG-synthesizing enzymes from pomegranate. As shown in Table S4.1, enzymes from tung tree (*Vernicia fordii*), castor bean (*Ricinus communis*), and flax (*Linum usitatissimum*) that are involved in the synthesis of UFAs or PUFAs were used as queries. Results indicated the presence of three pomegranate DGAT2s, three phospholipid: diacylglycerol acyltransferases (PDATs), and one DGAT1, PDCT, LPCAT, glycerol-3-phosphate acyltransferase 9 (GPAT9), lysophosphatidic acid acyltransferase 2 (LPAT2),

phospholipase A2 (PLA2), phospholipase C (PLC), and long-chain acyl-CoA synthetase 8 (LACS8), respectively.

In previous studies in plants, PDAT and DGAT have often been the subject of investigation owing to their direct contribution to the final step of TAG synthesis (Chen et al., 2022; Xu et al., 2018a). Given their critical roles, we first conducted a functional validation assay of these proteins. Genes encoding PgDGAT1, PgDGAT2.a, PgDGAT2.b, PgDGAT2.c, PgPDAT.a, PgPDAT.b, and PgPDAT.c were cloned from pomegranate cDNA and transformed into *S. cerevisiae* mutant strain H1246. H1246 is a yeast quadruple mutant that lacks genes that encode yeast native DGAT, PDAT, and acyl-CoA: sterol acyltransferases, and is thus devoid of TAG synthesizing ability (Sandager et al., 2002; Siloto et al., 2009). As such, expressing heterologous TAG assembly enzymes in this yeast mutant will result in the reconstitution of TAG biosynthesis if the enzyme is fully functional. As shown in Figure 4.1B, after 72h culture, yeast cells expressing *PgDGAT1*, *PgDGAT2.a*, and *PgDGAT2.b* produced strong TAG bands, suggesting their strong complementary activity in restoring TAG synthesis using yeast native fatty acids.

Moreover, since pomegranate contains high levels of PuA, it is plausible to assume that pomegranate-derived TAG assembly enzymes may have evolved a preference for PuA-containing substrate. Therefore, to further evaluate their abilities, recombinant yeast strains were cultured in the presence of exogenously added pomegranate oil hydrolysate which contains free PuA. Interestingly, pomegranate PgDGAT2.c and PgPDAT.a produced weak TAG bands when pomegranate oil hydrolysate was provided (Figure 4.1C). It is also worth noting that PgDGAT2.a, PgDGAT2.b, and PgDGAT2.c produced TAG with higher unsaturation levels, which have a slower migration rate on the thin layer chromatography (TLC) plate. Subsequent

GC-FID analysis of the TAG bands confirmed a reduction of saturated fatty acid (SFA) content in cells expressing *PgDGAT2* compared to those expressing *PgDGAT1* (Figure 4.1D). When pomegranate oil hydrolysate was added to the culture, PuA accounted for over 20% of the TAG fraction of strain expressing *PgDGAT2.c*, which suggested that this enzyme might prefer substrates containing PuA. While yeast has been extensively used as a model organism to study TAG assembly genes in plant species, it has been shown that some plant-derived enzymes accumulate poorly in yeast cells (Pan et al., 2013). This could potentially account for the unsuccessful complementation of PgPDAT.b and c to TAG synthesis in H1246, and the lower activity of PgDGAT2.c and PgPDAT.a compared to PgDGAT1 when free PuA was supplied.

Various protein fusions have been used to enhance enzyme performance in metabolic engineering efforts (Andre et al., 2013; Jia et al., 2015; Xu et al., 2020a). For instance, our previous study revealed that fusing algal DGAT with an acyl-CoA binding protein, which attracts the substrates for DGAT-catalyzed reactions, led to a kinetic improvement of the enzyme (Xu et al., 2020a). Additionally, protein fusion can also be used to remove harmful byproducts, as shown in a previous study where combining aldehyde deformylating oxygenase with catalase alleviated inhibition from H_2O_2 accumulation (Andre et al., 2013; Jia et al., 2015). Therefore, selected sequences encoding phosphatidylcholine-binding protein (SCP2), oxygen carrier-protein (Vhb), soluble domain of electron transporter (CB5SD) or catalase (CAT) were cloned and linked with PgFADX by a flexible peptide linker since PC is the substrate for PgFADX (Iwabuchi et al., 2003), molecular oxygen and electrons are needed for the desaturase-like enzyme activity (Pugh and Kates, 1979; Yazawa et al., 2010), and H_2O_2 may inhibit the activity of desaturase-like enzyme (Browse and Slack, 1981). The expression cassettes containing these protein fusions were transformed into the BY4741 *snf2Δ* mutant, which exhibits an elevated

level of fatty acid synthesis (Chumnanpuen et al., 2012; Kamisaka et al., 2010b, 2007b). As shown in Figure 4.1E, except for the fusion with catalase, all other PgFADX variants showed a slight increase in PuA levels. Given the larger size of catalase compared to other proteins, it is possible that combining this enzyme with FADX potentially disrupted the structure of PgFADX. In addition, we also constructed a BY4741 *snf2Δ snf1Δ* double knockout mutant by replacing the *snf1* gene with an *AtSCP2-PgFADX* expression cassette. Yeast SNF1 (Sucrose Non-Fermenting 1) is a protein kinase and master regulator that plays a critical role in regulating yeast energy metabolism and glucose homeostasis (Seip et al., 2013; Usaite et al., 2009). SNF1 is activated when the ATP level *in vivo* is low, leading to the degradation of storage lipids and the inhibition of lipid synthesis (Mayer et al., 2011). As shown in Figure 4.1E, when *AtCB5SD-PgFADX* was expressed in this strain background, PuA accounted for 6.2% of total fatty acids.

In addition to the proposed function, modifications to the N-terminus of PgFADX may also influence the turnover rate of this key enzyme. For instance, a previous study showed the N-terminal sequences of *Brassica* and tung tree fatty acid desaturase 3 (FAD3) proteins confer a rapid degradation of a fluorescent reporter in both plant and yeast cells (Khuu et al., 2011; O'Quin et al., 2010). For FAD2 expression, the N-terminus also plays an important role in controlling the protein half-life (Tang et al., 2005). Given the structural similarities between various UFA-producing enzymes and FAD2, further characterization of their protein half-life in transgenic plant and yeast cells could aid in the design of a more stable enzyme, thereby improving UFA production.

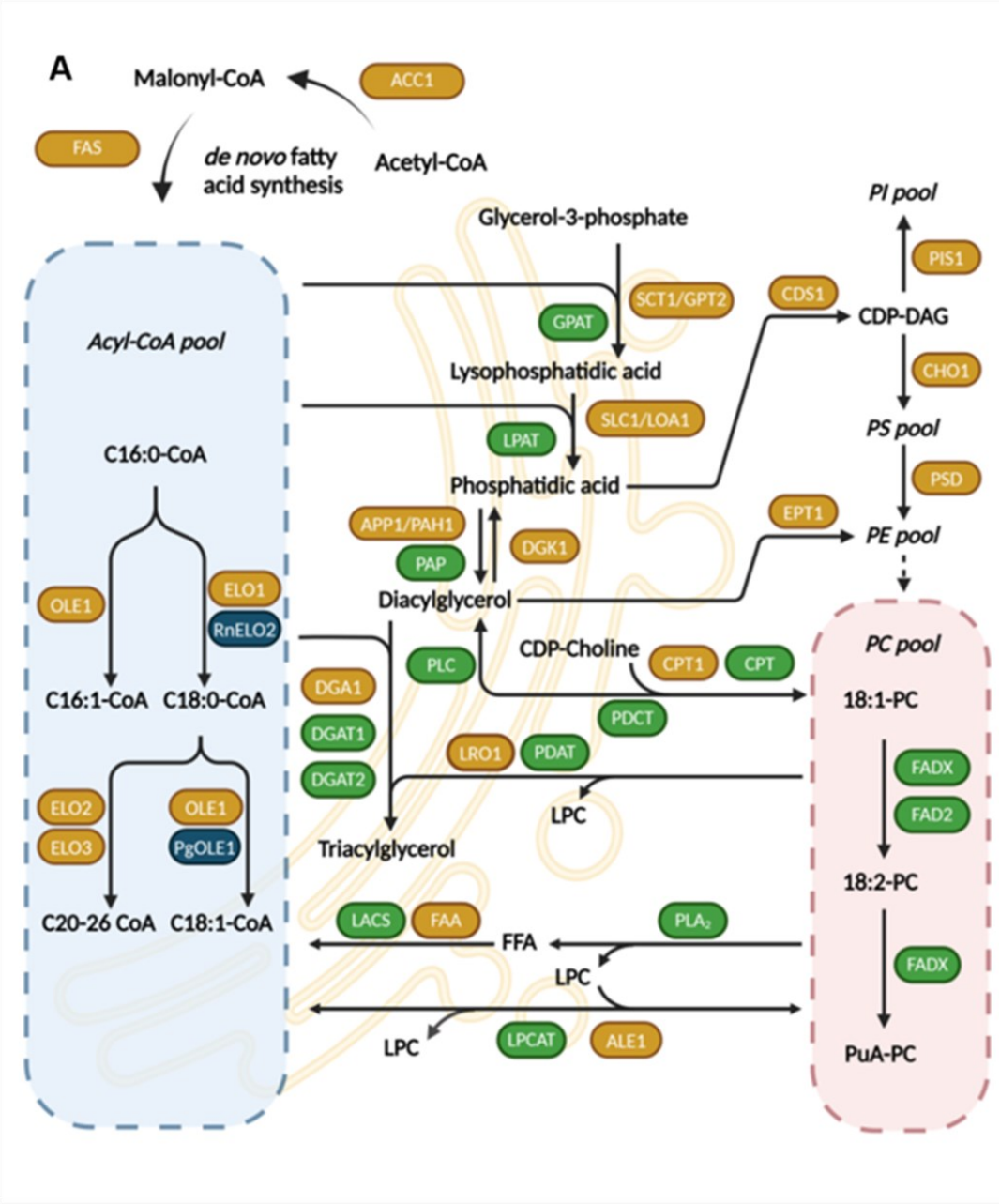
A
Malonyl-CoA
ACC1
FAS
de novo fatty acid synthesis
Acetyl-CoA
Glycerol-3-phosphate
PI pool
PIS1
SCT1/GPT2
CDS1
GPAT
CDP-DAG
Acyl-CoA pool
CHO1
Lysophosphatidic acid
SLC1/LOA1
PS pool
C16:0-CoA
LPAT
PSD
Phosphatidic acid
EPT1
APP1/PAH1
PE pool
DGK1
PAP
OLE1
ELO1
Diacylglycerol
RnELO2
CDP-Choline
PC pool
PLC
CPT1
CPT
C16:1-CoA
C18:0-CoA
18:1-PC
DGA1
PDCT
DGAT1
LRO1
PDAT
FADX
DGAT2
LPC
FAD2
ELO2
OLE1
Triacylglycerol
18:2-PC
ELO3
PgOLE1
C20-26 CoA
C18:1-CoA
LACS
FAA
PLA2
FFA
FADX
LPC
LPC
LPCAT
ALE1
PuA-PC

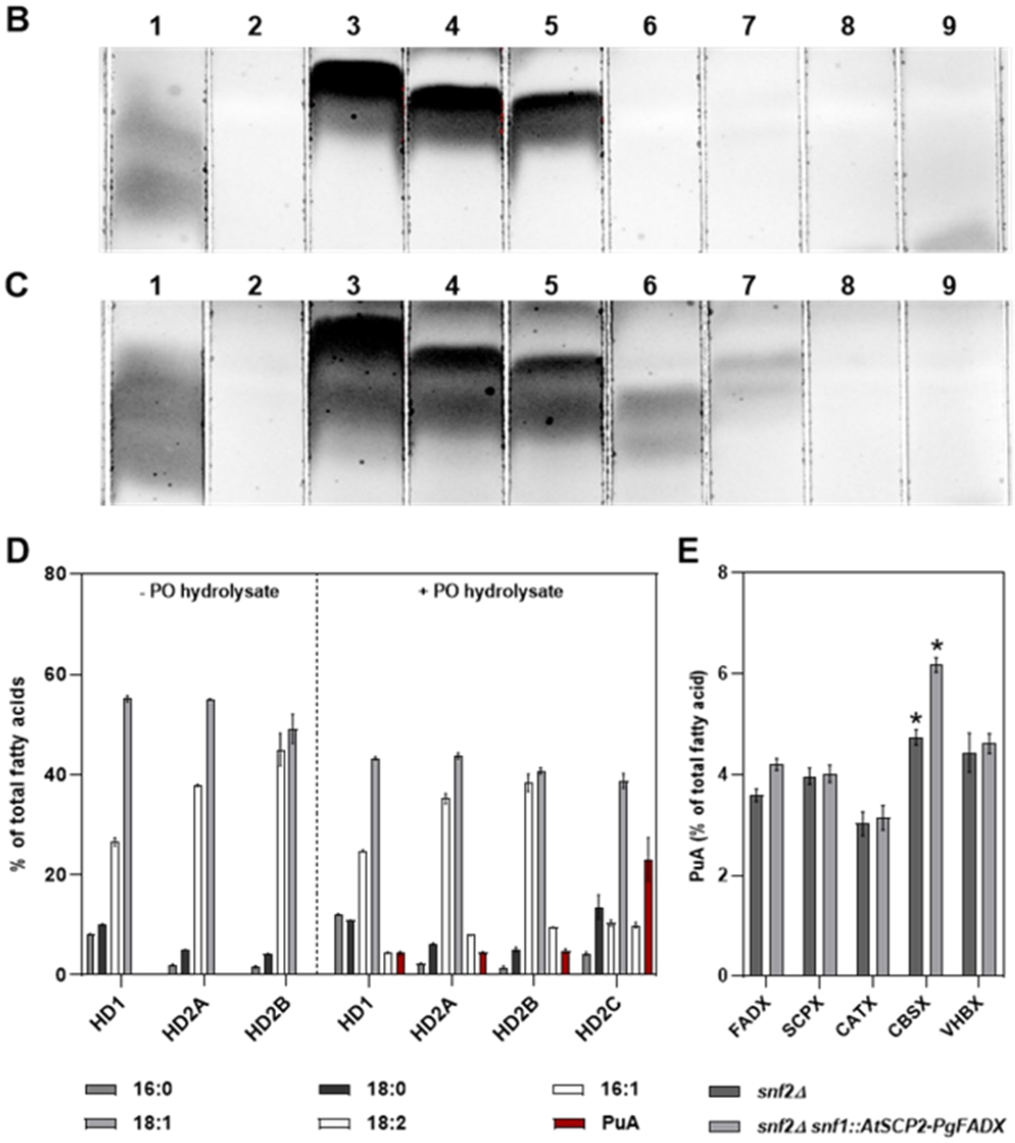

Figure 4.1. TAG and UFA synthetic pathways.

(A) Rewiring the lipid biosynthetic pathway in *S. cerevisiae* to produce PuA. Yellow ellipses indicate *S. cerevisiae* native enzymes. Green ellipses indicate enzymes from *P. granatum*. Blue ellipses indicate enzymes from other sources. DGAT/DGA1, acyl-CoA: diacylglycerol

acyltransferase; GPAT/SCT1/GPT2, glycerol-3-phosphate acyltransferase; LACS/FAA, long-chain acyl-CoA synthetase; LPAT/SLC1, lysophosphatidic acid acyltransferase; LPC, lysophosphatidylcholine; LPCAT, lysophosphatidylcholine acyltransferase; PAP/APP1/PAH1, phosphatidate phosphatase; PC, phosphatidylcholine; PDAT/LRO1, phospholipid: diacylglycerol acyltransferase; PDCT, phosphatidylcholine: diacylglycerol cholinephosphotransferase; PLA2, phospholipase A2; ACC1, acetyl-CoA carboxylase; FAS, fatty acid synthase; OLE1, acyl-CoA desaturase; ELO, fatty acid elongase; LOA1, lysophosphatidic acid: oleoyl-CoA acyltransferase; DGK1, diacylglycerol kinase; CDS1, phosphatidate cytidylyltransferase; EPT1, choline/ethanolamine phosphotransferase; PIS1, CDP-diacylglycerol--inositol 3-phosphatidyltransferase; PSD, phosphatidylserine decarboxylase; CPT, cholinephosphotransferase; PLC, phospholipase C; ALE1, lysophospholipid acyltransferase; FADX, bifunctional fatty acid conjugase/Delta(12)-oleate desaturase; FAD2, delta(12)-fatty-acid desaturase; PI, phosphatidylinositol; PE, phosphatidylethanolamine; CHO1, CDP-diacylglycerol-serine O-phosphatidyltransferase; PS, phosphatidylserine. Made with biorender.com. (B, C) Functional complementation assay in yeast strain H1246 without/with pomegranate oil hydrolysate. Lane 1-9, pomegranate oil, empty vector control, PgDGAT1, PgDGAT2a, PgDGAT2b, PgDGAT2c, PgPDAT.a, PgPDAT.b, PgPDAT.c respectively. (D) Fatty acid profiles of recombinant H1246 strains expressing different TAG assembly genes in the absence or presence of pomegranate oil hydrolysate. (E) PuA level in yeast strains transformed with various PgFADX protein fusions. Data represents mean ± SD of triplicates. ∗, $P < 0.005$ (Student's t-test).

4.3.2. Improved bioconversion from LA to PuA in yeast cells constructed by Ty retrotransposon-targeted random gene shuffling

The above result was obtained using a plasmid-based expression system, which is less stable without selective pressure and may lead to lower expression levels as well as *in vivo* enzyme concentrations (Karim et al., 2013; Lian et al., 2016). Therefore, following the characterization of pomegranate genes, we developed a workflow aiming for the effective integration and testing of pathway genes responsible for UFA accumulation directly in the yeast genome (Figure 4.2). To deliver this objective, yeast Ty retrotransposon elements were chosen as the locus for integration, and a CRISPR/Cas9 system was used to facilitate the process. The *S. cerevisiae* genome contains a large number of Ty retrotransposon elements (Curcio et al., 2015; Hanasaki and Masumoto, 2019; Malcı et al., 2020; McCarty et al., 2020), and since they do not participate in yeast metabolism, the integration of pathway genes into these regions will lead to greater copy numbers with lower interference with cellular fitness (Kato et al., 2013; Krastanova et al., 2005; Shi et al., 2016). Therefore, sequence analysis of yeast Ty retrotransposons and their long terminal repeats (delta sequence) was conducted initially. In total, 299 sequences were pulled from the yeast genome based on the genomic sequence of S288C. After sequence alignment, *YERCdelta20* (Table S4.2), *YDRWdelta23* (Table S4.3), and *TyA Gag* genes (Table S4.4) were chosen as the targets for gene shuffling due to their high similarity with other analyzed sequences. A brief description of the developed workflow is shown in Figure 4.2A. First, the expression cassettes for providing the donor DNA were constructed. Homology arms targeting yeast Ty retrotransposons were added as flanking sequences. Since previous studies have shown the defective promoter of a selection marker will cause selective pressure for cells to increase the copy number of the cassettes (Alper et al., 2005), auxotrophic markers with

truncated promoter regions (down to 20-50bp) were also linked with candidate genes to enhance the probability of obtaining positive transformants (Figure 4.2B). Next, the cassette was linearized and co-transformed into yeast cells with a CRISPR/Cas9 system. Various transformants were then individually cultured in small tubes and tested for intracellular lipid and PuA levels. 0.03% LA was added to the liquid culture in rounds 1 and 2 but was omitted in round 3 screening, which aimed for PuA neosynthesis.

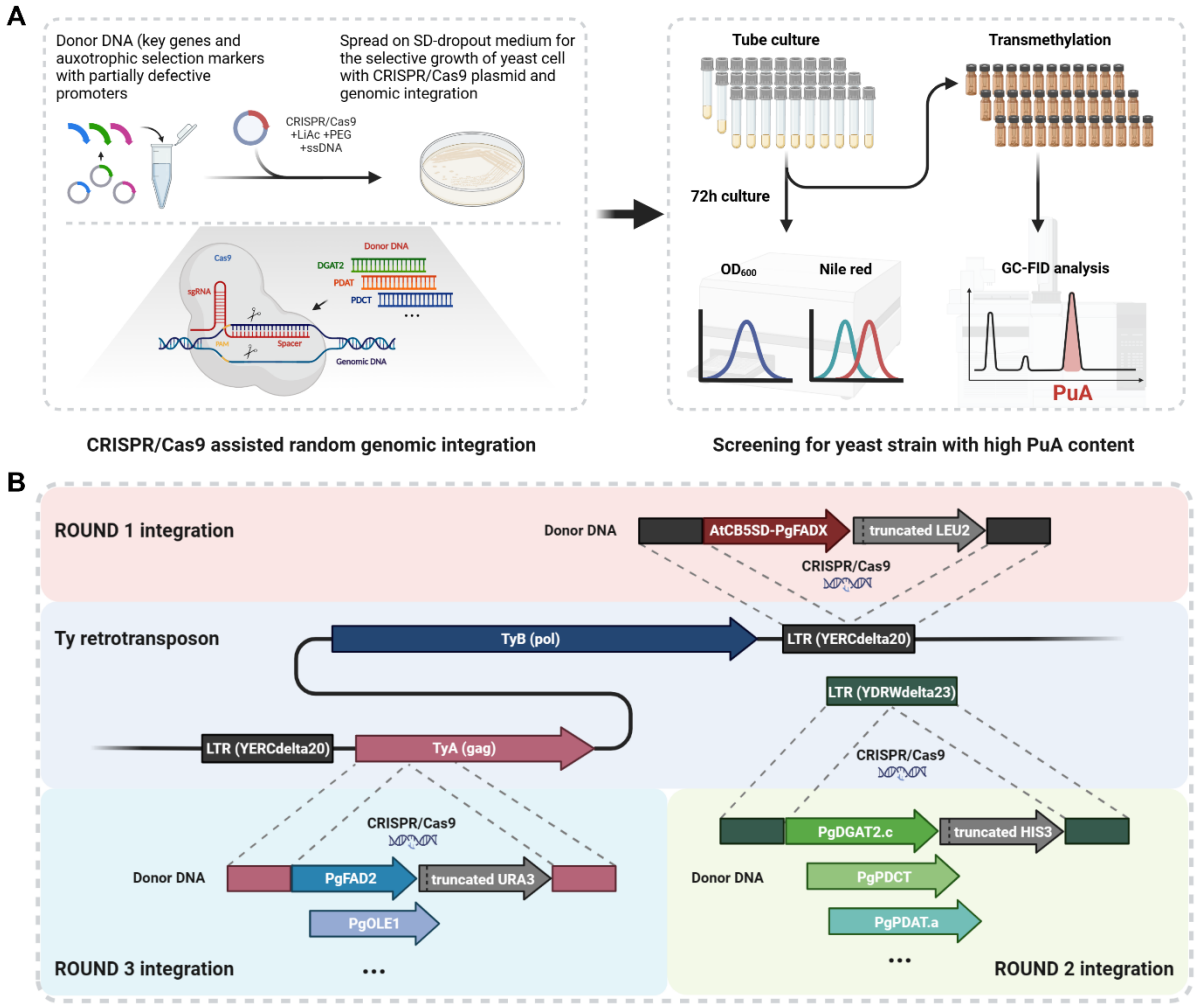

Figure 4.2. Workflow of the Ty retrotransposon-targeted random gene shuffling.

(A) Schematic diagram depicting the screening procedure for Ty retrotransposon-targeted random gene shuffling by CRISPR/Cas9. (B) Schematic diagram of donor DNA design for integration into yeast Ty retrotransposons. Made with biorender.com.

Given the critical role of PgFADX, the first round of yeast Ty retrotransposon-targeted integration was conducted to integrate the *AtCB5SD-PgFADX* expression cassette into the BY4741 *snf2Δ snf1Δ* double knockout mutant. As shown in Figure 4.3A, 360 strains were screened in total. With LA feeding, PuA accumulation was detected in all tested transformants. Merely 10.3% of strain candidates accumulated PuA levels at less than 6% of total fatty acids. The majority of the strain candidates (83.7%) accumulated 6%-10% PuA, and 6.1% of the strain candidates accumulated more than 10% of total fatty acids as PuA. The PuA content in the best strain, designated as CARIA266, reached nearly 11%. To further probe the performance of CARIA266, we conducted a growth analysis of this strain in shake flasks under different culturing temperatures. As shown in Figure 4.3B, CARIA266 maintained a high PuA level of up to 12.6% at 96h of cultivation at 20 °C. Compared to 30 °C, CARIA266 accumulates more monounsaturated fatty acid (MFA) at 20 °C, and the level of PuA gradually increased during the 4-day period. When cultured at 30 °C, the level of PuA was relatively stable and lower than the level obtained at 20 °C. The highest titer of PuA in the liquid culture on day 5 corresponded to 68.7 mg/L.

Instead of being converted to PuA, LA was enriched in CARIA266's lipids by nearly 50% (Figure 4.3B). Even though the PuA level obtained by Ty retrotransposon-targeted integration is significantly higher than the plasmid-based approach, the unexpected buildup of

LA indicated that this fatty acid precursor was not efficiently converted to PuA. One possible cause for this is the lack of specialized enzymes from the pomegranate acyl-editing and TAG assembly network (Figure 4.1A). Therefore, a second round of Ty retrotransposon-targeted random gene shuffling was conducted, focusing on the genomic integration of those enzymes. Since PgDGAT1, PgDGAT2a, PgDGAT2b, PgDGAT2c, and PgPDAT.a showed successful complementation of TAG synthesis in yeast H1246 (Figure 4.1B, 1C, 1D), their encoding genes along with *PgPDCT*, *PgLPCAT*, *PgGPAT9*, *PgLPAT2*, *PgPLA2*, *PgPLC*, and *PgLACS8* were selected as the candidates for round 2 integration. These donor DNAs were pooled together and co-transformed into CARIA266 with *YDRWdelta23*-targeting CRISPR/Cas9. The resulting transformants were again cultured in the presence of 0.03% LA. As shown in Figure 4.3C, 792 strains were screened in total for round 2 integration. 22.6% produced PuA below 8% of total fatty acids, 69.8% produced 8%-12% PuA, and 7.6% produced PuA higher than 12% of total fatty acids. Compared to round 1 integration (Figure 4.3A), the average signal intensity of the PuA from round 2 samples was significantly higher (Figure 4.3C), indicating the enhanced production of PuA. The majority of the population (96%) of round 2 transformants also had higher Nile red fluorescence, suggesting the improvement in neutral lipid accumulation caused by the pomegranate acyl-editing and TAG assembly genes. The PuA content in the best strain, designated as CARIB650, reached 16% in tube culture. As shown in Figure 4.3D, when CARIB650 was cultured in the shake flask at 20 °C, the highest PuA content further increased to over 17.7% of total fatty acids, and the highest PuA titer reached 94 mg/L. Compared to CARIA266, the content of LA on day 4 significantly dropped by 25%, indicating an improved conversion rate of this fatty acid precursor.

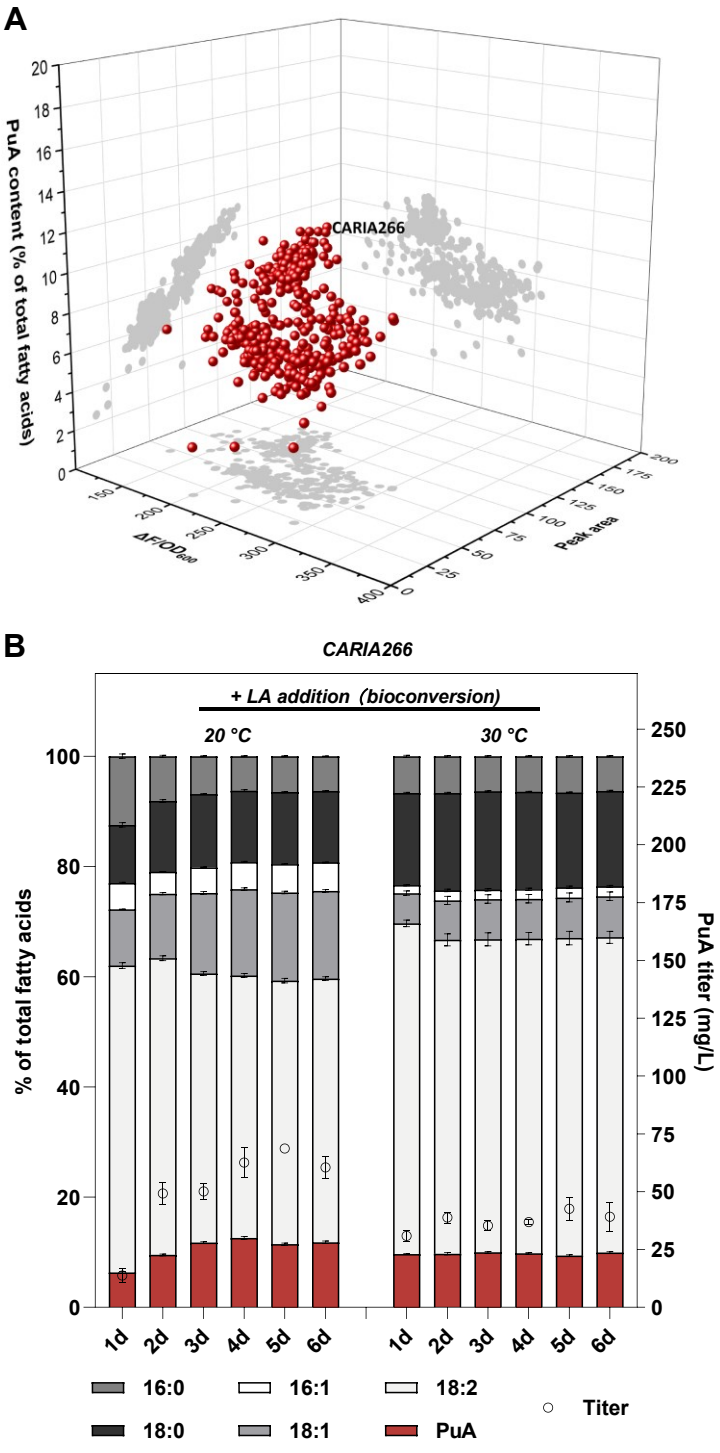
A
PuA content (% of total fatty acids)
CARIA266
ΔF/OD600
Peak area
B
CARIA266
+ LA addition (bioconversion)
20 °C
30 °C
% of total fatty acids
PuA titer (mg/L)
1d
2d
3d
4d
5d
6d
16:0
16:1
18:2
18:0
18:1
PuA
Titer

C

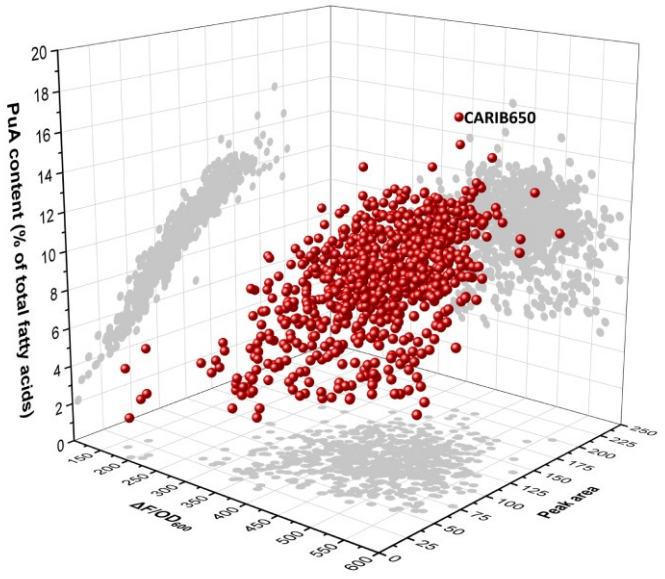
CARIB650
PuA content (% of total fatty acids)
ΔFIOD600
Peak area

D

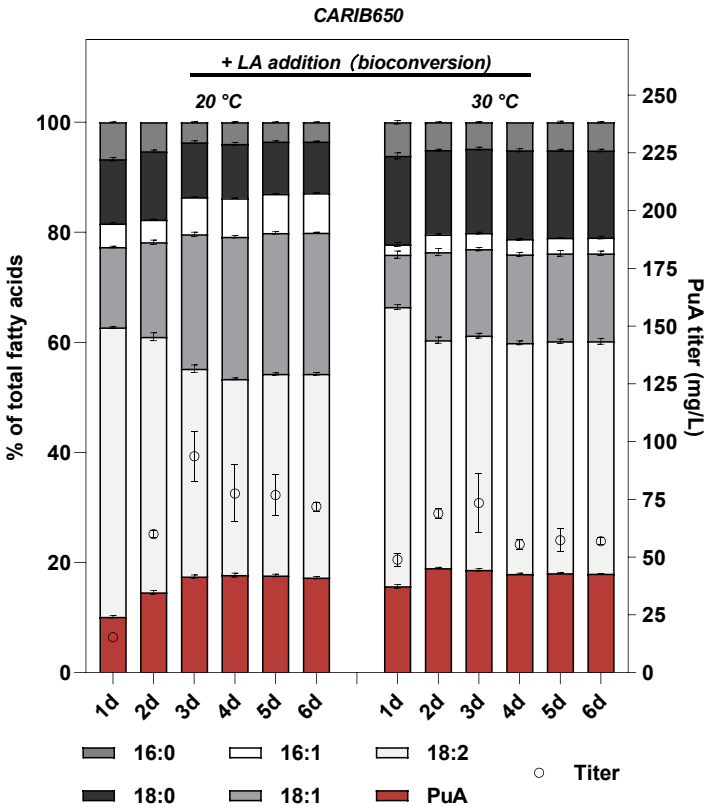
CARIB650
+ LA addition（bioconversion)
20 °C
30 °C
% of total fatty acids
PuA titer (mg/L)
1d
2d
3d
4d
5d
6d
16:0
16:1
18:2
18:0
18:1
PuA
Titer

E

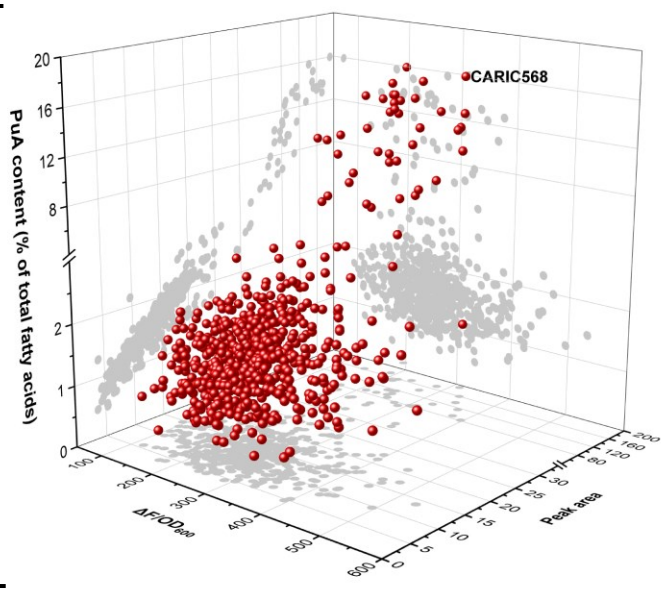
CARIC568
PuA content (% of total fatty acids)
ΔFlOD600
Peak area

F

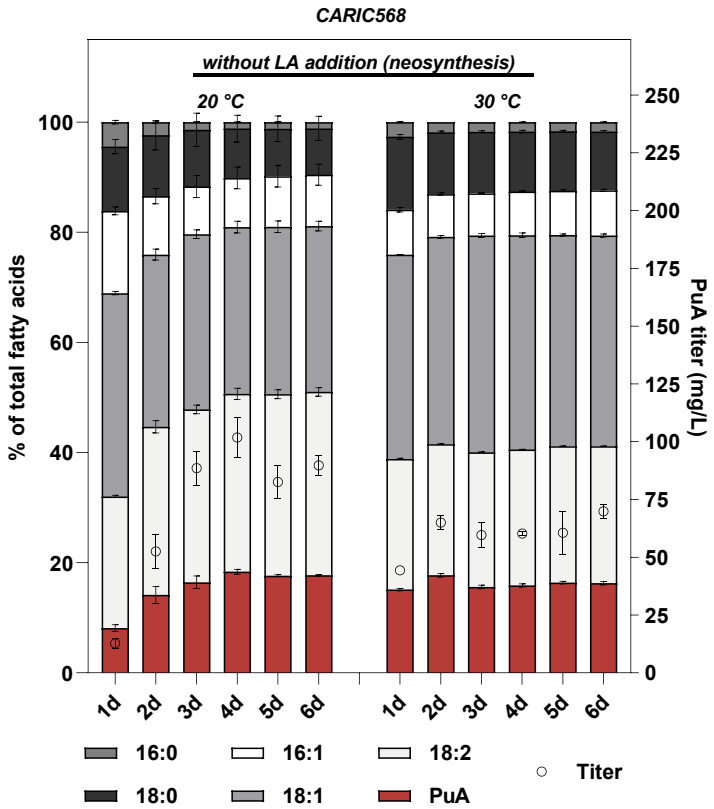
CARIC568
without LA addition (neosynthesis)
20 °C
30 °C
% of total fatty acids
PuA titer (mg/L)
1d
2d
3d
4d
5d
6d
16:0
16:1
18:2
18:0
18:1
PuA
Titer

Figure 4.3. PuA production in *S. cerevisiae* strains constructed by Ty retrotransposon-targeted random gene shuffling.

(A, C, E) Three-dimensional scatter plots of the results from round 1, round 2, and round 3 CRISPR/Cas9-assisted random integration, respectively. Each red dot represents an individual yeast transformant. The yeast transformant's PuA content (represented by the percentage of PuA in total fatty acids, Z-axis), PuA amount (represented by the integrated area of PuA's peak, Y-axis), and neutral lipid level (represented by the Nile red fluorescence, X-axis) are shown. (B, D, F) Fatty acid composition and PuA production of CARIA266, CARIB650, and CARIC568 at different incubation times under different culturing temperatures. Data represent mean ± SD of triplicates.

4.3.3. High-level neosynthesis of PuA in yeast cells using yeast Ty retrotransposon-targeted random gene shuffling and culture condition optimization.

The above results were obtained by bioconversion of manually fed LA precursor to PuA. Given the additional cost and requirement for constant precursor quality associated with the bioconversion method, neosynthesis might represent a more advantageous choice. Therefore, a round 3 integration was conducted to generate LA precursor *in vivo*, directly on the *sn*-2 position of PC. The codon-optimized donor DNA encoding AtCB5SD-FADX, PgFAD2, *Puccinia graminis* acyl-CoA desaturase (PgOLE1), and *R. norvegicus* fatty acid elongase (RnELO2) (Table S4.5) were transformed into the CARIB650 strain to obtain the library for round 3 screening. In total, 600 strains were screened without LA feeding (Figure 4.3E). Via neosynthesis, 15.5% of the strain candidates produced 2%-10% PuA, 3.3% produced 10%-14% PuA and 0.8% produced PuA higher than 14%. 80% of the strain candidates only produced 1%-

2% PuA, which is possibly caused by the lack of *PgFAD2* integration. The best strain, designated as CARIC568, accumulated 16% PuA in tube culture. The shake flask cultivation of CARIC568 over 6 days showed it was capable of accumulating 18.4% PuA (102 mg/L) at 20 °C on day 4 without LA feeding (Figure 4.3F).

In total, 1752 yeast transformants were screened using the workflow proposed by this study. The PuA content and product titer have been improved significantly, and the content of total unsaturated fatty acid was increased from 81% of total fatty acids (with LA feeding) in CARIA266 to 90% in CARIC568 (without LA feeding). Previous studies have shown that PUFA concentrations in plant cells rise with decreasing temperature due to the post-transcriptional regulation of fatty acid desaturase (Lou et al., 2014). Culturing temperature also influences the abundance of plant FAD2 and FAD3 proteins expressed in yeast cells (O'Quin et al., 2010; Tang et al., 2005). Therefore, a lower temperature may extend the half-life of heterologous desaturases, stimulate the synthesis of unsaturated fatty acid precursors, and lead to improved PuA production. In line with this, as shown in Figure 4.3, the PuA titer was higher at 20 °C compared to 30 °C.

Subsequently, on the level of shake flask culture, a response surface methodology using a multifactorial Box-Behnken design was employed for culture condition optimization to test CARIC568's potential in PuA production. The chosen variables included carbon (X1), initial pH (X2), and initial OD (X3), which were varied at three levels (-1, 0, and +1) as detailed in Table S4.6. Results showed carbon source level and initial pH were the most significant factors affecting PuA content in CARIC568 (Figure 4.4A and 4B). Higher pH, carbon, and initial OD_{600} levels promoted PuA content and production (Figure S4.1 and S4.2). Second-order polynomial equations were fitted to the experimental results to predict the optimal points within

experimental constraints (Table S4.6), which led to optimized conditions at 12% glucose, pH 7.04, and an initial OD_{600} of 0.72. A verification experiment with the optimized conditions was then carried out to determine the accuracy of the prediction. Following 120h of incubation, CARIC568 produced 425 mg/L PuA (Table 4). The lipid content reached 15.5% of dry cell weight, with PuA accounting for 26.7% of total fatty acids. The results validated the predictions provided by the statistically based experimental designs used in this study. To the best of our knowledge, this is the highest content and titer reported to date for PuA production in *S. cerevisiae*.

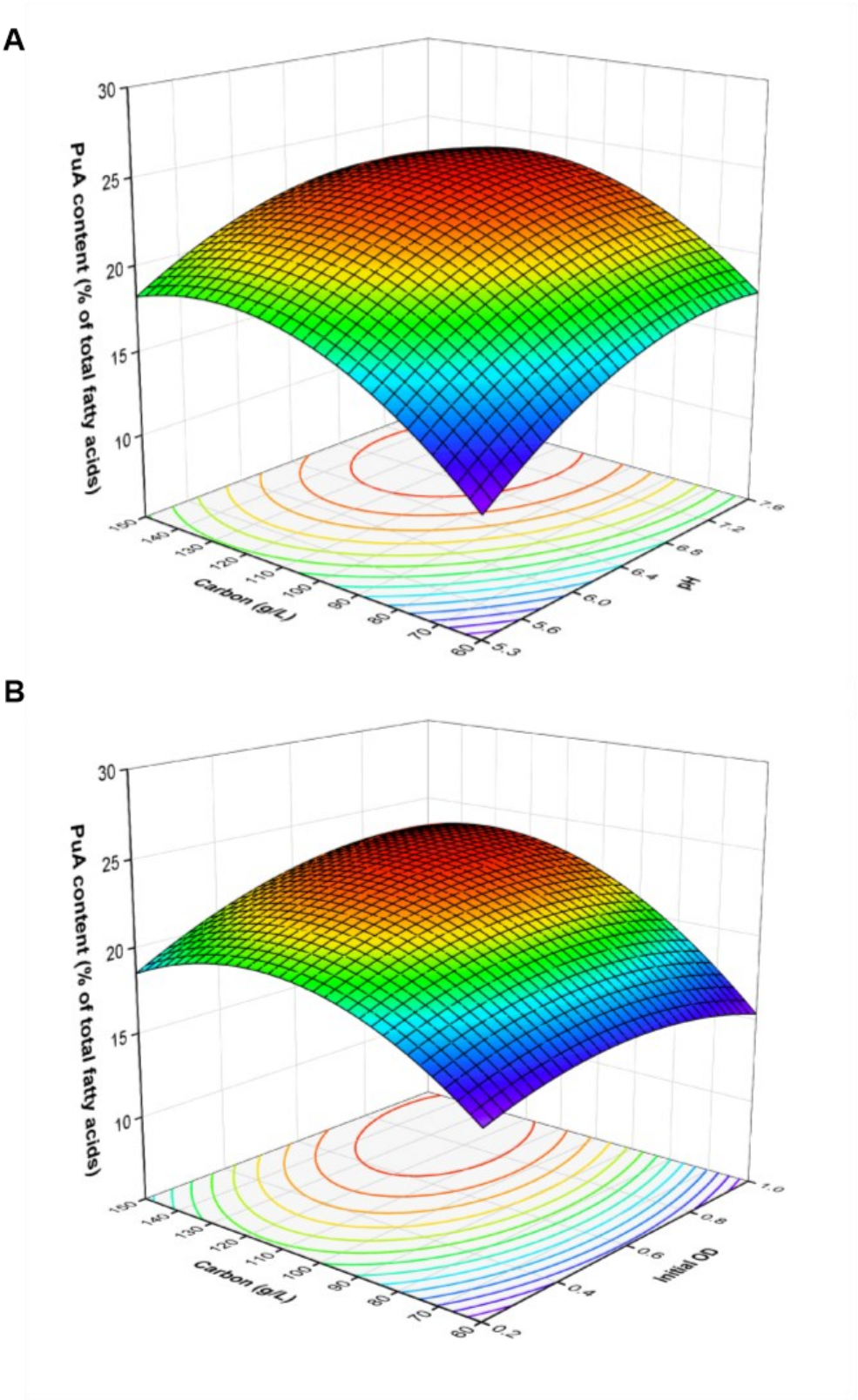
A
PuA content (% of total fatty acids)
30
25
20
15
10
Carbon (g/L)
150
140
130
120
110
100
90
80
70
60
pH
7.6
7.2
6.8
6.4
6.0
5.6
5.3
B
PuA content (% of total fatty acids)
30
25
20
15
10
Carbon (g/L)
150
140
130
120
110
100
90
80
70
60
Initial OD
1.0
0.8
0.6
0.4
0.2

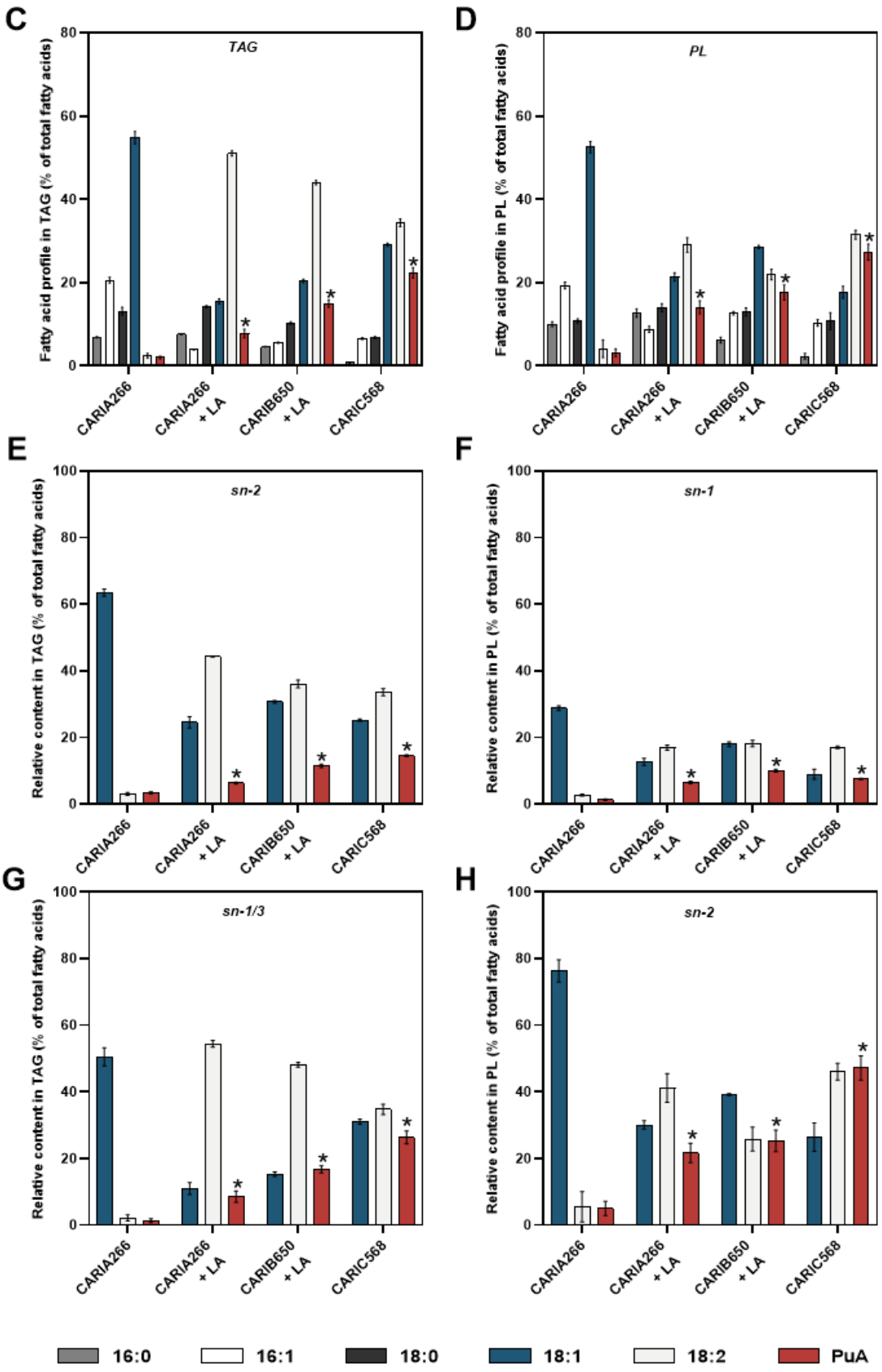
C
TAG
Fatty acid profile in TAG (% of total fatty acids)
D
PL
Fatty acid profile in PL (% of total fatty acids)
E
sn-2
Relative content in TAG (% of total fatty acids)
F
sn-1
Relative content in PL (% of total fatty acids)
G
sn-1/3
Relative content in TAG (% of total fatty acids)
H
sn-2
Relative content in PL (% of total fatty acids)
CARIA266
CARIA266 + LA
CARIB650 + LA
CARIC568
16:0
16:1
18:0
18:1
18:2
PuA

Figure 4.4. Growth condition optimization and the relative content of PuA in TAG and polar lipids.

(A, B) Three-dimensional surface plot of PuA content's response to carbon source level, and initial pH or initial OD_{600}. (C) Fatty acid composition of TAG. (D) Fatty acid composition of polar lipids. (E) Fatty acid composition at the *sn-2* position of TAG. (F) Fatty acid composition at the *sn-1* position of polar lipids. (G) The relative content of fatty acid at the *sn-1/3* positions of TAG. (H) The relative content of fatty acid at the *sn-2* position of polar lipids. Data represents mean ± SD of triplicates. ∗, $P < 0.05$ (Student's t-test).

Table 4. Fatty acid profile and PuA production of CARIC568 over a 6-day growth period in the optimized medium.

	Fatty acid content (% of total fatty acids)						PuA titer (mg/L)
	C16:0	C16:1	C18:0	C18:1	C18:2	PuA	
24h	6.5 ± 0.1	15.4 ± 1.2	13.3 ± 0.4	31.0 ± 1.0	26.4 ± 0.2	7.3 ± 0.4	26 ± 10
48h	2.8 ± 0.2	9.8 ± 0.4	13.0 ± 0.2	27.2 ± 0.2	31.4 ± 0.5	15.8 ± 0.7	180 ± 48
72h	1.4 ± 0.1	7.6 ± 0.3	11.0 ± 0.5	27.4 ± 0.3	31.1 ± 0.4	21.5 ± 0.1	272 ± 36
96h	0.9 ± 0.04	7.0 ± 0.5	8.8 ± 0.6	26.4 ± 0.9	31.8 ± 0.7	25.1 ± 0.4	331 ± 32
120h	0.8 ± 0.1	7.0 ± 0.9	7.3 ± 0.6	26.5 ± 0.9	31.7 ± 0.3	26.7 ± 1.0	425 ± 33
144h	0.6 ± 0.04	6.8 ± 0.8	6.8 ± 0.2	26.9 ± 0.9	32.3 ± 0.4	26.6 ± 1.2	380 ± 59

To date, the precise roles of enzymes involved in plant UFA biosynthesis are still under investigation. Individually determining the functions and optimal expression levels of these proteins in plant or microbial hosts adds to the challenge of developing an efficient platform for the heterologous production of UFAs. Instead of using traditional gene stacking strategies, where the exact gene candidates, combinations, and ratios are determined before the experiment, this study randomly combined and integrated potentially necessary pathway genes into the yeast genome using CRISPR/Cas9, resulting in a pool of transformants. The candidates were then

screened, yielding a strain with a gene combination that is best suited for UFA synthesis under specific culture conditions. Accordingly, subsequent analysis detected the presence of *AtCB5SD-PgFADX* as well as *PgPDCT, PgLPCAT, PgDGAT2.c*, *PgFAD2* and *RnELO2* in CARIC568.

Normally when *S. cerevisiae* BY4741 was cultured at 30 °C, C16 fatty acids accounted for over 60% of its total fatty acid composition (He et al., 2018; Sec et al., 2015). In comparison, total C16 fatty acid accounted for only 9% at 72h in BY4741-derived CARIC568 grown at 20 °C (Table 4). Combining the effects of PgFAD2 and RnELO2, these enzymes greatly contributed to the *in vivo* increase of C18 fatty acid precursor levels and stimulated PuA production. This result is consistent with previous studies, in which the expression of the gene encoding rat elongase 2 (rELO2) reversed the relative quantities of C16:1 and C18:1 in yeast cells and introducing the elongase rather than the desaturase was more efficient in raising the quantity of C18:1 (Inagaki et al., 2002; Yazawa et al., 2011).

On the other hand, PDCT, LPCAT, and DGAT2 hold special positions in plant TAG assembly and acyl-editing pathways. *Arabidopsis* PDCT, encoded by the *ROD1* gene, plays a critical role in sending C18:1 to PC for desaturation and transferring PUFA products into TAG synthesis (Lu et al., 2009). Moreover, castor PDCT and DGAT2, which have been well characterized to prefer UFA-containing acyl-CoA, were proposed to work in concert to increase tri-ricinoleoyl glycerol levels in castor seeds while also generating nonricinoleate lipids for membrane biosynthesis (Demski et al., 2022). LPCAT was also involved in this process. As illustrated in Figure 4.1A, plant LPCAT enzymes play an important role in regulating acyl-CoA composition by catalyzing both the forward reaction to synthesize PC and the reverse reaction to release acyl-CoA (Lager et al., 2013). Certain plant LPCATs were shown to have lower activity with the UFA group in the forward reaction, but higher activity on common unsaturated C18

fatty acids (Arroyo-Caro et al., 2013a; Lager et al., 2013), suggesting a role in the recruitment of specific precursor acyl-CoAs into PC for UFA synthesis.

It should be noted that given *S. cerevisiae*'s limited PuA accumulating capabilities (0.3–3.7%) observed in our previous study (Wang et al., 2021), for round 2 integration, we chose to screen pomegranate genes in the yeast genome under the condition of bioconversion. As a result, in the future, it would be interesting to conduct another round of Ty retrotransposon-targeted random gene shuffling of pomegranate acyl-editing and TAG assembly genes in CARIC568. Given the presence of a complete pathway for PuA neosynthesis, a better combination of pomegranate genes in terms of *de novo* PuA production could be found. In addition, considering the potential contribution of yeast native lipid anabolism to PuA accumulation, the genes encoding yeast native fatty acid synthesis and TAG assembly enzymes in CARIC568 were kept intact. However, a previous report suggested that isozyme competition might be a limiting factor in the engineering of UFA production in heterologous hosts (van Erp et al., 2015). Similarly, in this study, yeast native enzymes may also compete with heterologous enzymes and preferentially integrate fatty acids other than PuA into the glycerol backbone of the TAG. Therefore, replacing them with equivalent pomegranate genes may further enhance PuA levels in yeast lipids.

4.3.4. Lipidomic analysis revealed substantial changes in yeast lipidomes

After three rounds of genomic integration, three strains with medium to high PuA content were developed, making them excellent candidates for investigating the impact of heterologous PuA synthesis on the yeast native lipidome. To this end, lipids were extracted from CARIA266 and CARIC568 without LA feeding, as well as CARIA266 and CARIB650 with 0.03% LA feeding. All strains were cultivated in the optimized medium for 96h. Extracted lipids were then separated by TLC for the distribution analysis of PuA. As shown in Figures 4.4C and D, when

LA was omitted in the culture medium, the PuA level in CARIA266 was relatively low. When LA was available, CARIA266 accumulated 7.8% and 51% of TAG as PuA and LA, respectively. CARIB650 accumulated 15% PuA in TAG after transforming pomegranate acyl-editing and TAG assembly genes, representing a 92% increase over CARIA266. Meanwhile, the content of LA in both TAG and PL fractions was lowered in CARIB650. By synthesizing LA directly on PC, CARIC568 accumulated the highest PuA (22.4%) and the lowest LA (34.4%) in the TAG fraction compared to other strains. The level of PuA achieved in the TAG fraction was a substantial improvement over our prior study, in which two genetically engineered oilseed plants *A. thaliana* and *B. napus* only accumulated 6.6% and 10.6% of the fatty acid in TAG as PuA (Mietkiewska et al., 2014; Xu et al., 2020b).

Positional analysis of TAG revealed that in CARIA266, the *sn*-2 position of TAG contained 44.3% LA and 6.3% PuA (Figure 4.4E). After round 2 integration, the LA content of CARIB650 at the *sn*-2 position of TAG decreased by 19% whereas PuA increased by 81.7%. In terms of CARIC568, PuA accounted for 14.5% of fatty acids in the *sn*-2 position of TAG (Figure 4.4E) and 26.3% of fatty acids in the *sn*-1/3 positions of TAG (Figure 4.4G), suggesting a slight preference for enriching PuA at the *sn*-1/3 positions in this strain. Positional analysis of PL indicated that the *sn*-1 position generally contained a relatively low level of PuA (Figure 4.4F). In contrast, PuA accounted for 21.7% (CARIA266+LA), 25.3% (CARIB650+LA), and 47.1% (CARIC568) of fatty acids at the *sn*-2 position of PL (Figure 4.4H), which is consistent with the widely held opinion that the *sn*-2 position of polar lipids is the location for acyl-editing.

To better examine the impact of PuA production on the yeast lipidome, lipidomic analysis was conducted. Principal components analysis (PCA) was first carried out to determine differences between the lipidomes of CARIA266, CARIA266 with LA addition, CARIB650 with

LA addition, and CARIC568 (Figure S4.3). Analysis of the entire lipid dataset, including different PL, TAG, and diacylglycerol (DAG), revealed a clear distinction between the four lipidomes. The first component clearly distinguished between the CARIA266 and the CARIC568, accounting for 59.3% of the differences. The second major component accounted for approximately 25% of the changes and showed the difference between groups with LA addition and without LA addition. When LA was added exogenously, CARIA266+LA clustered firmly with CARIC568+LA and away from groups without LA feeding, indicating that fatty acid precursor uptake dominated the shift in the yeast lipidome. The distance between the final strain CARIC568 and starting strain CARIA266 on the PCA plot indicated significant alterations in the yeast lipidome as a result of genetic modifications made by Ty retrotransposon-targeted integration.

The TAG species in yeast lipidomes were separated into SFA-containing TAG, MFA-containing TAG, and PUFA-containing TAG. Heatmaps displaying the relative abundance of different TAG species are shown separately in Figure 4.5A-C using a color scale. The most abundant SFA-containing TAG in CARIA266, CARIA266+LA, CARIB650+LA, and CARIC568 were TAG (54:2_18:0), TAG (54:4_18:0), TAG (54:4_18:0), and TAG (54:3_18:0), respectively (Figure 4.5A). In CARIA266, the overall content of TAG containing SFA was noticeably greater. Compared with the CARIC568, CARIA266 accumulated more TAG with shorter chain SFA, such as TAG (50:2_16:0) and TAG (52:2_16:0). In terms of MFA-containing TAG, CARIA266 accumulated a higher content of C16:1-containing TAG, and the overall saturation of CARIA266 TAG was higher (Figure 4.5B). As seen in Figure 4.5C, the content of C18:2-containing TAG was relatively greater in CARIA266+LA and CARIB650+LA as a result of exogenously added LA. In this regard, CARIB650 led to a lower level of C18:2-containing

TAG than CARIA266, indicating that the introduction of pomegranate TAG assembly and acyl-editing genes reduced the level of TAG species with LA. Since *S. cerevisiae* does not naturally accumulate C18:3 fatty acids (Sec et al., 2015), the C18:3 detected in the TAG fraction reflected the content of PuA. CARIC568 generated the highest content of PuA-containing TAG species, led by TAG (54:6_18:3) and TAG (54:5_18:3) (Figure 4.5C). Compared to the other three lipidomes, CARIC568 had a significantly higher level of TAG species with a high unsaturation degree (5-8 double bonds in total). However, in contrast to pomegranate seed oil, where the majority of PuA incorporated into TAG occupies all three positions of the glycerol backbone (Holic et al., 2018), the lack of TAG (54:9) in the top-ranking TAG species in all yeast lipidomes suggested that the PuA product was still primarily found at a single or double position of TAG glycerol backbones.

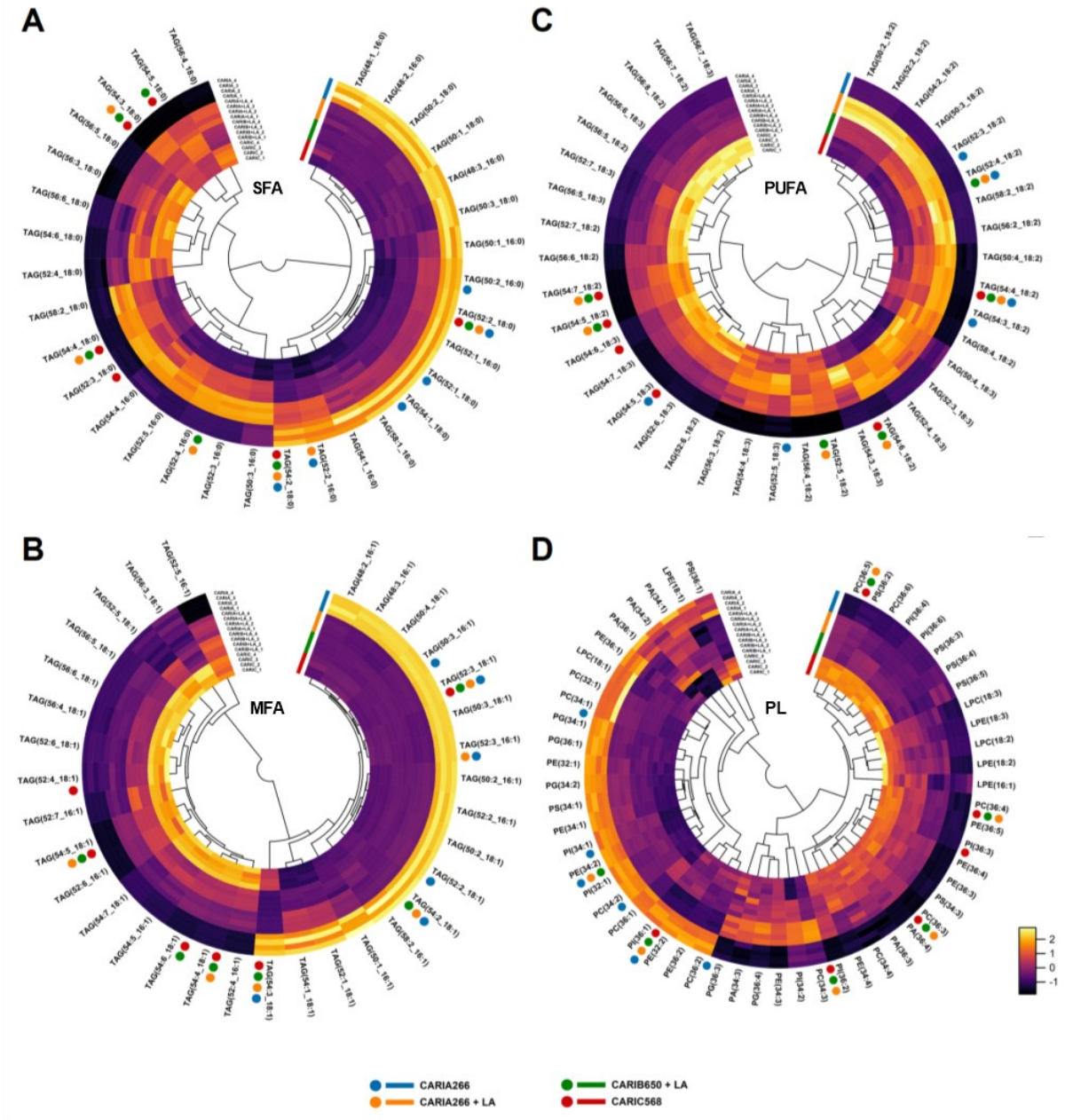
A
SFA
B
MFA
C
PUFA
D
PL
2
1
0
-1
CARIA266
CARIA266 + LA
CARIB650 + LA
CARIC568

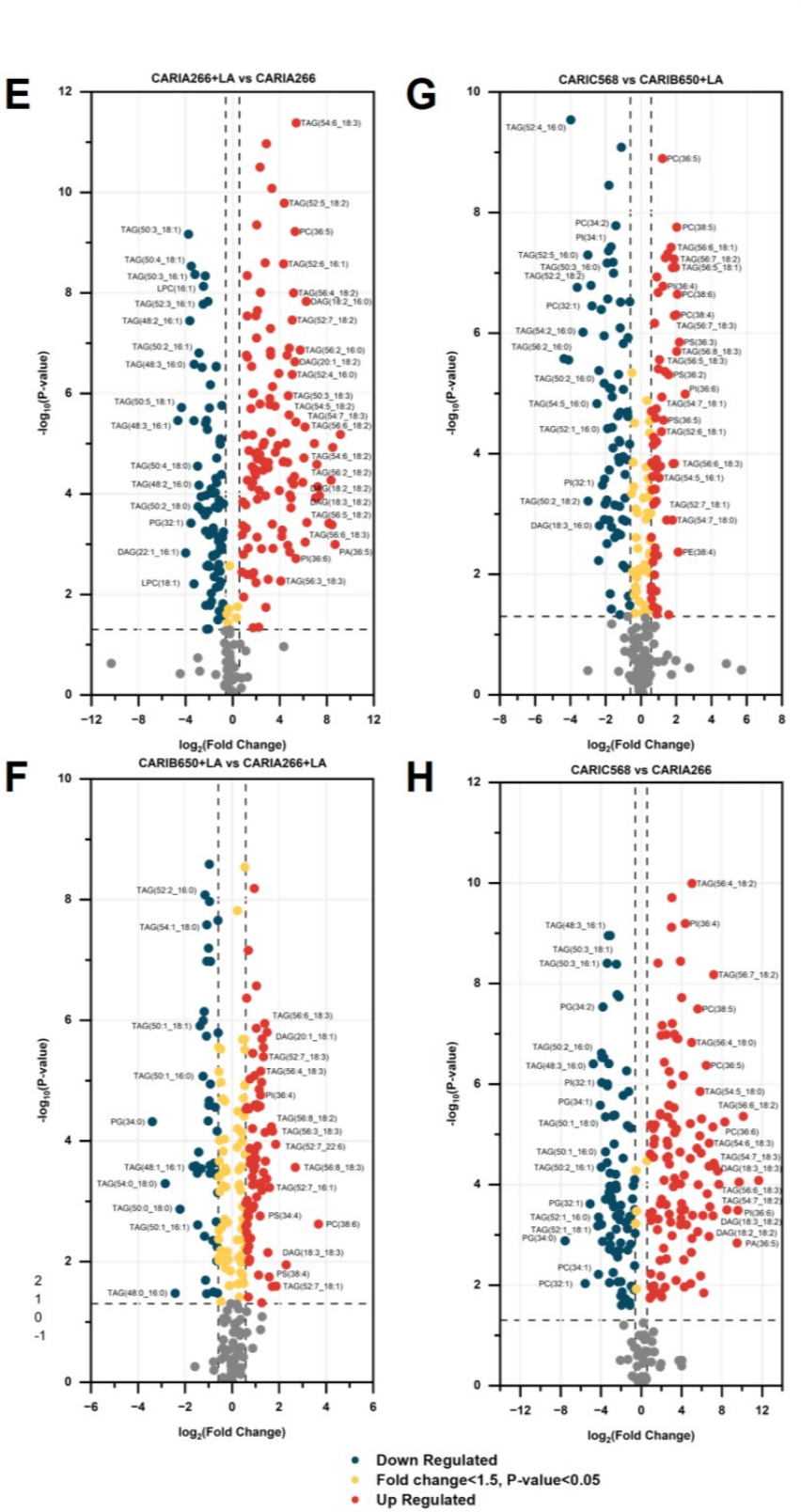
E
CARIA266+LA vs CARIA266
G
CARIC568 vs CARIB650+LA
F
CARIB650+LA vs CARIA266+LA
H
CARIC568 vs CARIA266
-log10(P-value)
log2(Fold Change)
Down Regulated
Fold change<1.5, P-value<0.05
Up Regulated

Figure 4.5. Yeast lipidomes containing PuA with or without LA feeding.

(A) Heatmap of top-ranking SFA-containing TAG. (B) Heatmap of top-ranking MFA-containing TAG. (C) Heatmap of top-ranking PUFA-containing TAG. (D) Heatmap of top-ranking polar lipid species. The intensities of single lipid species are presented on a color scale ranging from black (low values) to yellow (high values), as described in the legend. (E-H) Volcano plots showing log2 (fold change) and -log10 (p values) of molecular lipid species comparing CARIA266+LA vs CARIA266, CARIB650+LA vs CARIA266+LA, CARIC568 vs CARIB650+LA, and CARIC568 vs CARIA266, respectively. Red or blue dots indicate up- or down-regulated lipid species, respectively, with a fold change >1.5 and p-value < 0.05.

Comparison of differentially expressed lipids between various strains is shown in volcano maps (Figure 4.5E-H). As indicated in Figure 4.5E, when exogenous LA was made accessible to CARIA266, TAG accounted for 60% of the up-regulated lipid species with C18:2-containing lipids being the majority. After round 2 integration, 82 lipid species and 45 lipid species were up- and down-regulated, respectively, with TAG accounting for 50%-78% of them (Figure 4.5F). By switching from bioconversion to neosynthesis, 34 TAG and 25 polar lipid species were up-regulated, whereas 47 TAG and 20 polar lipid species with saturated acyl chains were down-regulated (Figure 4.5G). When comparing the final strain CARIC568 with the starting strain CARIA266, significant changes in 205 lipid species were observed. TAG accounted for 55% of both up and down-regulated lipids (Figure 4.5H). Most up-regulated lipids had more than four double bonds, whereas the down-regulated lipids consisted of shorter acyl chains with fewer double bonds (Figure 4.5H).

The tested yeast samples contained a variety of PLs, including PC, lysophosphatidylcholine (LPC), lysophosphatidylethanolamine (LPE), phosphatidylserine (PS), phosphatidylethanolamine (PE), phosphatidylglycerol (PG), phosphatidylinositol (PI), and phosphatidic acid (PA) (Figure 4.5D). In CARIA266, CARIA266+LA, CARIB650+LA, and CARIC568, the most abundant PL species were PE (34:2), PI (36:2), PC (36:4), and PC (36:5), respectively. A previous study found that the parental strain of BY4741 (S288c) lacks PL-containing fatty acids with more than two double bonds (Hein and Hayen, 2012). This remained the case for strain CARIA266 without LA feeding. *S. cerevisiae'*s physiology and cellular processes rely heavily on phospholipids. For example, PC, the most abundant phospholipid in *S. cerevisiae* membranes, contributes to the maintenance of membrane integrity, fluidity, and stability (Hein and Hayen, 2012). Therefore, ideally, the introduced PuA-producing pathway should cause as little disturbance as possible to the yeast's native polar lipid species. However, as shown in Figure 4.5D, the content of PL with more than two double bonds was raised following PuA accumulation capability, and this up-regulation was observed across major PL species, such as PC (36:5), PC (36:6), PI (36:3), PI (36:6), PE (36:5), and PS (36:4). Certain important branching points exist in yeast phospholipid biosynthesis that may control the acyl-chain species. For example, yeast PE-producing enzyme (EPT1) showed the highest activity towards di-unsaturated DAG species as substrates and yeast PC-producing enzyme (CPT1) favored C32:2 substrates (Boumann et al., 2004). A previous study on human CDP-diacylglycerol synthases (CDS) also revealed that this key enzyme, catalyzing the formation of CDP-diacylglycerol, exhibited acyl-chain specificities for its lipid substrate (D'Souza et al., 2014). Although little information is known concerning baker's yeast native lipid synthetic enzymes' selectivity on

conjugated PUFA, the polar lipidomic profile obtained in this study suggested substantial crosstalk between PuA and yeast major polar lipid synthetic pathways.

On the other hand, the presence of PuA in yeast PL and its accompanied influence on cellular fitness may contribute to the design of novel rapid screening methods, targeting cells with higher PuA. Since screening by gas chromatography is relatively time-consuming and labor-intensive, previous studies have used UV spectral scans to detect the amount of conjugated dienes and trienes in bacterial isolates or pomegranate oils (Liu et al., 2012; Ülker et al., 2016). However, such methods still require the prior extraction of conjugated fatty acids. Alternatively, the membrane lipid composition of *S. cerevisiae* is known to affect strain survival under stress conditions (Henderson and Block, 2014). For instance, when *Arabidopsis FAD2* was expressed in *S. cerevisiae*, yeast cells acquired greater resistance to ethanol stress (Kajiwara et al., 1996). Expressing *FAD2* from the rubber tree (*Hevea brasiliensis*) increased *S. cerevisiae*'s susceptibility to oxidative stress, triggered by paraquat, tertbutyl hydroperoxide, and hydrogen peroxide-induced lipid peroxidation (Cipak et al., 2006). From a future perspective, it would be intriguing to examine how CARIC568 responds to these stress factors. These stress conditions could serve as selective or counter-selective measures to identify the strain with the highest PuA levels among the transformants produced by Ty retrotransposon-targeted random gene shuffling.

4.4. Conclusions

In this study, genes potentially contributing to plant-derived UFA synthesis were directly integrated and shuffled in the *S. cerevisiae* genome. Screening 1752 strains led to the identification of a recombinant capable of accumulating 26.7% of total fatty acids as PuA without LA precursor feeding. In shake flask cultivation, the PuA titer reached 425 mg/L. PuA comprised over 22% of total fatty acids in the TAG fraction of yeast single-cell oil, a significant

increase compared to transgenic *A. thaliana* and *B. napus*. Subsequent analysis revealed significant lipidome changes due to PuA synthesis. Based on these results, the PuA level in this PuA-enriched yeast platform could be further enhanced by iterative integration using the same workflow.

4.5. Supplementary material

Supplementary Table S4.1. Pomegranate acyl-editing and TAG assembly genes

Enzyme	Query species	Annotation	*Subject species*	*No.*	Designation	Subject protein
DGAT1	*Vernicia fordii*	Tung DGAT1, natural producer of UFA; producer of conjugated 18:3 PUFA	*Punica granatum*	*1*	PgDGAT1	>XP_031382678.1
DGAT2	*Vernicia fordii*	Tung DGAT2, natural producer of UFA; producer of conjugated 18:3 PUFA	*Punica granatum*	*2*	PgDGAT2.a	>XP_031388774.1
				3	PgDGAT2.b	>XP_031401853.1
				4	PgDGAT2.c	>XP_031401854.1
PDAT	*Linum usitatissimum*	Flax LuPDAT2, a natural producer of 18:3 PUFA, is expressed in vegetative tissue but has high protein accumulation in yeast, Similar preference with flax LuPDAT1, which is a seed-specific PDAT	*Punica granatum*	*5*	PgPDAT.a	>XP_031388206.1
				6	PgPDAT.b	>XP_031380888.1
				7	PgPDAT.c	>XP_031388207.1
GPAT9	*Ricinus communis*	Castor GPAT9, a natural producer of UFA	*Punica granatum*	*8*	PgGPAT9	>XP_031383927.1
LPAT2	*Vernicia fordii*	Tung LPAT2, natural producer of UFA; producer of conjugated 18:3 PUFA	*Punica granatum*	*9*	PgLPAT2	>XP_031398075.1
LACS8	*Linum usitatissimum*	Flax LACS8, natural producer of 18:3 PUFA, has high preference towards18:3 fatty acid	*Punica granatum*	*10*	PgLACS8	>XP_031372442.1
LPCAT	*Linum usitatissimum*	Flax LPCAT, a natural producer of 18:3 PUFA	*Punica granatum*	*11*	PgLPCAT	>XP_031394089.1
PDCT	*Linum usitatissimum*	Flax PDCT, a natural producer of 18:3 PUFA	*Punica granatum*	*12*	PgPDCT	>XP_031389447.1

PLA2a	*Ricinus communis*	Castor PLA2a, a natural producer of UFA	*Punica granatum*	*13*	PgPLA2a	>XP_031374260.1
PLC	*Ricinus communis*	Castor PLC, a natural producer of UFA	*Punica granatum*	*14*	PgPLC	>XP_031386572.1

Supplementary Table S4.2. Sequence similarity and identity search for YERCdelta20 using the Basic Local Alignment Search Tool (BLAST)

	Short name	Total Score	Query Cover	E value	Per. ident	Acc. Len
1	YPLWdelta4	623	100%	0	100	337
2	YPLWdelta3	623	100%	0	100	337
3	YCLWdelta15	623	100%	0	100	337
4	YARCdelta5	623	100%	0	100	337
5	YARCdelta4	623	100%	0	100	337
6	YLRCdelta8	619	99%	7.00E-180	100	335
7	YLRCdelta7	619	99%	7.00E-180	100	335
8	YMLWdelta5	612	100%	1.00E-177	99	337
9	YERCdelta19	606	100%	6.00E-176	99	337
10	YMLWdelta6	562	93%	1.00E-162	99	316
1	YPRCdelta19	508	100%	2.00E-146	94	334
2	YPRCdelta18	508	100%	2.00E-146	94	334
3	YLRWdelta11	508	100%	2.00E-146	94	334
4	YDRWdelta27	508	100%	2.00E-146	94	334
5	YNLWdelta4	503	100%	8.00E-145	94	334
6	YNLWdelta3	503	100%	8.00E-145	94	334
7	YLRWdelta10	497	100%	4.00E-143	93	334
8	YJRWdelta12	497	100%	4.00E-143	93	334
9	YGRCdelta16	497	100%	4.00E-143	93	334
10	YDRWdelta28	497	100%	4.00E-143	93	334
11	YDRCdelta22	497	100%	4.00E-143	93	334
12	YPRCdelta23	490	100%	6.00E-141	93	338
13	YOLWdelta5	490	100%	6.00E-141	93	338
14	YLRWdelta13	486	100%	8.00E-140	93	334
15	YJRWdelta13	484	100%	3.00E-139	93	338
16	YJRWdelta11	484	100%	3.00E-139	93	338
17	YGRWdelta14	484	100%	3.00E-139	93	338
18	YGRWdelta13	484	100%	3.00E-139	93	338
19	YGRCdelta15	477	94%	5.00E-137	94	334
20	YPRCdelta24	473	100%	6.00E-136	92	338
21	YLRWdelta14	466	94%	1.00E-133	93	334
22	YDRCdelta8	466	94%	1.00E-133	93	334
23	YDRCdelta7	466	94%	1.00E-133	93	334
24	YDRCdelta21	466	94%	1.00E-133	93	334
25	YPRWdelta21	453	94%	8.00E-130	92	338
26	YPRWdelta20	453	94%	8.00E-130	92	338

27	YOLWdelta4	453	94%	8.00E-130	92	338
28	YMRCdelta9	453	94%	8.00E-130	92	338
29	YMRCdelta10	453	94%	8.00E-130	92	338
30	YLRCdelta2	453	94%	8.00E-130	92	338
31	YDRWdelta24	453	94%	8.00E-130	92	338
32	YDRWdelta23	453	94%	8.00E-130	92	338
33	YLRCdelta3	448	94%	4.00E-128	92	338
34	YERCdelta24	448	94%	4.00E-128	92	338
35	YLRCdelta18	448	97%	4.00E-128	91	333
36	YHLCdelta1	446	97%	1.00E-127	91	328
37	YNRCdelta8	444	97%	5.00E-127	91	332
38	YHRCdelta10	440	97%	6.00E-126	91	333
39	YNLCdelta2	440	100%	6.00E-126	91	332
40	YNLCdelta1	440	100%	6.00E-126	91	332
41	YMLCdelta2	438	98%	2.00E-125	91	333
42	YILWdelta2	436	97%	8.00E-125	91	333
43	YDRWdelta7	435	93%	3.00E-124	92	329
44	YORWdelta17	435	97%	3.00E-124	91	333
45	YELWdelta2	435	97%	3.00E-124	91	333
46	YELWdelta1	435	97%	3.00E-124	91	676
47	YMRCdelta8	435	100%	3.00E-124	90	332
48	YMRCdelta7	435	100%	3.00E-124	90	332
49	YKRCdelta12	435	100%	3.00E-124	90	332
50	YBLWdelta10	435	100%	3.00E-124	90	332
51	YORWdelta24	433	97%	1.00E-123	91	332
52	YORWdelta23	433	97%	1.00E-123	91	332
53	YMRWdelta19	433	97%	1.00E-123	91	332
54	YELCdelta4	433	97%	1.00E-123	91	328
55	YDRWdelta29	433	97%	1.00E-123	91	332
56	YDRCdelta5	433	97%	1.00E-123	91	332
57	YERCdelta14	429	97%	1.00E-122	90	333
58	YPRWdelta12	429	100%	1.00E-122	90	332
59	YGRWdelta11	429	100%	1.00E-122	90	332
60	YORCdelta21	429	99%	1.00E-122	90	333
61	YORCdelta20	429	99%	1.00E-122	90	333
62	YLRCdelta26	427	97%	5.00E-122	91	332
63	YLRCdelta25	427	97%	5.00E-122	91	332
64	YGRCdelta17	427	97%	5.00E-122	91	333
65	YERWdelta22	427	97%	5.00E-122	91	332
66	YDRWdelta14	427	97%	5.00E-122	91	332

67	YDRWdelta13	427	97%	5.00E-122	91	332
68	YDRCdelta4	427	97%	5.00E-122	91	329
69	YBLWdelta2	427	97%	5.00E-122	91	332
70	YJLCdelta3	427	97%	5.00E-122	90	332
71	YGRWdelta32	424	100%	6.00E-121	90	332
72	YPLWdelta5	422	97%	2.00E-120	90	332
73	YGRWdelta27	422	97%	2.00E-120	90	332
74	YFLWdelta4	422	97%	2.00E-120	90	332
75	YFLWdelta3	422	97%	2.00E-120	90	328
76	YDRWdelta20	422	97%	2.00E-120	90	332
77	YDRWdelta19	422	97%	2.00E-120	90	332
78	YJRCdelta19	418	97%	3.00E-119	90	333
79	YPLWdelta8	416	97%	1.00E-118	90	322
80	YLRWdelta23	416	97%	1.00E-118	90	332
81	YLRWdelta22	416	97%	1.00E-118	90	332
82	YJRWdelta17	416	97%	1.00E-118	90	332
83	YCLWdelta5	416	97%	1.00E-118	90	332
84	YCLWdelta4	416	97%	1.00E-118	90	332
85	YGRWdelta28	414	93%	4.00E-118	91	324
86	YNLCdelta6	411	97%	5.00E-117	90	333
87	YNLCdelta5	411	97%	5.00E-117	90	332
88	YGRCdelta18	411	97%	5.00E-117	90	332
89	YCLWdelta3	411	97%	5.00E-117	90	332
90	YBLWdelta4	411	97%	5.00E-117	90	332
91	YKLWdelta7	409	93%	2.00E-116	90	332
92	YORWdelta14	409	94%	2.00E-116	90	332
93	YORWdelta13	409	94%	2.00E-116	90	332
94	YGRCdelta30	409	94%	2.00E-116	90	332
95	YGRCdelta29	409	94%	2.00E-116	90	332
96	YMLWdelta4	403	94%	8.00E-115	90	332
97	YMLWdelta3	403	94%	8.00E-115	90	332
98	YHRCdelta15	403	94%	8.00E-115	90	332
99	YBRWdelta13	403	94%	8.00E-115	90	332
100	YBRWdelta12	403	94%	8.00E-115	90	332

Supplementary Table S4.3. Sequence similarity and identity search for YDRWdelta23 using the Basic Local Alignment Search Tool (BLAST)

	Short name	Total Score	Query Cover	E value	Per. ident	Acc. Len
1	YPRWdelta21	625	100%	0	100	338
2	YPRWdelta20	625	100%	0	100	338
3	YMRCdelta9	625	100%	0	100	338
4	YMRCdelta10	625	100%	0	100	338
5	YLRCdelta2	625	100%	0	100	338
6	YLRCdelta3	619	100%	7.00E-180	100	338
7	YERCdelta24	619	100%	7.00E-180	100	338
8	YDRWdelta24	619	100%	7.00E-180	100	338
9	YOLWdelta4	614	100%	3.00E-178	99	338
10	YPRCdelta24	597	95%	3.00E-173	100	338
11	YPRCdelta23	588	94%	2.00E-170	100	338
12	YOLWdelta5	588	94%	2.00E-170	100	338
13	YJRWdelta13	586	100%	7.00E-170	98	338
14	YJRWdelta11	586	100%	7.00E-170	98	338
15	YGRWdelta14	586	100%	7.00E-170	98	338
16	YGRWdelta13	586	100%	7.00E-170	98	338
1	YMLWdelta4	569	100%	7.00E-165	97	332
2	YHRCdelta15	569	100%	7.00E-165	97	332
3	YGRCdelta30	569	100%	7.00E-165	97	332
4	YGRCdelta29	569	100%	7.00E-165	97	332
5	YORWdelta14	568	99%	3.00E-164	97	332
6	YORWdelta13	568	99%	3.00E-164	97	332
7	YMLWdelta3	564	100%	3.00E-163	97	332
8	YHRCdelta16	564	100%	3.00E-163	97	332
9	YBRWdelta13	564	100%	3.00E-163	97	332
10	YBRWdelta12	564	100%	3.00E-163	97	332
11	YNLCdelta2	532	94%	1.00E-153	97	332
12	YNLCdelta1	532	94%	1.00E-153	97	332
13	YGRWdelta32	532	94%	1.00E-153	97	332
14	YMRCdelta8	527	94%	5.00E-152	97	332
15	YMRCdelta7	527	94%	5.00E-152	97	332
16	YKRCdelta12	527	94%	5.00E-152	97	332
17	YGRWdelta11	527	94%	5.00E-152	97	332
18	YBLWdelta10	527	94%	5.00E-152	97	332
19	YPRWdelta12	521	94%	2.00E-150	97	332
20	YGLWdelta7	521	94%	2.00E-150	97	332

21	YBLWdelta9	518	94%	3.00E-149	96	334
22	YHRCdelta3	516	94%	1.00E-148	96	332
23	YKRCdelta8	499	94%	1.00E-143	95	332
24	YCRWdelta10	497	94%	4.00E-143	95	331
25	YFRCdelta8	494	94%	5.00E-142	95	332
26	YCRCdelta6	494	94%	5.00E-142	95	332
27	YDRWdelta11	486	94%	8.00E-140	95	331
28	YORCdelta25	486	93%	8.00E-140	95	332
29	YDRWdelta26	483	92%	1.00E-138	95	332
30	YDRWdelta25	464	94%	4.00E-133	93	330
31	YERCdelta19	462	95%	1.00E-132	93	337
32	YDRCdelta3	460	94%	5.00E-132	93	332
33	YMLWdelta5	457	100%	6.00E-131	91	337
34	YPLWdelta4	453	94%	8.00E-130	92	337
35	YPLWdelta3	453	94%	8.00E-130	92	337
36	YLRCdelta8	453	94%	8.00E-130	92	335
37	YLRCdelta7	453	94%	8.00E-130	92	335
38	YERCdelta20	453	94%	8.00E-130	92	337
39	YCLWdelta15	453	94%	8.00E-130	92	337
40	YARCdelta5	453	94%	8.00E-130	92	337
41	YARCdelta4	453	94%	8.00E-130	92	337
42	YHRWdelta7	449	91%	1.00E-128	93	325
43	YLRCdelta21	448	94%	4.00E-128	92	331
44	YARWdelta6	438	94%	2.00E-125	92	333
45	YELWdelta6	433	94%	1.00E-123	92	333
46	YLLCdelta1	433	93%	1.00E-123	92	332
47	YMLWdelta6	429	93%	1.00E-122	91	316
48	YJRWdelta18	414	94%	4.00E-118	91	322
49	YMRWdelta17	409	100%	2.00E-116	89	332
50	YJLCdelta4	691	94%	6.00E-116	92	667
51	YOLCdelta3	407	93%	6.00E-116	90	333
52	YILCdelta1	405	94%	2.00E-115	89	349

Supplementary Table S4.4. Sequence similarity and identity search for TyA Gag gene using Basic Local Alignment Search Tool (BLAST)

	Short name	Total Score	Query Cover	E value	Per. ident	Acc. Len
1	YHRCTy1-1	1198	100%	0	99	6028
2	YPLWTy1-1	1016	100%	0	100	5924
3	YOLWTy1-1	1016	100%	0	100	5926
4	YMLWTy1-2	1016	100%	0	100	5903
5	YLRWTy1-3	1016	100%	0	100	5920
6	YLRWTy1-2	1016	100%	0	100	5918
7	YLRCTy1-1	1016	100%	0	100	5922
8	YJRWTy1-1	1016	100%	0	100	5922
9	YERCTy1-1	1016	100%	0	100	5924
10	YDRWTy1-5	1016	100%	0	100	5918
11	YDRCTy1-3	1016	100%	0	100	5493
12	YPRCTy1-4	1005	100%	0	100	5926
13	YPRWTy1-3	989	100%	0	99	5929
14	YORWTy1-2	989	100%	0	99	5914
15	YGRCTy1-3	989	100%	0	99	5914
16	YGRCTy1-2	989	100%	0	99	5918
17	YDRWTy1-4	989	100%	0	99	5926
18	YDRCTy1-2	989	100%	0	99	5918
19	YDRCTy1-1	989	100%	0	99	5918
20	YBRWTy1-2	989	100%	0	99	5917
21	YMRCTy1-4	983	100%	0	99	5926
22	YMLWTy1-1	983	100%	0	99	5914
23	YERCTy1-2	983	100%	0	99	5727
24	YPRCTy1-2	977	100%	0	99	5918
25	YJRWTy1-2	977	100%	0	99	5922
26	YGRWTy1-1	977	100%	0	99	5926
27	YARCTy1-1	977	100%	0	99	5925
1	YNLWTy1-2	928	100%	0	97	5900
2	YNLCTy1-1	889	100%	0	96	5914
3	YBLWTy1-1	601	100%	2.00E-60	86	5916
4	YMRCTy1-3	590	100%	2.00E-60	86	5914
5	YORCTy2-1	226	50%	2.00E-60	82	5961
6	YNLCTy2-1	226	50%	2.00E-60	82	5297
7	YLRWTy2-1	226	50%	2.00E-60	82	5959
8	YDRWTy2-3	226	50%	2.00E-60	82	5955
9	YDRCTy2-1	226	50%	2.00E-60	82	5956

10	YGRCTy2-1	224	49%	9.00E-60	81	5961
11	YORWTy2-2	220	50%	1.00E-58	81	5959
12	YLRCTy2-2	220	50%	1.00E-58	81	5443
13	YGRWTy2-2	220	50%	1.00E-58	81	5951
14	YFLWTy2-1	220	50%	1.00E-58	81	5959
15	YDRWTy2-2	220	50%	1.00E-58	81	5959
16	YCLWTy2-1	220	50%	1.00E-58	81	5959
17	YBLWTy2-1	220	50%	1.00E-58	81	5959

Supplementary Table S4.5. Codon optimization of *AtCB5SD-FADX, PgFAD2, PgOLE1 and RnELO2*

Name	Length	CAI	%G+C	%G+C(1)	%G+C(2)	%G+C(3)	Nc
fadx_before	1575	0.665	51.9	52.8	42.1	61	55.4
fadx_after	1575	0.891	41.3	45	41.9	37	29
fad2_before	1164	0.591	58.6	54.9	42	78.9	46.4
fad2_after	1164	0.939	36.5	44.1	41.8	23.7	26.8
ole1_before	1524	0.702	51	57.5	43.3	52.4	52.4
ole1_after	1524	0.896	41.5	46.7	43.3	34.4	27.9
elo2_before	804	0.676	48.5	44	32.1	69.4	44.8
elo2_after	804	0.842	40.3	33.2	32.5	55.2	29.8

Supplementary Table S4.6. Optimization of culture conditions using response surface methodology.

Run	Carbon	pH	OD	Titer mean	Content means
1	60	6.5	0.2	102.5	15.3
2	105	5.3	1	214.5	18.7
3	105	6.5	0.6	330.3	23.3
4	105	7.6	0.2	292.8	21.2
5	150	6.5	1	278.8	23.1
6	150	5.3	0.6	266.5	18.2
7	150	6.5	0.2	219.6	19.5
8	105	6.5	0.6	331.5	21.7
9	60	7.6	0.6	142.6	17.7
10	105	5.3	0.2	220.6	13.9
11	150	7.6	0.6	265.8	21.5
12	105	6.5	0.6	371.7	24.4
13	60	5.3	0.6	108.9	12.6
14	105	6.5	0.6	380.6	22.1
15	105	6.5	0.6	371.4	23.2
16	105	7.6	1	343.4	23.4
17	60	6.5	1	102.1	14.4
PuA content= 22.9458 + 2.78723 * X1 + 2.49504 * X2 + 1.20784 * X3 + -0.461944 * X1X2 + 1.16779 * X1X3 -0.689039 * X2X3 -3.32149 * X1^2 -2.19481 * X2^2 -1.54413 * X3^2					
PuA titer= 357.115 + 71.6532 * X1 + 27.4837 * X2 + 13.2087 * X3 -8.89518 * X1X2 + 14.9048 * X1X3 + 14.8339 * X2X3 -126.632 * X1^2 -36.2917 * X2^2 -54.7395 * X3^2					

Supplementary Table S4.7. Strains and plasmids used in this study

Name	Description	Source
Strains		
E. coli DH5a	F– endA1 glnV44 thi-1 recA1 relA1 gyrA96 deoR nupG purB20 φ80dlacZΔM15Δ(lacZYA-argF) U169, hsdR17(rK–mK+), λ–	Invitrogen
S. cerevisiae BY4741	*MATa his3Δ1 leu2Δ0 met15Δ0 ura3Δ0*	(Baker Brachmann et al., 1998)
S. cerevisiae H1246	*MATα are1Δ::HIS3, are2Δ::LEU2, dga1Δ::KanMX4, lro1Δ::TRP1 ADE2*	Laboratory stock
S. cerevisiae snf2Δ	*S. cerevisiae* BY4741-*snf2Δ::KanMX*	Euroscarf
S. cerevisiae snf2Δ snf1Δ	*S. cerevisiae* BY4741-*snf2Δ::KanMX-snf1::AtSCP2-PgFADX*	This study
HD1	*S. cerevisiae* H1246/pST3-PgDGAT1	This study
HD2A	*S. cerevisiae* H1246/pST3-PgDGAT2.a	This study
HD2B	*S. cerevisiae* H1246/pST3-PgDGAT2.b	This study
HD2C	*S. cerevisiae* H1246/pST3-PgDGAT2.c	This study
HPA	*S. cerevisiae* H1246/pST3-PgPDAT.a	This study
HPB	*S. cerevisiae* H1246/pST3-PgPDAT.b	This study
HPC	*S. cerevisiae* H1246/pST3-PgPDAT.c	This study
FADX	*S. cerevisiae snf2Δ/*pHRPT-PgFADX	This study
SCPX-*snf2Δ*	*S. cerevisiae snf2Δ/*pHRPT-AtSCP2-PgFADX	This study
CATX-*snf2Δ*	*S. cerevisiae snf2Δ/*pHRPT-ScCAT-PgFADX	This study
CBSX-*snf2Δ*	*S. cerevisiae snf2Δ/*pHRPT-AtCB5SD-PgFADX	This study
VHBX-*snf2Δ*	*S. cerevisiae snf2Δ/*pHRPT-Vhb-PgFADX	This study

FADX-*snf1Δsnf2Δ*	*S. cerevisiae snf2Δ snf1Δ/*pHRPT-PgFADX	This study
SCPX-*snf1Δsnf2Δ*	*S. cerevisiae snf2Δ snf1Δ/*pHRPT-AtSCP2-PgFADX	This study
CATX-*snf1Δsnf2Δ*	*S. cerevisiae snf2Δ snf1Δ/*pHRPT-ScCAT-PgFADX	This study
CBSX-*snf1Δsnf2Δ*	*S. cerevisiae snf2Δ snf1Δ/*pHRPT-AtCB5SD-PgFADX	This study
VHBX-*snf1Δsnf2Δ*	*S. cerevisiae snf2Δ snf1Δ/*pHRPT-Vhb-PgFADX	This study
CARIC568	*S. cerevisiae snf2Δ snf1Δ* P_{PGK1}*-AtCB5SD-PgFADX-*T_{ADH1}*-LEU2* P_{TEF1}*- PgDGAT2.c-*T_{CYC1}*-HIS3* P_{TEF1}*-PgLPCAT-*T_{CYC1}*-HIS3* P_{TEF1}*-PgPDCT-*T_{CYC1}*-HIS3* P_{GAP}*-PgFAD2-*T_{ADH2}*-URA3* P_{GAP}*-RnELO2-*T_{ADH2}*-URA3*	This study
Plasmids		
pCRCT	TracrRNA/ iCas9/ Amp^R/ URA3	Addgene
pCRCT-MET	TracrRNA/ iCas9/ Amp^R/ MET15	This study
pDA-CRISPR	pCRCT/ YERCdelta20 crRNA	This study
pDB-CRISPR	pCRCT/ YDRWdelta23 crRNA	This study
pDC-CRISPR	pCRCT-MET/ TyA Gag gene crRNA	This study
pHRPT-AtCB5SD-PgFADX	Amp^R/URA3/ Hyg^R/P_{PGK1}*-AtCB5SD-PgFADX-*T_{ADH1}	This study
pHRPT-AtSCP2-PgFADX	Amp^R/URA3/ Hyg^R/P_{PGK1}- AtSCP2-PgFADX-T_{ADH1}	This study
pHRPT-PgFADX	Amp^R/URA3/ Hyg^R/P_{PGK1}-PgFADX -T_{ADH1}	This study
pHRPT-ScCAT-PgFADX	Amp^R/URA3/ Hyg^R/P_{PGK1}-ScCAT-PgFADX-T_{ADH1}	This study
pHRPT-VHB-PgFADX	Amp^R/URA3/ Hyg^R/P_{PGK1}-VHB-PgFADX-T_{ADH1}	This study
pST3-PgDGAT1	Amp^R/URA3/ Hyg^R/P_{TEF1}-PgDGAT1-T_{CYC1}	This study
pST3-PgDGAT2.a	Amp^R/URA3/ Hyg^R/P_{TEF1}-PgDGAT2.a-T_{CYC1}	This study
pST3-PgDGAT2.b	Amp^R/URA3/ Hyg^R/P_{TEF1}-PgDGAT2.b-T_{CYC1}	This study

pST3-PgDGAT2.c	Amp^R/URA3/ Hyg^R/P_{TEF1}-PgDGAT2.c-T_{CYC1}	This study
pST3-PgGPAT9	Amp^R/URA3/ Hyg^R/P_{TEF1}-PgGPAT9-T_{CYC1}	This study
pST3-PgLACS8	Amp^R/URA3/ Hyg^R/P_{TEF1}-PgLACS8-T_{CYC1}	This study
pST3-PgLACS9	Amp^R/URA3/ Hyg^R/P_{TEF1}-PgLACS9-T_{CYC1}	This study
pST3-PgLPAT2	Amp^R/URA3/ Hyg^R/P_{TEF1}-PgLPAT2-T_{CYC1}	This study
pST3-PgLPCAT	Amp^R/URA3/ Hyg^R/P_{TEF1}-PgLPCAT-T_{CYC1}	This study
pST3-PgPDAT.a	Amp^R/URA3/ Hyg^R/P_{TEF1}-PgPDAT.a-T_{CYC1}	This study
pST3-PgPDAT.b	Amp^R/URA3/ Hyg^R/P_{TEF1}-PgPDAT.b-T_{CYC1}	This study
pST3-PgPDAT.c	Amp^R/URA3/ Hyg^R/P_{TEF1}-PgPDAT.c-T_{CYC1}	This study
pST3-PgPDCT	Amp^R/URA3/ Hyg^R/P_{TEF1}-PgPDCT-T_{CYC1}	This study
pST3-PgPLA2a	Amp^R/URA3/ Hyg^R/P_{TEF1}-PgPLA2a-T_{CYC1}	This study
pST3-PgPLC	Amp^R/URA3/ Hyg^R/P_{TEF1}-PgPLC-T_{CYC1}	This study
pDAL-AtCB5SD-PgFADX	*YERCdelta20-left arm/*P_{PGK1}*-AtCB5SD-PgFADX-*T_{ADH1}*-LEU2/YERCdelta20-right arm*	This study
pDBH-PgDGAT1	*YDRWdelta23-left arm/*P_{TEF1}*-PgDGAT1-*T_{CYC1}*/YDRWdelta23-right arm*	This study
pDBH-PgDGAT2.a	*YDRWdelta23-left arm/*P_{TEF1}*-PgDGAT2.a-*T_{CYC1}*/YDRWdelta23-right arm*	This study
pDBH-PgDGAT2.b	*YDRWdelta23-left arm/*P_{TEF1}*-PgDGAT2.b-*T_{CYC1}*/YDRWdelta23-right arm*	This study
pDBH-PgDGAT2.c	*YDRWdelta23-left arm/*P_{TEF1}*-PgDGAT2.c-*T_{CYC1}*/YDRWdelta23-right arm*	This study
pDBH-PgGPAT9	*YDRWdelta23-left arm/*P_{TEF1}*-PgGPAT9-*T_{CYC1}*/YDRWdelta23-right arm*	This study
pDBH-PgLACS8	*YDRWdelta23-left arm/*P_{TEF1}*-PgLACS8-*T_{CYC1}*/YDRWdelta23-right arm*	This study
pDBH-PgLPAT2	*YDRWdelta23-left arm/*P_{TEF1}*-PgLPAT2-*T_{CYC1}*/YDRWdelta23-right arm*	This study
pDBH-PgLPCAT	*YDRWdelta23-left arm/*P_{TEF1}*-PgLPCAT-*T_{CYC1}*/YDRWdelta23-right arm*	This study

pDBH-PgPDAT.a	*YDRWdelta23-left arm/P_{TEF1}-PgPDAT.a-T_{CYC1}/YDRWdelta23-right arm*	This study
pDBH-PgPDCT	*YDRWdelta23-left arm/P_{TEF1}-PgPDCT-T_{CYC1}/YDRWdelta23-right arm*	This study
pDBH-PgPLA2a	*YDRWdelta23-left arm/P_{TEF1}-PgPLA2a-T_{CYC1}/YDRWdelta23-right arm*	This study
pDBH-PgPLC	*YDRWdelta23-left arm/P_{TEF1}-PgPLC-T_{CYC1}/YDRWdelta23-right arm*	This study
pDCU-AtCB5SD-FADX OPED	*TyA Gag-left arm/P_{GAP}-AtCB5SD-FADX OPED-T_{ADH2}-URA3/ TyA Gag-right arm*	This study
pDCU-PgFAD2 OPED	*TyA Gag-left arm/P_{GAP}-PgFAD2 OPED-T_{ADH2}-URA3/ TyA Gag-right arm*	This study
pDCU-PgOLE1 OPED	*TyA Gag-left arm/P_{GAP}-PgOLE1 OPED-T_{ADH2}-URA3/ TyA Gag-right arm*	This study
pDCU-RnELO2 OPED	*TyA Gag-left arm/P_{GAP}-RnELO2 OPED-T_{ADH2}-URA3/ TyA Gag-right arm*	This study

Supplementary Table S4.8. Guide sequences and target regions used in this study

Target region	Sequence
YERCdelta20-crRNA	TATACTAGAAGTTCTCCTCG/**AGG**
YDRWdelta23-crRNA	GCAAGGATTGATAATGTAAT/**AGG**
TyA Gag-crRNA	TCAGGTGATGGAGTGCTCAG/**AGG**
YERCdelta20	TGTTGGAATAGAAATCAACTATCATCTACTAACTAGTATTTACATT ACTAGTATATTATCATATACGGTGTTAGAAGATGACGCAAATGAT GAGAAATAGTCATCTAAATTAGTGGAAGCTGAAACGCAAGGATTG ATAATGTAATAGGATCAATGAATATAAACATATAAAACGGAATGA GGAATAATCGTAATATTAGTATGTAGAAATATAGATTCCATTTTGA GGATTCCTATATCCTCGAGGAGAACTTCTAGTATATTCTGTATACC TAATATTATAGCCTTTATCAACAATGGAATCCCAACAATTATCTCA ACATTCACCCATTTCTCATGGTAGCGCCTGTGCTTCGGTTACTTCTA AGGAAGTCCACACAAATCAAGATCCGTTAGACGTTTCAGCTTCCA
YDRWdelta23	TGTTGGAATAAAAATCCACTATCGTCTATCAACTAATAGTTATATT ATCAATATATTATCATATACGGTGTTAAGATGATGACATAAGTTAT GAGAAGCTGTCATCGATGTTAGAGGAAGCTGAAACGCAAGGATTG ATAATGTAATAGGATCAATGAATATAAACATATAAAACGGAATGA GGAATAATCGTAATATTAGTATGTAGAAATATAGATTCCATTTTGA GGATTCCTATATCCTCGA

TyA Gag	ATGGAATCCCAACAATTATCTCAACATTCACCCATTTCTCATGGTA
	GCGCCTGTGCTTCGGTTACTTCTAAGGAAGTCCACACAAATCAAGA
	TCCGTTAGACGTTTCAGCTTCCAAAACAGAAGAATGTGAGAAGGC
	TTCCACTAAGGCTAACTCTCAACAGACAACAACACCTGCTTCATCA
	GCTGTTCCAGAGAACCCCCATCATGCCTCTCCTCAACCTGCTTCAG
	TACCACCTCCACAGAATGGGCCGTACCCACAGCAGTGCATGATGA
	CCCAAAACCAAGCCAATCCATCTGGTTGGTCATTTTACGGACACCC
	ATCTATGATTCCGTATACACCTTATCAAATGTCGCCTATGTACTTTC
	CACCTGGGCCACAATCACAGTTTCCGCAGTATCCATCATCAGTTGG
	AACGCCTCTGAGCACTCCATCACCTGAGTCAGGTAATACATTTACT
	GATTCATCCTCAGCGGACTCTGATATGACATCCACTAAAAAATATG
	TCAGACCACCACCAATGTTAACCTCACCTAATGACTTTCCAAATTG
	GGTTAAAACATACATCAAATTTTTACAAAACTCGAATCTCGGTGGT
	ATTATTCCGACAGTAAACGGAAAACCCGTACGTCAGATCACTGAT
	GATGAACTCACCTTCTTGTATAACACTTTTCAAATATTTGCTCCCTC
	TCAATTCCTACCTACCTGGGTCAAAGACATCCTATCCGTTGATTAT
	ACGGATATCATGAAAATTCTTTCCAAAAGTATTGAAAAAATGCAA
	TCTGATACCCAAGAGGCAAACGACATTGTGACCCTGGCAAATTTG
	CAATATAATGGCAGTACACCTGCAGATGCATTTGAAACAAAAGTC
	ACAAACATTATCGACAGACTGAACAATAATGGCATTCATATCAAT
	AACAAGGTCGCATGCCAATTAATTATGAGAGGTCTATCTGGCGAA
	TATAAATTTTTACGCTACACACGTCATCGACATCTAAATATGACAG
	TCGCTGAACTGTTCTTAGATATCCATGCTATTTATGAAGAACAACA
	GGGATCGAGAAACAGCAAACCTAATTACAGGAGAAATCTGAGTGA
	TGAGAAGAATGATTCTCGCAGCTATACGAATACAACCAAACCCAA
	AGTTATAGCTCGGAATCCTCAAAAAACAAATAATTCGAAATCGAA
	AACAGCCAGGGCTCACAATGTATCCACATCTAATAACTCTCCCAGC
	ACGGACAACGATTCCATCAGTAAATCAACTACTGAACCGATTCAA
	TTGAACAATAAGCACGACCTTCACCTTAGGCCAGGAACTTACTGA

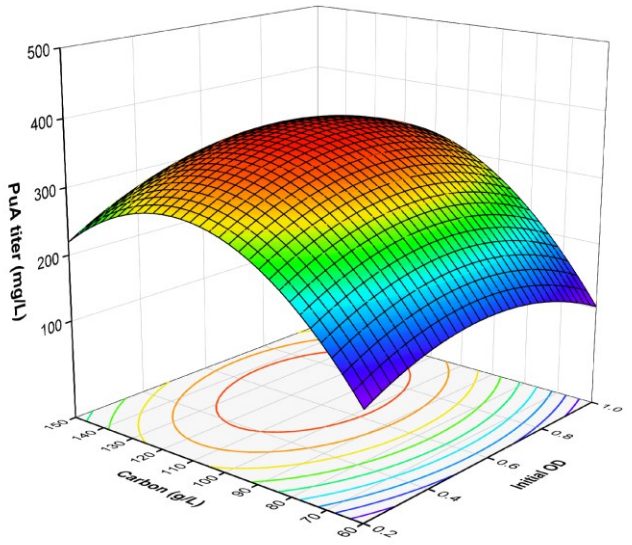

Supplementary Figure S4.1. Three-dimensional surface plot of PuA titer to carbon source level and initial OD.

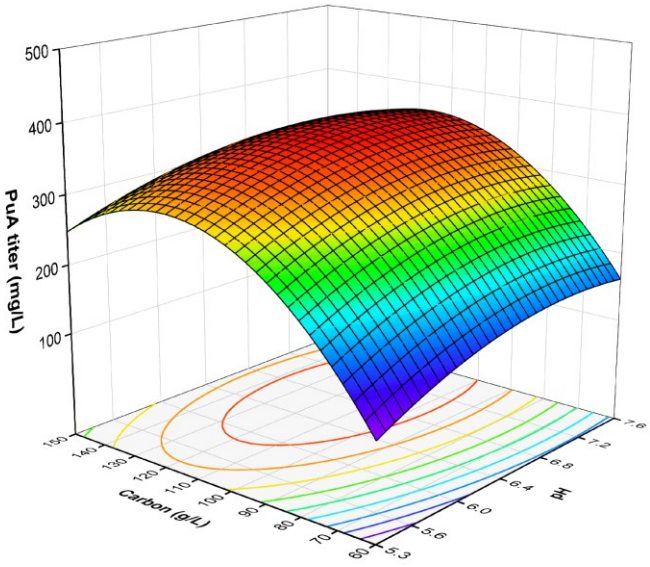

Supplementary Figure S4.2. Three-dimensional surface plot of PuA titer to carbon source level and initial pH.

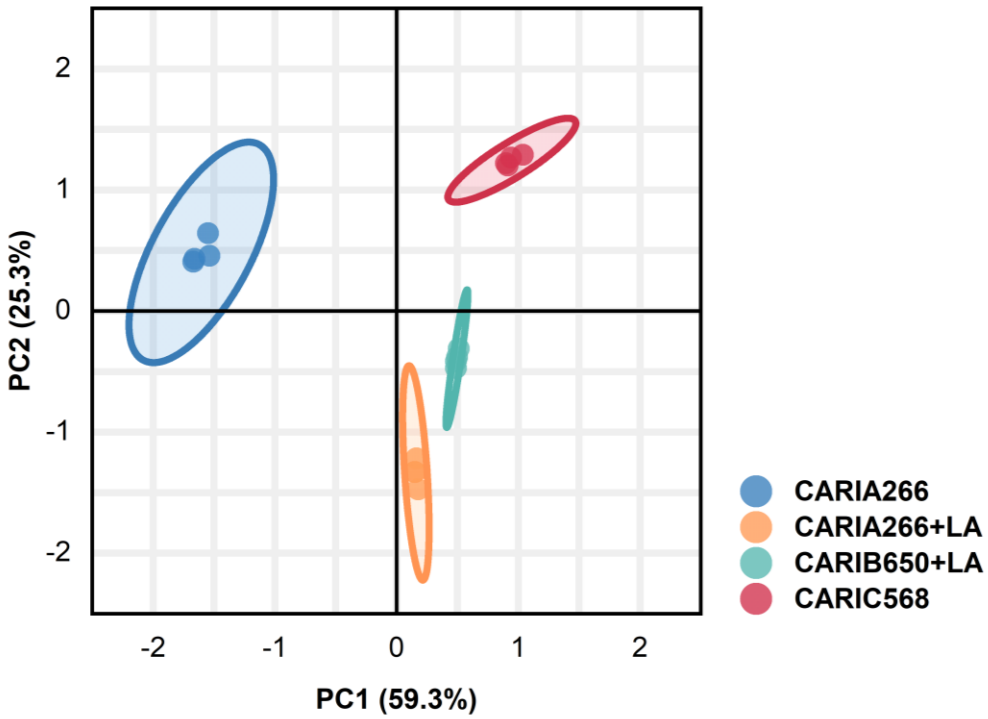

Supplementary Figure S4.3. Two-dimensional plot of principal component analysis.

PCA was performed including all the lipid data in 16 yeast cultures under investigation.

Chapter 5 – Engineering *Rhodosporidium toruloides* for the Production of Pomegranate-Derived Punicic Acid

5.1. Introduction

In our previous study, we modified baker's yeast (*Saccharomyces cerevisiae*) to produce 3.7% of total fatty acids as PuA using LA precursor feeding (Wang et al., 2021). In another study, the metabolic engineering of *Schizosaccharomyces pombe*, a yeast with high oleic acid content, led to 25.1% of total fatty acid as PuA (Garaiova et al., 2017). However, since *S. cerevisiae* and *S. pombe* have very limited ability to accumulate lipids, the PuA titer was only 7.2 mg/L and 38.7 mg/L, respectively. In this regard, it is attractive to search and develop new microbial platforms for the production of this plant-derived unusual fatty acid via metabolic engineering.

Some yeast species are well-recognized for their potential to produce single-cell oil. Oleaginous yeasts, such as *Trichosporon fermentans*, *Yarrowia lipolytica,* and *Rhodosporidium toruloides*, can accumulate more than 20% of their biomass as lipids. For instance, *T. fermentans* was able to convert rice straw hydrolysate or waste molasse to 40% - 60% of single cell oil (Huang et al., 2009; Zhu et al., 2008). *Y. lipolytica* has the ability to grow on various carbon sources including fatty acids, glucose, fructose, or glycerol, and accumulating 36% of its biomass as lipids (Zhang et al., 2014), and it has been tested for the production of several UFAs (Imatoukene et al., 2020; Park and Hahn, 2024; Urbanikova et al., 2023; Xue et al., 2013). *R. toruloides*, an unconventional yeast capable of the concomitant synthesis of lipids and carotenoids, is typically regarded as a promising candidate for biofuel production due to its excellent lipid accumulation capability, which often exceeds 60% of dry cell weight (González-García et al., 2017; Ratledge and Wynn, 2002). More interestingly, *R. toruloides* has the natural

ability to use a wide range of substrates, including pentose sugars such as xylose (Adamczyk et al., 2023; Boviatsi et al., 2020; Coradetti et al., 2023; Qi et al., 2020) (Figure 5.1A). This advantage makes *R. toruloides* promising for sustainable bioindustry and agriculture applications since xylose assimilation capability is essential for converting lignocellulosic biomass, the most abundant raw material derived from agriculture and forestry waste, into value-added UFAs.

In this study, we evaluated the potential of engineering the nonconventional yeast *R. toruloides* for the production of PuA, a plant-derived value-added UFA. *R. toruloides* transformed with *PgFADX* was able to accumulate PuA to 3.7% of total fatty acids. By further integrating codon-optimized *PgFAD2* or *PgDGAT2* into *R. toruloides'* genome, PuA contents were significantly improved. The best-engineered strain *R. toruloides* RX2 containing both *PgFADX* and *PgFAD2* accumulated 12% of total lipid as PuA using glucose as substrate and a titer of 452 mg/L PuA was achieved in flask cultivation. Lipid fraction analysis revealed that, when cultured under the nitrogen-limited condition to induce lipid accumulation, the recombinant *R. toruloides* cells accumulated higher PuA content in TAG compared to its content in PL. Finally, we tested if *R. toruloides* RX2 could use wood hydrolysate as the feedstock for PuA production, and the results revealed that the strain could accumulate 6.4% of its lipid as PuA, which demonstrated a good potential of *R. toruloides* in converting low-value agricultural waste into value-added PuA.

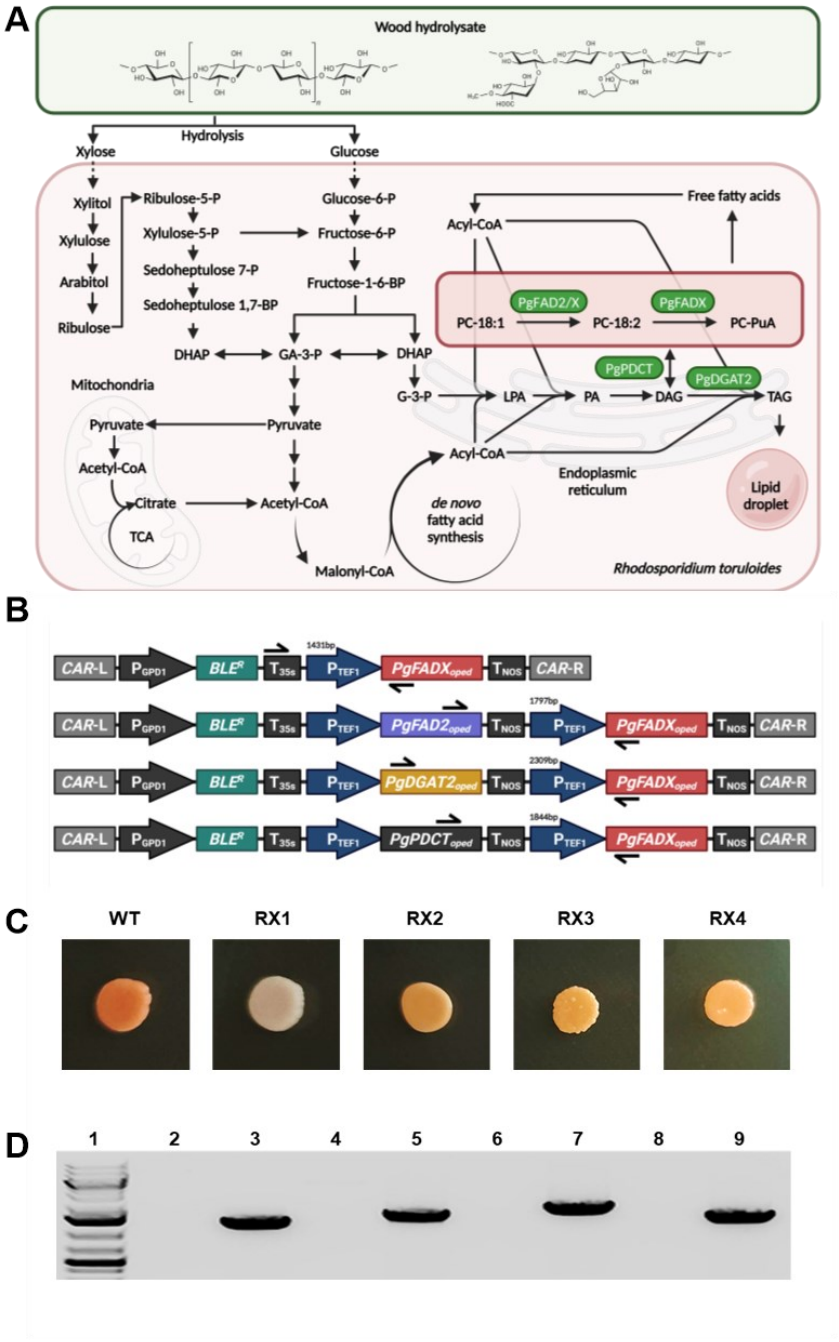

Figure 5.1. Metabolic engineering of PuA-producing *R. toruloides*.

A) Illustration of the metabolic pathway involved in PuA biosynthesis in *R. toruloides*. Abbreviations: PgDGAT2, *P. granatum* acyl-CoA: diacylglycerol acyltransferase 2; PgFAD2, *P. granatum* fatty acid desaturase 2; PgFADX, *P. granatum* fatty acid desaturase and conjugase;

PgPDCT, *P. granatum* phosphatidylcholine: diacylglycerol cholinephosphotransferase; GA-3-P, glyceraldehyde 3-phosphate; DHAP, dihydroxyacetone phosphate; G-3-P, glycerol-3-phosphate; LPA, lysophosphatidic acid; PA, phosphatidic acid; DAG, diacylglycerol; TAG, triacylglycerol; PC, phosphatidylcholine. Made with biorender.com. B) Donor DNA structures and genomic integrations of codon-optimized *PgFADX, PgFAD2, PgDGAT2,* and *PgPDCT* into *R. toruloides.* C) Colony color of *R. toruloides* wild-type strain as well as engineered strains RX1, RX2, RX3 and RX4. D) Detection of positive transformants. Lane 1, GeneRuler 1 kb Plus DNA ladder; Lane 2/4/6/8, *R. toruloides* wild type strain; Lane 3/5/7/9, detection of integrated cassettes in strain RX1, RX2, RX3, and RX4, respectively.

5.2. Materials and methods

5.2.1. Strains, plasmids and culture conditions

Strains and plasmids used in this study are listed in Table 5 and Table S5.1. *Escherichia coli* DH5α was used for routine plasmid construction and preparation. The wild-type *R. toruloides* ATCC 204091 (formerly known as *Rhodotorula glutinis*) was obtained from the American Type Culture Collection (ATCC, Manassas, VA, USA). To construct mutants with various gene deletions, the 1 kb upstream and downstream flanking sequences of the *CAR2* gene were amplified from the *R. toruloides* genomic DNA and linked with expression cassettes containing the zeocin-resistance gene and the target gene. *CAR2* encodes lycopene cyclase, which is responsible for carotenoid pigment biosynthesis (Qi et al., 2020). Insertion into the *CAR2* gene by homologous recombination leads to white colonies due to the disruption of carotenoid biosynthesis, which serves as a visual marker besides antibiotic selection for identifying transformants with successful integration. *EcoRV* restriction sites were introduced to both ends of the flanking sequences in the primer design. The zeocin-resistance gene was under

the control of the *GPD1* promoter and *35S* terminator. The target genes, including codon-optimized *PgFADX*, *PgFAD2*, *PgDGAT2*, and *PgPDCT*, were placed under the control of the *translation elongation factor 1* (*TEF1*) promoter, which is a strong constitutive promoter with robust performance under various growth conditions and *NOS* terminator (Nora et al., 2019) (Figure 5.1B). To release donor DNAs from the plasmid backbone, either PCR or double digestion of *EcoRV* sites flanking the donor DNA was conducted.

E. coli was cultured in Luria-Bertani (LB) medium at 37 °C with constant shaking at 200 rpm. Kanamycin (50 μg/L) was added to maintain a stable inheritance of plasmids. *R. toruloides* was routinely maintained with yeast extract peptone dextrose (YPD) medium containing 10 g/L yeast extract, 20 g/L peptone, and 20 g/L glucose at 30 °C. To induce lipid production, a seed culture of *R. toruloides* was first grown in a 50 mL falcon tube containing 5mL YPD medium at 30 °C and 250 rpm and then inoculated into 1 L shake flasks containing 200 mL of nutrient-limited media (100 g/L glucose; 0.1 g/L $NaNO_3$, 4.5 g/L KH_2PO_4, 0.2 g/L $MgSO_4 \cdot 7H_2O$, and 0.11 g/L $CaCl_2 \cdot 2H_2O$) to an initial OD_{600} of 0.8 (González-García et al., 2017).

5.2.2. RNA extraction, cDNA synthesis, and gene expression analysis with quantitative RT-PCR

Total RNA was extracted from various recombinant *R. toruloides* strains cultured in the nitrogen-limited medium using the Spectrum Total RNA Kit (Sigma-Aldrich, Oakville, Canada). First-strand cDNA was synthesized with the SuperScript IV first-strand cDNA synthesis kit (Invitrogen, Carlsbad, USA) according to the manufacturer's instructions, and then diluted 10 times and used as the template for analysis of *PgFADX* expression with quantitative RT-PCR (qPCR). *R. toruloides GPD1* was used as the internal reference. qPCR was conducted with three biological replicates on a StepOnePlus Real-Time PCR System (Applied Biosystems, USA)

using the GB-Amp™ Sybr Green qPCR Mix (GeneBio, Burlington, Canada) according to the manufacturer's instructions. Results were analyzed using the comparative Ct method ($2^{-\Delta\Delta Ct}$ method).

5.2.3. Chemical transformation of *R. toruloides*

Yeast transformation was performed using the lithium acetate and PEG method (Nora et al., 2019; Tsai et al., 2017). Briefly, the wild-type *R. toruloides* strain was first cultured in YPD medium at 30°C and 200 rpm overnight. The next day, the cell was diluted with fresh medium to OD_{600} of 0.2 and grown to OD_{600} of 0.8. Biomass was then recovered, washed, and resuspended in 1 mL of 100 mM lithium acetate. After centrifugation, 10 μL single-stranded salmon sperm DNA (10 mg/mL), 240 μL PEG4000, 36μL lithium acetate (1.0 M), and 5 μg DNA of interest was added to the cells, which were then incubated at 30 °C for 40 min. Subsequently, 34 μL dimethylsulfoxide (DMSO) was added to the mixture, followed by heat shock at 42 °C for 15 min. Transformed yeast cells were allowed to recover overnight at 30 °C in the YPD medium with shaking. The cells were plated on YPD agar plates containing 150 μg/mL of Zeocin and incubated at 30 °C.

5.2.4. Lipid extraction

Yeast biomass was harvested from liquid culture via centrifugation and then mixed with 800 μL of a precooled lipid extraction mixture containing chloroform and isopropanol (2:1, v/v) along with glass beads (0.5mm). Butylated hydroxytoluene (BHT) was added as the antioxidant at a final concentration of 0.01% to protect PuA from degradation. Subsequently, *R. toruloides* cells were disrupted via three cycles of bead beating (1-minute duration each) using a Biospec bead beater (Biospec, Bartlesville, OK), with a 2-minute cooling on ice between each cycle. The

extraction process was repeated twice. The collected organic phase was pooled together, dried under nitrogen, resuspended in chloroform, and stored under -20 °C until further analysis.

5.2.5. Separation of lipid class using thin-layer chromatography (TLC)

For the detailed analysis of lipid classes, extracted lipids were separated using silica gel-coated plates (0.25 mm Silica gel, DCFertigplatten, Macherey-Nagel, Germany) in a solvent mixture consisting of hexane, diethyl ether, and acetic acid in a 70:30:1 volume ratio (Mietkiewska et al., 2014). Once the TLC plates were developed, lipid fractions were visualized using a 0.05% primulin dissolved in acetone: water (8:2 v/v), which allows for the non-destructive identification of lipid bands. Following the identification of lipid fractions, the bands corresponding to the target lipid classes were scraped from the plates. These collected fractions were then subjected to lipid extraction and base-catalyzed lipid derivatization.

5.2.6. Positional analysis of TAG with enzymatic hydrolysis

The distribution of fatty acids within the *sn*-2 and *sn*-1/3 positions of TAG was conducted with enzymatic hydrolysis (Luddy et al., 1964; Xu et al., 2020b). Briefly, TAG fractions recovered from the TLC plate were moved to clean tubes and dried under a stream of nitrogen. For enzymatic hydrolysis, lipids were mixed with 1 mL Tris-HCl buffer (1 mM, pH 8.0), 100 μL 2.2% $CaCl_2$, and 250 μL 0.1% deoxycholate. This mixture was then vortexed and sonicated briefly for lipid emulsification. After being pre-warmed for 30 seconds at 40°C, 20 mg of pancreatic lipase (pancreatic lipase type II, Sigma) was added to the mixture to initiate hydrolysis. This enzyme specifically targets the acyl chain on the *sn-1/3* positions in TAGs. The reaction was continued for 3 minutes at 40°C and quenched with 500 μL of 6 M HCl. Lipids were then extracted twice with diethyl ether, followed by a secondary TLC separation. The band

corresponding to the *sn-2* monoacylglycerol fraction was recovered, transmethylated, and analyzed on the gas chromatograph (Xu et al., 2020b).

5.2.7. Lipid transmethylation and analysis

Briefly, for preparing fatty acid methyl esters (FAMEs), transmethylation was conducted via a base-catalyzed method using 1 mL of 5% sodium methoxide dissolved in methanol (Mietkiewska et al., 2014). After incubation in the dark at 30 °C for 1 hour, the transmethylation reaction was stopped by adding 1.5 mL of 0.9% (w/v) sodium chloride solution. FAMEs were extracted twice with hexane, dried under nitrogen, and analyzed on an Agilent 6890N Gas Chromatograph equipped with a 5975 inert XL Mass Selective Detector (for qualification) and a Flame Ionization Detector (for quantification). FAMEs were separated on a capillary DB23 column (30 222 m×0.25 mm×0.25 µm, Agilent Technologies, Wilmington, DE, USA) with split injection (5:1 split ratio, 1 µL injection) using the following program: 165 °C for 4 min, increased to 180 °C (10 °C/ min) and held for 5 min, and then increased to 230 °C at 10 °C/min and held for 5 min.

Table 5. Strains used in this study

Strain	Relevant genotype/property	Source
E. coli DH5a	*F– endA1 glnV44 thi-1 recA1 relA1 gyrA96 deoR nupG purB20 φ80dlacZΔM15Δ(lacZYA-argF) U169, hsdR17(rK– mK+), λ–*	Invitrogen
Wild type *R. toruloides*	*R. toruloides* ATCC 204091	ATCC
RX1	*R. toruloides* ATCC 204091 transformed with codon-optimized *PgFADX*	This study
RX2	*R. toruloides* ATCC 204091 transformed with codon-optimized *PgFAD2 and PgFADX*	This study
RX3	*R. toruloides* ATCC 204091 transformed with codon-optimized *PgDGAT2 and PgFADX*	This study
RX4	*R. toruloides* ATCC 204091 transformed with codon-optimized *PgPDCT and PgFADX*	This study

5.3. Results and Discussions

5.3.1. Reconstitution of punicic acid synthesis in *R. toruloides* via the heterologous expression of *PgFADX*

Since controlling the carbon/nitrogen ratio in the culture medium significantly impacts lipid metabolism in oleaginous microorganisms, to improve PuA production and lipid content, wild-type and recombinant *R. toruloides* were cultured in a nitrogen-limited medium optimized for lipid induction (González-García et al., 2017; Osorio-González et al., 2023; Ratledge, 2002). As shown in Figure 5.2A, after 96h of cultivation under nitrogen-limited conditions, the wild-type yeast cell accumulated C18:1 and C18:2 to 47% and 10% of total fatty acids, respectively. In contrast, there was only a limited amount of C18:3 fatty acids (<2.7%), and no conjugated fatty acids were detected in the wild-type strain. The combined C18 fatty acid occupied over 70% of total fatty acids, which is conducive to PuA accumulation since C18:1 and C18:2 are the important fatty acid precursors to PuA synthesis.

For the reconstitution of the PuA synthetic pathway in *R. toruloides*, a donor DNA cassette was first assembled (Figure 5.1B). Since *R. toruloides* genes have very high (~60%) GC contents (Hu and Ji, 2016; Bonturi et al., 2022), the gene encoding pomegranate-derived *PgFADX* was codon optimized to accommodate *R. toruloides*' specific codon usage bias (Table S5.2) and integrated into *R. toruloides*' genome targeting the *CAR2* region, which was shown to have higher gene editing efficiency compared to other commonly used loci, such as *URA3* (Otoupal et al., 2019). As shown in Figure 5.1C, after the transformation of *PgFADX*, strains with white colonies were obtained on the zeocin agar plate. Subsequent analysis detected the *PgFADX* cassette on the genomic DNA recovered from positive transformants (Figure 5.1D). In order to examine their PuA-accumulating ability, seven single white colonies were tested in the

nitrogen-limited medium. As shown in Figure 5.2B, the transformation of *PgFADX* led to 1.6%-2.6% of total fatty acids as PuA, with an average content of 2.3%. Notably, the linolenic acid content in transformed *R. toruloides* decreased to less than 0.3% (Figure 5.2B). Since linolenic acid synthesis competes with PuA synthesis for LA substrate, in our previous study, a mutant *Arabidopsis* line lacking fatty acid desaturase 3 activity was used to limit competition and improve PuA production (Mietkiewska et al., 2014). Although a bifunctional Δ12/Δ15 fatty acid desaturase was suggested to carry out further desaturation converting LA into linolenic acid in oleaginous yeasts such as *R. toruloides* and *Lipomyces starkeyi* (Y. Liu et al., 2021; Matsuzawa et al., 2018), the very low content of linolenic acid content in the transgenic *R. toruloides* strains indicated that PgFADX may effectively compete with *R. toruloides*' endogenous desaturase for LA substrate. Therefore, removing the activities of native desaturases may not be necessary.

To further characterize the influence of *PgFADX* overexpression, the transformant with the highest PuA content, designated as RX1, was tested in a 10-day shake flask cultivation. As shown in Figure 5.2C, the level of LA and PuA in strain RX1 gradually increased in the 10-day period, and PuA accounted for 3.7% of total fatty acids at the end of cultivation. A concomitant increase in LA and PuA was also observed, which was possibly due to PgFADX's bifunctional activity to produce both LA and PuA (Garaiova et al., 2017). On the contrary, the content of oleic acid level was reduced from 58% to 50% between day 2 and day 10. The PuA titer at the end of the cultivation reached 88.8 mg/L, which was higher than the level previously achieved in *S. cerevisiae* and *Y. lipolytica* with single *PgFADX* expression (Urbanikova et al., 2023; Wang et al., 2021). Taken together, the results indicated that *R. toruloides* has great potential to become a yeast platform for producing plant-derived PuA.

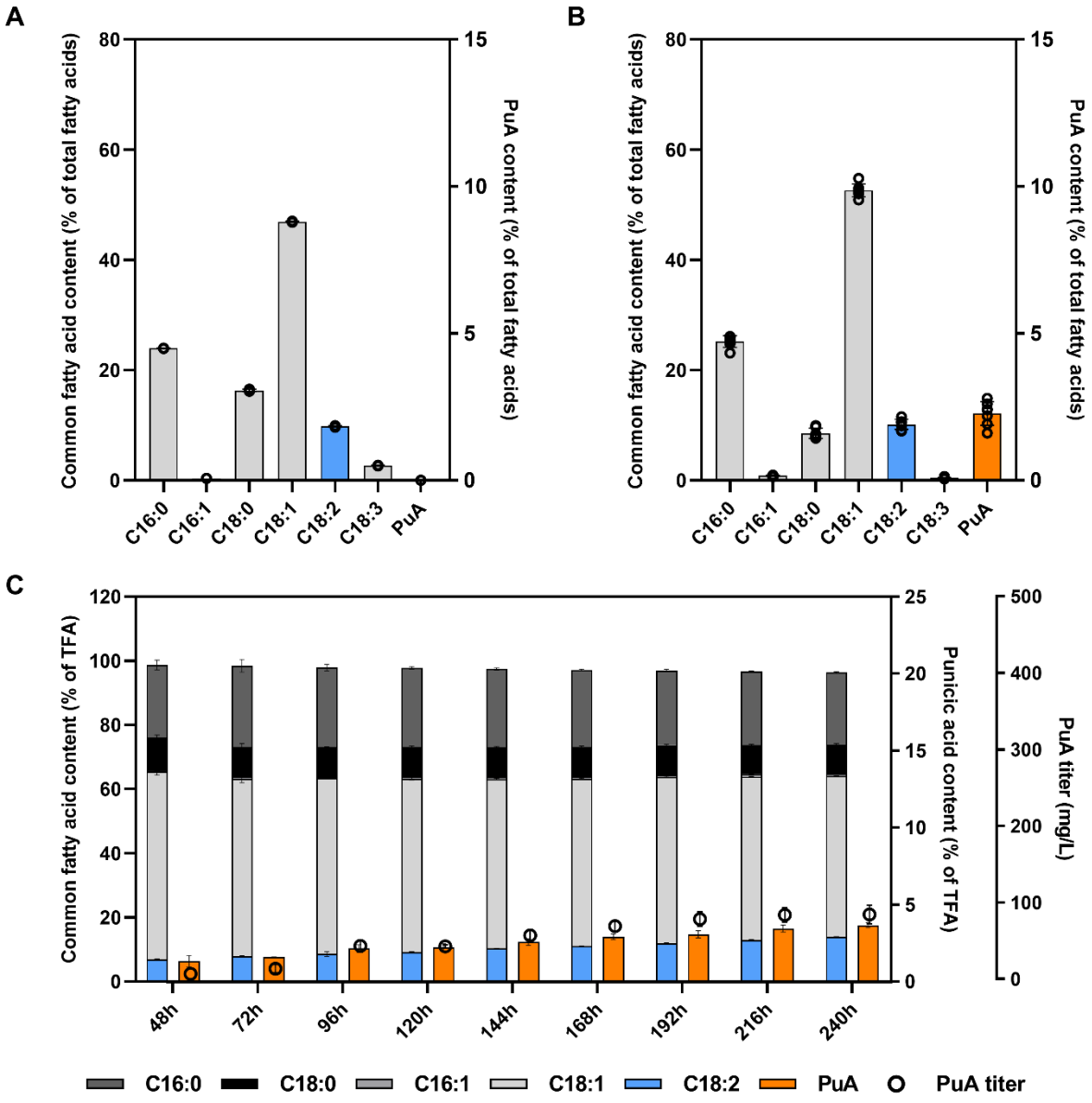

Figure 5.2. Genomic integration of pomegranate *PgFADX* expression cassette led to PuA-producing *R. toruloides* strain RX1.

A) Fatty acid composition of wild-type *R. toruloides* cultured in chemically defined medium. B) Integration of *PgFADX* led to PuA product. C) Fatty acid composition and PuA titer of RX1 strain from 48h to 240h. Data represents mean ± SD of triplicates.

5.3.2. Coexpression of *PgFADX* with *PgFAD2* or *PgDGAT2* significantly improved punicic acid content in recombinant *R. toruloides*

Considering the importance of LA precursor to PuA synthesis, we further constructed a *PgFAD2* and *PgFADX* coexpression cassette, aiming to provide more LA precursor to PgFADX on top of *R. toruloides*' native LA synthesis. Moreover, since the channeling of UFAs in the natural producer also requires a series of downstream enzymes such as DGAT2 and PDCT (Burgal et al., 2008; Demski et al., 2022; Shockey et al., 2006), strains coexpressing *PgFADX* with *PgDGAT2* or *PgPDCT* were also constructed, respectively (Table 5). Only a few transformants harboring the coexpression of two genes were recovered from the zeocin selection plate, and all of them displayed an orange pigmentation (Figure 5.1C), indicating the incomplete *CAR2*-targeted insertion and disruption by the cassettes. The incomplete disruption may have been caused by the much longer length of the co-expression cassettes, in comparison to the single *PgFADX* expression cassettes (Figure 5.1B), or by the preference for nonhomologous end joining (NHEJ) over homologous recombination (HR) for DNA repair in the *R. toruloides* strain (Schultz et al., 2019). Indeed, earlier studies indicated that high *CAR2* deletion efficiency up to 75.3% was only obtained in the KU70-deficient *R. toruloides* strain, which has a mutation of Ku70/80 regulatory DNA-binding subunits that is critical to the NHEJ system, whereas in the wild-type *R. toruloides* strain, the targeted deletion frequency of *CAR2* was only 10.5% (Koh et al., 2014). The donor DNA cassettes generated for coexpression appeared to be randomly integrated into the *R. toruloides* genome by NHEJ, in line with a previous study using a similar transformation method (Tsai et al., 2017).

To take into account positional effects, in which surrounding genetic elements may enhance or inhibit gene expression, different transformants were examined for their varying

abilities to accumulate PuA. As shown in Figure 5.3A, *PgFADX-PgFAD2* coexpression led to 5.8%-9.6% of total fatty acids as PuA, with an average of 7.4%, representing a 2.3-fold increase compared to *PgFADX* single expression (Figure 5.2). In addition, the average LA content increased by 30% at the expense of oleic acid content (Figure 5.3A). Similarly, the coexpression of *PgDGAT2* with *PgFADX* resulted in a 2-fold rise in PuA content, whereas LA content decreased by 14% (Figure 5.3B). In contrast, the coexpression of *PgPDCT* with *PgFADX* only increased the PuA content by merely 17% (Figure 5.3C). The transformants with highest PuA content for *PgFADX-PgFAD2*, *PgFADX-PgDGAT2*, and *PgFADX-PgPDCT* coexpression, designated as strains RX2, RX3, and RX4, were subsequently investigated in shake flask culture (Figure 5.3D, E and F). By the end of the 10-day cultivation, LA and PuA accounted for 13.8% and 12% of total fatty acids in RX2, respectively (Figure 5.3D). The final lipid content was 66% of dry cell weight, and the PuA titer of strain RX2 reached 452 mg/L, which was 5-fold that of RX1. In strain RX3, the PuA levels reached 8% of total fatty acids at the end of cultivation and led to a final PuA titer of 285 mg/L (Figure 5.3E), which was 3.2-fold that of RX1. To determine whether the increase in PuA production resulted from changes in *PgFADX* expression levels or from the beneficial effects of the coexpressed enzymes, the relative expression levels of *PgFADX* in RX2, RX3, and RX4 were also quantified using RT-PCR (Figure 5.4A). Results showed that *PgFADX* expression was not higher in RX2, RX3, and RX4 when compared to the level in strain RX1. Collectively, the results indicate that *PgFAD2* and *PgDGAT2* could significantly further improve PuA production in *R. toruloides.*

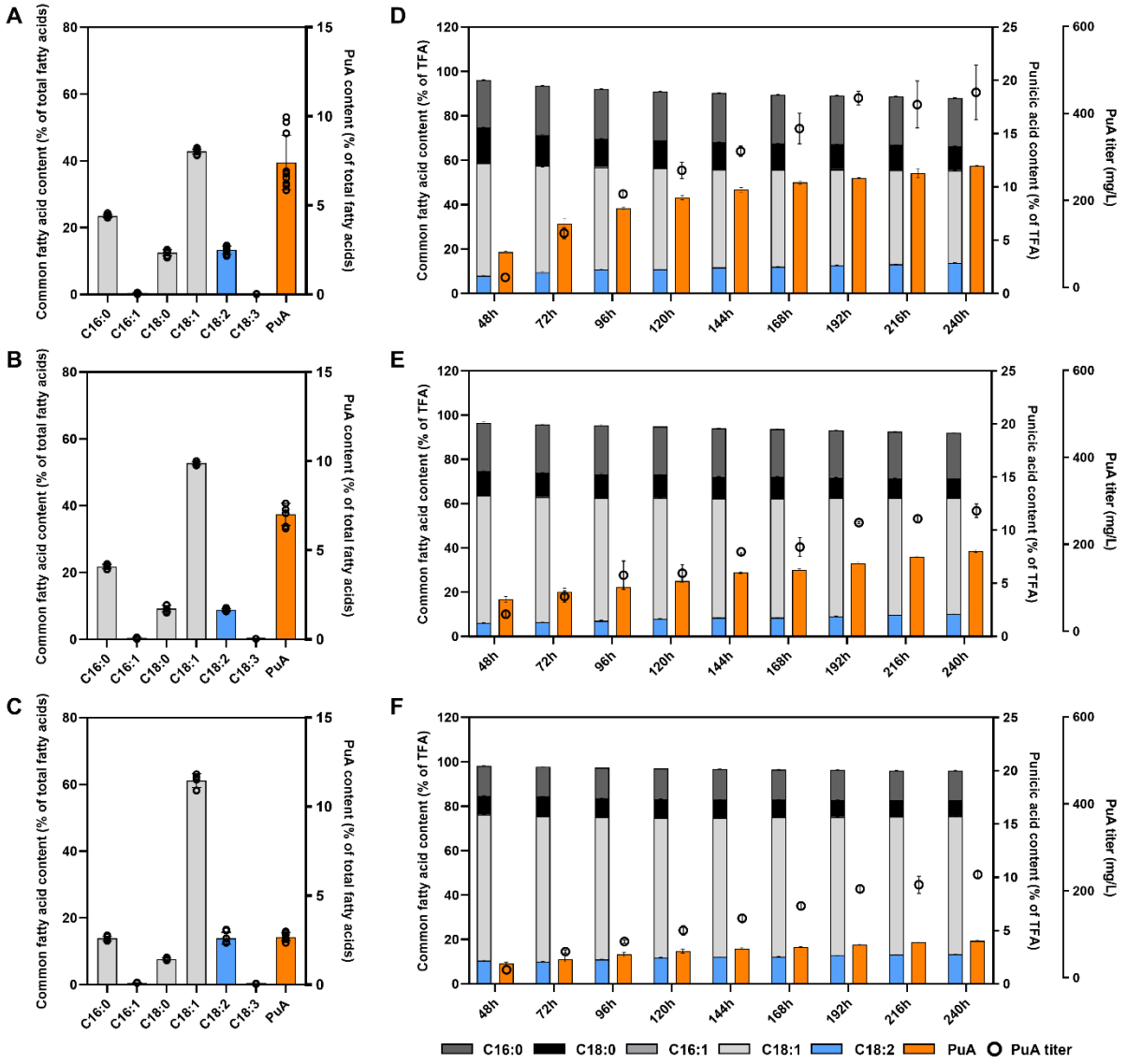

Figure 5.3. Coexpression of pomegranate *PgFAD2*, *PgDGAT2*, and *PgPDCT*, respectively, with *PgFADX* led to increased PuA production.

A-C) Fatty acid composition of *R. toruloides* strains coexpressing *PgFAD2-PgFADX, PgDGAT2-PgFADX, and PgPDCT-PgFADX*. D-F) Fatty acid composition and PuA titer of *R. toruloides* strains RX2, RX3, and RX4 from 48h to 240h. Data represent mean ± SD of triplicates.

In the previous study, when coexpressing *PgFAD2* with *PgFADX* in *S. cerevisiae*, the LA content was increased to over 6%, whereas PuA content was only 0.3% of total fatty acids, indicating that LA was not effectively converted to PuA (Wang et al., 2021). In the metabolically engineered oleaginous *Y. lipolytica* with *PgFADX* overexpression, the level of LA (2.9%) was also much higher than the PuA level (0.5%) (Urbanikova et al., 2023). In this study, the level of LA and PuA obtained in the recombinant *R. toruloides* strain RX2 was relatively more balanced, which, together with its high oleaginicity and enhanced PuA content, led to a high PuA titer of 452 mg/L in the flask culture. Although previous studies demonstrated that both DGAT2 and PDCT could improve the production of UFAs in transgenic hosts (Burgal et al., 2008; Yu et al., 2019), the different PuA content in RX3 and RX4 indicated the varied performance of PgDGAT2 and PgPDCT in transgenic *R. toruloides*. Indeed, many plant-derived DGAT2s have distinct acyl-CoA and DAG substrate preferences, which considerably contribute to the accumulation of UFAs (Burgal et al., 2008; Shockey et al., 2006). Correspondingly, *PgFADX-PgDGAT2* coexpression in *R. toruloides* RX3 also substantially increased PuA content compared with RX1. In contrast, although PDCT activity was proposed to play an important role in regulating UFA exchange between DAG and polar lipid pools, which facilitates the enrichment of UFAs in TAG (Demski et al., 2022; Lu et al., 2009; Yu et al., 2019), *PgFADX-PgPDCT* coexpression in *R. toruloides* RX4 did not substantially enhance PuA production (Figure 5.3). This result could be due to the use of nitrogen-limited culture conditions, in which the nutritional stress already limited the synthesis of phospholipids for cell membrane proliferation, and concentrated *Rhodosporidium*'s native lipid metabolism towards TAG biosynthesis (Patel et al., 2017).

5.3.3. Distribution of punicic acid in polar and neutral lipids extracted from recombinant *R. toruloides*

To further elucidate the PuA distribution among different lipid classes, total lipids extracted from strains RX1, RX2, RX3, and RX4 cultured in nitrogen-limited conditions, as well as wild-type *R. toruloides* cultured in the 2*YPD medium, were separated by TLC (Figure 5.4B). Under nitrogen-limited conditions, all recombinant *R. toruloides* cultures produced a higher amount of neutral lipids compared to polar lipids (PL). In terms of fatty acid distribution, 4.9% PuA, 17% LA, and 47% oleic acid were found in the TAG isolated from strain RX1 (Figure 5.4C), while PuA made up just 0.8% of the total fatty acids in the PL fraction of RX1 lipid (Figure 5.4D). With *PgFADX-PgFAD2* coexpression, strain RX2 accumulated 13.6% PuA in TAG, representing a 1.78-fold increase compared to strain RX1 (Figure 5.4C). Meanwhile, the levels of LA and oleic acid were reduced by 9% and 15%, respectively. The PL fraction separated from strain RX2 lipid mainly comprised 1.4% PuA, 32% LA, and 46% oleic acid. Since both PgFAD2 and PgFADX use C18:1-PC as substrate, the amount of oleic acid in RX2's PL was considerably reduced by 46% compared to RX1. Albeit at a lower level relative to RX2, strains RX3 and RX4 also accumulated 10.7% and 5.5% PuA in TAG, respectively, indicating a 1.2- and 0.13-fold increase compared to RX1.

In the seed lipid of pomegranate, PuA made up 60% of the fatty acids in TAG and merely 0.8% of the fatty acids in PC (Mietkiewska et al., 2014). In contrast, the distribution of UFAs between PL and TAG significantly varies in transgenic hosts (Mietkiewska et al., 2014; Wang et al., 2021; Xu et al., 2020b). For example, in PuA-producing transgenic *Arabidopsis*, the PuA content of TAG was only 6.6%, whereas PC contained up to 12.5% of total fatty acids as PuA (Mietkiewska et al., 2014). On the contrary, in recombinant PuA-accumulating *S. cerevisiae,*

PuA accounted for 4.8% of total fatty acids in PL, which was 1.3-fold higher than its content in TAG (Wang et al., 2021). However, in this study, recombinant *R. toruloides* led to significantly higher PuA content in TAG than in PL. A similar observation was also reported in eicosapentaenoic acid (EPA)-producing *Y. lipolytica* (Xue et al., 2013). A possible explanation is that under nitrogen-limited conditions, TAG synthesis in oleaginous yeast undergoes a significant upregulation, channeling more fatty acid toward TAG assembly instead of being utilized for membrane expansion and PL synthesis.

Positional analysis of TAG was also conducted for all strains (Figure 5.4E, 4F). Results revealed that PuA was preferentially attached to the *sn*-1/3 positions on TAG, with the highest percentage (19.3%) in RX2 (Figure 5.4E, F). A similar result was found in a prior study, in which metabolically engineered EPA-producing *Y. lipolytica* preferably concentrated EPA at the *sn*-1/3 positions of TAG (Xue et al., 2013). The rearrangement of EPA across the glycerol backbone suggested significant lipid remodeling between the PL and TAG fractions in *Y. lipolytica* (Xue et al., 2013); a process that might similarly occur in *R. toruloides*. Moreover, the results also indicated that a further rationally designed metabolic engineering strategy could be developed to target the improvement of PuA content at the *sn*-2 position of TAG. Without reducing its content at the *sn*-1/3 positions, such a strategy may further enrich PuA content in the TAG fraction.

Although some naturally occurring polar lipids are being investigated for their potential in nutraceutical applications (Da Costa et al., 2021; Venkat et al., 2024), the presence of phospholipids in crude oils is sometimes considered to negatively affect the oil's appearance and flavor (Liu et al., 2023). Since the oxidation of phospholipids has a substantial influence on the stability, shelf life, and quality of food oils, in food lipid production, degumming is often

required to remove phospholipids from crude oils (Li et al., 2023). In the case of PuA-containing oils produced by heterologous hosts, removing PL may result in product loss, especially if a larger ratio of PuA is retained in the PL fraction rather than the neutral lipid fraction. From the biological perspective, the buildup of UFAs in PL may also lead to fitness costs (Yazawa et al., 2013; Yu et al., 2019). In this regard, the ability of engineered *R. toruloides* to accumulate a high amount of PuA in TAG under nitrogen-limited conditions makes it valuable for industrial purposes.

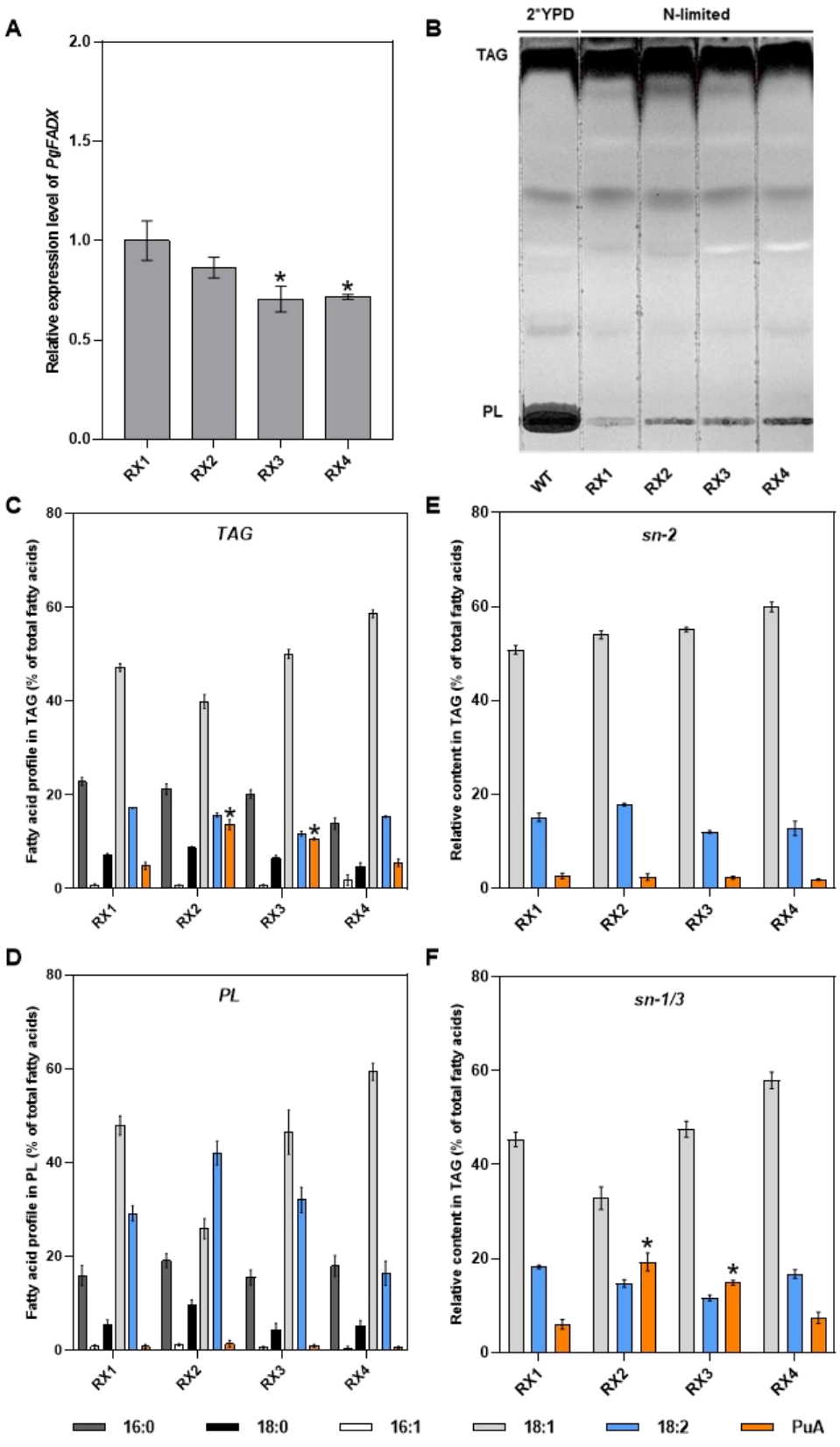
A
Relative expression level of PgFADX
2.0
1.5
1.0
0.5
0.0
RX1
RX2
RX3
RX4
B
2*YPD
N-limited
TAG
PL
WT
RX1
RX2
RX3
RX4
C
TAG
Fatty acid profile in TAG (% of total fatty acids)
D
PL
Fatty acid profile in PL (% of total fatty acids)
E
sn-2
Relative content in TAG (% of total fatty acids)
F
sn-1/3
Relative content in TAG (% of total fatty acids)
16:0
18:0
16:1
18:1
18:2
PuA

Figure 5.4. Analysis of *PgFADX* expression levels and PuA distribution in engineered *R. toruloides* strains.

A) Relative expression of *PgFADX* gene in recombinant *R. toruloides* strains. *R. toruloides* GPD1 gene was used as the internal reference gene. B) TLC separation of lipids extracted from the wild-type and four engineered strains. C) Fatty acid composition of TAG. D) Fatty acid composition of polar lipids. E) Fatty acid composition at the *sn-2* position of TAG. F) Fatty acid composition at the *sn-1/3* positions of TAG. Data represents mean ± SD of triplicates. ∗, $P < 0.05$ (Student's t-test).

5.3.4. Converting wood hydrolysate into punicic acid-containing single-cell oil

R. toruloides has a broad substrate range and is notable for its inherent ability to metabolize pentose sugars, attracting interest for its potential in converting lignocellulosic biomass into valuable bioproducts (Boviatsi et al., 2020; Qi et al., 2020; Sunder et al., 2023). Moreover, *R. toruloides* has shown strong growth in the presence of various inhibitors that are typically found in pretreated agricultural wastes, demonstrating its tolerance to stressful conditions compared to other yeasts (Jiao et al., 2021; Y. Zhang et al., 2022b). In this regard, we examined the capability of the best-engineered *R. toruloides* strain RX2 in converting lignocellulose feedstock into PuA-containing single-cell oil. We first generated wood pulp hydrolysate and analyzed its sugar composition. Enzymatic hydrolysis of wood pulp yielded a liquid wood hydrolysate containing 62 mg/mL glucose and 16 mg/mL xylose, which was differentially diluted and used to replace the glucose in the nitrogen-limited medium (González-García et al., 2017).

As shown in Figure 5.5A, RX2 could successfully convert wood hydrolysate to PuA containing single-cell oil. When cultivated in 80% wood hydrolysate, RX2 accumulated 5.5% of

total fatty acids as PuA. A slight increase in PuA content and titer was observed when using a higher concentration of wood hydrolysate and a higher initial OD_{600}. Subsequently, a 10-day cultivation in 100% wood hydrolysate was conducted (Figure 5.5B). By the end of the cultivation, the strain accumulated 6.4% of its fatty acids as PuA, and the PuA titer reached 310 mg/L in shake flask conditions. These results demonstrated the potential of *R. toruloides* in producing PuA, and likely other value-added UFAs, from low-cost feedstock, which is particularly valuable in sustainable bioindustries.

Lignocellulose feedstock, along with many other renewable feedstocks, is frequently regarded as a suitable substrate for microbial cell factories due to its availability and renewable nature (Sunder et al., 2023; de Paula et al., 2019; Ling et al., 2014). Lignocellulosic biomass can be obtained from agriculture and forestry waste, and unlike starch or sugar, the abundance of lignocellulose feedstock ensures a long-term and secure supply of substrates for industrial bioprocesses without competing with food sources (Fatma et al., 2018; Inyang et al., 2022; Kumar and Sharma, 2017; Somerville et al., 2010). To transform lignocellulosic substrates into bioproducts, a microorganism must be capable of utilizing both pentose and hexose sugars. However, not all industrially significant strains have this capability. In the yeast *S. cerevisiae*, the introduction of heterologous xylose reductase/xylitol dehydrogenase pathway or xylose isomerase pathway was needed to enable the use of xylose as the carbon source (Gao et al., 2023). Although the oleaginous yeast *Y. lipolytica* has emerged as a promising host for lipid and bioproduct synthesis, it is also unable to grow with xylose as the sole carbon source (Ledesma-Amaro et al., 2016; Zhao et al., 2015). The co-expression of xylose reductase and xylitol dehydrogenase from *Scheffersomyces stipitis* coupled with overexpression of the endogenous

xylulokinase are necessary to permit normal growth of engineered *Y. lipolytica* on xylose (Ledesma-Amaro et al., 2016).

On the contrary, oleaginous *R. toruloides* can naturally assimilate pentose sugars, which is a great advantage in serving as a platform for converting low-value lignocellulose feedstock to high-value UFAs via metabolic engineering. Moreover, previous studies indicated that *R. toruloides*' ability to convert lignocellulosic feedstock into bioproducts could be improved through the enhancement of xylose assimilation and the adaptive evolution of the engineered strain (Coradetti et al., 2023; Díaz et al., 2018; Z. Liu et al., 2021). *R. toruloides* has an unusual xylose metabolism featuring the reduction to D-arabitol, oxidation to D-ribulose, and phosphorylation to ribulose 5-phosphate (Adamczyk et al., 2023). By overexpressing a putative transcription factor (RTO4_12978, Pnt1) that acts as a major regulator of pentose metabolism, the expression of enzymes involved in xylose catabolism was increased and the specific growth rate was improved significantly in cultures on xylose (Coradetti et al., 2023). Furthermore, the adaptation of *R. toruloides* through evolutionary strategies has also led to the development of strains with increased tolerance to the major inhibitors present in lignocellulosic hydrolysates (Díaz et al., 2018; Z. Liu et al., 2021). In the future, through additional adaptation of PuA-producing *R. toruloides* in lignocellulosic medium and metabolic engineering of the xylose assimilation pathway, both the cell growth and the production of PuA could be further enhanced.

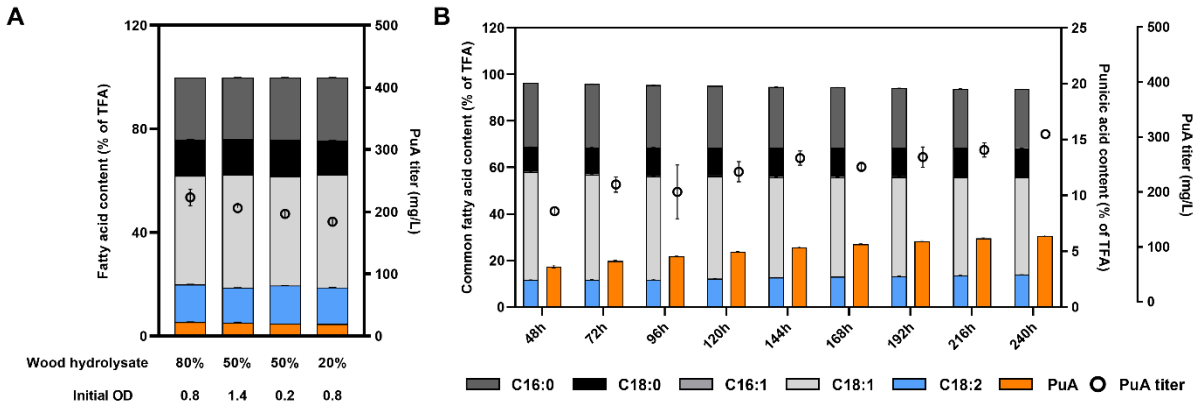

Figure 5.5. Converting wood hydrolysate into PuA-containing single-cell oil by strain RX2. A) Examining the influence of wood hydrolysate concentration and initial OD_{600} on PuA production. B) Fatty acid composition and PuA titer of *R. toruloides* strain RX2 cultured in 100% wood hydrolysate from 48h to 240h. Data represents mean ± SD of triplicates.

5.4. Conclusions

In this study, the unconventional oleaginous yeast *R. toruloides* was engineered for the first time to produce PuA, a unique and valuable conjugated fatty acid synthesized in plants. By integrating codon-optimized *PgFADX*, strain RX1 successfully synthesized 3.7% PuA. Further coexpression of *PgFAD2* or *PgDGAT2* led to a notable increase in PuA levels. The engineered strain RX2 hosting *PgFADX* and *PgFAD2* could produce 12% of total fatty acids as PuA and achieve 452 mg/L PuA production using glucose as the carbon source. Utilizing wood hydrolysate as the feedstock, RX2 produced 6.4% of total fatty acids as PuA with a titer of 310 mg/L in the shake flask culture. Taken together, our results demonstrated that *R. toruloides* could serve as an ideal platform for the production of plant-derived high-value conjugated fatty acids via metabolic engineering from agricultural waste.

5.5. Supplementary material

Supplementary Table S5.1. Plasmids and qPCR primers used in this study

Name	Description	Source
Plasmids		
pRT-FADX	Kan^R/ *RtCAR2-left arm*/ P_{GPD1}*-codon-optimized* BLE^R-T_{35s} / P_{TEF1}- *PgFADX-*T_{NOS}/ *RtCAR2-right arm*	This study
pRT-FAD2-FADX	Kan^R/ *RtCAR2-left arm*/ P_{GPD1}*-codon-optimized* BLE^R-T_{35s}/ P_{TEF1}- *PgFAD2-*T_{NOS} / P_{TEF1}- *PgFADX-*T_{NOS}/ *RtCAR2-right arm*	This study
pRT-DGAT2-FADX	Kan^R/ *RtCAR2-left arm*/ P_{GPD1}*-codon-optimized* BLE^R-T_{35s}/ P_{TEF1}- *PgDGAT2-*T_{NOS} / P_{TEF1}- *PgFADX-*T_{NOS}/ *RtCAR2-right arm*	This study
pRT-PDCT-FADX	Kan^R/ *RtCAR2-left arm*/ P_{GPD1}*-codon-optimized* BLE^R-T_{35s}/ P_{TEF1}- *PgPDCT-*T_{NOS} / P_{TEF1}- *PgFADX-*T_{NOS}/ *RtCAR2-right arm*	This study
qPCR primers		
qRt-GPD1-F	GTACGACCAGATCAAGCAGAC	This study
qRt-GPD1-R	ACAAAGTCGGTTGAGACGAG	This study
qRT-FADX-F1	ACGGCTTTGCATCACACTAC	This study
qRT-FADX-R1	GAGGCGGTAGAGGATGTAGTAG	This study

Supplementary Table S5.2. Codon-optimized sequences used in this study

Name	Sequence
PgFADX-OPTIMIZED-RT	ATGGGCGCCGACGGCACCATGTCGCCGGTCCTCACCAAGCGCCGCC CGGACCAGGAGATCAACAAGCTCGACATCAAGCCGAACCACGAGGT CGACATCGCCCGCCGCGCACCGCATTCGAAGCCGCCGTTCACCCTCT CGGACCTCCGCTCGGCCATCCCGCCGCACTGCTTCCATCGCTCACTC CTCATGTCGTCGTCGTACCTCATCCGCGACTTCGCCCTCGCCTTCCTC TTCTACCACTCGGCCGTCACCTACATCCCGCTCCTCCCGAAGCCGCT CGCCTGCATGGCATGGCCGGTCTACTGGTTCCTCCAGGGCTCGAACA TGCTCGGCATCTGGGTCATCGCCCACGAGTGCGGCCACCAGGCCTTC TCGAACTACGGCTGGGTCAACGACGCCGTCGGCTTCTTCCTCCACAC CTCGCTCCTCGTCCCGTACTTCCCGTTCAAGTACTCGCACCGCCGCCA CCACTCGAACACCAACTCGGTCGAGCACGACGAGGTCTTCGTCCCGC GCCACAAGGACGGCGTCCAGTGGTACTACCGCTTCTTCAACAACACC CCGGGCCGCGTCCTCACACTCACCCTCACCCTCCTCGTCGGCTGGCC GTCGTACCTCGCCTTCAACGCCTCGGGCCGCCCGTACGACGGCTTTG CATCACACTACAACCCGAACGCCCAGATCTTCAACCTCCGCGAGCGC TTCTGGGTCCACGTCTCGAACATCGGCATCCTCGCCATCTACTACAT CCTCTACCGCCTCGCCACCACCAAGGGCCTCCCGTGGCTCCTCTCGA TCTACGGCGTCCCGGTCCTCATCCTCAACGCCTTCGTCGTCCTCATCA CCTTCCTCCAGCACTCGCACCCGGCCCTCCCGCACTACAACTCGGAC GAGTGGGACTGGCTCCGCGGCGCACTCGCCACCGTCGACCGAGACT ACGGCTTCCTCAACGAGGTCTTCCACGACATCACCGACACCCACGTC ATCCACCACCTCTTCCCGACCATGCCGCACTACAACGCCAAGGAGGC CACCGTCTCGATCCGCCCGATCCTCAAGGACTACTACAAGTTCGACC GCACCCCGATCTGGCGCGCCCTCTGGCGCGAAGCCAAGGAGTGCCT CTACGTCGAGGCCGACGGCACCGGCTCGAAGGGCGTCCTCTGGTTCA AGTCGAAGTTCTAG
PgFAD2-OPTIMIZED-RT	ATGGGCGCCGGCGGCCGAATGACCGTCCCGAACAAGTGGGAGGGCG AGGGCGACGAGAAGTCGCAGAAGCCGGTCCAGCGCGTCCCGTCGGC CAAACCACCATTCACCCTCTCGGAGATCAAGAAGGCCATCCCGCCGC ACTGCTTCAAGCGCTCGCTCCTCAAGTCGTTCTCGTACGTCCTCTACG ACCTCACCCTCGTCGCCATCTTCTACTACGTCGCCACCACCTACATCG ACGCCCTCCCGGGCCCACTACGCTACGCCGCATGGCCAGTCTACTGG GCCCTCCAGGGCTGCGTCCTCACCGGCGTATGGGTCATCGCCCACGA GTGTGGACACCACGCCTTCTCGGACTACCAGTGGGTCGACGACTGCG TCGGCCTCGTCCTCCACTCGGCCCTCCTCGTCCCGTACTTCTCGTGGA AGTACTCGCACCGCCGCCACCACTCGAACACCGGCTCGCTCGAGCGC

GACGAGGTCTTCGTCCCGAAGCCGAAGTCGAAGATGCCGTGGTTCTC
GAAGTACCTCAACAACCCGCCGGGCCGCGTCATGACCCTCATCGTCA
CCCTCACCCTCGGCTGGCCGCTCTACCTCGCCCTCAACGTCTCGGGC
CGCCCGTACGACCGCTTTGCATGCCACTTCGACCCGTACGGCCCGAT
CTACACCGACCGCGAGCGCCTCCAGATCTACATCTCGGACGTCGGCA
TCATGGCCGCCACCTACACCCTCTACAAGATCGCCGCCGCCCGAGGA
CTAGCCTGGCTCGTCTGCGTCTACGGCGTCCCGCTCCTCATCGTCAA
CGCCTTCCTCGTCACCATCACCTACCTCCAGCACACCCACCCGGCCC
TCCCGCACTACGACTCGTCGGAGTGGGACTGGCTCCGCGGCGCACTA
GCCACCGCCGATCGAGACTACGGCATCCTCAACAAGGTCTTCCACAA
CATCACCGACACCCACGTCGCCCACCACCTCTTCTCGACCATGCCGC
ACTACCACGCCATGGAGGCCACCAAGGCCATCAAGCCGATCCTCGG
CGACTACTACCAGTTCGACGGCACCCCGGTCTACAAGGCCATGTGGC
GCGAGGCCCGCGAGTGTCTCTACGTCGAGCCGGACGACGGCGCCAA
CTCGAAGGGCGTCTTCTGGTACAAGAAGAACCTCTAG

ATGGGCGAGGAGGCCTCGGTCAAGCTCGGCGAGGACCAGCAGCGCG
AGGTCTTCACCGGCCGCAAGGAGTCGCCGTCGCCGGTCACCTTCCAC
GCCCTCCTCGCCCTCGCCATCTGGGTCGGCACCATCCACTTCTTCGGC
TTCCTCGTCTCGGTCTCGCTCCTCGTCCTCCCGCTCTCGAAGGCCCTC
CTCGTCTTCGGCCTCCTCGGCGCCCTCGTCGTCATCCCGGCCGACGA
CCGCTCGAAGTTCGGCGAGCGCGTCACCCGCTACATCCTCAAGCACG
CCTGCCCGTACTTCCCGATGACCCTCCACGCCGAGGAGTTCGGCTGC
ATCGACCCGAACCGCGCCTACGTCTTCGGCTACGAGCCGCACTCGGT
CATGCCGGTCGGCACCGTCGCCCTCGCCCAGCTCTACGGCCTCATCA
CCATCCCGAAGCTCAAGGTCCTCGCCTCGACCGTCGTCTTCCGCACC
PgDGAT2-OPTIMIZED-RT CCGTTCATCCGCCACGTCTGGACCTGGATGGGCCTCACCCCGGCCAC
CCGCAAGAACTTCATCTCGCTCCTCGAGTCGGGCTACTCGTGCATCG
TCGTCCCGGGCGGCGTCCAGGAGACCTTCTACATGGAGCACGGCTTC
GAGGTCGTCTTCCTCAAGAAGCGCCGCGGCTTCGTCCGCATCGCCCT
CGAGACCGGCTGCCCGCTCGTCCCGGTCTTCTGCTTCGGCCAGTCGC
AGCTCTACAAGTGGTGGAAGCCGTCGTGGGGCCTCTTCCTCAAGATC
TGCCGCGTCGTCAAGTTCACCCCGATGTTCTTCTGGGGCATGCTCGG
CTCGCCGCTCCCGTTCCGCCACCCGCTCCACATCGTCGTCGGCAAGC
CGATCGAGGTCAAGCGCACCCCGAACCCGACCGCCGAGGAGGTCGA
CGAGCTCCACAAGCAGTACGTCGAGGCCCTCCGCGACCTCTTCGAGC
GCCACAAGGCCCAGGTCGGCCACGAGGACCTCGTCCTCAAGATCCT
CTAG

PgPDCT-OPTIMIZED-RT

ATGAACGGCGCCAAGTCGACCACCGCCACCATCACCCGCCGCCGAG
ACCCACGCTCGCCATCGAACGGCCTCGTCCTCGACCCGGTCGCAGGA
ATGGCCAACGGAAAGCGCGCAGTCGTCAACGGCGGCTACGGAGACT
ACAACAAGGCCAAGGCCGCCGTCGCCTTCATGCGCTGGACCCGCGA
CGACGTCTTCAACCTAGCACGCTACCACCGCCTCCCGTGCCTCTTCG
CAGCCGGCCTCCTCTTCTTCATGGGCGTCGAGTACACCCTCCTCATG
GTCCCGGACGACCTCCCGCCGTTCGACCTCGGCTTCGTCGCCACCCG
CTCGCTCCACCGAGTCCTATCGTCGTCGTCGGAGCTCAACACCATCC
TCGCCGCCCTCAACACCGTCTTCGTCGGCATGCAGACCGCCTACATC
CTCTGGGCCTGGCTCATCGAGGGCCGCCCACGAGCCACCATCTCGGC
ACTCTTCATGTTCACCTGCCGCGGCATCCTCGGCTACTCGACCCAGC
TCCCGCTCCCGCAGGGCTTCCTCGGCTCAGGCGTCGACTTCCCGGTC
GGCAACGTCTCGTTCTTCCTCTTCTTCTCGGGCCACGTCGCCGGCTCA
GTCATCGCCTCGCTCGACATGCGCCGCATGAAGCGCTGGGAGCTCGC
CTGGACCTTCGACGTCCTCAACGTCCTCCAGGCCGTCCGCCTCCTAG
GCACACGAGGCCACTACACCATCGACCTCGCCGTCGGCCTCGGAGC
AGGCATCCTCTTCGACTCGCTCGCCGGCAAGTACGAGGAGTCGCACA
AGATGCGCAAGGGCATCATCCACCACGTCAACGGCATGAACGGCTC
GAAGGAGGGCCCGATGATCTAG

TEF1 PROMOTER

CGCGAAGCGGTAGAAGCAATGAAGCGAGGCGAGAGCGAGAGAGGC
AGGGCTTCAGCCATGTCCAGCTGATCGGCTGTAACGTCGCGCCGGGC
CAGTCTGTTGAATTTGTTGCGTCGCCTGAGCGTAATAGAAGTGCAGT
AGTCTACTCCGCATGCCGAGAACGTCGAAGAGCGCGAAGTAGGGAG
TCGAGGGAAGCGAGGGTGGCAAACACAGCAACGACAAGCGGTTCCG
CTTCGCTCAAAAGCTCGTTGACGTTGTTTTGACGTTTTGAAGACAGT
ACAACAGCAGCAAGAGGCGTGCGAAGCGTTGGTGGCGAGAGCAGC
GACAAGGAGGGAGGAATGAGGGAGTGGTGGCGAGGGCTCGCAAAC
GGGCGTACGCCTCGAATGGAGACGTGCGAGTCGTTCTTCGACGTCCG
AGGGATGCCGAGCGCCGAGACGGAGCACGCAACGAGCGAGAGGAG
AGCAGCCGCGCAAGGTGATTCGAGTGGCGCAAGCGGAGGACGACGA
GGAGACGGACGAGGGAGGAGGAGGGATGGCGAGCGAGCATCGGAC
GGCGGGGCGCGAGAGACGGCGTGAGGAGCCGGGTGTGGAGAGTTTG
AGGAGGCGCGGGATGCGAAGTGGCTGGGTGTGCGGAGTGAGCGGTG
GCAAAGAGCGCACTTAGAGTCTAGAGCGAGGCAGTAGTAGTAGAGC
TGTATGAATGAATACAAAGTGTGAATACAACAGTTTGTAATGCGATT
CTGAGCTTGGACGTGTGCGCGCGAGAGGGCGACTTGCAAGCCAGCG
CCCGCTCGCTCTTCTTCCTTCTGCACCTCGCGTCAACCCTCGCATCTC
ACACCTACACTCGCATTCAAAGTGCGTACACTCTCCCACGACACACG
GGGACGGCGCACACCACCGCGCGTCGCTTGAACGGCGTCGCCACTT

	CGAGCCGTCACTGACTTCGTCCTCGTCCTCCCTCCTCTACTCTCTTGT ACTGTActgtgtactgggggggatag
RtGPD1 promoter	TCTTCAGACGGCTTGTTCTCTCCTGCTCTGGTGGGCTGGCCTGACATG TAATGTGCTCCGCCGCAAGTCCGTCGTCGGTCTCAATTCGACGTTGA AAGGGCATAGCGCAAGGAAGAACCCTCTGCGGACATGCAGAATTAC TGGCTCGCCTGCTCCTTCGTCTACTGGAATAAGTCCTGTCTCGTTAAA GCCCCAACGTCGTTTTTCGACGTTTGTAAGGCGCAAGAGGTGCTATG GGCTACGCAGGAAGCTGAGAGGACATAGAAGTCGGGGGAGGAACG GCGCAGAGCGGCAGTTGCGGAAGCATGAGGAAAGCGAGACGGTCC AGCATCTGCAGCGCCAATCCGCAATCTCCTGGTTGAGCCTGCACCGG AAGCGTCGGAACAGTATGCGCAGAGTCGAACGCAAGTAAGAAAGAC GCACCCTCACACTCGCTTACTTCGAGCCATACAACGGATCAAAGCTG CGCGTATCTCGGCTTGTAAGGGCCGGAAAGCAACCTCGGAGATGGA CACGTCACATCACCAACTTATCGATCTCGGCCGTCGACGTCGCAGAG AGGGCGAGAGAAGCGGTGAAGGAGGGAAACAACCCCTCGAGAGCA TGATCCGACCGAATCTGCAGCGCAGGAAGCCGTTACAAGCCCGCCT CGAGCGCAGGTCGGGTCCAGCCGGGGGACGAAACGCGCGAGGCTGA TTCGTGAGCGAAGGAAGCCGCATCGACAAGTTCGCTCCCCTTTGCCC TCTTTCCCATCACCCGTTCTCGCCTTACCCGCTCAGAACAACACCAG ATCACTCACA
BLE- OPTIMZE D-RT	ATGGCCAAGCTCACCTCGGCCGTCCCGGTCCTCACCGCCCGAGACGT CGCAGGAGCAGTCGAGTTCTGGACCGACCGCCTCGGCTTCTCGCGCG ACTTCGTCGAGGACGACTTCGCCGGCGTCGTCCGCGACGACGTCACC CTCTTCATCTCGGCCGTCCAGGACCAGGTCGTCCCGGACAACACATT AGCATGGGTCTGGGTCCGAGGCCTAGACGAGCTCTACGCCGAGTGG TCGGAGGTCGTCTCGACCAACTTCCGCGACGCCTCGGGACCAGCCAT GACCGAGATCGGCGAGCAGCCGTGGGGACGCGAGTTCGCCCTCCGC GATCCGGCAGGCAACTGCGTCCACTTCGTAGCCGAGGAGCAGGACT AG
35S terminator	acgctgaaatcaccagtctctctctacaaatctatctctctctatttttctccataaataatgtgtgagtagtttcccgataa gggaaattagggttcttatagggtttcgctcatgtgttgagcatataagaaacccttagtatgtatttgtatttgtaaaat acttctatcaataaaatttctaattcctaaaaccaaAATCCAGTACTAAAATCCAGA
NOS terminator	gatcgttcaaacatttggcaataaagtttcttaagattgaatcctgttgccggtcttgcgatgattatcatataatttctgtt gaattacgttaagcatgtaataattaacatgtaatgcatgacgttatttatgagatgggtttttatgattagagtcccgca attatacatttaatacgcgatagaaaacaaaatatagcgcgcaaactaggataaattatcgcgcgcGGTGTCA TCTATGTTACTAGATC

Chapter 6 – Summary and Future Directions

PuA has promising potential applications in the nutraceutical and chemical industries due to its conjugated double-bond configuration (Holic et al., 2018). Although initial efforts are underway to produce PuA in transgenic plants, the productivity of this UFA has been relatively low thus far (Mietkiewska et al., 2014; Xu et al., 2020b). Therefore, there is a growing interest in producing PuA in microorganisms via metabolic engineering and fermentation. However, despite the benefits of microbial platforms in terms of growth rate and fermentation capability, improving PuA content in the microorganisms remains highly challenging, which is partially due to insufficient precursor supply and channeling of PuA from PC to TAG, and rather limited lipid accumulating ability in non-oleaginous microbial species. Therefore, this study aimed to improve the performance of the heterologous production of PuA in yeast, focusing on testing and understanding the pomegranate-derived biosynthesis apparatus, developing an efficient strategy to obtain stains with ideal gene combinations and high PuA content, as well as converting a non-conventional oleaginous yeast into a PuA-producing microbial platform (Table 6).

Table 6. Summary of PuA production in heterologous yeast cells developed in this study

Platform	Type	Feedstock	LA	PuA content	PuA yield	References
S. cerevisiae	Model yeast	Glucose	+	3.4%	7.2 mg/L	Chapter 3
S. cerevisiae	Model yeast	Glucose	-	26.6%	425 mg/L	Chapter 4
R. toruloides	Oleaginous yeast	Glucose	-	12%	450 mg/L	Chapter 5
R. toruloides	Oleaginous yeast	Wood hydrolysate	-	6.4%	310 mg/L	Chapter 5

In the first part of the thesis, the model *S. cerevisiae* strain BY4741 was engineered to test the potential of producing PuA. Using a traditional plasmid-based system, a recombinant yeast strain containing 0.3% PuA was obtained. Subsequently, by using the “push and pull”

approach, PuA production was improved in a stepwise manner to 3.4% of total fatty acids with LA feeding. In the second part of the thesis, a high-throughput workflow was developed, aiming to directly shuffle genes potentially contributing to PuA synthesis in the yeast genome. By screening 1752 strains, a recombinant *S. cerevisiae* that is capable of accumulating 26.7% of total fatty acids as PuA without requiring LA precursor feeding was obtained (Figure 6). In shake flask cultivation, the PuA titer reached 425 mg/L, which to the best of our knowledge is the highest PuA level achieved in *S. cerevisiae*. In the third part of the thesis, a non-conventional oleaginous yeast *R. toruloides* was engineered to produce PuA from glucose or wood hydrolysate. The production of PuA in the strain with the best gene combination reached 452 mg/L in shake flask cultivation using glucose as the substrate.

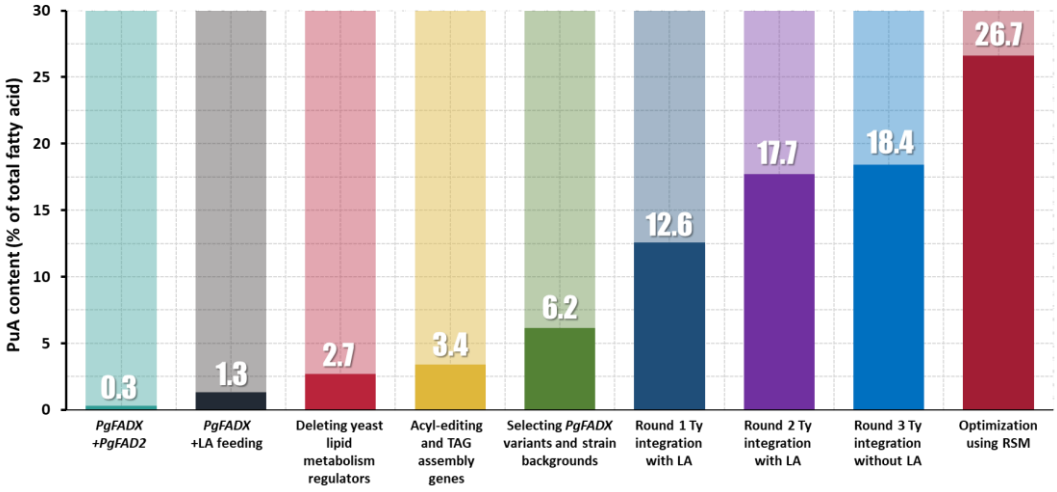

Figure 6. Summary of the stepwise increase in PuA content by engineered *S. cerevisiae*. Abbreviations: PgFADX, pomegranate fatty acid conjugase; PgFAD2, pomegranate Δ12 fatty acid desaturase; PuA, punicic acid; LA, linoleic acid; Ty, transposons of yeast; RSM, response surface methodology.

To facilitate PuA accumulation, this study extensively engineered yeast native lipid metabolism and rewired it toward PuA synthesis. From a future perspective, a thorough

investigation of regulators responsive to yeast total lipid or PUFA accumulation would be beneficial. As demonstrated by previous studies, the influence of various regulators is often complex and multifaceted. For instance, SNF2 was proposed to regulate a large number of genes involved in the metabolism of phospholipids, storage lipids, and fatty acid assimilation by altering chromatin dynamics in certain regions, and thus has complex effects on lipid biosynthesis (Kamisaka et al., 2006; Kodaki et al.,1995). Furthermore, in the *snf2Δ* mutant background, overexpression of *DGAT* resulted in higher enzyme activity compared to the wild-type strain (Kamisaka et al., 2010a, 2007a). The research in this thesis indicated that the knockout of master regulators improved PuA content. However, it remained unclear whether these knockouts would affect other metabolic pathways and therefore the performance of the engineered strain under certain growth conditions. In the future, conducting RNA-seq analysis of the PuA-accumulating strains produced by this study would provide insights into global changes in yeast gene expression, potentially identifying unforeseen effects. On the other hand, an increasing number of genes and regulators that have a substantial influence on yeast lipid accumulation are being discovered (Fei et al., 2011; Arhar et al., 2021). Using the PuA level as an indicator, continuing the genome-wide search for genes and regulators that influence PuA production will facilitate further metabolic engineering efforts.

In contrast to yeast native acyl-CoA desaturase (OLE1), which contains a cytochrome b5 domain as an integral part of its enzyme structure (Martin et al., 2007), many plant desaturases, such as FAD2, FAD3, and desaturase-like FADX, typically do not have a cytochrome b5 domain. Instead, they often require external cytochrome b5s to transfer electrons necessary for the desaturation reaction (Kumar et al., 2012). This implies that by solely expressing plant desaturase in yeast cells, its activity has to rely on yeast's native electron transporter, which may

not be fully compatible (Martin et al., 2007; Yazawa et al., 2010). Given that higher plants, including pomegranate, usually possess several isoforms of cytochrome b5 (Hu and Ji, 2016; Kumar et al., 2012), further investigating their compatibility with PgFADX in the heterologous host could be quite interesting.

Moreover, the activity and protein half-life of some plant desaturases could be influenced by post-translational regulation. For instance, a previous study suggested that the soybean FAD2-1 enzyme could be phosphorylated and downregulated (Tang et al., 2005). Also, in the heterologous host, the plant desaturase's protein half-life has been found to be associated with its N-terminal sequences, which was able to confer a rapid proteasome-dependent protein degradation in yeast cells (Khuu et al., 2011; O'Quin et al., 2010; Tang et al., 2005). Hence, a more detailed analysis of the PgFADX protein sequence, including its N-terminus, could reveal insights into enhancing protein stability and increasing PuA accumulation.

Since shake flask cultivation was used to test the PuA-enriched *S. cerevisiae* obtained through the result-driven gene stacking strategy developed in this study, subsequent bioprocess optimization in bioreactors would provide more controlled environmental conditions and thus further increase PuA production. Moreover, strains with higher PuA content could be generated in the future. In terms of the target sites, yeast Ty retrotransposon elements were chosen as the locus for integration (Curcio et al., 2015, p. 201; Krastanova et al., 2005). In addition to Ty elements, many studies have also selected abundant ribosomal DNA (rDNA) clusters as the location for multiplex genome engineering in yeast (Dai et al., 2013; Wang et al., 2018). Moreover, in certain studies, rDNA sites and Ty elements were both targeted for engineering (Park and Hahn, 2019). From a future perspective, by targeting additional Ty elements or rDNA sites, iterative integration of pomegranate genes using the workflow outlined in Chapter 4 may

further increase PuA production in engineered yeast cells. Furthermore, it has been shown that by crossing haploid *S. cerevisiae* strains with different genetic backgrounds, a descendant with better lipid accumulating capability could be obtained (Arhar et al., 2021). Also, an industrial-relevant *S. cerevisiae* strain D5A (ATCC 200062) was shown to be naturally oleaginous and has certain beneficial traits such as high biomass accumulating ability (He et al., 2018; Ranatunga et al., 1997). By choosing these strains as a chassis, PuA production could be further enhanced using the advanced genetic tools available for *S. cerevisiae*, alongside the workflow established in this thesis.

In this thesis, the investigation of converting the non-conventional oleaginous yeast *R. toruloides* into a PuA-producing yeast platform paved the foundation for conjugated fatty acid production in this yeast species. It also sheds light on the production of PuA in other oleaginous yeast species. Due to difficulties in the genetic manipulation of *R. toruloides*, an unmodified wild-type strain was used as the starting strain. Nevertheless, as molecular tools for *R. toruloides* continue to advance (Jiao et al., 2019; Otoupal et al., 2019; Schultz et al., 2019), it becomes increasingly possible to create strains with specific gene knockouts that favor lipid or PuA accumulation. For example, in non-conventional yeast species, the *snf1* knockout significantly increased target lipid production in *Y. lipolytica* (Seip et al., 2013) and *L. starkeyi* (Sato et al., 2024). Further testing the deletion of *snf1* in PuA-producing *R. toruloides* using newly developed molecular tools may further enhance PuA production. In addition, the main advantage of using non-conventional oleaginous yeast to produce lipids derives from their capacity to utilize a wide variety of carbon sources. In this thesis, the content of PuA reached 6.4% in engineered *R. toruloides* when wood hydrolysate was used as the substrate. In the future, it would be beneficial

to test *R. toruloides'* capability to transform other low-cost agricultural or industrial wastes into value-added lipid products.

Collectively, the PuA-producing microbial platforms obtained by this study will be of value for the heterologous production of high-value fatty acids via fermentation. The result of this research also provides insights into the enrichment mechanism of plant-derived UFAs in microbial hosts, which may further facilitate the heterologous production of other value-added fatty acids.

References

Abbadi, A., Brummel, M., Spener, F., 2000. Knockout of the regulatory site of 3-ketoacyl-ACP synthase III enhances short- and medium-chain acyl-ACP synthesis. Plant J. 24, 1–9. https://doi.org/10.1046/j.1365-313x.2000.00841.x

Abdullah, H.M., Pang, N., Chilcoat, B., Shachar-Hill, Y., Schnell, D.J., Dhankher, O.P., 2024. Overexpression of the *Phosphatidylcholine: Diacylglycerol Cholinephosphotransferase* (*PDCT*) gene increases carbon flux toward triacylglycerol (TAG) synthesis in *Camelina sativa* seeds. Plant Physiol. Biochem. 208, 108470. https://doi.org/10.1016/j.plaphy.2024.108470

Adamczyk, P.A., Coradetti, S.T., Gladden, J.M., 2023. Non-canonical d-xylose and l-arabinose metabolism via d-arabitol in the oleaginous yeast *Rhodosporidium toruloides*. Microb. Cell Factories 22, 145. https://doi.org/10.1186/s12934-023-02126-x

Adams, C., Godfrey, V., Wahlen, B., Seefeldt, L., Bugbee, B., 2013. Understanding precision nitrogen stress to optimize the growth and lipid content tradeoff in oleaginous green microalgae. Bioresour. Technol. 131, 188–194. https://doi.org/10.1016/j.biortech.2012.12.143

Adekunle, K.F., 2015. A review of vegetable oil-based polymers: synthesis and applications. Open J. Polym. Chem. 05, 34–40. https://doi.org/10.4236/ojpchem.2015.53004

Adhikari, N.D., Bates, P.D., Browse, J., 2016. *WRINKLED1* rescues feedback inhibition of fatty acid synthesis in hydroxylase-expressing seeds. Plant Physiol. 171, 179–191. https://doi.org/10.1104/pp.15.01906

Ali, U., Lu, S., Fadlalla, T., Iqbal, S., Yue, H., Yang, B., Hong, Y., Wang, X., Guo, L., 2022. The functions of phospholipases and their hydrolysis products in plant growth, development

and stress responses. Prog. Lipid Res. 86, 101158. https://doi.org/10.1016/j.plipres.2022.101158

Alper, H., Fischer, C., Nevoigt, E., Stephanopoulos, G., 2005. Tuning genetic control through promoter engineering. Proc. Natl. Acad. Sci. 102, 12678–12683. https://doi.org/10.1073/pnas.0504604102

Alvarez, H.M., Hernández, M.A., Lanfranconi, M.P., Silva, R.A., Villalba, M.S., 2021. *Rhodococcus* as biofactories for microbial oil production. Molecules 26, 4871. https://doi.org/10.3390/molecules26164871

Amara, S., Seghezzi, N., Otani, H., Diaz-Salazar, C., Liu, J., Eltis, L.D., 2016. Characterization of key triacylglycerol biosynthesis processes in *rhodococci*. Sci. Rep. 6, 24985. https://doi.org/10.1038/srep24985

Andre, C., Kim, S.W., Yu, X.-H., Shanklin, J., 2013. Fusing catalase to an alkane-producing enzyme maintains enzymatic activity by converting the inhibitory byproduct H_2O_2 to the cosubstrate O_2. Proc. Natl. Acad. Sci. 110, 3191–3196. https://doi.org/10.1073/pnas.1218769110

Arhar, S., Gogg-Fassolter, G., Ogrizović, M., Pačnik, K., Schwaiger, K., Žganjar, M., Petrovič, U., Natter, K., 2021. Engineering of *Saccharomyces cerevisiae* for the accumulation of high amounts of triacylglycerol. Microb. Cell Factories 20, 147. https://doi.org/10.1186/s12934-021-01640-0

Arroyo-Caro, J.M., Chileh, T., Alonso, D.L., García-Maroto, F., 2013a. Molecular characterization of a lysophosphatidylcholine acyltransferase gene belonging to the MBOAT family in *Ricinus communis* L. Lipids 48, 663–674. https://doi.org/10.1007/s11745-013-3797-z

Arroyo-Caro, J.M., Chileh, T., Kazachkov, M., Zou, J., Alonso, D.L., García-Maroto, F., 2013b. The multigene family of lysophosphatidate acyltransferase (LPAT)-related enzymes in *Ricinus communis*. Cloning and molecular characterization of two LPAT genes that are expressed in castor seeds. Plant Sci. 199–200, 29–40. https://doi.org/10.1016/j.plantsci.2012.09.015

Aruna, P., Venkataramanamma, D., Singh, A.K., Singh, R.P., 2015. Health benefits of punicic acid: a review. Compr. Rev. Food Sci. Food Saf. 15, 16–27. https://doi.org/10.1111/1541-4337.12171

Aryal, N., Lu, C., 2018. A phospholipase C-like protein from *Ricinus communis* increases hydroxy fatty acids accumulation in transgenic seeds of Camelina sativa. Front. Plant Sci. 9. https://doi.org/10.3389/fpls.2018.01576

Athenstaedt, K., Daum, G., 2003. YMR313c/TGL3 encodes a novel triacylglycerol lipase located in lipid particles of *Saccharomyces cerevisiae*. J. Biol. Chem. 278, 23317–23323. https://doi.org/10.1074/jbc.M302577200

Aznar-Moreno, J.A., Venegas-Calerón, M., Martínez-Force, E., Garcés, R., Salas, J.J., 2016. Acyl carrier proteins from sunflower (*Helianthus annuus* L.) seeds and their influence on FatA and FatB acyl-ACP thioesterase activities. Planta 244, 479–490. https://doi.org/10.1007/s00425-016-2521-7

Badami, R.C., Patil, K.B., 1980. Structure and occurrence of unusual fatty acids in minor seed oils. Prog. Lipid Res. 19, 119–153. https://doi.org/10.1016/0163-7827(80)90002-8

Bafor, M., Smith, M.A., Jonsson, L., Stobart, K., Stymne, S., 1991. Ricinoleic acid biosynthesis and triacylglycerol assembly in microsomal preparations from developing castor-bean

(*Ricinus communis*) endosperm. Biochem. J. 280, 507–514. https://doi.org/10.1042/bj2800507

Baker Brachmann, C., Davies, A., Cost, G.J., Caputo, E., Li, J., Hieter, P., Boeke, J.D., 1998. Designer deletion strains derived from *Saccharomyces cerevisiae* S288C: A useful set of strains and plasmids for PCR-mediated gene disruption and other applications. Yeast 14, 115–132. https://doi.org/10.1002/(SICI)1097-0061(19980130)14:2<115::AID-YEA204>3.0.CO;2-2

Banaś, A., Jasieniecka-Gazarkiewicz, K., Klińska, S., 2023. Biosynthesis and transfer of α-elostearic acid *in vivo* in *Momordica charantia* L. developing seeds and *in vitro* in microsomal fractions of these seed. Int. J. Mol. Sci. 24, 848. https://doi.org/10.3390/ijms24010848

Banaś, W., Sanchez Garcia, A., Banaś, A., Stymne, S., 2013. Activities of acyl-CoA:diacylglycerol acyltransferase (DGAT) and phospholipid:diacylglycerol acyltransferase (PDAT) in microsomal preparations of developing sunflower and safflower seeds. Planta 237, 1627–1636. https://doi.org/10.1007/s00425-013-1870-8

Bao, Z., Xiao, H., Liang, J., Zhang, L., Xiong, X., Sun, N., Si, T., Zhao, H., 2015. Homology-integrated CRISPR–Cas (HI-CRISPR) system for one-step multigene disruption in *Saccharomyces cerevisiae*. ACS Synth. Biol. 4, 585–594. https://doi.org/10.1021/sb500255k

Basak, S., Duttaroy, A.K., 2020. Conjugated linoleic acid and its beneficial effects in obesity, cardiovascular disease, and cancer. Nutrients 12, 1913. https://doi.org/10.3390/nu12071913

Bassaganya-Riera, J., DiGuardo, M., Climent, M., Vives, C., Carbo, A., Jouni, Z.E., Einerhand, A.W.C., O'Shea, M., Hontecillas, R., 2011. Activation of PPARγ and δ by dietary punicic acid ameliorates intestinal inflammation in mice. Br. J. Nutr. 106, 878–886. https://doi.org/10.1017/S0007114511001188

Bates, P.D., Browse, J., 2011. The pathway of triacylglycerol synthesis through phosphatidylcholine in *Arabidopsis* produces a bottleneck for the accumulation of unusual fatty acids in transgenic seeds. Plant J. Cell Mol. Biol. 68, 387–399. https://doi.org/10.1111/j.1365-313X.2011.04693.x

Bates, P.D., Fatihi, A., Snapp, A.R., Carlsson, A.S., Browse, J., Lu, C., 2012. Acyl editing and headgroup exchange are the major mechanisms that direct polyunsaturated fatty acid flux into triacylglycerols. Plant Physiol. 160, 1530–1539. https://doi.org/10.1104/pp.112.204438

Bates, P.D., Johnson, S.R., Cao, X., Li, J., Nam, J.-W., Jaworski, J.G., Ohlrogge, J.B., Browse, J., 2014. Fatty acid synthesis is inhibited by inefficient utilization of unusual fatty acids for glycerolipid assembly. Proc. Natl. Acad. Sci. 111, 1204–1209. https://doi.org/10.1073/pnas.1318511111

Bayon, S., Chen, G., Weselake, R.J., Browse, J., 2015. A small phospholipase A2-α from castor catalyzes the removal of hydroxy fatty acids from phosphatidylcholine in transgenic *Arabidopsis* seeds. Plant Physiol. 167, 1259–1270. https://doi.org/10.1104/pp.114.253641

Beld, J., Blatti, J.L., Behnke, C., Mendez, M., Burkart, M.D., 2014. Evolution of acyl-ACP thioesterases and β-ketoacyl-ACP synthases revealed by protein–protein interactions. J. Appl. Phycol. 26, 1619–1629. https://doi.org/10.1007/s10811-013-0203-4

Beopoulos, A., Verbeke, J., Bordes, F., Guicherd, M., Bressy, M., Marty, A., Nicaud, J.-M., 2014. Metabolic engineering for ricinoleic acid production in the oleaginous yeast *Yarrowia lipolytica*. Appl. Microbiol. Biotechnol. 98, 251–262. https://doi.org/10.1007/s00253-013-5295-x

Bianchini, J.-P., Ralaimanarivo, A., Gaydou, E.M., 1983. Effects of heat and hydrogenation on cyclopropenoid fatty acid composition of baobab (*Adansonia suarezensis*) seed oil. J. Food Sci. 48, 253–255. https://doi.org/10.1111/j.1365-2621.1983.tb14837.x

Billault, I., Mantle, P.G., Robins, R.J., 2004. Deuterium NMR used to indicate a common mechanism for the biosynthesis of ricinoleic acid by *Ricinus communis* and *Claviceps purpurea*. J. Am. Chem. Soc. 126, 3250–3256. https://doi.org/10.1021/ja038814d

Bonturi, N., Pinheiro, M.J., de Oliveira, P.M., Rusadze, E., Eichinger, T., Liudžiūtė, G., De Biaggi, J.S., Brauer, A., Remm, M., Miranda, E.A., Ledesma-Amaro, R., Lahtvee, P.-J., 2022. Development of a dedicated Golden Gate assembly platform (RtGGA) for *Rhodotorula toruloides*. Metab. Eng. Commun. 15, e00200. https://doi.org/10.1016/j.mec.2022.e00200

Borgeson, C.E., Blomquist, G.J., 1993. Subcellular location of the Δ12 desaturase rules out bacteriocyte contribution to linoleate biosynthesis in the house cricket and the American cockroach. Insect Biochem. Mol. Biol. 23, 297–302. https://doi.org/10.1016/0965-1748(93)90011-G

Boumann, H.A., de Kruijff, B., Heck, A.J.R., de Kroon, A.I.P.M., 2004. The selective utilization of substrates in vivo by the phosphatidylethanolamine and phosphatidylcholine biosynthetic enzymes Ept1p and Cpt1p in yeast. FEBS Lett. 569, 173–177. https://doi.org/10.1016/j.febslet.2004.05.043

Boviatsi, E., Papadaki, A., Efthymiou, M., Nychas, G.E., Papanikolaou, S., Da Silva, J.A.C., Freire, D.M.G., Koutinas, A., 2020. Valorisation of sugarcane molasses for the production of microbial lipids via fermentation of two *Rhodosporidium* strains for enzymatic synthesis of polyol esters. J. Chem. Technol. Biotechnol. 95, 402–407. https://doi.org/10.1002/jctb.5985

Brian, B.L., Gardner, E.W., 1968. A simple procedure for detecting the presence of cyclopropane fatty acids in bacterial lipids. Appl. Microbiol. 16, 549–552. https://doi.org/10.1128/am.16.4.549-552.1968

Broadwater, J.A., Whittle, E., Shanklin, J., 2002. Desaturation and hydroxylation. Residues 148 and 324 of *Arabidopsis* FAD2, in addition to substrate chain length, exert a major influence in partitioning of catalytic specificity. J. Biol. Chem. 277, 15613–15620. https://doi.org/10.1074/jbc.M200231200

Broun, P., Boddupalli, S., Somerville, C., 1998a. A bifunctional oleate 12-hydroxylase: desaturase from *Lesquerella fendleri*. Plant J. Cell Mol. Biol. 13, 201–210. https://doi.org/10.1046/j.1365-313x.1998.00023.x

Broun, P., Shanklin, J., Whittle, E., Somerville, C., 1998b. Catalytic plasticity of fatty acid modification enzymes underlying chemical diversity of plant lipids. Science 282, 1315–1317. https://doi.org/10.1126/science.282.5392.1315

Broun, P., Somerville, C., 1997. Accumulation of ricinoleic, lesquerolic, and densipolic acids in seeds of transgenic *Arabidopsis* plants that express a fatty acyl hydroxylase cDNA from castor bean. Plant Physiol. 113, 933–942. https://doi.org/10.1104/pp.113.3.933

Browse, J.A., Slack, C.R., 1981. Catalase stimulates linoleate desaturase activity in microsomes from developing linseed cotyledons. FEBS Lett. 131, 111–114. https://doi.org/10.1016/0014-5793(81)80899-X

Burgal, J., Shockey, J., Lu, C., Dyer, J., Larson, T., Graham, I., Browse, J., 2008. Metabolic engineering of hydroxy fatty acid production in plants: RcDGAT2 drives dramatic increases in ricinoleate levels in seed oil. Plant Biotechnol. J. 6, 819–831. https://doi.org/10.1111/j.1467-7652.2008.00361.x

Cahoon, E.B., Carlson, T.J., Ripp, K.G., Schweiger, B.J., Cook, G.A., Hall, S.E., Kinney, A.J., 1999. Biosynthetic origin of conjugated double bonds: Production of fatty acid components of high-value drying oils in transgenic soybean embryos. Proc. Natl. Acad. Sci. 96, 12935–12940. https://doi.org/10.1073/pnas.96.22.12935

Cahoon, E.B., Dietrich, C.R., Meyer, K., Damude, H.G., Dyer, J.M., Kinney, A.J., 2006. Conjugated fatty acids accumulate to high levels in phospholipids of metabolically engineered soybean and *Arabidopsis* seeds. Phytochemistry 67, 1166–1176. https://doi.org/10.1016/j.phytochem.2006.04.013

Cahoon, E.B., Li-Beisson, Y., 2020. Plant unusual fatty acids: learning from the less common. Curr. Opin. Plant Biol. 55, 66–73. https://doi.org/10.1016/j.pbi.2020.03.007

Cai, G., Fan, C., Liu, S., Yang, Q., Liu, D., Wu, J., Li, J., Zhou, Y., Guo, L., Wang, X., 2020. Nonspecific phospholipase C6 increases seed oil production in oilseed *Brassicaceae* plants. New Phytol. 226, 1055–1073. https://doi.org/10.1111/nph.16473

Cao, Y., Zhang, X., 2013. Production of long-chain hydroxy fatty acids by microbial conversion. Appl. Microbiol. Biotechnol. 97, 3323–3331. https://doi.org/10.1007/s00253-013-4815-z

Cappelletti, M., Presentato, A., Piacenza, E., Firrincieli, A., Turner, R.J., Zannoni, D., 2020. Biotechnology of *Rhodococcus* for the production of valuable compounds. Appl. Microbiol. Biotechnol. 104, 8567–8594. https://doi.org/10.1007/s00253-020-10861-z

Carlsson, A.S., Thomaeus, S., Hamberg, M., Stymne, S., 2004. Properties of two multifunctional plant fatty acid acetylenase/desaturase enzymes. Eur. J. Biochem. 271, 2991–2997. https://doi.org/10.1111/j.1432-1033.2004.04231.x

Carmichael, A.B., Wong, L., 2001. Protein engineering of *Bacillus megaterium* CYP102. Eur. J. Biochem. 268, 3117–3125. https://doi.org/10.1046/j.1432-1327.2001.02212.x

Carpenter, D.L., Slover, H.T., 1973. Lipid composition of selected margarines. J. Am. Oil Chem. Soc. 50, 372–376. https://doi.org/10.1007/BF02640843

Caupin, H.-J., 1997. Products from castor oil: Past, present, and future, in: Lipid Technologies and Applications. Routledge.

Chapman, K.D., Ohlrogge, J.B., 2012. Compartmentation of triacylglycerol accumulation in plants. J. Biol. Chem. 287, 2288–2294. https://doi.org/10.1074/jbc.R111.290072

Chatterjee, A., DeLorenzo, D.M., Carr, R., Moon, T.S., 2020. Bioconversion of renewable feedstocks by *Rhodococcus opacus*. Curr. Opin. Biotechnol. 64, 10–16. https://doi.org/10.1016/j.copbio.2019.08.013

Chatterjee, M., Patel, J.B., Stober, S.T., Zhang, X., 2022. Heterologous synthesis and secretion of ricinoleic acid in *Starmerella bombicola* with sophorolipid as an intermediate. ACS Synth. Biol. 11, 1178–1185. https://doi.org/10.1021/acssynbio.1c00457

Chen, D.-J., Yan, L.-H., Li, Q., Zhang, C., Si, C.-L., Li, Z.-Y., Song, Y.-J., Zhou, H., Zhang, T.-C., Luo, X.-G., 2017. Bioconversion of conjugated linoleic acid by *Lactobacillus*

plantarum CGMCC8198 supplemented with *Acer truncatum bunge* seeds oil. Food Sci. Biotechnol. 26, 1595–1611. https://doi.org/10.1007/s10068-017-0218-8

Chen, G., Harwood, J.L., Lemieux, M.J., Stone, S.J., Weselake, R.J., 2022. Acyl-CoA:diacylglycerol acyltransferase: Properties, physiological roles, metabolic engineering and intentional control. Prog. Lipid Res. 88, 101181. https://doi.org/10.1016/j.plipres.2022.101181

Chen, G., Snyder, C.L., Greer, M.S., Weselake, R.J., 2011. Biology and biochemistry of plant phospholipases. Crit. Rev. Plant Sci. 30, 239–258. https://doi.org/10.1080/07352689.2011.572033

Chen, G., van Erp, H., Martin-Moreno, J., Johnson, K., Morales, E., Browse, J., Eastmond, P., Lin, J.-T., 2016. Expression of castor LPAT2 enhances ricinoleic acid content at the *sn-2* position of triacylglycerols in *Lesquerella* seed. Int. J. Mol. Sci. 17, 507. https://doi.org/10.3390/ijms17040507

Chen, G., Woodfield, H.K., Pan, X., Harwood, J.L., Weselake, R.J., 2015. Acyl-trafficking during plant oil accumulation. Lipids 50, 1057–1068. https://doi.org/10.1007/s11745-015-4069-x

Chen, J., Gao, J., Zhang, Lingling, Zhang, Lin, 2023. Tung tree stearoyl-acyl carrier protein Δ9 desaturase improves oil content and cold resistance of *Arabidopsis* and *Saccharomyces cerevisiae*. Front. Plant Sci. 14. https://doi.org/10.3389/fpls.2023.1144853

Chen, Y.-H., Chen, J.-H., Luo, Y.-M., 2012. Complementary biodiesel combination from tung and medium-chain fatty acid oils. Renew. Energy 44, 305–310. https://doi.org/10.1016/j.renene.2012.01.098

Chhikara, S., Abdullah, H.M., Akbari, P., Schnell, D., Dhankher, O.P., 2018. Engineering *Camelina sativa* (L.) Crantz for enhanced oil and seed yields by combining diacylglycerol acyltransferase1 and glycerol-3-phosphate dehydrogenase expression. Plant Biotechnol. J. 16, 1034–1045. https://doi.org/10.1111/pbi.12847

Chisti, Y., 2008. Biodiesel from microalgae beats bioethanol. Trends Biotechnol. 26, 126–131. https://doi.org/10.1016/j.tibtech.2007.12.002

Chumnanpuen, P., Zhang, J., Nookaew, I., Nielsen, J., 2012. Integrated analysis of transcriptome and lipid profiling reveals the co-influences of inositol–choline and Snf1 in controlling lipid biosynthesis in yeast. Mol. Genet. Genomics 287, 541–554. https://doi.org/10.1007/s00438-012-0697-5

Cipak, A., Hasslacher, M., Tehlivets, O., Collinson, E.J., Zivkovic, M., Matijevic, T., Wonisch, W., Waeg, G., Dawes, I.W., Zarkovic, N., Kohlwein, S.D., 2006. *Saccharomyces cerevisiae* strain expressing a plant fatty acid desaturase produces polyunsaturated fatty acids and is susceptible to oxidative stress induced by lipid peroxidation. Free Radic. Biol. Med. 40, 897–906. https://doi.org/10.1016/j.freeradbiomed.2005.10.039

Cipak, A., Jaganjac, M., Tehlivets, O., Kohlwein, S.D., Zarkovic, N., 2008. Adaptation to oxidative stress induced by polyunsaturated fatty acids in yeast. Biochim. Biophys. Acta BBA - Mol. Cell Biol. Lipids 1781, 283–287. https://doi.org/10.1016/j.bbalip.2008.03.010

Coakley, M., Ross, R.P., Nordgren, M., Fitzgerald, G., Devery, R., Stanton, C., 2003. Conjugated linoleic acid biosynthesis by human-derived *Bifidobacterium* species. J. Appl. Microbiol. 94, 138–145. https://doi.org/10.1046/j.1365-2672.2003.01814.x

Coradetti, S.T., Adamczyk, P.A., Liu, D., Gao, Y., Otoupal, P.B., Geiselman, G.M., Webb-Robertson, B.-J.M., Burnet, M.C., Kim, Y.-M., Burnum-Johnson, K.E., Magnuson, J., Gladden, J.M., 2023. Engineering transcriptional regulation of pentose metabolism in *Rhodosporidium toruloides* for improved conversion of xylose to bioproducts. Microb. Cell Factories 22, 144. https://doi.org/10.1186/s12934-023-02148-5

Costantini, S., Rusolo, F., De Vito, V., Moccia, S., Picariello, G., Capone, F., Guerriero, E., Castello, G., Volpe, M.G., 2014. Potential anti-inflammatory effects of the hydrophilic fraction of pomegranate (*Punica granatum* L.) seed oil on breast cancer cell lines. Mol. Basel Switz. 19, 8644–8660. https://doi.org/10.3390/molecules19068644

Cripps, C., Borgeson, C., Blomquist, G.J., de Renobales, M., 1990. The Δ12-desaturase from the house cricket, *Acheta domesticus* (Orthoptera: Gryllidae): Characterization and form of the substrate. Arch. Biochem. Biophys. 278, 46–51. https://doi.org/10.1016/0003-9861(90)90229-R

Curcio, M.J., Lutz, S., Lesage, P., 2015. The Ty1 LTR-retrotransposon of budding yeast, *Saccharomyces cerevisiae*. Microbiol. Spectr. 3, 3.2.19. https://doi.org/10.1128/microbiolspec.MDNA3-0053-2014

C. Whitehouse, C.J., G. Bell, S., Wong, L.-L., 2012. P450 BM3 (CYP102A1): connecting the dots. Chem. Soc. Rev. 41, 1218–1260. https://doi.org/10.1039/C1CS15192D

Czerwiec, Q., Idrissitaghki, A., Imatoukene, N., Nonus, M., Thomasset, B., Nicaud, J.-M., Rossignol, T., 2019. Optimization of cyclopropane fatty acids production in *Yarrowia lipolytica*. Yeast 36, 143–151. https://doi.org/10.1002/yea.3379

Da Costa, E., Melo, T., Reis, M., Domingues, P., Calado, R., Abreu, M.H., Domingues, M.R., 2021. Polar lipids composition, antioxidant and anti-inflammatory activities of the

Atlantic red seaweed *Grateloupia turuturu*. Mar. Drugs 19, 414. https://doi.org/10.3390/md19080414

da Silva Ramos, L.C., Tango, J.S., Savi, A., Leal, N.R., 1984. Variability for oil and fatty acid composition in castor bean varieties. J. Am. Oil Chem. Soc. 61, 1841–1843. https://doi.org/10.1007/BF02540812

Dahlqvist, A., Ståhl, U., Lenman, M., Banas, A., Lee, M., Sandager, L., Ronne, H., Stymne, S., 2000. Phospholipid:diacylglycerol acyltransferase: An enzyme that catalyzes the acyl-CoA-independent formation of triacylglycerol in yeast and plants. Proc. Natl. Acad. Sci. 97, 6487–6492. https://doi.org/10.1073/pnas.120067297

Dai, Z., Liu, Y., Zhang, Xianan, Shi, M., Wang, B., Wang, D., Huang, L., Zhang, Xueli, 2013. Metabolic engineering of *Saccharomyces cerevisiae* for production of ginsenosides. Metab. Eng. 20, 146–156. https://doi.org/10.1016/j.ymben.2013.10.004

Dauk, M., Lam, P., Kunst, L., Smith, M.A., 2007. A FAD2 homologue from *Lesquerella lindheimeri* has predominantly fatty acid hydroxylase activity. Plant Sci. 173, 43–49. https://doi.org/10.1016/j.plantsci.2007.03.015

de Paula, R.G., Antoniêto, A.C.C., Ribeiro, L.F.C., Srivastava, N., O'Donovan, A., Mishra, P.K., Gupta, V.K., Silva, R.N., 2019. Engineered microbial host selection for value-added bioproducts from lignocellulose. Biotechnol. Adv., Microbial Engineering Biotechnologies 37, 107347. https://doi.org/10.1016/j.biotechadv.2019.02.003

De Sousa, N.L., Cabral, G.B., Aragão, F.J.L., 2022. Herbicide tolerance and gene silencing stability over generations in the ricin bio-detoxicated castor bean. J. Genet. Eng. Biotechnol. 20, 16. https://doi.org/10.1186/s43141-022-00303-w

Demski, K., Jeppson, S., Lager, I., Misztak, A., Jasieniecka-Gazarkiewicz, K., Waleron, M., Stymne, S., Banaś, A., 2019. Isoforms of acyl-CoA:diacylglycerol acyltransferase2 differ substantially in their specificities toward erucic acid. Plant Physiol. 181, 1468–1479. https://doi.org/10.1104/pp.19.01129

Demski, K., Jeppson, S., Stymne, S., Lager, I., 2022. Phosphatidylcholine:diacylglycerol cholinephosphotransferase's unique regulation of castor bean oil quality. Plant Physiol. 189, 2001–2014. https://doi.org/10.1093/plphys/kiac209

den Hartigh, L.J., 2019. Conjugated linoleic acid effects on cancer, obesity, and atherosclerosis: A review of pre-clinical and human trials with current perspectives. Nutrients 11, 370. https://doi.org/10.3390/nu11020370

Díaz, T., Fillet, S., Campoy, S., Vázquez, R., Viña, J., Murillo, J., Adrio, J.L., 2018. Combining evolutionary and metabolic engineering in *Rhodosporidium toruloides* for lipid production with non-detoxified wheat straw hydrolysates. Appl. Microbiol. Biotechnol. 102, 3287–3300. https://doi.org/10.1007/s00253-018-8810-2

Dib, S., Mostefa-Kara, B., Villemin, D., 2023. Extraction and composition of lipids from pomegranate seed oil from West Algeria. Chem. Proc. 14, 78. https://doi.org/10.3390/ecsoc-27-16115

D'Souza, K., Kim, Y.J., Balla, T., Epand, R.M., 2014. Distinct properties of the two isoforms of CDP-diacylglycerol synthase. Biochemistry 53, 7358–7367. https://doi.org/10.1021/bi501250m

Dyer, J.M., Chapital, D.C., Cary, J.W., Pepperman, A.B., 2001. Chilling-sensitive, post-transcriptional regulation of a plant fatty acid desaturase expressed in yeast. Biochem. Biophys. Res. Commun. 282, 1019–1025. https://doi.org/10.1006/bbrc.2001.4667

Dyer, J.M., Chapital, D.C., Kuan, J.-C.W., Mullen, R.T., Turner, C., McKeon, T.A., Pepperman, A.B., 2002. Molecular analysis of a bifunctional fatty acid conjugase/desaturase from tung. Implications for the evolution of plant fatty acid diversity. Plant Physiol. 130, 2027–2038. https://doi.org/10.1104/pp.102.010835

Fadavi, A., Barzegar, M., Hossein Azizi, M., 2006. Determination of fatty acids and total lipid content in oilseed of 25 pomegranates varieties grown in Iran. J. Food Compos. Anal., Biodiversity and nutrition: a common path 19, 676–680. https://doi.org/10.1016/j.jfca.2004.09.002

Fan, R., Zhao, F., Gong, Z., Chen, Y., Yang, B., Zhou, C., Zhang, J., Du, Z., Wang, X., Yin, P., Guo, L., Liu, Z., 2023. Insights into the mechanism of phospholipid hydrolysis by plant non-specific phospholipase C. Nat. Commun. 14, 194. https://doi.org/10.1038/s41467-023-35915-4

Farhi, M., Marhevka, E., Masci, T., Marcos, E., Eyal, Y., Ovadis, M., Abeliovich, H., Vainstein, A., 2011. Harnessing yeast subcellular compartments for the production of plant terpenoids. Metab. Eng. 13, 474–481. https://doi.org/10.1016/j.ymben.2011.05.001

Fatma, S., Hameed, A., Noman, M., Ahmed, T., Shahid, M., Tariq, M., Sohail, I., Tabassum, R., 2018. Lignocellulosic biomass: A sustainable bioenergy source for the future. Protein Pept. Lett. 25, 148–163. https://doi.org/10.2174/0929866525666180122144504

Fei, W., Shui, G., Zhang, Y., Krahmer, N., Ferguson, C., Kapterian, T.S., Lin, R.C., Dawes, I.W., Brown, A.J., Li, P., Huang, X., Parton, R.G., Wenk, M.R., Walther, T.C., Yang, H., 2011. A role for phosphatidic acid in the formation of "supersized" lipid droplets. PLoS Genet. 7, e1002201. https://doi.org/10.1371/journal.pgen.1002201

Fernandes, M.A., Mota, M.N., Faria, N.T., Sá-Correia, I., 2023. An evolved strain of the oleaginous yeast *Rhodotorula toruloides*, multi-tolerant to the major inhibitors present in lignocellulosic hydrolysates, exhibits an altered cell envelope. J. Fungi 9, 1073. https://doi.org/10.3390/jof9111073

Fillet, S., Ronchel, C., Callejo, C., Fajardo, M.-J., Moralejo, H., Adrio, J.L., 2017. Engineering *Rhodosporidium toruloides* for the production of very long-chain monounsaturated fatty acid-rich oils. Appl. Microbiol. Biotechnol. 101, 7271–7280. https://doi.org/10.1007/s00253-017-8461-8

Friedlander, J., Tsakraklides, V., Kamineni, A., Greenhagen, E.H., Consiglio, A.L., MacEwen, K., Crabtree, D.V., Afshar, J., Nugent, R.L., Hamilton, M.A., Joe Shaw, A., South, C.R., Stephanopoulos, G., Brevnova, E.E., 2016. Engineering of a high lipid producing *Yarrowia lipolytica* strain. Biotechnol. Biofuels 9, 77. https://doi.org/10.1186/s13068-016-0492-3

Fu, J., Song, X., 2018. Fitness cost of transgenic *cry1Ab/c* rice under saline-alkaline soil condition. Front. Plant Sci. 9. https://doi.org/10.3389/fpls.2018.01552

Gao, H., Yang, B., Stanton, C., Ross, R.P., Zhang, H., Liu, Z., Chen, H., Chen, W., 2020. Characteristics of bifidobacterial conjugated fatty acid and hydroxy fatty acid production and its potential application in fermented milk. LWT 120, 108940. https://doi.org/10.1016/j.lwt.2019.108940

Gao, J., Yu, W., Li, Y., Jin, M., Yao, L., Zhou, Y.J., 2023. Engineering co-utilization of glucose and xylose for chemical overproduction from lignocellulose. Nat. Chem. Biol. 19, 1524–1531. https://doi.org/10.1038/s41589-023-01402-6

Garaiova, M., Hua, Q., Holic, R., 2023. Heterologous production of calendic acid naturally found in *Calendula officinalis* by recombinant fission yeast. J. Agric. Food Chem. 71, 3842–3851. https://doi.org/10.1021/acs.jafc.2c08967

Garaiova, M., Mietkiewska, E., Weselake, R.J., Holic, R., 2017. Metabolic engineering of *Schizosaccharomyces pombe* to produce punicic acid, a conjugated fatty acid with nutraceutic properties. Appl. Microbiol. Biotechnol. 101, 7913–7922. https://doi.org/10.1007/s00253-017-8498-8

Gietz, R.D., Schiestl, R.H., 2007a. Frozen competent yeast cells that can be transformed with high efficiency using the LiAc/SS carrier DNA/PEG method. Nat. Protoc. 2, 1–4. https://doi.org/10.1038/nprot.2007.17

Gietz, R.D., Schiestl, R.H., 2007b. High-efficiency yeast transformation using the LiAc/SS carrier DNA/PEG method. Nat. Protoc. 2, 31–34. https://doi.org/10.1038/nprot.2007.13

González-García, Y., Rábago-Panduro, L.M., French, T., Camacho-Córdova, D.I., Gutiérrez-González, P., Córdova, J., 2017. High lipids accumulation in *Rhodosporidium toruloides* by applying single and multiple nutrients limitation in a simple chemically defined medium. Ann. Microbiol. 67, 519–527. https://doi.org/10.1007/s13213-017-1282-2

Greenspan, F.P., Gall, R.J., 1956. Epoxy fatty acid ester plasticizers. Preparation and properties. J. Am. Oil Chem. Soc. 33, 391–394. https://doi.org/10.1007/BF02630763

Greer, M.S., Truksa, M., Deng, W., Lung, S.-C., Chen, G., Weselake, R.J., 2015. Engineering increased triacylglycerol accumulation in *Saccharomyces cerevisiae* using a modified type 1 plant diacylglycerol acyltransferase. Appl. Microbiol. Biotechnol. 99, 2243–2253. https://doi.org/10.1007/s00253-014-6284-4

Grossmann, M.E., Mizuno, N.K., Schuster, T., Cleary, M.P., 2010. Punicic acid is an ω-5 fatty acid capable of inhibiting breast cancer proliferation. Int. J. Oncol. 36, 421–426. https://doi.org/10.3892/ijo_00000515

Guil-Guerrero, J.L., 2007. Stearidonic acid (18:4n-3): Metabolism, nutritional importance, medical uses and natural sources. Eur. J. Lipid Sci. Technol. 109, 1226–1236. https://doi.org/10.1002/ejlt.200700207

Guo, Y., Mietkiewska, E., Francis, T., Katavic, V., Brost, J.M., Giblin, M., Barton, D.L., Taylor, D.C., 2009. Increase in nervonic acid content in transformed yeast and transgenic plants by introduction of a *Lunaria annua* L. 3-ketoacyl-CoA synthase (KCS) gene. Plant Mol. Biol. 69, 565–575. https://doi.org/10.1007/s11103-008-9439-9

Gupta, P., Dash, P.K., 2017. Molecular details of secretory phospholipase A2 from flax (*Linum usitatissimum* L.) provide insight into its structure and function. Sci. Rep. 7, 11080. https://doi.org/10.1038/s41598-017-10969-9

Hackett, S.C., Bonsall, M.B., 2016. Type of fitness cost influences the rate of evolution of resistance to transgenic Bt crops. J. Appl. Ecol. 53, 1391–1401. https://doi.org/10.1111/1365-2664.12680

Hanasaki, M., Masumoto, H., 2019. CRISPR/Transposon gene integration (CRITGI) can manage gene expression in a retrotransposon-dependent manner. Sci. Rep. 9, 15300. https://doi.org/10.1038/s41598-019-51891-6

Hancock, J.F., 2003. A framework for assessing the risk of transgenic crops. BioScience 53, 512–519. https://doi.org/10.1641/0006-3568(2003)053[0512:AFFATR]2.0.CO;2

Hao, D., Chen, H., Hao, G., Yang, B., Zhang, B., Zhang, H., Chen, W., Chen, Y.Q., 2015. Production of conjugated linoleic acid by heterologous expression of linoleic acid

isomerase in oleaginous fungus *Mortierella alpina*. Biotechnol. Lett. 37, 1983–1992. https://doi.org/10.1007/s10529-015-1871-8

Harwood, J.L., Woodfield, H.K., Chen, G., Weselake, R.J., 2017. Modification of oil crops to produce fatty acids for industrial applications, in: Fatty Acids. Elsevier, pp. 187–236. https://doi.org/10.1016/B978-0-12-809521-8.00005-2

Hayes, D.G., Kleiman, R., 1996. A detailed triglyceride analysis of *Lesquerella fendleri* oil: Column chromatographic fractionation followed by supercritical fluid chromatography. J. Am. Oil Chem. Soc. 73, 267–269. https://doi.org/10.1007/BF02523908

He, Q., Bennett, G.N., San, K.-Y., Wu, H., 2019. Biosynthesis of medium-chain ω-hydroxy fatty acids by AlkBGT of *Pseudomonas putida* GPo1 with native FadL in engineered *Escherichia coli*. Front. Bioeng. Biotechnol. 7. https://doi.org/10.3389/fbioe.2019.00273

He, Q., Yang, Y., Yang, S., Donohoe, B.S., Van Wychen, S., Zhang, M., Himmel, M.E., Knoshaug, E.P., 2018. Oleaginicity of the yeast strain *Saccharomyces cerevisiae* D5A. Biotechnol. Biofuels 11, 258. https://doi.org/10.1186/s13068-018-1256-z

He, X., Chen, G.Q., Kang, S.T., McKeon, T.A., 2007. *Ricinus communis* contains an acyl-CoA synthetase that preferentially activates ricinoleate to its CoA thioester. Lipids 42, 931–938. https://doi.org/10.1007/s11745-007-3090-0

He, X., Chen, G.Q., Lin, J.-T., McKeon, T.A., 2004a. Regulation of diacylglycerol acyltransferase in developing seeds of castor. Lipids 39, 865–871. https://doi.org/10.1007/s11745-004-1308-1

He, X., Turner, C., Chen, G.Q., Lin, J.-T., McKeon, T.A., 2004b. Cloning and characterization of a cDNA encoding diacylglycerol acyltransferase from castor bean. Lipids 39, 311–318. https://doi.org/10.1007/s11745-004-1234-2

He, Z., Chapital, D.C., Cheng, H.N., Thomas Klasson, K., Olanya, O.M., Uknalis, J., 2014. Application of tung oil to improve adhesion strength and water resistance of cottonseed meal and protein adhesives on maple veneer. Ind. Crops Prod. 61, 398–402. https://doi.org/10.1016/j.indcrop.2014.07.031

Hein, E.-M., Hayen, H., 2012. Comparative lipidomic profiling of *S. cerevisiae* and four other hemiascomycetous yeasts. Metabolites 2, 254–267. https://doi.org/10.3390/metabo2010254

Henderson, C.M., Block, D.E., 2014. Examining the role of membrane lipid composition in determining the ethanol tolerance of *Saccharomyces cerevisiae*. Appl. Environ. Microbiol. 80, 2966–2972. https://doi.org/10.1128/AEM.04151-13

Hennessy, A.A., Ross, P.R., Fitzgerald, G.F., Stanton, C., 2016. Sources and bioactive properties of conjugated dietary fatty acids. Lipids 51, 377–397. https://doi.org/10.1007/s11745-016-4135-z

Hernández, M.A., Mohn, W.W., Martínez, E., Rost, E., Alvarez, A.F., Alvarez, H.M., 2008. Biosynthesis of storage compounds by *Rhodococcus jostii* RHA1 and global identification of genes involved in their metabolism. BMC Genomics 9, 600. https://doi.org/10.1186/1471-2164-9-600

Herrera-Meza, S., Martínez, A., Sánchez-Otero, M.-G., Mendoza, M., García-Barradas, O., Viveros, G., Oliart-Ros, R., 2014. Fatty acid composition and some physicochemical characteristics of Sterculia apetala seed oils. Grasas Aceites 65, e039. https://doi.org/10.3989/gya.0223141

Holic, R., Xu, Y., Caldo, K.M.P., Singer, S.D., Field, C.J., Weselake, R.J., Chen, G., 2018. Bioactivity and biotechnological production of punicic acid. Appl. Microbiol. Biotechnol. 102, 3537–3549. https://doi.org/10.1007/s00253-018-8883-y

Holic, R., Yazawa, H., Kumagai, H., Uemura, H., 2012. Engineered high content of ricinoleic acid in fission yeast *Schizosaccharomyces pombe*. Appl. Microbiol. Biotechnol. 95, 179–187. https://doi.org/10.1007/s00253-012-3959-6

Hornung, E., Krueger, C., Pernstich, C., Gipmans, M., Porzel, A., Feussner, I., 2005. Production of (10E,12Z)-conjugated linoleic acid in yeast and tobacco seeds. Biochim. Biophys. Acta BBA - Mol. Cell Biol. Lipids 1738, 105–114. https://doi.org/10.1016/j.bbalip.2005.11.004

Hornung, E., Pernstich, C., Feussner, I., 2002. Formation of conjugated Δ11Δ13-double bonds by Δ12-linoleic acid (1,4)-acyl-lipid-desaturase in pomegranate seeds. Eur. J. Biochem. 269, 4852–4859. https://doi.org/10.1046/j.1432-1033.2002.03184.x

Hu, J., Ji, L., 2016. Draft genome sequences of *Rhodosporidium toruloides* strains ATCC 10788 and ATCC 10657 with compatible mating types. Genome Announc. 4, e00098-16. https://doi.org/10.1128/genomeA.00098-16

Hu, Z., Ren, Z., Lu, C., 2012. The phosphatidylcholine diacylglycerol cholinephosphotransferase is required for efficient hydroxy fatty acid accumulation in transgenic *Arabidopsis*. Plant Physiol. 158, 1944–1954. https://doi.org/10.1104/pp.111.192153

Huai, D., Zhang, Y., Zhang, C., Cahoon, E.B., Zhou, Y., 2015. Combinatorial effects of fatty acid elongase enzymes on nervonic acid production in *Camelina sativa*. PLOS ONE 10, e0131755. https://doi.org/10.1371/journal.pone.0131755

Huang, C., Zong, M., Wu, H., Liu, Q., 2009. Microbial oil production from rice straw hydrolysate by *Trichosporon fermentans*. Bioresour. Technol. 100, 4535–4538. https://doi.org/10.1016/j.biortech.2009.04.022

Hussain, S.K.A., Srivastava, A., Tyagi, A., Shandilya, U.K., Kumar, A., Kumar, S., Panwar, S., Tyagi, A.K., 2016. Characterization of CLA-producing *Butyrivibrio* spp. reveals strain-specific variations. 3 Biotech 6, 90. https://doi.org/10.1007/s13205-016-0401-2

Imatoukene, N., Back, A., Nonus, M., Thomasset, B., Rossignol, T., Nicaud, J.-M., 2020. Fermentation process for producing CFAs using *Yarrowia lipolytica*. J. Ind. Microbiol. Biotechnol. 47, 403–412. https://doi.org/10.1007/s10295-020-02276-6

Imatoukene, N., Verbeke, J., Beopoulos, A., Idrissi Taghki, A., Thomasset, B., Sarde, C.-O., Nonus, M., Nicaud, J.-M., 2017. A metabolic engineering strategy for producing conjugated linoleic acids using the oleaginous yeast *Yarrowia lipolytica*. Appl. Microbiol. Biotechnol. 101, 4605–4616. https://doi.org/10.1007/s00253-017-8240-6

Inagaki, K., Aki, T., Fukuda, Y., Kawamoto, S., Shigeta, S., Ono, K., Suzuki, O., 2002. Identification and expression of a rat fatty acid elongase involved in the biosynthesis of C18 fatty acids. Biosci. Biotechnol. Biochem. 66, 613–621. https://doi.org/10.1271/bbb.66.613

Inyang, V., Laseinde, O.T., Kanakana, G.M., 2022. Techniques and applications of lignocellulose biomass sources as transport fuels and other bioproducts. Int. J. Low-Carbon Technol. 17, 900–909. https://doi.org/10.1093/ijlct/ctac068

Isbell, T.A., Mund, M.S., Evangelista, R.L., Dierig, D.A., 2008. Method for analysis of fatty acid distribution and oil content on a single *Lesquerella fendleri* seed. Ind. Crops Prod. 28, 231–236. https://doi.org/10.1016/j.indcrop.2008.02.010

Iwabuchi, M., Kohno-Murase, J., Imamura, J., 2003. Delta 12-oleate desaturase-related enzymes associated with formation of conjugated trans-delta 11, cis-delta 13 double bonds. J. Biol. Chem. 278, 4603–4610. https://doi.org/10.1074/jbc.M210748200

Jaakola, S., Vahvaselkä, M., Laakso, S., 2006. Positional distribution of conjugated linoleic acid in triacylglycerol of *Saccharomyces cerevisiae*. J. Agric. Food Chem. 54, 5611–5616. https://doi.org/10.1021/jf060682v

Jia, C., Li, M., Li, J., Zhang, J., Zhang, H., Cao, P., Pan, X., Lu, X., Chang, W., 2015. Structural insights into the catalytic mechanism of aldehyde-deformylating oxygenases. Protein Cell 6, 55–67. https://doi.org/10.1007/s13238-014-0108-2

Jia, Y.-L., Zhang, Q.-M., Du, F., Yang, W.-Q., Zhang, Z.-X., Xu, Y.-S., Ma, W., Sun, X.-M., Huang, H., 2024. Identification of lipid synthesis genes in *Schizochytrium* sp. and their application in improving eicosapentaenoic acid synthesis in *Yarrowia lipolytica*. Biotechnol. Biofuels Bioprod. 17, 1–17. https://doi.org/10.1186/s13068-024-02471-y

Jiang, Y., Peng, W., Li, Z., You, C., Zhao, Y., Tang, D., Wang, B., Li, S., 2021. Unexpected reactions of α,β-unsaturated fatty acids provide insight into the mechanisms of CYP152 peroxygenases. Angew. Chem. Int. Ed. 60, 24694–24701. https://doi.org/10.1002/anie.202111163

Jiao, X., Lyu, L., Zhang, Y., Huang, Q., Zhou, R., Wang, Shian, Wang, Shuang, Zhang, S., Zhao, Z.K., 2021. Reduction of lipid-accumulation of oleaginous yeast *Rhodosporidium toruloides* through CRISPR/Cas9-mediated inactivation of lipid droplet structural proteins. FEMS Microbiol. Lett. 368, fnab111. https://doi.org/10.1093/femsle/fnab111

Jiao, X., Zhang, Y., Liu, X., Zhang, Q., Zhang, S., Zhao, Z.K., 2019. Developing a CRISPR/Cas9 system for genome editing in the basidiomycetous yeast *Rhodosporidium toruloides*. Biotechnol. J. 14, 1900036. https://doi.org/10.1002/biot.201900036

Joo, Y.-C., Seo, E.-S., Kim, Y.-S., Kim, K.-R., Park, J.-B., Oh, D.-K., 2012. Production of 10-hydroxystearic acid from oleic acid by whole cells of recombinant *Escherichia coli* containing oleate hydratase from *Stenotrophomonas maltophilia*. J. Biotechnol. 158, 17–23. https://doi.org/10.1016/j.jbiotec.2012.01.002

Jumper, J., Evans, R., Pritzel, A., Green, T., Figurnov, M., Ronneberger, O., Tunyasuvunakool, K., Bates, R., Žídek, A., Potapenko, A., Bridgland, A., Meyer, C., Kohl, S.A.A., Ballard, A.J., Cowie, A., Romera-Paredes, B., Nikolov, S., Jain, R., Adler, J., Back, T., Petersen, S., Reiman, D., Clancy, E., Zielinski, M., Steinegger, M., Pacholska, M., Berghammer, T., Bodenstein, S., Silver, D., Vinyals, O., Senior, A.W., Kavukcuoglu, K., Kohli, P., Hassabis, D., 2021. Highly accurate protein structure prediction with AlphaFold. Nature 596, 583–589. https://doi.org/10.1038/s41586-021-03819-2

Jung, S.T., Lauchli, R., Arnold, F.H., 2011. Cytochrome P450: taming a wild type enzyme. Curr. Opin. Biotechnol. 22, 809–817. https://doi.org/10.1016/j.copbio.2011.02.008

Kajiwara, S., Shirai, A., Fujii, T., Toguri, T., Nakamura, K., Ohtaguchi, K., 1996. Polyunsaturated fatty acid biosynthesis in *Saccharomyces cerevisiae*: expression of ethanol tolerance and the FAD2 gene from *Arabidopsis thaliana*. Appl. Environ. Microbiol. 62, 4309–4313. https://doi.org/10.1128/aem.62.12.4309-4313.1996

Kalinger, R.S., Rowland, O., 2023. Determinants of substrate specificity in a catalytically diverse family of acyl-ACP thioesterases from plants. BMC Plant Biol. 23, 1. https://doi.org/10.1186/s12870-022-04003-y

Kamisaka, Y., Kimura, K., Uemura, H., Shibakami, M., 2010a. Activation of diacylglycerol acyltransferase expressed in *Saccharomyces cerevisiae*: overexpression of Dga1p lacking the N-terminal region in the Δsnf2 disruptant produces a significant increase in its enzyme activity. Appl. Microbiol. Biotechnol. 88, 105–115. https://doi.org/10.1007/s00253-010-2725-x

Kamisaka, Y., Kimura, K., Uemura, H., Shibakami, M., 2010b. Activation of diacylglycerol acyltransferase expressed in *Saccharomyces cerevisiae*: overexpression of Dga1p lacking the N-terminal region in the Δsnf2 disruptant produces a significant increase in its enzyme activity. Appl. Microbiol. Biotechnol. 88, 105–115. https://doi.org/10.1007/s00253-010-2725-x

Kamisaka, Y., Kimura, K., Uemura, H., Yamaoka, M., 2013. Overexpression of the active diacylglycerol acyltransferase variant transforms *Saccharomyces cerevisiae* into an oleaginous yeast. Appl. Microbiol. Biotechnol. 97, 7345–7355. https://doi.org/10.1007/s00253-013-4915-9

Kamisaka, Y., Noda, N., Tomita, N., Kimura, K., Kodaki, T., Hosaka, K., 2006. Identification of genes affecting lipid content using transposon mutagenesis in *Saccharomyces cerevisiae*. Biosci. Biotechnol. Biochem. 70, 646–653. https://doi.org/10.1271/bbb.70.646

Kamisaka, Y., Tomita, N., Kimura, K., Kainou, K., Uemura, H., 2007a. *DGA1* (diacylglycerol acyltransferase gene) overexpression and leucine biosynthesis significantly increase lipid accumulation in the Δ *snf2* disruptant of *Saccharomyces cerevisiae*. Biochem. J. 408, 61–68. https://doi.org/10.1042/BJ20070449

Kamisaka, Y., Tomita, N., Kimura, K., Kainou, K., Uemura, H., 2007b. DGA1 (diacylglycerol acyltransferase gene) overexpression and leucine biosynthesis significantly increase lipid

accumulation in the *Δsnf2* disruptant of *Saccharomyces cerevisiae*. Biochem. J. 408, 61–68. https://doi.org/10.1042/BJ20070449

Kannengiesser, J., Sakaguchi-Söder, K., Mrukwia, T., Jager, J., Schebek, L., 2016. Extraction of medium chain fatty acids from organic municipal waste and subsequent production of bio-based fuels. Waste Manag., Biowaste to Fuel 47, 78–83. https://doi.org/10.1016/j.wasman.2015.05.030

Karim, A.S., Curran, K.A., Alper, H.S., 2013. Characterization of plasmid burden and copy number in *Saccharomyces cerevisiae* for optimization of metabolic engineering applications. FEMS Yeast Res. 13, 107–116. https://doi.org/10.1111/1567-1364.12016

Kato, H., Matsuda, F., Yamada, R., Nagata, K., Shirai, T., Hasunuma, T., Kondo, A., 2013. Cocktail δ-integration of xylose assimilation genes for efficient ethanol production from xylose in *Saccharomyces cerevisiae*. J. Biosci. Bioeng. 116, 333–336. https://doi.org/10.1016/j.jbiosc.2013.03.020

Kaufman, M., Wiesman, Z., 2007. Pomegranate oil analysis with emphasis on MALDI-TOF/MS triacylglycerol fingerprinting. J. Agric. Food Chem. 55, 10405–10413. https://doi.org/10.1021/jf072741q

Kazaz, S., Barthole, G., Domergue, F., Ettaki, H., To, A., Vasselon, D., De Vos, D., Belcram, K., Lepiniec, L., Baud, S., 2020. Differential activation of partially redundant Δ9 stearoyl-ACP desaturase genes is critical for omega-9 monounsaturated fatty acid biosynthesis during seed development in *Arabidopsis*. Plant Cell 32, 3613–3637. https://doi.org/10.1105/tpc.20.00554

Kennedy, E.P., 1961. Biosynthesis of complex lipids. Presented at the Fed. Proc., pp. 934–940.

Khoddami, A., Man, Y.B.C., Roberts, T.H., 2014. Physico-chemical properties and fatty acid profile of seed oils from pomegranate (*Punica granatum* L.) extracted by cold pressing. Eur. J. Lipid Sci. Technol. 116, 553–562. https://doi.org/10.1002/ejlt.201300416

Khuu, N., Gidda, S., Shockey, J.M., Dyer, J.M., Mullen, R.T., 2011. The N termini of *Brassica* and tung omega-3 fatty acid desaturases mediate proteasome-dependent protein degradation in plant cells. Plant Signal. Behav. 6, 422–425. https://doi.org/10.4161/psb.6.3.14522

Kim, H.M., Chae, T.U., Choi, S.Y., Kim, W.J., Lee, S.Y., 2019. Engineering of an oleaginous bacterium for the production of fatty acids and fuels. Nat. Chem. Biol. 15, 721–729. https://doi.org/10.1038/s41589-019-0295-5

Kim, H.U., Lee, K.-R., Go, Y.S., Jung, J.H., Suh, M.-C., Kim, J.B., 2011. Endoplasmic reticulum-located PDAT1-2 from castor bean enhances hydroxy fatty acid accumulation in transgenic plants. Plant Cell Physiol. 52, 983–993. https://doi.org/10.1093/pcp/pcr051

Kim, H.U., Park, M.-E., Lee, K.-R., Suh, M.C., Chen, G.Q., 2020. Variant castor lysophosphatidic acid acyltransferases acylate ricinoleic acid in seed oil. Ind. Crops Prod. 150, 112245. https://doi.org/10.1016/j.indcrop.2020.112245

Kim, K.-R., Oh, D.-K., 2013. Production of hydroxy fatty acids by microbial fatty acid-hydroxylation enzymes. Biotechnol. Adv. 31, 1473–1485. https://doi.org/10.1016/j.biotechadv.2013.07.004

Kim, Y.J., Liu, R.H., Bond, D.R., Russell, J.B., 2000. Effect of linoleic acid concentration on conjugated linoleic acid production by *Butyrivibrio fibrisolvens* A38. Appl. Environ. Microbiol. 66, 5226–5230. https://doi.org/10.1128/AEM.66.12.5226-5230.2000

Kishino, S., Park, S.-B., Takeuchi, M., Yokozeki, K., Shimizu, S., Ogawa, J., 2011. Novel multi-component enzyme machinery in lactic acid bacteria catalyzing C C double bond migration useful for conjugated fatty acid synthesis. Biochem. Biophys. Res. Commun. 416, 188–193. https://doi.org/10.1016/j.bbrc.2011.11.022

Kleiner, A.C., Cladis, D.P., Santerre, C.R., 2015. A comparison of actual versus stated label amounts of EPA and DHA in commercial omega-3 dietary supplements in the United States. J. Sci. Food Agric. 95, 1260–1267. https://doi.org/10.1002/jsfa.6816

Klińska, S., Jasieniecka-Gazarkiewicz, K., Banaś, A., 2019. Acyl-CoA:lysophosphatidylcholine acyltransferases (LPCATs) of *Camelina sativa* seeds: biochemical properties and function. Planta 250, 1655–1670. https://doi.org/10.1007/s00425-019-03248-6

Klug, L., Daum, G., 2014. Yeast lipid metabolism at a glance. FEMS Yeast Res. 14, 369–388. https://doi.org/10.1111/1567-1364.12141

Knoshaug, E.P., Van Wychen, S., Singh, A., Zhang, M., 2018. Lipid accumulation from glucose and xylose in an engineered, naturally oleaginous strain of *Saccharomyces cerevisiae*. Biofuel Res. J. 5, 800–805. https://doi.org/10.18331/BRJ2018.5.2.3

Kodaki, T., Hosaka, K., Nikawa, J. -i., Yamashita, S., 1995. The *SNF2/SWI2/GAM1/TYE3/RIC1* gene is involved in the coordinate regulation of phospholipid synthesis in *Saccharomyces cerevisiae*. J. Biochem. (Tokyo) 117, 362–368. https://doi.org/10.1093/jb/117.2.362

Koh, C.M.J., Liu, Y., Moehninsi, Du, M., Ji, L., 2014. Molecular characterization of KU70 and KU80 homologues and exploitation of a KU70-deficient mutant for improving gene deletion frequency in *Rhodosporidium toruloides*. BMC Microbiol. 14, 50. https://doi.org/10.1186/1471-2180-14-50

Krastanova, O., Hadzhitodorov, M., Pesheva, M., 2005. Ty elements of the yeast *Saccharomyces cerevisiae*. Biotechnol. Biotechnol. Equip. 19, 19–26. https://doi.org/10.1080/13102818.2005.10817272

Kroon, J.T.M., Wei, W., Simon, W.J., Slabas, A.R., 2006. Identification and functional expression of a type 2 acyl-CoA:diacylglycerol acyltransferase (DGAT2) in developing castor bean seeds which has high homology to the major triglyceride biosynthetic enzyme of fungi and animals. Phytochemistry 67, 2541–2549. https://doi.org/10.1016/j.phytochem.2006.09.020

Kumar, A.K., Sharma, S., 2017. Recent updates on different methods of pretreatment of lignocellulosic feedstocks: a review. Bioresour. Bioprocess. 4, 7. https://doi.org/10.1186/s40643-017-0137-9

Kumar, K., Gambhir, G., Dass, A., Tripathi, A.K., Singh, A., Jha, A.K., Yadava, P., Choudhary, M., Rakshit, S., 2020. Genetically modified crops: current status and future prospects. Planta 251, 91. https://doi.org/10.1007/s00425-020-03372-8

Kumar, R., Tran, L.-S.P., Neelakandan, A.K., Nguyen, H.T., 2012. Higher plant cytochrome b5 polypeptides modulate fatty acid desaturation. PLoS ONE 7, e31370. https://doi.org/10.1371/journal.pone.0031370

Kunst, L., Taylor, D., Underhill, E.W., 1992. Fatty acid elongation in developing seeds of *Arabidopsis thaliana*. Plant Physiol Biochem 30, 425–434.

Lager, I., Yilmaz, J.L., Zhou, X.-R., Jasieniecka, K., Kazachkov, M., Wang, P., Zou, J., Weselake, R., Smith, M.A., Bayon, S., Dyer, J.M., Shockey, J.M., Heinz, E., Green, A., Banas, A., Stymne, S., 2013. Plant acyl-CoA:lysophosphatidylcholine acyltransferases (LPCATs)

have different specificities in their forward and reverse reactions. J. Biol. Chem. 288, 36902–36914. https://doi.org/10.1074/jbc.M113.521815

Lan, E.I., Chuang, D.S., Shen, C.R., Lee, A.M., Ro, S.Y., Liao, J.C., 2015. Metabolic engineering of cyanobacteria for photosynthetic 3-hydroxypropionic acid production from CO2 using *Synechococcus elongatus* PCC 7942. Metab. Eng. 31, 163–170. https://doi.org/10.1016/j.ymben.2015.08.002

Lansky, E.P., Newman, R.A., 2007. *Punica granatum* (pomegranate) and its potential for prevention and treatment of inflammation and cancer. J. Ethnopharmacol. 109, 177–206. https://doi.org/10.1016/j.jep.2006.09.006

Ledesma-Amaro, R., Lazar, Z., Rakicka, M., Guo, Z., Fouchard, F., Coq, A.-M.C.-L., Nicaud, J.-M., 2016. Metabolic engineering of *Yarrowia lipolytica* to produce chemicals and fuels from xylose. Metab. Eng. 38, 115–124. https://doi.org/10.1016/j.ymben.2016.07.001

Lee, H.S., Lee, S.M., Park, S.L., Choi, T.-R., Song, H.-S., Kim, H.-J., Bhatia, S.K., Gurav, R., Kim, Y.-G., Kim, J.-H., Choi, K.-Y., Yang, Y.-H., 2021. Tung oil-based production of high 3-hydroxyhexanoate-containing terpolymer poly(3-hydroxybutyrate-co-3-hydroxyvalerate-co-3-hydroxyhexanoate) using engineered *Ralstonia eutropha*. Polymers 13, 1084. https://doi.org/10.3390/polym13071084

Lee, K.-R., Chen, G.Q., Kim, H.U., 2015. Current progress towards the metabolic engineering of plant seed oil for hydroxy fatty acids production. Plant Cell Rep. 34, 603–615. https://doi.org/10.1007/s00299-015-1736-6

Lee, M., Lenman, M., Banaś, A., Bafor, M., Singh, S., Schweizer, M., Nilsson, R., Liljenberg, C., Dahlqvist, A., Gummeson, P.-O., Sjödahl, S., Green, A., Stymne, S., 1998. Identification

of non-heme diiron proteins that catalyze triple bond and epoxy group formation. Science 280, 915–918. https://doi.org/10.1126/science.280.5365.915

Leonard, J.M., Knapp, S.J., Slabaugh, M.B., 1998. A *Cuphea* β-ketoacyl-ACP synthase shifts the synthesis of fatty acids towards shorter chains in *Arabidopsis* seeds expressing *Cuphea* FatB thioesterases *in vivo*. Plant J. 13, 621–628. https://doi.org/10.1046/j.1365-313X.1998.00066.x

Leplat, C., Nicaud, J.-M., Rossignol, T., 2018. Overexpression screen reveals transcription factors involved in lipid accumulation in *Yarrowia lipolytica*. FEMS Yeast Res. 18. https://doi.org/10.1093/femsyr/foy037

Li, D.-W., Xie, W.-H., Hao, T.-B., Cai, J.-X., Zhou, T.-B., Balamurugan, S., Yang, W.-D., Liu, J.-S., Li, H.-Y., 2018. Constitutive and chloroplast-targeted expression of acetyl-CoA carboxylase in oleaginous microalgae elevates fatty acid biosynthesis. Mar. Biotechnol. 20, 566–572. https://doi.org/10.1007/s10126-018-9841-5

Li, J.-J., Zhang, C.-L., Zhang, Y.-L., Gao, H.-N., Wang, H.-B., Jiang, H., Li, Y.-Y., 2022. An apple long-chain acyl-CoA synthase, MdLACS1, enhances biotic and abiotic stress resistance in plants. Plant Physiol. Biochem. 189, 115–125. https://doi.org/10.1016/j.plaphy.2022.08.021

Li, Q., Chen, J., Yu, X., Gao, J.-M., 2019. A mini review of nervonic acid: Source, production, and biological functions. Food Chem. 301, 125286. https://doi.org/10.1016/j.foodchem.2019.125286

Li, R., Yu, K., Hatanaka, T., Hildebrand, D.F., 2010a. *Vernonia* DGATs increase accumulation of epoxy fatty acids in oil. Plant Biotechnol. J. 8, 184–195. https://doi.org/10.1111/j.1467-7652.2009.00476.x

Li, R., Yu, K., Hildebrand, D.F., 2010b. *DGAT1, DGAT2* and *PDAT* expression in seeds and other tissues of epoxy and hydroxy fatty acid accumulating plants. Lipids 45, 145–157. https://doi.org/10.1007/s11745-010-3385-4

Li, X., Teitgen, A.M., Shirani, A., Ling, J., Busta, L., Cahoon, R.E., Zhang, W., Li, Z., Chapman, K.D., Berman, D., Zhang, C., Minto, R.E., Cahoon, E.B., 2018. Discontinuous fatty acid elongation yields hydroxylated seed oil with improved function. Nat. Plants 4, 711–720. https://doi.org/10.1038/s41477-018-0225-7

Li, Z., Wang, W., Liu, X., Qi, S., Lan, D., Wang, Y., 2023. Effect of different degumming processes on the retention of bioactive components, acylglycerol and phospholipid composition of rapeseed oil. Process Biochem. 133, 190–199. https://doi.org/10.1016/j.procbio.2023.08.019

Lian, J., Jin, R., Zhao, H., 2016. Construction of plasmids with tunable copy numbers in *Saccharomyces cerevisiae* and their applications in pathway optimization and multiplex genome integration: plasmid copy number engineering. Biotechnol. Bioeng. 113, 2462–2473. https://doi.org/10.1002/bit.26004

Liao, P., Lechon, T., Romsdahl, T., Woodfield, H., Fenyk, S., Fawcett, T., Wallington, E., Bates, R.E., Chye, M.-L., Chapman, K.D., Harwood, J.L., Scofield, S., 2022. Transgenic manipulation of triacylglycerol biosynthetic enzymes in *B. napus* alters lipid-associated gene expression and lipid metabolism. Sci. Rep. 12, 3352. https://doi.org/10.1038/s41598-022-07387-x

Liavonchanka, A., Hornung, E., Feussner, I., Rudolph, M.G., 2006. Structure and mechanism of the *Propionibacterium acnes* polyunsaturated fatty acid isomerase. Proc. Natl. Acad. Sci. 103, 2576–2581. https://doi.org/10.1073/pnas.0510144103

Li-Beisson, Y., Shorrosh, B., Beisson, F., Andersson, M.X., Arondel, V., Bates, P.D., Baud, S., Bird, D., DeBono, A., Durrett, T.P., Franke, R.B., Graham, I.A., Katayama, K., Kelly, A.A., Larson, T., Markham, J.E., Miquel, M., Molina, I., Nishida, I., Rowland, O., Samuels, L., Schmid, K.M., Wada, H., Welti, R., Xu, C., Zallot, R., Ohlrogge, J., 2013. Acyl-lipid metabolism. Arab. Book 11, e0161. https://doi.org/10.1199/tab.0161

Lin, J., Turner, C., Liao, L.P., McKeon, T.A., 2003. Identification and quantification of the molecular species of acylglycerols in castor oil by HPLC using ELSD. J. Liq. Chromatogr. Relat. Technol. 26, 773–780. https://doi.org/10.1081/JLC-120018421

Lin, J.-T., Arcinas, A., 2007. Regiospecific analysis of diricinoleoylacylglycerols in castor (*Ricinus communis* L.) oil by electrospray ionization-mass spectrometry. J. Agric. Food Chem. 55, 2209–2216. https://doi.org/10.1021/jf063105f

Lin, Y., Chen, G., Mietkiewska, E., Song, Z., Caldo, K.M.P., Singer, S.D., Dyer, J., Smith, M., McKeon, T., Weselake, R.J., 2019. Castor patatin-like phospholipase A IIIβ facilitates removal of hydroxy fatty acids from phosphatidylcholine in transgenic *Arabidopsis* seeds. Plant Mol. Biol. 101, 521–536. https://doi.org/10.1007/s11103-019-00915-w

Ling, H., Teo, W., Chen, B., Leong, S.S.J., Chang, M.W., 2014. Microbial tolerance engineering toward biochemical production: from lignocellulose to products. Curr. Opin. Biotechnol., Cell and Pathway Engineering 29, 99–106. https://doi.org/10.1016/j.copbio.2014.03.005

Liu, W., Mao, W., Zhang, C., Lu, X., Xiao, X., Zhao, Z., Lin, J., 2020. Co-fermentation of a sugar mixture for microbial lipid production in a two-stage fermentation mode under non-sterile conditions. Sustain. Energy Fuels 4, 2380–2385. https://doi.org/10.1039/D0SE00003E

Liu, X., Li, H., Chen, Y., Cao, Y., 2012. Method for screening of bacterial strains biosynthesizing specific conjugated linoleic acid isomers. J. Agric. Food Chem. 60, 9705–9710. https://doi.org/10.1021/jf3032843

Liu, X., Wang, W., Zhao, Z., Xu, L., Yang, B., Lan, D., Wang, Y., 2023. Monoacylglycerol lipase from marine *Geobacillus* sp. showing lysophospholipase activity and its application in efficient soybean oil degumming. Food Chem. 406, 134506. https://doi.org/10.1016/j.foodchem.2022.134506

Liu, X.-X., Xiong, Z.-Q., Wang, G.-Q., Wang, L.-F., Xia, Y.-J., Song, X., Ai, L.-Z., 2021. LysR family regulator LttR controls production of conjugated linoleic acid in *Lactobacillus plantarum* by directly activating the cla operon. Appl. Environ. Microbiol. 87, e02798-20. https://doi.org/10.1128/AEM.02798-20

Liu, Y., Koh, C.M.J., Yap, S.A., Cai, L., Ji, L., 2021. Understanding and exploiting the fatty acid desaturation system in *Rhodotorula toruloides*. Biotechnol. Biofuels 14, 73. https://doi.org/10.1186/s13068-021-01924-y

Liu, Ying, Chen, Y., Yue, X., Liu, Yingying, Ning, J., Li, L., Wu, J., Luo, X., Zhang, S., 2024. Proteomics and metabolomics analysis reveal the regulation mechanism of linoleate isomerase activity and function in *Propionibacterium acnes*. ACS Omega 9, 1643–1655. https://doi.org/10.1021/acsomega.3c08243

Liu, Z., Radi, M., Mohamed, E.T.T., Feist, A.M., Dragone, G., Mussatto, S.I., 2021. Adaptive laboratory evolution of *Rhodosporidium toruloides* to inhibitors derived from lignocellulosic biomass and genetic variations behind evolution. Bioresour. Technol. 333, 125171. https://doi.org/10.1016/j.biortech.2021.125171

Lou, Y., Schwender, J., Shanklin, J., 2014. FAD2 and FAD3 desaturases form heterodimers that facilitate metabolic channeling *in vivo*. J. Biol. Chem. 289, 17996–18007. https://doi.org/10.1074/jbc.M114.572883

Lu, B.-R., Yang, X., Ellstrand, N.C., 2016. Fitness correlates of crop transgene flow into weedy populations: a case study of weedy rice in China and other examples. Evol. Appl. 9, 857–870. https://doi.org/10.1111/eva.12377

Lu, C., Fulda, M., Wallis, J.G., Browse, J., 2006. A high-throughput screen for genes from castor that boost hydroxy fatty acid accumulation in seed oils of transgenic *Arabidopsis*. Plant J. Cell Mol. Biol. 45, 847–856. https://doi.org/10.1111/j.1365-313X.2005.02636.x

Lu, C., Xin, Z., Ren, Z., Miquel, M., Browse, J., 2009. An enzyme regulating triacylglycerol composition is encoded by the ROD1 gene of *Arabidopsis*. Proc. Natl. Acad. Sci. 106, 18837–18842. https://doi.org/10.1073/pnas.0908848106

Luddy, F.E., Barford, R.A., Herb, S.F., Magidman, P., Riemenschneider, R.W., 1964. Pancreatic lipase hydrolysis of triglycerides by a semimicro technique. J. Am. Oil Chem. Soc. 41, 693–696. https://doi.org/10.1007/BF02661412

Lunn, D., Le, A., Wallis, J.G., Browse, J., 2020. Castor LPCAT and PDAT1A act in concert to promote transacylation of hydroxy-fatty acid onto triacylglycerol. Plant Physiol. 184, 709–719. https://doi.org/10.1104/pp.20.00691

Lunn, D., Wallis, J.G., Browse, J., 2019. Tri-hydroxy-triacylglycerol is efficiently produced by position-specific castor acyltransferases. Plant Physiol. 179, 1050–1063. https://doi.org/10.1104/pp.18.01409

Luo, X., Li, H., Wu, Z., Yao, W., Zhao, P., Cao, D., Yu, H., Li, K., Poudel, K., Zhao, D., Zhang, F., Xia, X., Chen, L., Wang, Q., Jing, D., Cao, S., 2020. The pomegranate (*Punica*

granatum L.) draft genome dissects genetic divergence between soft- and hard-seeded cultivars. Plant Biotechnol. J. 18, 955–968. https://doi.org/10.1111/pbi.13260

Machado, M., Costa, E.M., Silva, S., Rodriguez-Alcalá, L.M., Gomes, A.M., Pintado, M., 2022. Pomegranate oil's potential as an anti-obesity ingredient. Molecules 27, 4958. https://doi.org/10.3390/molecules27154958

Macouzet, M., Lee, B.H., Robert, N., 2010. Genetic and structural comparison of linoleate isomerases from selected food-grade bacteria. J. Appl. Microbiol. 109, 2128–2134. https://doi.org/10.1111/j.1365-2672.2010.04844.x

Maeo, K., Tokuda, T., Ayame, A., Mitsui, N., Kawai, T., Tsukagoshi, H., Ishiguro, S., Nakamura, K., 2009. An AP2-type transcription factor, WRINKLED1, of *Arabidopsis thaliana* binds to the AW-box sequence conserved among proximal upstream regions of genes involved in fatty acid synthesis. Plant J. 60, 476–487. https://doi.org/10.1111/j.1365-313X.2009.03967.x

Malcı, K., Walls, L.E., Rios-Solis, L., 2020. Multiplex genome engineering methods for yeast cell factory development. Front. Bioeng. Biotechnol. 8, 589468. https://doi.org/10.3389/fbioe.2020.589468

Mannino, F., Imbesi, C., Bitto, A., Minutoli, L., Squadrito, F., D'Angelo, T., Booz, C., Pallio, G., Irrera, N., 2023. Anti-oxidant and anti-inflammatory effects of ellagic and punicic acid in an in vitro model of cardiac fibrosis. Biomed. Pharmacother. 162, 114666. https://doi.org/10.1016/j.biopha.2023.114666

Mapelli-Brahm, A., Sánchez, R., Pan, X., Moreno-Pérez, A.J., Garcés, R., Martínez-Force, E., Weselake, R.J., Salas, J.J., Venegas-Calerón, M., 2020. Functional characterization of

lysophosphatidylcholine: acyl-CoA acyltransferase genes from sunflower (*Helianthus annuus* L.). Front. Plant Sci. 11, 403. https://doi.org/10.3389/fpls.2020.00403

Markham, K.A., Alper, H.S., 2018. Engineering *Yarrowia lipolytica* for the production of cyclopropanated fatty acids. J. Ind. Microbiol. Biotechnol. 45, 881–888. https://doi.org/10.1007/s10295-018-2067-8

Martin, C.E., Oh, C.-S., Jiang, Y., 2007. Regulation of long chain unsaturated fatty acid synthesis in yeast. Biochim. Biophys. Acta BBA - Mol. Cell Biol. Lipids 1771, 271–285. https://doi.org/10.1016/j.bbalip.2006.06.010

Matsuzawa, T., Maehara, T., Kamisaka, Y., Ara, S., Takaku, H., Yaoi, K., 2018. Identification and characterization of Δ12 and Δ12/Δ15 bifunctional fatty acid desaturases in the oleaginous yeast *Lipomyces starkeyi*. Appl. Microbiol. Biotechnol. 102, 8817–8826. https://doi.org/10.1007/s00253-018-9345-2

Mavraganis, I., Meesapyodsuk, D., Vrinten, P., Smith, M., Qiu, X., 2010. Type II diacylglycerol acyltransferase from *Claviceps purpurea* with ricinoleic acid, a hydroxyl fatty acid of industrial importance, as preferred substrate. Appl. Environ. Microbiol. 76, 1135–1142. https://doi.org/10.1128/AEM.02297-09

Mayer, F.V., Heath, R., Underwood, E., Sanders, M.J., Carmena, D., McCartney, R.R., Leiper, F.C., Xiao, B., Jing, C., Walker, P.A., Haire, L.F., Ogrodowicz, R., Martin, S.R., Schmidt, M.C., Gamblin, S.J., Carling, D., 2011. ADP regulates SNF1, the *Saccharomyces cerevisiae* homolog of AMP-activated protein kinase. Cell Metab. 14, 707–714. https://doi.org/10.1016/j.cmet.2011.09.009

McCartney, A.W., Dyer, J.M., Dhanoa, P.K., Kim, P.K., Andrews, D.W., McNew, J.A., Mullen, R.T., 2004. Membrane-bound fatty acid desaturases are inserted co-translationally into

the ER and contain different ER retrieval motifs at their carboxy termini. Plant J. Cell Mol. Biol. 37, 156–173. https://doi.org/10.1111/j.1365-313x.2004.01949.x

McCarty, N.S., Graham, A.E., Studená, L., Ledesma-Amaro, R., 2020. Multiplexed CRISPR technologies for gene editing and transcriptional regulation. Nat. Commun. 11, 1281. https://doi.org/10.1038/s41467-020-15053-x

McKeon, T., Hayes, D.G., Hildebrand, D., Weselake, R., 2016. Industrial oil crops. Elsevier.

McKeon, T.A., He, X., 2015. Castor diacylglycerol acyltransferase type 1 (DGAT1) displays greater activity with diricinolein than *Arabidopsis* DGAT1. Biocatal. Agric. Biotechnol. 4, 276–278. https://doi.org/10.1016/j.bcab.2015.01.005

Meesapyodsuk, D., Chen, Y., Ng, S.H., Chen, J., Qiu, X., 2015. Metabolic engineering of *Pichia pastoris* to produce ricinoleic acid, a hydroxy fatty acid of industrial importance. J. Lipid Res. 56, 2102–2109. https://doi.org/10.1194/jlr.M060954

Meesapyodsuk, D., Qiu, X., 2008. An oleate hydroxylase from the fungus *Claviceps purpurea*: cloning, functional analysis, and expression in *Arabidopsis*. Plant Physiol. 147, 1325–1333. https://doi.org/10.1104/pp.108.117168

Mei, Y., Chen, H., Yang, B., Zhao, J., Zhang, H., Chen, W., 2022. Research progress on conjugated linoleic acid bio-conversion in *Bifidobacterium*. Int. J. Food Microbiol. 369, 109593. https://doi.org/10.1016/j.ijfoodmicro.2022.109593

Metzger, J.O., Bornscheuer, U., 2006. Lipids as renewable resources: current state of chemical and biotechnological conversion and diversification. Appl. Microbiol. Biotechnol. 71, 13–22. https://doi.org/10.1007/s00253-006-0335-4

Mietkiewska, E., Miles, R., Wickramarathna, A., Sahibollah, A.F., Greer, M.S., Chen, G., Weselake, R.J., 2014. Combined transgenic expression of *Punica granatum* conjugase

(FADX) and FAD2 desaturase in high linoleic acid *Arabidopsis thaliana* mutant leads to increased accumulation of punicic acid. Planta 240, 575–583. https://doi.org/10.1007/s00425-014-2109-z

Misra, A., Khan, K., Niranjan, A., Kumar, V., Sane, V.A., 2017. Heterologous expression of two GPATs from *Jatropha curcas* alters seed oil levels in transgenic *Arabidopsis thaliana*. Plant Sci. 263, 79–88. https://doi.org/10.1016/j.plantsci.2017.07.003

Mitchelhill, K.I., Stapleton, D., Gao, G., House, C., Michell, B., Katsis, F., Witters, L.A., Kemp, B.E., 1994. Mammalian AMP-activated protein kinase shares structural and functional homology with the catalytic domain of yeast Snf1 protein kinase. J. Biol. Chem. 269, 2361–2364. https://doi.org/10.1016/S0021-9258(17)41951-X

Napier, J.A., 2007. The production of unusual fatty acids in transgenic plants. Annu. Rev. Plant Biol. 58, 295–319. https://doi.org/10.1146/annurev.arplant.58.032806.103811

Noiriel, A., Benveniste, P., Banas, A., Stymne, S., Bouvier-Navé, P., 2004. Expression in yeast of a novel phospholipase A1 cDNA from *Arabidopsis thaliana*. Eur. J. Biochem. 271, 3752–3764. https://doi.org/10.1111/j.1432-1033.2004.04317.x

Nora, L.C., Wehrs, M., Kim, J., Cheng, J.-F., Tarver, A., Simmons, B.A., Magnuson, J., Harmon-Smith, M., Silva-Rocha, R., Gladden, J.M., Mukhopadhyay, A., Skerker, J.M., Kirby, J., 2019. A toolset of constitutive promoters for metabolic engineering of *Rhodosporidium toruloides*. Microb. Cell Factories 18, 117. https://doi.org/10.1186/s12934-019-1167-0

Ohadi, S., Hodnett, G., Rooney, W., Bagavathiannan, M., 2017. Gene flow and its consequences in *Sorghum* spp. Crit. Rev. Plant Sci. 36, 367–385. https://doi.org/10.1080/07352689.2018.1446813

Ohlrogge, J., Thrower, N., Mhaske, V., Stymne, S., Baxter, M., Yang, W., Liu, J., Shaw, K., Shorrosh, B., Zhang, M., Wilkerson, C., Matthäus, B., 2018. PlantFAdb: a resource for exploring hundreds of plant fatty acid structures synthesized by thousands of plants and their phylogenetic relationships. Plant J. 96, 1299–1308. https://doi.org/10.1111/tpj.14102

O'Quin, J.B., Bourassa, L., Zhang, D., Shockey, J.M., Gidda, S.K., Fosnot, S., Chapman, K.D., Mullen, R.T., Dyer, J.M., 2010. Temperature-sensitive post-translational regulation of plant omega-3 fatty-acid desaturases is mediated by the endoplasmic reticulum-associated degradation pathway. J. Biol. Chem. 285, 21781–21796. https://doi.org/10.1074/jbc.M110.135236

Osorio-González, C.S., Saini, R., Hegde, K., Brar, S.K., Lefebvre, A., Avalos Ramirez, A., 2023. Carbon/nitrogen ratio as a tool to enhance the lipid production in *Rhodosporidium toruloides*-1588 using C5 and C6 wood hydrolysates. J. Clean. Prod. 384, 135687. https://doi.org/10.1016/j.jclepro.2022.135687

Otoupal, P.B., Ito, M., Arkin, A.P., Magnuson, J.K., Gladden, J.M., Skerker, J.M., 2019. Multiplexed CRISPR-Cas9-based genome editing of *Rhodosporidium toruloides*. mSphere 4, 13. https://doi.org/10.1128/msphere.00099-19

Özgül-Yücel, S., 2005. Determination of conjugated linolenic acid content of selected oil seeds grown in Turkey. J. Am. Oil Chem. Soc. 82, 893–897. https://doi.org/10.1007/s11746-005-1161-7

Pan, X., Chen, G., Kazachkov, M., Greer, M.S., Caldo, K.M.P., Zou, J., Weselake, R.J., 2015. *In vivo* and *in vitro* evidence for biochemical coupling of reactions catalyzed by lysophosphatidylcholine acyltransferase and diacylglycerol acyltransferase. J. Biol. Chem. 290, 18068–18078. https://doi.org/10.1074/jbc.M115.654798

Pan, X., Siloto, R.M.P., Wickramarathna, A.D., Mietkiewska, E., Weselake, R.J., 2013. Identification of a pair of phospholipid:diacylglycerol acyltransferases from developing flax (*Linum usitatissimum* L.) seed catalyzing the selective production of trilinolenin. J. Biol. Chem. 288, 24173–24188. https://doi.org/10.1074/jbc.M113.475699

Park, K., Hahn, J.-S., 2024. Engineering *Yarrowia lipolytica* for sustainable ricinoleic acid production: A pathway to free fatty acid synthesis. Metab. Eng. 81, 197–209. https://doi.org/10.1016/j.ymben.2023.12.002

Park, M.-E., Lee, K.-R., Chen, G.Q., Kim, H.U., 2022. Enhanced production of hydroxy fatty acids in *Arabidopsis* seed through modification of multiple gene expression. Biotechnol. Biofuels Bioprod. 15, 66. https://doi.org/10.1186/s13068-022-02167-1

Park, S.-H., Hahn, J.-S., 2019. Development of an efficient cytosolic isobutanol production pathway in *Saccharomyces cerevisiae* by optimizing copy numbers and expression of the pathway genes based on the toxic effect of α-acetolactate. Sci. Rep. 9, 3996. https://doi.org/10.1038/s41598-019-40631-5

Pasha, M.Khysar., Ahmad, Fasih., 1992. Analysis of triacylglycerols containing cyclopropane fatty acids in *Sterculia fostida* (Linn.) seed lipids. J. Agric. Food Chem. 40, 626–629. https://doi.org/10.1021/jf00016a020

Patel, A., Pruthi, V., Pruthi, P.A., 2017. Synchronized nutrient stress conditions trigger the diversion of CDP-DG pathway of phospholipids synthesis towards *de novo* TAG synthesis in oleaginous yeast escalating biodiesel production. Energy 139, 962–974. https://doi.org/10.1016/j.energy.2017.08.052

Paul, A., Radhakrishnan, M., 2020. Pomegranate seed oil in food industry: Extraction, characterization, and applications. Trends Food Sci. Technol. 105, 273–283. https://doi.org/10.1016/j.tifs.2020.09.014

Payá-Milans, M., Aznar-Moreno, J.A., Balbuena, T.S., Haslam, R.P., Gidda, S.K., Pérez-Hormaeche, J., Mullen, R.T., Thelen, J.J., Napier, J.A., Salas, J.J., Garcés, R., Martínez-Force, E., Venegas-Calerón, M., 2016. Sunflower HaGPAT9-1 is the predominant GPAT during seed development. Plant Sci. 252, 42–52. https://doi.org/10.1016/j.plantsci.2016.07.002

Petranovic, D., Nielsen, J., 2008. Can yeast systems biology contribute to the understanding of human disease? Trends Biotechnol. 26, 584–590. https://doi.org/10.1016/j.tibtech.2008.07.008

Phippen, W.B., Isbell, T.A., Phippen, M.E., 2006. Total seed oil and fatty acid methyl ester contents of *Cuphea* accessions. Ind. Crops Prod. 24, 52–59. https://doi.org/10.1016/j.indcrop.2006.02.001

Pugh, E.L., Kates, M., 1979. Membrane-bound phospholipid desaturases. Lipids 14, 159–165. https://doi.org/10.1007/BF02533867

Qi, F., Shen, P., Hu, R., Xue, T., Jiang, X., Qin, L., Chen, Y., Huang, J., 2020. Carotenoids and lipid production from *Rhodosporidium toruloides* cultured in tea waste hydrolysate. Biotechnol. Biofuels 13, 74. https://doi.org/10.1186/s13068-020-01712-0

Qiu, X., Reed, D.W., Hong, H., MacKenzie, S.L., Covello, P.S., 2001. Identification and analysis of a gene from *Calendula officinalis* encoding a fatty acid conjugase. Plant Physiol. 125, 847–855. https://doi.org/10.1104/pp.125.2.847

Rahman, H., Harwood, J., Weselake, R., 2013. Increasing seed oil content in *Brassica* species through breeding and biotechnology. Lipid Technol. 25, 182–185. https://doi.org/10.1002/lite.201300291

Ranatunga, T.D., Jervis, J., Helm, R.F., McMillan, J.D., Hatzis, C., 1997. Toxicity of hardwood extractives toward *Saccharomyces cerevisiae* glucose fermentation. Biotechnol. Lett. 19, 1125–1127. https://doi.org/10.1023/A:1018400912828

Ratledge, C., 2004. Fatty acid biosynthesis in microorganisms being used for Single Cell Oil production. Biochimie 86, 807–815. https://doi.org/10.1016/j.biochi.2004.09.017

Ratledge, C., 2002. Regulation of lipid accumulation in oleaginous micro-organisms. Biochem. Soc. Trans. 30, 1047–1050. https://doi.org/10.1042/bst0301047

Ratledge, C., Wynn, J.P., 2002. The biochemistry and molecular biology of lipid accumulation in oleaginous microorganisms, in: Advances in Applied Microbiology. Elsevier, pp. 1–52. https://doi.org/10.1016/S0065-2164(02)51000-5

Rawat, R., Yu, X.-H., Sweet, M., Shanklin, J., 2012. Conjugated fatty acid synthesis. J. Biol. Chem. 287, 16230–16237. https://doi.org/10.1074/jbc.M111.325316

Regmi, A., Shockey, J., Kotapati, H.K., Bates, P.D., 2020. Oil-producing metabolons containing DGAT1 use separate substrate pools from those containing DGAT2 or PDAT. Plant Physiol. 184, 720–737. https://doi.org/10.1104/pp.20.00461

Robin, J., Gueroult, M., Cheikhrouhou, R., Guicherd, M., Borsenberger, V., Marty, A., Bordes, F., 2019. Identification of a crucial amino acid implicated in the hydroxylation/desaturation ratio of CpFAH12 bifunctional hydroxylase. Biotechnol. Bioeng. 116, 2451–2462. https://doi.org/10.1002/bit.27102

Román-Figueroa, C., Cea, M., Paneque, M., González, M.E., 2020. Oil content and fatty acid composition in castor bean naturalized accessions under Mediterranean conditions in Chile. Agronomy 10, 1145. https://doi.org/10.3390/agronomy10081145

Russell, F.D., Bürgin-Maunder, C.S., 2012. Distinguishing health benefits of eicosapentaenoic and docosahexaenoic acids. Mar. Drugs 10, 2535–2559. https://doi.org/10.3390/md10112535

Ryu, S.B., Lee, H.Y., Doelling, J.H., Palta, J.P., 2005. Characterization of a cDNA encoding *Arabidopsis* secretory phospholipase A2-alpha, an enzyme that generates bioactive lysophospholipids and free fatty acids. Biochim. Biophys. Acta 1736, 144–151. https://doi.org/10.1016/j.bbalip.2005.08.005

Saini, R., Osorio-Gonzalez, C.S., Hegde, K., Brar, S.K., Vezina, P., 2021. Effect of creating a fed-batch like condition using carbon to nitrogen ratios on lipid accumulation in *Rhodosporidium toruloides*-1588. Bioresour. Technol. 337, 125354. https://doi.org/10.1016/j.biortech.2021.125354

Salas, J.J., Ohlrogge, J.B., 2002. Characterization of substrate specificity of plant FatA and FatB acyl-ACP thioesterases. Arch. Biochem. Biophys. 403, 25–34. https://doi.org/10.1016/S0003-9861(02)00017-6

Salie, M.J., Thelen, J.J., 2016. Regulation and structure of the heteromeric acetyl-CoA carboxylase. Biochim. Biophys. Acta 1861, 1207–1213. https://doi.org/10.1016/j.bbalip.2016.04.004

Salimon, J., Abdullah, B.M., Salih, N., 2011. Hydrolysis optimization and characterization study of preparing fatty acids from *Jatropha curcas*seed oil. Chem. Cent. J. 5, 67. https://doi.org/10.1186/1752-153X-5-67

Samuelsson, J., Johansson, M., 2001. A study of fatty acid methyl esters with epoxy or alkyne functionalities. J Am Oil Chem Soc 78, 1191–1196. https://doi.org/10.1007/s11745-001-0412-y

Sandager, L., Gustavsson, M.H., Ståhl, U., Dahlqvist, A., Wiberg, E., Banas, A., Lenman, M., Ronne, H., Stymne, S., 2002. Storage lipid synthesis is non-essential in yeast. J. Biol. Chem. 277, 6478–6482. https://doi.org/10.1074/jbc.M109109200

Sato, R., Fujii, Y., Ara, S., Yamazaki, H., Aburatani, S., Ogasawara, W., Takaku, H., 2024. Deletion of *LsSNF1* enhances lipid accumulation in the oleaginous yeast *Lipomyces starkeyi*. J. Biosci. Bioeng. https://doi.org/10.1016/j.jbiosc.2024.01.014

Savakis, P., Hellingwerf, K.J., 2015. Engineering cyanobacteria for direct biofuel production from CO2. Curr. Opin. Biotechnol. 33, 8–14. https://doi.org/10.1016/j.copbio.2014.09.007

Scherer, G.F.E., Ryu, S.B., Wang, X., Matos, A.R., Heitz, T., 2010. Patatin-related phospholipase A: nomenclature, subfamilies and functions in plants. Trends Plant Sci. 15, 693–700. https://doi.org/10.1016/j.tplants.2010.09.005

Schultz, J.C., Cao, M., Zhao, H., 2019. Development of a CRISPR/Cas9 system for high efficiency multiplexed gene deletion in *Rhodosporidium toruloides*. Biotechnol. Bioeng. 116, 2103–2109. https://doi.org/10.1002/bit.27001

Sec, P., Garaiova, M., Gajdos, P., Certik, M., Griac, P., Hapala, I., Holic, R., 2015. Baker's yeast deficient in storage lipid synthesis uses cis-vaccenic acid to reduce unsaturated fatty acid toxicity. Lipids 50, 621–630. https://doi.org/10.1007/s11745-015-4022-z

Seip, J., Jackson, R., He, H., Zhu, Q., Hong, S.-P., 2013. Snf1 is a regulator of lipid accumulation in *Yarrowia lipolytica*. Appl. Environ. Microbiol. 79, 7360–7370. https://doi.org/10.1128/AEM.02079-13

Seo, M.-H., Kim, K.-R., Oh, D.-K., 2013. Production of a novel compound, 10,12-dihydroxystearic acid from ricinoleic acid by an oleate hydratase from *Lysinibacillus fusiformis*. Appl. Microbiol. Biotechnol. 97, 8987–8995. https://doi.org/10.1007/s00253-013-4728-x

Shabbir, M.A., Khan, M.R., Saeed, M., Pasha, I., Khalil, A.A., Siraj, N., 2017. Punicic acid: A striking health substance to combat metabolic syndromes in humans. Lipids Health Dis. 16, 99. https://doi.org/10.1186/s12944-017-0489-3

Shi, S., Liang, Y., Zhang, M.M., Ang, E.L., Zhao, H., 2016. A highly efficient single-step, markerless strategy for multi-copy chromosomal integration of large biochemical pathways in *Saccharomyces cerevisiae*. Metab. Eng. 33, 19–27. https://doi.org/10.1016/j.ymben.2015.10.011

Shi, Y., Wang, D., Li, R., Huang, L., Dai, Z., Zhang, X., 2021. Engineering yeast subcellular compartments for increased production of the lipophilic natural products ginsenosides. Metab. Eng. 67, 104–111. https://doi.org/10.1016/j.ymben.2021.06.002

Shockey, J., Lager, I., Stymne, S., Kotapati, H.K., Sheffield, J., Mason, C., Bates, P.D., 2019. Specialized lysophosphatidic acid acyltransferases contribute to unusual fatty acid accumulation in exotic *Euphorbiaceae* seed oils. Planta 249, 1285–1299. https://doi.org/10.1007/s00425-018-03086-y

Shockey, J., Regmi, A., Cotton, K., Adhikari, N., Browse, J., Bates, P.D., 2016a. Identification of *Arabidopsis GPAT9* (At5g60620) as an essential gene involved in triacylglycerol biosynthesis. Plant Physiol. 170, 163–179. https://doi.org/10.1104/pp.15.01563

Shockey, J., Rinehart, T., Chen, Y., Yangdong, W., Zhiyong, Z., Lisong, H., 2016b. Tung (*Vernicia fordii* and *Vernicia montana*), in: McKeon, T.A., Hayes, D.G., Hildebrand, D.F., Weselake, R.J. (Eds.), Industrial Oil Crops. AOCS Press, pp. 243–273. https://doi.org/10.1016/B978-1-893997-98-1.00010-5

Shockey, J.M., Gidda, S.K., Chapital, D.C., Kuan, J.-C., Dhanoa, P.K., Bland, J.M., Rothstein, S.J., Mullen, R.T., Dyer, J.M., 2006. Tung tree DGAT1 and DGAT2 have nonredundant functions in triacylglycerol biosynthesis and are localized to different subdomains of the endoplasmic reticulum. Plant Cell 18, 2294–2313. https://doi.org/10.1105/tpc.106.043695

Siloto, R.M.P., Truksa, M., He, X., McKeon, T., Weselake, R.J., 2009. Simple methods to detect triacylglycerol biosynthesis in a yeast-based recombinant system. Lipids 44, 963–973. https://doi.org/10.1007/s11745-009-3336-0

Singer, S.D., Chen, G., Mietkiewska, E., Tomasi, P., Jayawardhane, K., Dyer, J.M., Weselake, R.J., 2016. *Arabidopsis* GPAT9 contributes to synthesis of intracellular glycerolipids but not surface lipids. J. Exp. Bot. 67, 4627–4638. https://doi.org/10.1093/jxb/erw242

Singh, S., Thomaeus, S., Lee, M., Stymne, S., Green, A., 2001. Transgenic expression of a Δ12-epoxygenase gene in *Arabidopsis* seeds inhibits accumulation of linoleic acid. Planta 212, 872–879. https://doi.org/10.1007/s004250000456

Siriwardhana, N., Kalupahana, N.S., Moustaid-Moussa, N., 2012. Chapter 13 - Health benefits of n-3 polyunsaturated fatty acids: eicosapentaenoic acid and docosahexaenoic acid, in:

Kim, S.-K. (Ed.), Advances in Food and Nutrition Research, Marine Medicinal Foods. Academic Press, pp. 211–222. https://doi.org/10.1016/B978-0-12-416003-3.00013-5

Slabaugh, M.B., Leonard, J.M., Knapp, S.J., 1998. Condensing enzymes from *Cuphea wrightii* associated with medium chain fatty acid biosynthesis. Plant J. 13, 611–620. https://doi.org/10.1046/j.1365-313X.1998.00065.x

Smith, M.A., Moon, H., Chowrira, G., Kunst, L., 2003. Heterologous expression of a fatty acid hydroxylase gene in developing seeds of *Arabidopsis thaliana*. Planta 217, 507–516. https://doi.org/10.1007/s00425-003-1015-6

Snow, A.A., 2002. Transgenic crops—why gene flow matters. Nat. Biotechnol. 20, 542–542. https://doi.org/10.1038/nbt0602-542

Somerville, C., Youngs, H., Taylor, C., Davis, S.C., Long, S.P., 2010. Feedstocks for lignocellulosic biofuels. Science 329, 790–792. https://doi.org/10.1126/science.1189268

Spector, A.A., Kim, H.-Y., 2015. Cytochrome P450 epoxygenase pathway of polyunsaturated fatty acid metabolism. Biochim. Biophys. Acta BBA - Mol. Cell Biol. Lipids, Oxygenated metabolism of PUFA: analysis and biological relevance 1851, 356–365. https://doi.org/10.1016/j.bbalip.2014.07.020

Ståhl, U., Carlsson, A.S., Lenman, M., Dahlqvist, A., Huang, B., Banaś, W., Banaś, A., Stymne, S., 2004. Cloning and functional characterization of a phospholipid:diacylglycerol acyltransferase from *Arabidopsis*. Plant Physiol. 135, 1324–1335. https://doi.org/10.1104/pp.104.044354

Sunder, S., Gupta, A., Kataria, R., Ruhal, R., 2023. Potential of *Rhodosporidium toruloides* for fatty acids production using lignocellulose biomass. Appl. Biochem. Biotechnol. https://doi.org/10.1007/s12010-023-04681-w

Takagi, T., Itabashi, Y., 1981. Occurrence of mixtures of geometrical isomers of conjugated octadecatrienoic acids in some seed oils: Analysis by open-tubular gas liquid chromatography and high performance liquid chromatography. Lipids 16, 546–551. https://doi.org/10.1007/BF02535054

Tan, X., Zheng, X., Zhang, Z., Wang, Z., Xia, H., Lu, C., Gu, S., 2014. Long chain acyl-coenzyme A synthetase 4 (BnLACS4) gene from *Brassica napus* enhances the yeast lipid contents. J. Integr. Agric. 13, 54–62. https://doi.org/10.1016/S2095-3119(13)60583-3

Tang, G.-Q., Novitzky, W.P., Carol Griffin, H., Huber, S.C., Dewey, R.E., 2005. Oleate desaturase enzymes of soybean: evidence of regulation through differential stability and phosphorylation. Plant J. Cell Mol. Biol. 44, 433–446. https://doi.org/10.1111/j.1365-313X.2005.02535.x

Taylor, D.C., Francis, T., Guo, Y., Brost, J.M., Katavic, V., Mietkiewska, E., Michael Giblin, E., Lozinsky, S., Hoffman, T., 2009. Molecular cloning and characterization of a KCS gene from *Cardamine graeca* and its heterologous expression in *Brassica* oilseeds to engineer high nervonic acid oils for potential medical and industrial use. Plant Biotechnol. J. 7, 925–938. https://doi.org/10.1111/j.1467-7652.2009.00454.x

Tezaki, S., Iwama, R., Kobayashi, S., Shiwa, Y., Yoshikawa, H., Ohta, A., Horiuchi, H., Fukuda, R., 2017. Δ12-fatty acid desaturase is involved in growth at low temperature in yeast *Yarrowia lipolytica*. Biochem. Biophys. Res. Commun. 488, 165–170. https://doi.org/10.1016/j.bbrc.2017.05.028

Tsai, Y.-Y., Ohashi, T., Kanazawa, T., Polburee, P., Misaki, R., Limtong, S., Fujiyama, K., 2017. Development of a sufficient and effective procedure for transformation of an oleaginous

yeast, *Rhodosporidium toruloides* DMKU3-TK16. Curr. Genet. 63, 359–371. https://doi.org/10.1007/s00294-016-0629-8

Tsuzuki, T., Kawakami, Y., Abe, R., Nakagawa, K., Koba, K., Imamura, J., Iwata, T., Ikeda, I., Miyazawa, T., 2006. Conjugated linolenic acid is slowly absorbed in rat intestine, but quickly converted to conjugated linoleic acid. J. Nutr. 136, 2153–2159. https://doi.org/10.1093/jn/136.8.2153

Ülker, S., Placidi, C., Point, V., Gadenne, B., Serveau-Avesque, C., Canaan, S., Carrière, F., Cavalier, J.-F., 2016. New lipase assay using Pomegranate oil coating in microtiter plates. Biochimie 120, 110–118. https://doi.org/10.1016/j.biochi.2015.09.004

United States Food and Drug Administration, 2021. GRN No. 928. Dried *Saccharomyces cerevisiae* yeast fermentate. URL https://www.cfsanappsexternal.fda.gov/scripts/fdcc/index.cfm?set=GRASNotices&id=928 (accessed 3.9.24).

United States Food and Drug Administration, 2015. GRN No. 604. Baker's yeast (*Saccharomyces cerevisiae*) expressing asparaginase II. URL https://www.cfsanappsexternal.fda.gov/scripts/fdcc/index.cfm?set=GRASNotices&id=604 (accessed 3.9.24).

United States Food and Drug Administration, 2011. GRN No. 355. Eicosapentaenoic acid (EPA)-rich triglyceride oil from *Yarrowia lipolytica*. URL https://www.cfsanappsexternal.fda.gov/scripts/fdcc/index.cfm?set=GRASNotices&id=355 (accessed 3.9.24).

United States Food and Drug Administration, 2005. GRN No. 175. *Saccharomyces cerevisiae* strain ECMo01 with enhanced expression of urea amidolyase. URL

https://www.cfsanappsexternal.fda.gov/scripts/fdcc/index.cfm?set=GRASNotices&id=175 (accessed 3.9.24).

Urbanikova, V., Park, Y.-K., Krajciova, D., Tachekort, M., Certik, M., Grigoras, I., Holic, R., Nicaud, J.-M., Gajdos, P., 2023. *Yarrowia lipolytica* as a platform for punicic acid production. Int. J. Mol. Sci. 24, 8823. https://doi.org/10.3390/ijms24108823

Usaite, R., Jewett, M.C., Oliveira, A.P., Yates, J.R., Olsson, L., Nielsen, J., 2009. Reconstruction of the yeast Snf1 kinase regulatory network reveals its role as a global energy regulator. Mol. Syst. Biol. 5, 319. https://doi.org/10.1038/msb.2009.67

Vahvaselkä, M., Lehtinen, P., Sippola, S., Laakso, S., 2004. Enrichment of conjugated linoleic acid in oats (*Avena sativa* L.) by microbial isomerization. J. Agric. Food Chem. 52, 1749–1752. https://doi.org/10.1021/jf034996j

Van Bogaert, I.N.A., Groeneboer, S., Saerens, K., Soetaert, W., 2011. The role of cytochrome P450 monooxygenases in microbial fatty acid metabolism. FEBS J. 278, 206–221. https://doi.org/10.1111/j.1742-4658.2010.07949.x

van de Loo, F.J., Broun, P., Turner, S., Somerville, C., 1995. An oleate 12-hydroxylase from *Ricinus communis* L. is a fatty acyl desaturase homolog. Proc. Natl. Acad. Sci. 92, 6743–6747. https://doi.org/10.1073/pnas.92.15.6743

van Erp, H., Bates, P.D., Burgal, J., Shockey, J., Browse, J., 2011. Castor phospholipid:diacylglycerol acyltransferase facilitates efficient metabolism of hydroxy fatty acids in transgenic *Arabidopsis*. Plant Physiol. 155, 683–693. https://doi.org/10.1104/pp.110.167239

van Erp, H., Shockey, J., Zhang, M., Adhikari, N.D., Browse, J., 2015. Reducing isozyme competition increases target fatty acid accumulation in seed triacylglycerols of transgenic *Arabidopsis*. Plant Physiol. 168, 36–46. https://doi.org/10.1104/pp.114.254110

Varadi, M., Anyango, S., Deshpande, M., Nair, S., Natassia, C., Yordanova, G., Yuan, D., Stroe, O., Wood, G., Laydon, A., Žídek, A., Green, T., Tunyasuvunakool, K., Petersen, S., Jumper, J., Clancy, E., Green, R., Vora, A., Lutfi, M., Figurnov, M., Cowie, A., Hobbs, N., Kohli, P., Kleywegt, G., Birney, E., Hassabis, D., Velankar, S., 2022. AlphaFold Protein Structure Database: massively expanding the structural coverage of protein-sequence space with high-accuracy models. Nucleic Acids Res. 50, D439–D444. https://doi.org/10.1093/nar/gkab1061

Venkat, M., Chia, L.W., Lambers, T.T., 2024. Milk polar lipids composition and functionality: a systematic review. Crit. Rev. Food Sci. Nutr. 64, 31–75. https://doi.org/10.1080/10408398.2022.2104211

Verhulst, A., Janssen, G., Parmentier, G., Eyssen, H., 1987. Isomerization of polyunsaturated long chain fatty acids by propionibacteria. Syst. Appl. Microbiol. 9, 12–15. https://doi.org/10.1016/S0723-2020(87)80049-8

Vikbjerg, A.F., Mu, H., Xu, X., 2006. Elucidation of acyl migration during lipase-catalyzed production of structured phospholipids. J. Am. Oil Chem. Soc. 83, 609–614. https://doi.org/10.1007/s11746-006-1246-3

Vincent, T., Gaillet, B., Garnier, A., 2021. Optimisation of cytochrome P450 BM3 assisted by consensus-guided evolution. Appl. Biochem. Biotechnol. 193, 2893–2914. https://doi.org/10.1007/s12010-021-03573-1

Vrinten, P., Hu, Z., Munchinsky, M.-A., Rowland, G., Qiu, X., 2005. Two *FAD3* desaturase genes control the level of linolenic acid in flax seed. Plant Physiol. 139, 79–87. https://doi.org/10.1104/pp.105.064451

Vroegrijk, I.O.C.M., van Diepen, J.A., van den Berg, S., Westbroek, I., Keizer, H., Gambelli, L., Hontecillas, R., Bassaganya-Riera, J., Zondag, G.C.M., Romijn, J.A., Havekes, L.M., Voshol, P.J., 2011. Pomegranate seed oil, a rich source of punicic acid, prevents diet-induced obesity and insulin resistance in mice. Food Chem. Toxicol. 49, 1426–1430. https://doi.org/10.1016/j.fct.2011.03.037

Wang, J., Singer, S.D., Souto, B.A., Asomaning, J., Ullah, A., Bressler, D.C., Chen, G., 2022. Current progress in lipid-based biofuels: Feedstocks and production technologies. Bioresour. Technol. 351, 127020. https://doi.org/10.1016/j.biortech.2022.127020

Wang, J., Xu, Y., Holic, R., Yu, X., Singer, S.D., Chen, G., 2021. Improving the production of punicic acid in baker's yeast by engineering genes in acyl channeling processes and adjusting precursor supply. J. Agric. Food Chem. 69, 9616–9624. https://doi.org/10.1021/acs.jafc.1c03256

Wang, K., Shi, T.-Q., Wang, J., Wei, P., Ledesma-Amaro, R., Ji, X.-J., 2022. Engineering the lipid and fatty acid metabolism in *Yarrowia lipolytica* for sustainable production of high oleic oils. ACS Synth. Biol. 11, 1542–1554. https://doi.org/10.1021/acssynbio.1c00613

Wang, K., Zhou, Y., Cao, L., Lin, L., Ledesma-Amaro, R., Ji, X.-J., 2024. Engineering *Yarrowia lipolytica* for sustainable production of the pomegranate seed oil-derived punicic acid. J. Agric. Food Chem. https://doi.org/10.1021/acs.jafc.3c08718

Wang, L., Deng, A., Zhang, Y., Liu, S., Liang, Y., Bai, H., Cui, D., Qiu, Q., Shang, X., Yang, Z., He, X., Wen, T., 2018. Efficient CRISPR–Cas9 mediated multiplex genome editing in yeasts. Biotechnol. Biofuels 11, 1–16. https://doi.org/10.1186/s13068-018-1271-0

Wang, L., Shen, W., Kazachkov, M., Chen, G., Chen, Q., Carlsson, A.S., Stymne, S., Weselake, R.J., Zou, J., 2012. Metabolic interactions between the Lands cycle and the Kennedy pathway of glycerolipid synthesis in *Arabidopsis* developing seeds. Plant Cell 24, 4652–4669. https://doi.org/10.1105/tpc.112.104604

Wang, L.-M., Lv, J.-P., Chu, Z.-Q., Cui, Y.-Y., Ren, X.-H., 2007. Production of conjugated linoleic acid by *Propionibacterium freudenreichii*. Food Chem. 103, 313–318. https://doi.org/10.1016/j.foodchem.2006.07.065

Wei, H., Movahedi, A., Zhang, Y., Aghaei-Dargiri, S., Liu, G., Zhu, S., Yu, C., Chen, Y., Zhong, F., Zhang, J., 2022. Long-chain acyl-CoA synthetases promote poplar resistance to abiotic stress by regulating long-chain fatty acid biosynthesis. Int. J. Mol. Sci. 23, 8401. https://doi.org/10.3390/ijms23158401

Wei, Q., Li, J., Zhang, L., Wu, P., Chen, Y., Li, M., Jiang, H., Wu, G., 2012. Cloning and characterization of a β-ketoacyl-acyl carrier protein synthase II from *Jatropha curcas*. J. Plant Physiol. 169, 816–824. https://doi.org/10.1016/j.jplph.2012.02.006

Wickramarathna, A.D., Siloto, R.M.P., Mietkiewska, E., Singer, S.D., Pan, X., Weselake, R.J., 2015. Heterologous expression of flax phospholipid:diacylglycerol cholinephosphotransferase (PDCT) increases polyunsaturated fatty acid content in yeast and *Arabidopsis* seeds. BMC Biotechnol. 15, 63. https://doi.org/10.1186/s12896-015-0156-6

Woods, A., Munday, M.R., Scott, J., Yang, X., Carlson, M., Carling, D., 1994. Yeast SNF1 is functionally related to mammalian AMP-activated protein kinase and regulates acetyl-CoA carboxylase in vivo. J. Biol. Chem. 269, 19509–19515. https://doi.org/10.1016/S0021-9258(17)32198-1

Xie, D., Jackson, E.N., Zhu, Q., 2015. Sustainable source of omega-3 eicosapentaenoic acid from metabolically engineered *Yarrowia lipolytica*: from fundamental research to commercial production. Appl. Microbiol. Biotechnol. 99, 1599–1610. https://doi.org/10.1007/s00253-014-6318-y

Xu, Y., Caldo, K.M.P., Falarz, L., Jayawardhane, K., Chen, G., 2020a. Kinetic improvement of an algal diacylglycerol acyltransferase 1 via fusion with an acyl-CoA binding protein. Plant J. 102, 856–871. https://doi.org/10.1111/tpj.14708

Xu, Y., Caldo, K.M.P., Holic, R., Mietkiewska, E., Ozga, J., Rizvi, S.M., Chen, G., Weselake, R.J., 2019. Engineering *Arabidopsis* long-chain acyl-CoA synthetase 9 variants with enhanced enzyme activity. Biochem. J. 476, 151–164. https://doi.org/10.1042/BCJ20180787

Xu, Y., Caldo, K.M.P., Pal-Nath, D., Ozga, J., Lemieux, M.J., Weselake, R.J., Chen, G., 2018a. Properties and biotechnological applications of acyl-CoA:diacylglycerol acyltransferase and phospholipid:diacylglycerol acyltransferase from terrestrial plants and microalgae. Lipids 53, 663–688. https://doi.org/10.1002/lipd.12081

Xu, Y., Caldo, K.M.P., Singer, S.D., Mietkiewska, E., Greer, M.S., Tian, B., Dyer, J.M., Smith, M., Zhou, X., Qiu, X., Weselake, R.J., Chen, G., 2021. *Physaria fendleri* and *Ricinus communis* lecithin:cholesterol acyltransferase-like phospholipases selectively cleave

hydroxy acyl chains from phosphatidylcholine. Plant J. 105, 182–196. https://doi.org/10.1111/tpj.15050

Xu, Y., Holic, R., Li, D., Pan, X., Mietkiewska, E., Chen, G., Ozga, J., Weselake, R.J., 2018b. Substrate preferences of long-chain acyl-CoA synthetase and diacylglycerol acyltransferase contribute to enrichment of flax seed oil with α-linolenic acid. Biochem. J. 475, 1473–1489. https://doi.org/10.1042/BCJ20170910

Xu, Y., Mietkiewska, E., Shah, S., Weselake, R.J., Chen, G., 2020b. Punicic acid production in *Brassica napus*. Metab. Eng. 62, 20–29. https://doi.org/10.1016/j.ymben.2020.08.011

Xue, Z., Sharpe, P.L., Hong, S.-P., Yadav, N.S., Xie, D., Short, D.R., Damude, H.G., Rupert, R.A., Seip, J.E., Wang, J., Pollak, D.W., Bostick, M.W., Bosak, M.D., Macool, D.J., Hollerbach, D.H., Zhang, H., Arcilla, D.M., Bledsoe, S.A., Croker, K., McCord, E.F., Tyreus, B.D., Jackson, E.N., Zhu, Q., 2013. Production of omega-3 eicosapentaenoic acid by metabolic engineering of *Yarrowia lipolytica*. Nat. Biotechnol. 31, 734–740. https://doi.org/10.1038/nbt.2622

Yazawa, H., Holic, R., Kumagai, H., Uemura, H., 2013. Toxicity of ricinoleic acid production in fission yeast *Schizosaccharomyces pombe* is suppressed by the overexpression of plg7, a phospholipase A2 of a platelet-activating factor (PAF) family homolog. Appl. Microbiol. Biotechnol. 97, 8193–8203. https://doi.org/10.1007/s00253-013-4987-6

Yazawa, H., Iwahashi, H., Kamisaka, Y., Kimura, K., Uemura, H., 2010. Improvement of polyunsaturated fatty acids synthesis by the coexpression of CYB5 with desaturase genes in *Saccharomyces cerevisiae*. Appl. Microbiol. Biotechnol. 87, 2185–2193. https://doi.org/10.1007/s00253-010-2679-z

Yazawa, H., Kamisaka, Y., Kimura, K., Yamaoka, M., Uemura, H., 2011. Efficient accumulation of oleic acid in *Saccharomyces cerevisiae* caused by expression of rat elongase 2 gene (rELO2) and its contribution to tolerance to alcohols. Appl. Microbiol. Biotechnol. 91, 1593–1600. https://doi.org/10.1007/s00253-011-3410-4

Ye, Y., Nikovics, K., To, A., Lepiniec, L., Fedosejevs, E.T., Van Doren, S.R., Baud, S., Thelen, J.J., 2020. Docking of acetyl-CoA carboxylase to the plastid envelope membrane attenuates fatty acid production in plants. Nat. Commun. 11, 6191. https://doi.org/10.1038/s41467-020-20014-5

Yin, Y., Raboanatahiry, N., Chen, K., Chen, X., Tian, T., Jia, J., He, H., He, J., Guo, Z., Yu, L., Li, M., 2022. Class A lysophosphatidic acid acyltransferase 2 from *Camelina sativa* promotes very long-chain fatty acids accumulation in phospholipid and triacylglycerol. Plant J. 112, 1141–1158. https://doi.org/10.1111/tpj.15999

Yu, X., Cahoon, R.E., Horn, P.J., Shi, H., Prakash, R.R., Cai, Y., Hearney, M., Chapman, K.D., Cahoon, E.B., Schwender, J., Shanklin, J., 2018. Identification of bottlenecks in the accumulation of cyclic fatty acids in camelina seed oil. Plant Biotechnol. J. 16, 926–938. https://doi.org/10.1111/pbi.12839

Yu, X.-H., Cai, Y., Chai, J., Schwender, J., Shanklin, J., 2019. Expression of a lychee phosphatidylcholine:diacylglycerol cholinephosphotransferase with an *Escherichia coli* cyclopropane synthase enhances cyclopropane fatty acid accumulation in camelina seeds. Plant Physiol. 180, 1351–1361. https://doi.org/10.1104/pp.19.00396

Yu, X.-H., Prakash, R.R., Sweet, M., Shanklin, J., 2014. Coexpressing *Escherichia coli* cyclopropane synthase with *Sterculia foetida* lysophosphatidic acid acyltransferase

enhances cyclopropane fatty acid accumulation. Plant Physiol. 164, 455–465. https://doi.org/10.1104/pp.113.230953

Yuan, L., Voelker, T.A., Hawkins, D.J., 1995. Modification of the substrate specificity of an acyl-acyl carrier protein thioesterase by protein engineering. Proc. Natl. Acad. Sci. 92, 10639–10643. https://doi.org/10.1073/pnas.92.23.10639

Zhan, Z., Chen, Y., Shockey, J., Han, X., Wang, Y., 2016. Proteomic analysis of tung tree (*Vernicia fordii*) oilseeds during the developmental stages. Mol. Basel Switz. 21, 1486. https://doi.org/10.3390/molecules21111486

Zhang, B., Chen, H., Li, M., Gu, Z., Song, Y., Ratledge, C., Chen, Y.Q., Zhang, H., Chen, W., 2013. Genetic engineering of *Yarrowia lipolytica* for enhanced production of trans-10, cis-12 conjugated linoleic acid. Microb. Cell Factories 12, 70. https://doi.org/10.1186/1475-2859-12-70

Zhang, B., Ni, L., Tang, X., Chen, X., Hu, B., 2022. Engineering the β-oxidation pathway in *Yarrowia lipolytica* for the production of trans-10, cis-12-conjugated linoleic acid. J. Agric. Food Chem. 70, 8377–8384. https://doi.org/10.1021/acs.jafc.2c02242

Zhang, B., Rong, C., Chen, H., Song, Y., Zhang, H., Chen, W., 2012. *De novo* synthesis of trans-10, cis-12 conjugated linoleic acid in oleaginous yeast *Yarrowia lipolytica*. Microb. Cell Factories 11, 51. https://doi.org/10.1186/1475-2859-11-51

Zhang, B., Song, Y., Chen, H., Zhang, H., Chen, W., 2016. Production of trans-10,cis-12-conjugated linoleic acid using permeabilized whole-cell biocatalyst of *Yarrowia lipolytica*. Biotechnol. Lett. 38, 1917–1922. https://doi.org/10.1007/s10529-016-2175-3

Zhang, H., Zhang, L., Chen, H., Chen, Y.Q., Chen, W., Song, Y., Ratledge, C., 2014. Enhanced lipid accumulation in the yeast *Yarrowia lipolytica* by over-expression of ATP:citrate

lyase from *Mus musculus*. J. Biotechnol. 192, 78–84. https://doi.org/10.1016/j.jbiotec.2014.10.004

Zhang, J., Liu, H., Sun, J., Li, B., Zhu, Q., Chen, S., Zhang, H., 2012. *Arabidopsis* fatty acid desaturase FAD2 is required for salt tolerance during seed germination and early seedling growth. PLoS ONE 7, e30355. https://doi.org/10.1371/journal.pone.0030355

Zhang, M., Barg, R., Yin, M., Gueta-Dahan, Y., Leikin-Frenkel, A., Salts, Y., Shabtai, S., Ben-Hayyim, G., 2005. Modulated fatty acid desaturation via overexpression of two distinct ω-3 desaturases differentially alters tolerance to various abiotic stresses in transgenic tobacco cells and plants. Plant J. 44, 361–371. https://doi.org/10.1111/j.1365-313X.2005.02536.x

Zhang, Y., Yang, C., Xia, J., Deng, L., Wang, F., Liu, J., 2022a. Overproducing nervonic acid by synergism of fatty acid elongases in engineered *Saccharomyces cerevisiae*. Process Biochem. 122, 341–346. https://doi.org/10.1016/j.procbio.2022.09.013

Zhang, Y., Zhang, S., Chu, Y., Zhang, Q., Zhou, R., Yu, D., Wang, S., Lyu, L., Xu, G., Zhao, Z.K., 2022b. Genetic manipulation of the interconversion between diacylglycerols and triacylglycerols in *Rhodosporidium toruloides*. Front. Bioeng. Biotechnol. 10. https://doi.org/10.3389/fbioe.2022.1034972

Zhao, C., Gu, D., Nambou, K., Wei, L., Chen, J., Imanaka, T., Hua, Q., 2015. Metabolome analysis and pathway abundance profiling of *Yarrowia lipolytica* cultivated on different carbon sources. J. Biotechnol. 206, 42–51. https://doi.org/10.1016/j.jbiotec.2015.04.005

Zhao, H., Kosma, D.K., Lü, S., 2021. Functional role of long-chain acyl-CoA synthetases in plant development and stress responses. Front. Plant Sci. 12. https://doi.org/10.3389/fpls.2021.640996

Zhao, L., Katavic, V., Li, F., Haughn, G.W., Kunst, L., 2010. Insertional mutant analysis reveals that long-chain acyl-CoA synthetase 1 (LACS1), but not LACS8, functionally overlaps with LACS9 in *Arabidopsis* seed oil biosynthesis. Plant J. 64, 1048–1058. https://doi.org/10.1111/j.1365-313X.2010.04396.x

Zhou, X.-R., Horne, I., Damcevski, K., Haritos, V., Green, A., Singh, S., 2008. Isolation and functional characterization of two independently-evolved fatty acid Δ12-desaturase genes from insects. Insect Mol. Biol. 17, 667–676. https://doi.org/10.1111/j.1365-2583.2008.00841.x

Zhou, X.-R., Shrestha, P., Yin, F., Petrie, J.R., Singh, S.P., 2013. AtDGAT2 is a functional acyl-CoA:diacylglycerol acyltransferase and displays different acyl-CoA substrate preferences than AtDGAT1. FEBS Lett. 587, 2371–2376. https://doi.org/10.1016/j.febslet.2013.06.003

Zhou, Y., Huang, X., Hu, T., Chen, S., Wang, Y., Shi, X., Yin, M., Li, R., Wang, J., Jia, X., 2023. Genome-wide analysis of glycerol-3-phosphate acyltransferase (GPAT) family in *Perilla frutescens* and functional characterization of PfGPAT9 crucial for biosynthesis of storage oils rich in high-value lipids. Int. J. Mol. Sci. 24, 15106. https://doi.org/10.3390/ijms242015106

Zhu, L.Y., Zong, M.H., Wu, H., 2008. Efficient lipid production with *Trichosporon fermentans* and its use for biodiesel preparation. Bioresour. Technol. 99, 7881–7885. https://doi.org/10.1016/j.biortech.2008.02.033

Appendix

The following list describes other publications and my contributions.

1. Wang, J., Singer, S.D., Souto, B.A., Asomaning, J., Ullah, A., Bressler, D.C., Chen, G., 2022. Current progress in lipid-based biofuels: Feedstocks and production technologies. Bioresource Technology 351, 127020. https://doi.org/10.1016/j.biortech.2022.127020
    - For this work, I wrote the major part of the manuscript, Souto, B.A. and Asomaning, J. from Dr. Bressler's lab also contributed to the writing and revision of the manuscript. All other coauthors contributed to the editing.
2. Lu, J., Xu, Y., Wang, J., Singer, S.D., Chen, G., 2020. The Role of Triacylglycerol in Plant Stress Response. Plants 9, 472. https://doi.org/10.3390/plants9040472
    - For this work, I participated in discussion and manuscript editing.
3. Shan, Q., Tian, G., Wang, J., Hui, H., Shou, Q., Fu, H., Hao, M., Wang, K., Wu, X., Cao, G., Chen, G., Qin, L., 2021. Change in the active component of processed *Tetradium ruticarpum* extracts leads to improvement in efficacy and toxicity attenuation. Journal of Ethnopharmacology 264, 113292. https://doi.org/10.1016/j.jep.2020.113292
    - For this work, I participated in manuscript editing.
4. Xu, Y., Pan, X., Lu, J., Wang, J., Shan, Q., Stout, J., Chen, G., 2021. Evolutionary and biochemical characterization of a *Chromochloris zofingiensis* MBOAT with wax synthase and diacylglycerol acyltransferase activity. Journal of Experimental Botany 72, 5584–5598. https://doi.org/10.1093/jxb/erab236
    - For this work, I contributed to microbial culture and carried out some lipid analysis experiments.